UNIVERSITY OF SOUTHAMPTON

DISTRIBUTION OF LEAKAGE FLUX AT THE STATOR CORE BACK OF THE SYNCHRONOUS MACHINE

by

Carlos Alberto Mariotoni

A thesis submitted for the degree of
Doctor of Philosophy

Department of Electrical Engineering
Faculty of Engineering and Applied Science

February 1981

DEDICO À MINHA COMPANHEIRA MARILI

E AO MEU PARCEIRO THIAGO

UNIVERSITY OF SOUTHAMPTON

ABSTRACT

FACULTY OF ENGINEERING AND APPLIED SCIENCE

ELECTRICAL ENGINEERING

Doctor of Philosophy

DISTRIBUTION OF LEAKAGE FLUX AT THE STATOR CORE BACK OF THE SYNCHRONOUS MACHINE

by Carlos Alberto Mariotoni

The importance of the leakage flux at the stator core back to the reliability of the synchronous machine has been increased with the constant growth in the machine size. The distribution of core back leakage flux is investigated during different operational conditions such as short and open circuits, and on-load. The radial, axial and circumferential components of leakage flux are measured at the air region of the stator core back. Those components help to estimate the leakage flux inside the stator core back and can be used to determine the effects of the leakage flux on the stator core structure.

The core back leakage flux can induce circulating currents which can damage the stator core. The distribution of this leakage flux depends on a large number of variables. The most important of them, which are discussed in this thesis, are: the levels of saturation in the stator core, the odd harmonics in the leakage flux waveform, the distribution of eddy currents, the overhang geometry and current, the power factor, and the geometry of the stator core and its mechanical structure.

The method of the electromagnetic sources is utilised in order to analyse the distribution of the leakage flux at the stator core back of the synchronous machine. The mathematical treatment of the electromagnetic sources is also presented.

CONTENTS

LIST OF SYMBOLS

A	Magnetic vector potential
a_n	Fourier series coefficient
b_n	Fourier series coefficient
B	Magnetic flux density
$B_{r_{ag}}$	Radial magnetic flux density at the air gap
B_{r_i}	Radial magnetic flux density at the iron
B_r	Radial magnetic flux density
B_{R_r}	Magnetic flux density at the rotor surface
$B_{R_{si}}$	Magnetic flux density at the inner surface of the stator
B_a	Axial magnetic flux density
B_θ	Circumferential magnetic flux density
c_n	Fourier series coefficient
$\cos \phi$	Power factor
D	Electric flux density
d_n	Fourier-Bessel series coefficient
E	Electric field strength
f	Frequency
f_n	Fourier series coefficient
F	Force
H	Magnetic field strength
H_{ag}	Air gap magnetic field
H_i	Magnetic field in the iron
I	Peak phase current
I_f	Field current
I_{sc}	Short circuit current
I_0, I_1, I_2	Modified Bessel functions of the first kind, and zero, first and second-order respectively

I_1'	Derivative of I_1
J	Current density
J_1, J_2	Bessel functions of first kind and first and second-order respectively
j	complex number
$\hat{J}_\theta, \hat{J}_z$	Peak value of the circumferential and axial surface current density respectively
$J_\theta(z), J_z(z)$	Circumferential and axial surface current density respectively
K	Constant
K_0, K_1, K_2	Modified Bessel functions of second kind and zero, first and second-order respectively
K_1'	Derivative of k_1
K_c	Chording factor
K_d	Distribution factor
l_{ap}	Half-length of the active part of the winding
l_c	Half-length of the stator core
l_{lw}	Half-length of the end winding
l_m	Distance between the
l_{oh}	Half-length of the overhang
l_{sp}	Half-length of the straight part of the overhang
l_s	Half-length of the rotor core
l_w	Half-length of the winding
n	Unit vector normal to the surface
N	Number of turns per phase
P	Dipole moment per unit volume
p	Number of pair poles
p*	Magnetic pole

$p^*_{cf}(r), P^*_{cf}$ Core front surface polarity

p^* Magnetic

$p^*_{si}(z), P^*_{si}$ Magnetic polarity at the inner surface of the stator

$p^*_r(z), P^*_r$ Magnetic polarity at the stator surface

r Radial distance

R_c Outer radius of the stator core

R_r Radius of the rotor

R_{si} Inner radius of the stator core

R_w Radius of the winding

v Volume

V Magnetic scalar potential

V_{oc} Open circuit voltage

z Axial distance

γ Stacking factor

δ_t Transverse skin depth

δ_z Axial skin depth

ε_o Electric permittivity of free space

ε_R Relative permittivity

θ Circumferential distance

λ_n Roots of the Bessel function J_1 for $n = 1, 2, 3, \ldots$

μ_o Air permeability

μ_r Relative permeability

ρ Charge density

ρ^* Magnetic pole density

σ Electromagnetic stress

ϕ Phase angle

∂ Conductivity

ACKNOWLEDGEMENTS

This thesis would not have been possible without many people's help and friendship throughout my research period.

I am really indebted to Professor P. Hammond who originated and supervised this research project and gave advice and guidance that significantly contributed to the realisation of this work.

My grateful thanks to Dr. R.L. Stoll for his kindly assistance and advice, and to Dr. P.J. Tavner for the useful suggestions and help in the vector field plotting.

Many thanks to Mr. A.J. Badden Fuller, Leicester University, for allowing us to use the Vect-3 program.

My sincere thanks to Dr. P.A. Kahan, Dr. A.G. Bailey, Dr. E.M. da Costa, Mr. A. Lenzi, Mr. S. Varella, Mr. J. Urriola, Mr. F.J. Mumford and Mr. J.H. Toyer for their help and encouragement.

I am also grateful to the Electrical Engineering Department technical staff and especially to Mr. R.L. Caldecutt for the great support given during the experimental investigations, and to Mr J.H. Johnstone for his help in taking the photographs used in this thesis.

I would like to thank Mrs. S. Frier for kindly typing this thesis and Mrs. J.C. Bennett for her help in typing the figure captions.

I would like to thank UNICAMP - Universidade Estadual de Campinas and CAPES - Coordenação do Aperfeiçoamento de Pessoal de Nível Superior - BRAZIL, for giving me the support and scholarship to do this research work.

Furthermore, I would like to express my gratitude to Marili and Thiago for their special support (the most important of all!).

CHAPTER ONE

INTRODUCTION

The demand for electric power has increased progressively all over the world and has contributed to the increase in rated power output of synchronous machines. The stator current of these machines has been increased in order to obtain the larger power output required since the increase of magnetic flux density is limited by the existing magnetic materials. The machine rating has increased more than ten times in the last twenty years, and nowadays there exists the possibility to construct synchronous machines around 1600MW and it may be possible to install machines greater than 2000MW in the near future.[1] The physical dimensions of the synchronous machines have had to increase in order to achieve the enlarged machine ratings, although the increase in dimensions is much less than the increase in ratings.

The price of each kW produced is decreased with the growth in the unity capacity and this stimulates the design of bigger power output synchronous machines. This has the disadvantage of difficult transportation since it is dealing with enlarged sizes and heavier weight. The active magnetic components present the greatest contribution to this problem while the conducting material quantity represents a smaller contribution.[1-3] Although the rates of material weight per unit power (kg/kW) has decreased with the increase in electrical machine capacity.

The increase in synchronous machine dimensions and power output has further forced the manufacturers to look constantly for new means to make machines more economic both in construction and operating costs and better in reliability, since the large synchronous machines have high efficiency and are expected to carry the largest

share of system load. This has contributed to increasing the need of seeking an improvement of the behaviour of both the magnetic and electric materials used in synchronous machine components in order to allow the required increase in the electric and magnetic loading. The improvement in the use of magnetic materials has not made much progress compared with the utilisation of conductive material. Therefore only a relatively modest growth in the air gap flux has taken place compared with the substantial increase in electric loading made possible by special cooling techniques.

To minimise the serious problems of heating noticed specially in the conductors and iron core, it has become customary to introduce direct water or gas or oil cooling and radial and/or axial cooling ducts in the stator iron.[4-7] In synchronous machines having a large stator core both radial and axial systems may be provided. The radial ducts are introduced between groups of laminations and have the disadvantage of reducing the core stacking factor. The axial ducts are made up of several holes punched in the laminations in such a way as to permit the flow of gas in the axial direction, but this has the disadvantage of disturbing the circumferential permeability. Both the radial and axial ducts can cause secondary effects disturbing the magnetic flux distribution.[8]

The design of the end region of the large synchronous machines has become particularly problematic owing mainly to the increase in both the fringing and leakage fluxes caused respectively by larger air gaps and increased currents. The specialists in synchronous machine design have drawn a lot of attention to the end region leakage fluxes perpendicular to the surface of the stator core front, specially near the toothed area.

It has been demonstrated that the axial leakage flux causes troublesome effects at the end region causing the establishment of excessive temperature affecting the integrity of the stator core end laminations leading, in some cases, to core damage. This flux induces eddy currents that circulate in the plane of the stator core laminations and cause an undesirable and additional joule loss which can reduce both the efficiency and the reliability of machines. Another effect of this leakage flux is the fact that it can cause local hotspots in the laminations. This has a cumulative effect and can degrade the inter-laminar dielectric properties, putting at risk the insulation between laminations and easing the establishment of circulating currents that can strongly damage the surrounding area.

Because of the necessity to develop techniques that could reduce the problems caused by the axial leakage flux at the core end, much research has been done[9-31], both theoretically and experimentally, using different available means: analytical, analogue representation, or by computational methods, in order to achieve both the best stator core end geometry and screening techniques that could help to reduce axial leakage flux effects. It has become customary to grade the corner of the stator core end which reduces the normally directed fluxes entering that core region, to place a copper or aluminium screen around magnetic plates which tends to deflect the flux away from the stator core front laminations preventing the flux penetration, and to split radially both the tooth at the end zone and the support finger to reduce the heating effects.

The damage in the stator cores is very much disliked by the electricity generating companies since any repair causes a very long period of inactivity of the machine and involves very high cost. Even if it is considered that just a part of the stator laminations

needs to be replaced this involves the necessity of removing the whole stator winding.

The biggest stator cores built up to now are those of synchronous machines. Despite the increased dimensions, their shape and construction forms have remained unaltered in their fundamental aspects, e.g. the stator core has been built up from packets of silicon steel laminations grouped and supported by iron bars and clamping plates which fix the laminations in a plane perpendicular to the mechanical axis, therefore, parallel to the direction of the main flux. The laminations are insulated from one another by a thin layer of varnish to increase the resistance of the eddy current paths. The effective thickness of the laminations influences the intensity of the induced circulating eddy currents and the thickness is made as small as possible to minimise this undesirable phenomenon. Usually laminations are 0.5mm or 0.35mm thick considering that a thickness thinner than 0.35mm is more difficult to produce, both more difficult and more expensive to assemble and also reduces the stacking factor. During assembly of the stator core body it is necessary to avoid any damage to the laminations' insulation in order to guarantee a highly effective inter-laminar insulation. The damaging of the laminations' insulation can cause an unexpected increase in the stator core losses. Owing to the great diameter of the stator core the laminations are constructed in sectors, nine or more, and they are overlapped from layer to layer, in halves or thirds, to ease the handling by builders, to give more consistency to the stator core and to diminish the troublesome effects of the transverse fluxes. The butt joints are mechanically necessary and result in the disadvantage of increased eddy current losses which could result in hotspots, caused by transverse fluxes in the region around the butt joints.[32-36]

To date attention paid to the stator core structure has been mainly linked with mechanical requirements, i.e. the building bars, key bars and many of the structure components have been designed and constructed mainly to guarantee the stiffness of the stator core, protecting against both vibration and mechanical forces. Less emphasis seems to have been given to their electromagnetic properties. Both the support finger and clamping plate used to compress and hold firmly the stator core laminations can be mentioned as examples of structure components where their magnetic properties can have a considerable effect on the leakage flux at the core end. The support finger and the clamping plates are made up of non-magnetic material (nodumag). Old synchronous machines have magnetic clamping plates. The substitution of the magnetic clamping plates by non-magnetic ones reduces considerably the effects of the leakage flux at the core front laminations. A copper or aluminium screening plate at the stator core front helps to reduce the penetration of the leakage flux in the core front.[38]

The mechanical properties and characteristics of the structural components have further been affected by the increase in the rated power output of synchronous machines because the forces between both turns of one coil and between coils and their supporting structures are proportional to the square of the machine current which has been increased considerably. Therefore it means that either the strength of the structural material needs to be improved or the dimensions need to be increased to support the greater applied forces.[39]

It is perfectly understandable that much attention is given to the mechanical qualities of the structure as a result of the increase in machine size, but it is further possible that some kind of loss

formerly considered as negligible, could be transformed into a reasonable amount or could have more significant effects, threatening the machine reliability since both the fringe and leakage fluxes have been largely increased.

Hitherto, very few investigations have been made dealing with leakage flux at the stator core back, but since core faults have increased this is starting to receive more attention by the research community. Many manufacturers have asked their electrical departments to give further attention to measuring and analysing the core back leakage flux during the standard open and short circuit tests, as well as during sudden short circuit tests. The measurements have been taken on large synchronous machines' stator cores, but the results are usually kept confidential and there are few publications on that subject.[41-46]

The leakage flux at the stator core back of synchronous machines may cause circulating currents which can damage the stator core laminations. Actually the core back leakage flux can penetrate the stator core structure inducing eddy currents since the flux is time varying and the structure components are made of solid steel. These eddy currents cause an undesirable amount of heating and can establish zones of high concentration of temperature at the stator core back likely contributing to the establishment of hotspots. Because the building bars are solid steel bodies the eddy currents induced will be greatly concentrated at the surface which is close to the stator core back surface and can transmit temperatures causing the increase in the core back temperature.

The core back leakage flux can also establish electric fields acting in adjacent laminations. These electric fields can cause a breakdown voltage which can damage the inter-laminar insulation and

easing the circulation of eddy currents between the adjacent laminations. The inter-laminar eddy current can cause high local concentration of temperature which has a tendency to expand the damaged area leading to core breakdown. The inter-laminar insulation is good enough to support the electric field caused by the synchronous machine main flux which is generally low. The resistance between each lamination and the building bars at the stator core back plays an important role in these phenomena.[41]

In view of these problems it has been decided to present in this thesis some analysis and discussions about the behaviour of the stator core back leakage flux and its relevance to synchronous machine design. This leakage flux has been analysed into its components and measurements were carried out mainly outside the stator core back. It would not be possible to measure the three components of the stator core back leakage flux without affecting the stator core integrity, disturbing the stacking factor. The determination of the leakage flux in the air region at the stator core back is important for two main reasons: firstly, it helps to estimate the leakage flux inside the stator core back and secondly, it can be used to determine the effects of leakage flux penetrating the stator core structure and its contribution to the core losses.

The stator core back leakage flux depends on a large number of variables including the geometry of the stator core and its supporting structure, the geometry of the overhang, levels of saturation in the stator core, the distribution of eddy currents, and the power factor of the synchronous machine. Two different laboratory models of synchronous machine were utilised in order to analyse the behaviour of the core back leakage flux during different operational conditions, and the geometry and dimensions' effects on the leakage flux

distribution. The laboratory synchronous machine was operated on both short and open circuit and on-load conditions. The leakage flux distributions were obtained for the three kinds of operation. During short circuit the overhang current effects on the core back leakage flux distribution were analysed. During open circuit the saturation effects on the distribution of leakage flux at the core back were obtained. During on-load conditions the power factor effects on the leakage flux distribution were obtained. The leakage flux distribution was also analysed for the different dimensions of overhang, different stator core laminations depth, different relative position between both the stator and rotor cores, different air gap lengths, screening plates, eddy currents and laminations rolling direction. The leakage flux is analysed by means of its electromagnetic sources and the magnetic field equations due to them are presented.

CHAPTER TWO

EXPERIMENTAL INVESTIGATION

2.1 GENERAL

It is common practice among manufacturers to undertake a number of standard tests on an electrical machine before it leaves the factory to be installed. Simultaneously with these tests different kinds of measurements are introduced in order to analyse problems observed in installed machines.

In most cases the industrial research community has facilities and advantages of experimenting with and analysing full-scale machines, while in universities research on scale models is generally substituted. It is possible to scale the models, but a perfect scaling of the effects to be analysed is always difficult and sometimes impossible. That is explained by the fact that not all the electrical machine parameters are dimensional and the non-dimensional parameters cannot be properly arranged to suit the model's requirements.

In order to investigate the core back leakage flux, two different laboratory machines were used. The first one is a laboratory synchronous machine which allowed us to analyse the leakage flux behaviour during different operational conditions such as: short circuit, open circuit and on-load. The second one is a laboratory model with stationary rotor which allowed us to investigate the effects of different machine dimensions and geometry on the stator core back leakage flux distribution. The eddy current effects have also been investigated.

In both laboratory models the axial, radial and circumferential components of the core back leakage flux were measured at the air region. The axial component is the only one which was measured inside

the core. The other two components were not measured inside the core because such measurement would cause a great disturbance to the stator core stacking factor. The values of the leakage flux intensities presented are RMS ones. The measurements of the leakage flux components at the air region close to the stator core back can help to estimate the leakage flux inside the core back by means of boundary conditions. They can also be used to investigate the effects of core back leakage flux penetrating the stator core structure and its contribution to the core losses.

2.2 MEASUREMENTS DESCRIPTION

2.2.1 Machine Under Different Operational Conditions

The core back leakage flux was measured with the laboratory synchronous machine operating in both open and short circuits and on-load conditions at the constant frequency of 50Hz. In order to present complete information about the behaviour of the stator core back leakage flux all over the core back region, the three components, axial, radial and circumferential, were measured at the different positions in the air region relative to the stator core body (figure 2.9).

The measurements of the leakage flux against position were taken maintaining a fixed condition when the machine was operating either on open and on short circuits or on-load conditions, and carefully varying the search coil location. Those measurements help to obtain the distribution of the core back leakage flux for the different operations.

The open circuit operation was obtained with the field winding fed with a 40A d.c. current and with the rotor rotating at a constant speed of 1500 RPM (the machine is a four pole one). The

stator winding terminals were left disconnected before exciting the machine. Three voltmeters were put between the phase terminals in order to measure the open circuit voltage. For safety reasons this open circuit voltage was fixed at 415V. During the open circuit operation the saturation effects on the core back leakage flux were investigated. The different levels of saturation were imposed to the synchronous machine varying the open circuit voltage controlling the field current at a constant frequency of 50Hz. The short circuit operation was obtained by having the stator winding terminals on symmetric short circuit before the machine was excited and gradually increasing the field current to the desirable value. The rotor speed was also equal to 1500 RPM in order to obtain a frequency equal to 50Hz. Finally, in order to investigate the leakage flux distribution during on-load conditions, the synchronous machine stator winding was connected in parallel with the mains by means of an autotransformer. In this case special care must be taken in order to guarantee a machine frequency equal to 50Hz before paralleling it with the mains. Therefore this arrangement allowed us to vary the synchronous machine power factor with the help of the transformer tap-changing switch. That switch permitted us to control the transformer voltage ratio, therefore the load could also be controlled. The field current was varied in order to control either the open circuit voltage or short circuit current. The laboratory synchronous machine characteristic curves are shown in figure 2.1.

To analyse the eddy current effects the machine frequency was varied. This was done during open circuit condition. The d.c. motor speed was varied. During open circuit operation the variation of frequency was obtained with a fixed current field and by letting the open circuit voltage vary freely. Figure 2.2 shows the variation

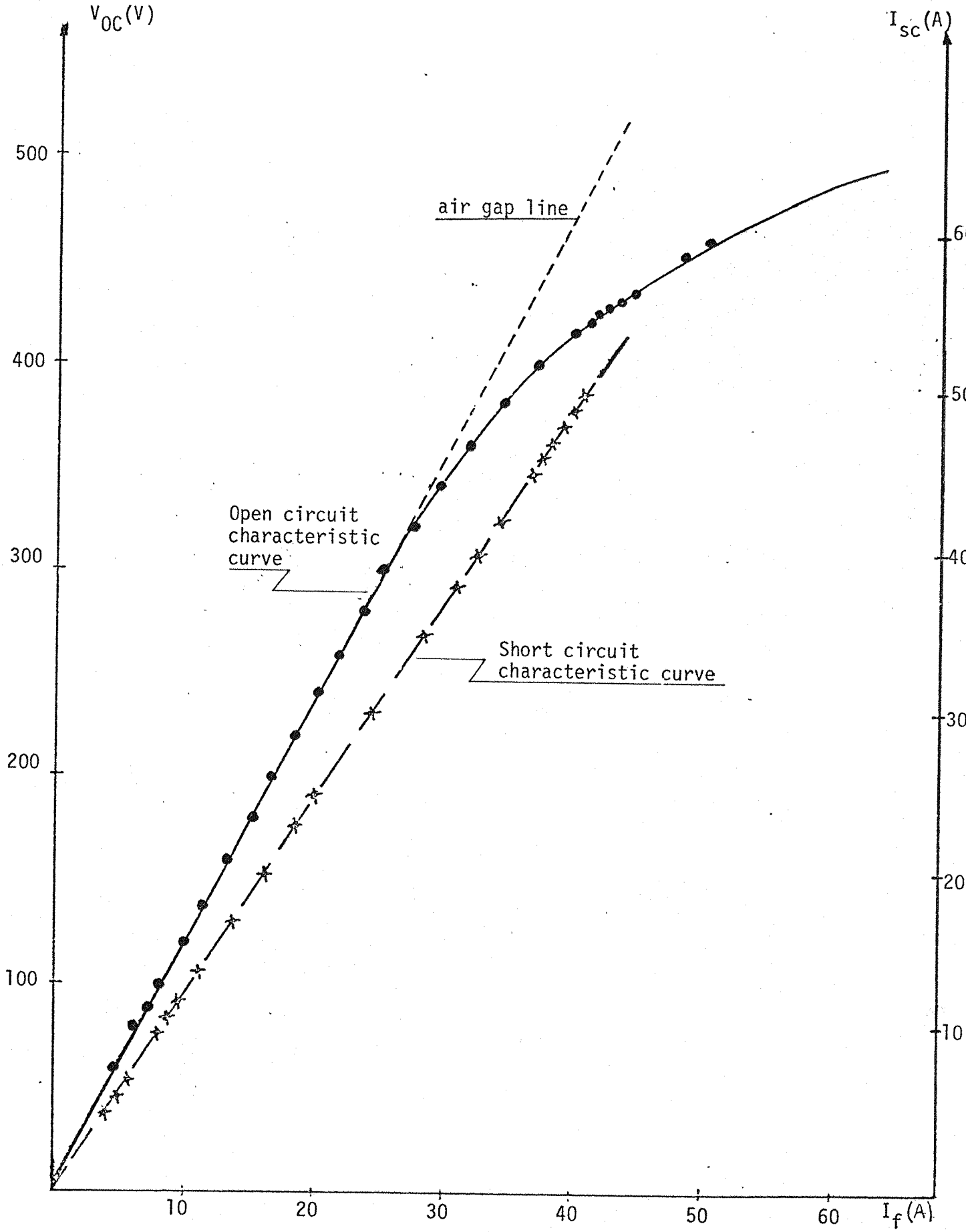

Fig.2.1 : Laboratory synchronous machine characteristic curves

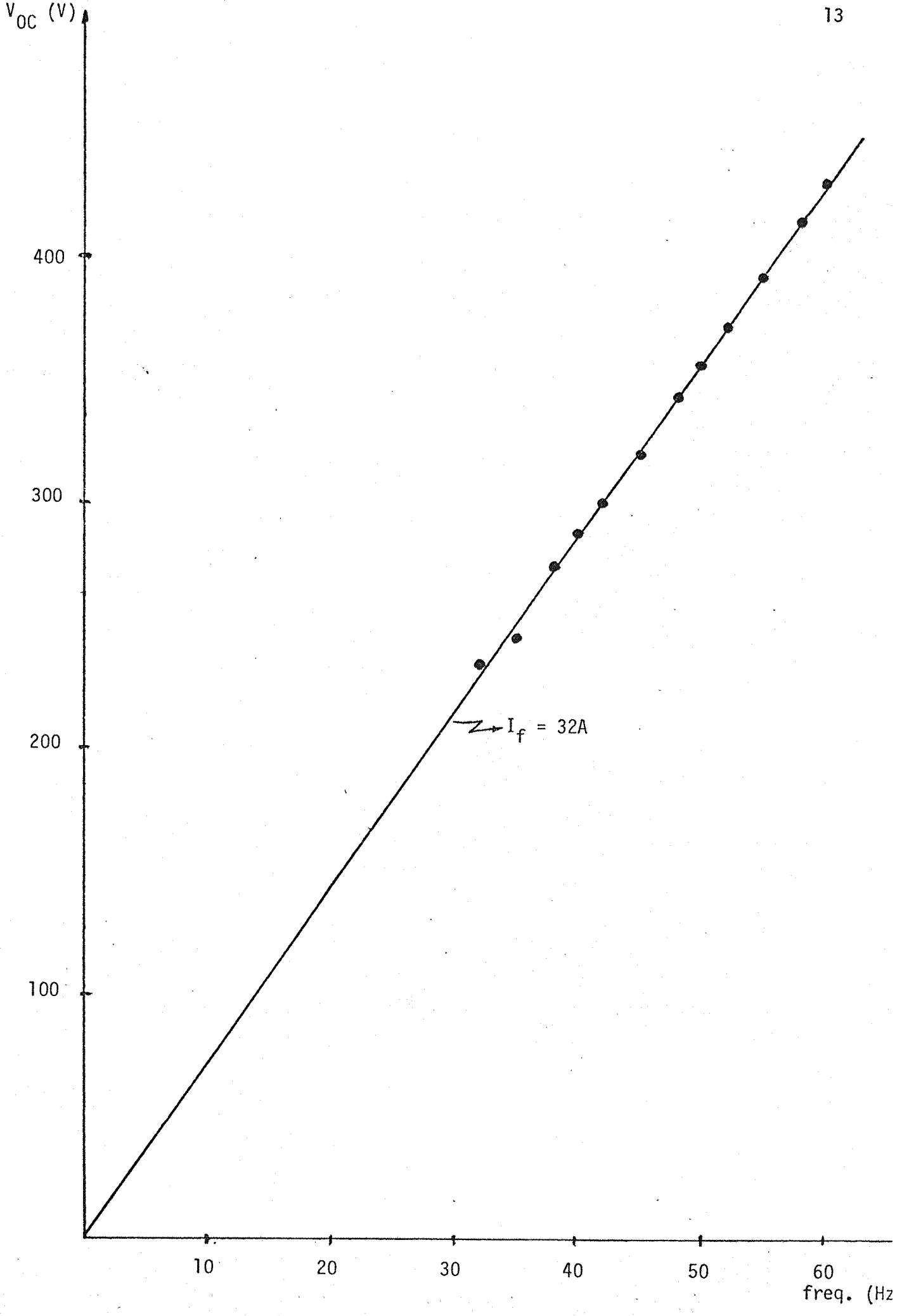

Fig. 2.2: Variation of the open circuit voltage against the frequency

of the open circuit voltage against the frequency for a fixed field current. Both the maximum and the minimum values of frequency were limited by the electrical and mechanical conditions established by the maximum voltage admissible in the stator windings, by maximum vibration levels supported by the system and by the maximum speed driven by the d.c. motor. The synchronous machine was fitted with a reference coil in order to measure the main frequency.

On both open and short circuits and on-load conditions the phase angles of the leakage flux components were not measured owing to the fact that the signals were full of harmonics. These harmonics did not allow us to obtain stable readings in the digital phase meter.

The laboratory synchronous machine used to obtain the measurements presented in this thesis is shown in figure 2.3. Nevertheless the results of this research are of particular interest with regard to large machines, the model used is not a scaled down version of such machines. However, the results obtained can give designers some useful information about the behaviour of the leakage flux which is likely to have some similarities to large machines. It is a 37KVA, 415V, four pole synchronous machine, formerly used to measure the axial leakage flux at the stator ends.

The machine has a rotor winding fed by a d.c. source, producing the machine field. The rotor winding is a full pitched four pole carried by 24 unskewed slots and has the terminals connected to a slip-ring assembly mounted externally to the bearing pedestal. The stator winding is a diamond one, four pole double layer 60^{o} spread, shorted chorded 8/9 of a pole pitch and carried by 36 slots. The rotor body is a laminated one as well as the stator body. The stator core is built up by packets of steel laminations, each one 0.5mm thick, conveniently grouped and stacked with the help of two rings placed

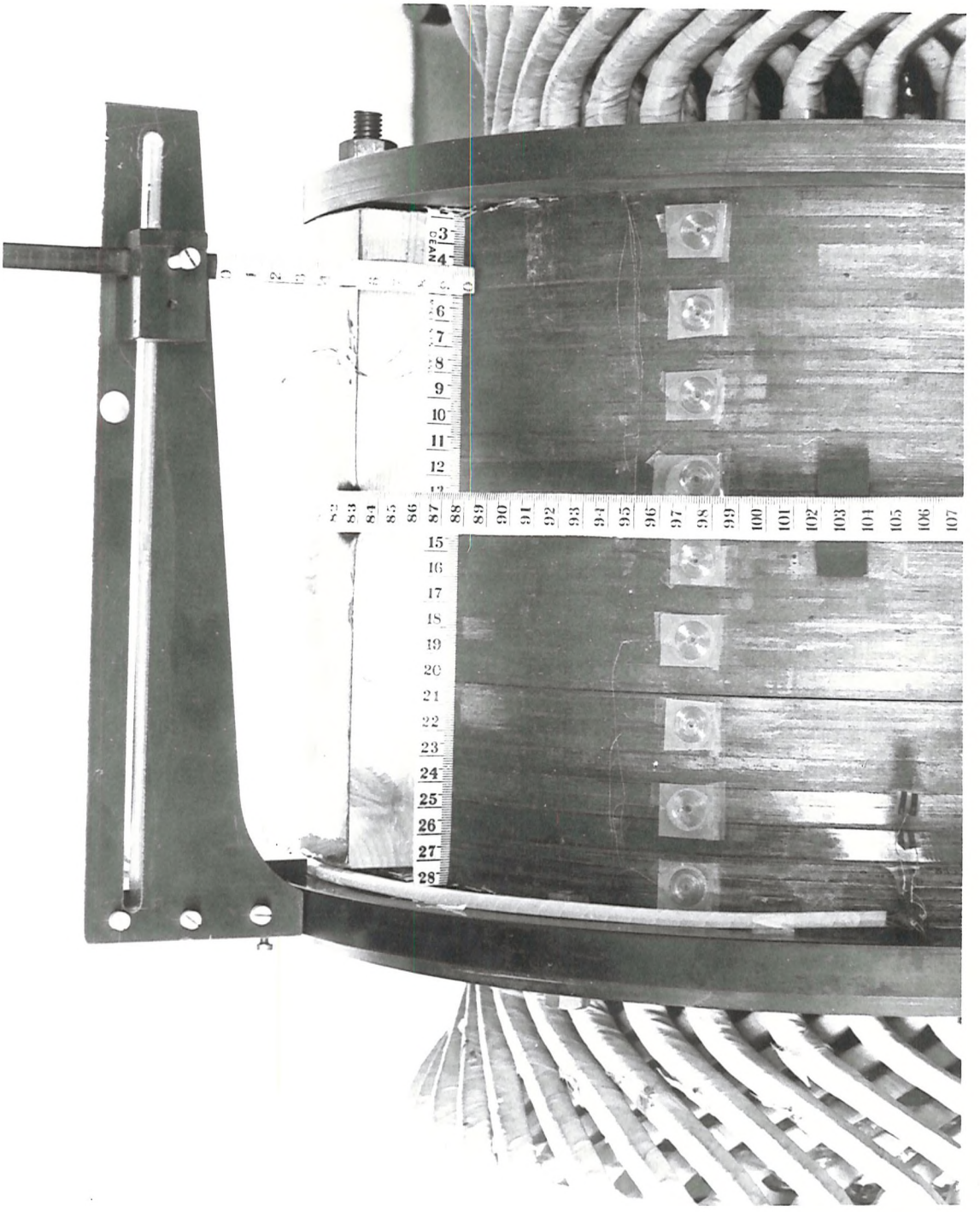

Fig. 2.3: Laboratory synchronous machine.

one at each of the stator ends. The laminations are complete ring stampings and are separated by a layer of insulation about 0.035mm thick.

The rotor and stator bodies are separated by a 2mm air gap. The stator and rotor teeth configurations and dimensions are shown below in figures 2.4 and figures 2.5 respectively.

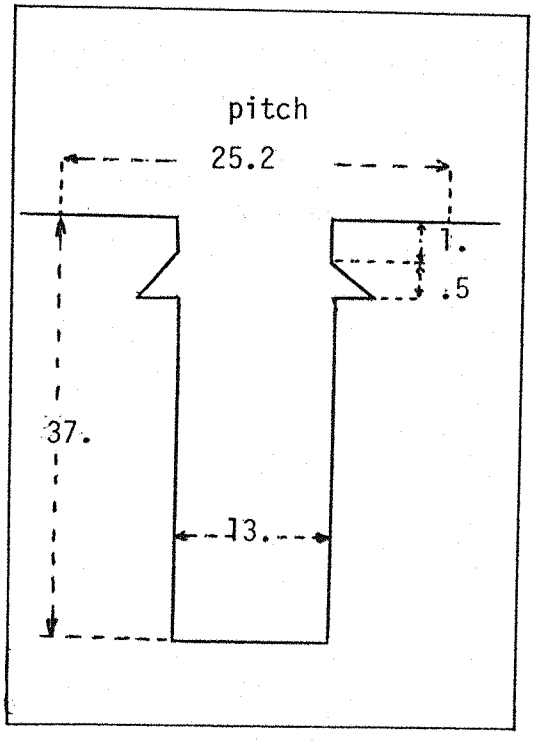

Fig. 2.4: Stator slot

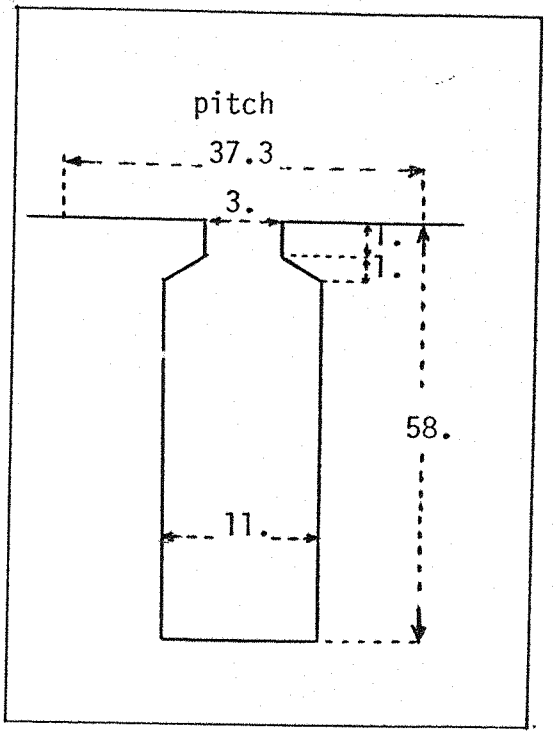

Fig. 2.5: Rotor slot

The main synchronous machine dimensions are:

Core length	300mm
Outside diameter	444mm
Bore diameter	289mm
Rotor diameter	285mm

Shaft diameter	108mm
Overhang length	110mm
Air gap length	2mm

The machine magnetic loadings are:

Stator yoke	1.1 Tesla
Rotor core	1.56 Tesla
Stator teeth	0.68 Tesla (min.)
	1.05 Tesla (max.)
Rotor teeth	0.775 Tesla (min.)
	1.83 Tesla (max.)
Air gap	0.47 Tesla

(all based on 1.28 x mean density).

The synchronous machine has an open frame to permit easy access to the core back region and to allow different locations of the search coils to measure the leakage flux at several points (figure 2.3). There are neither axial nor radial ventilating ducts in this laboratory machine. A d.c. motor drives the rotor and there is a set of switches, rheostats, voltmeters and ammeters, mounted in such a way that it is possible to vary and control the d.c. motor speed and consequently the machine main frequency as well as the field current. A three-phase Wattmeter/Varmeter has been used in order to measure the power factor of the synchronous machine during on-load operation.

2.2.2 Variation of the Model Dimensions and Geometry

The laboratory model with stationary rotor is shown in figure 2.6. That model has been used to investigate the effects on core back leakage flux distribution due to different machine dimensions and geometry. The stator has a diamond winding with diameter equal to 265mm,

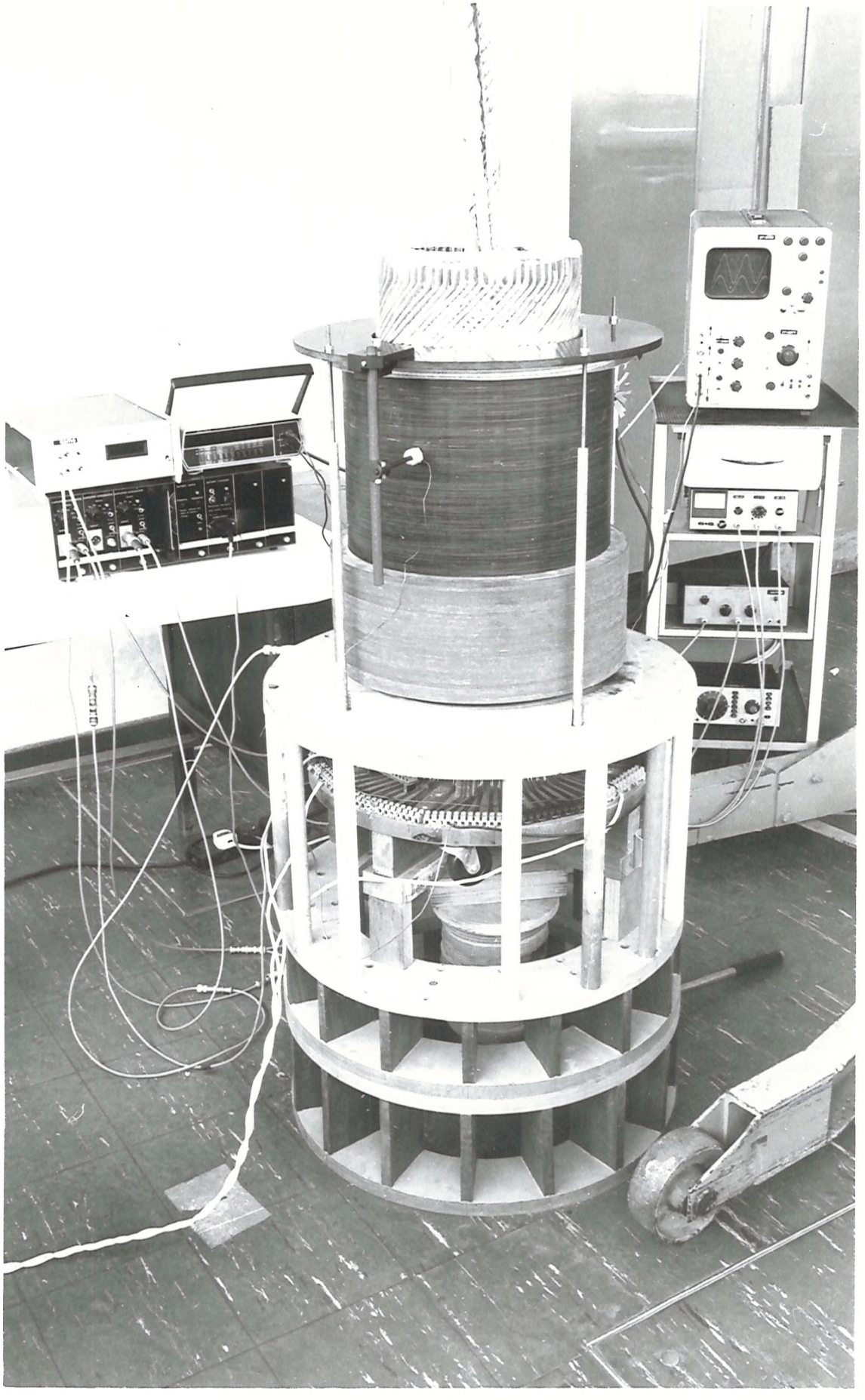

Fig. 2.6: Laboratory model with stationary rotor.

straight part 300mm long and an end winding length equal to 140mm. The stator winding has been excited by a balanced three-phase system obtained from the mains. A constant 6A phase current has been fed to the stator winding.

The stator core was built up from steel laminations 0.5mm thick, insulated with varnish and clamped together in a randomised way. The clamping system was such that a uniform stacking factor has been guaranteed. In order to analyse the effects of the core depth on the core back leakage flux, both the 45mm and 70mm depth laminations were used. The rotor core was also laminated and built up from steel laminations 0.5mm thick. Two different rotor bodies were utilised one had a diameter equal to 140mm and the other one a diameter equal to 225mm. These two rotors allowed us to introduce two different air gap lengths.

The model has been constructed in such a way that it was possible to vary the relative positions between the stator winding, stator and rotor cores. The stator core laminations rested on a wooden platform at a fixed position. The rotor core was held by a crane and the stator winding body was leaning on a jack. Both the crane and the jack allowed us to vary in an independent way the positions of the rotor core and the stator winding respectively. Those arrangements are shown in figure 2.6. The mechanical auxiliary equipments have been positioned in such a way that their conducting parts were far enough from the model in order to avoid interference on the measurements.

To investigate the eddy current effects on the core back leakage flux distribution the supply was provided by a group of three 3kW solid-state amplifiers, type 3000 WT (Derritron). The oscillator units enabled us to supply a sinusoidal waveform with a variable

frequency. The frequency could be varied from 1.5Hz to 22kHz. The variable frequency test was carried out with a constant stator winding current. Because of voltage limitations the maximum current was 1A. When the frequency was varied the stator winding voltage needed to be readjusted in order to maintain a constant phase current. Increasing the frequency, the voltage needed to be increased in order to maintain a constant phase current. That happens due to the variation on the stator winding inductance caused by the variation of frequency. The maximum values of the stator winding voltage with a fixed current was determined by the maximum power supplied by the 3kW solid-state amplifiers. Two copper screening plates 6mm thick were used to increase the effects of the eddy currents. They were 45mm and 70mm deep respectively.

The stator core laminations have been aligned, in a special arrangement, in order to investigate the effects of aligned rolling directions on the distribution of the core back leakage flux.

The measurements carried out on the laboratory model with stationary rotor were under unsaturated conditions since the field produced in the air gap was small. That model permitted us to investigate the effects on the core back leakage flux distribution caused by the:

- overhang
- relative position between both the stator and rotor cores
- air gap length
- stator core depth
- screening plates
- laminations rolling direction
- eddy currents
- stator winding current.

The effects of the presence of the iron on the magnetic field produced by the stator winding can also be shown.

In this model the leakage flux at the core back has been measured both in amplitude and phase since the signals had negligible harmonics.

When measuring the leakage flux distribution the stator winding current phase was maintained constant. Therefore, for the different arrangements done, the stator voltage needed to be carefully readjusted in order to compensate the variation on the inductance for each particular case.

2.2.3 Leakage Flux Measurements by Means of Search Coils[47]

Different kinds of search coils were used to measure the stator core back leakage flux components at the air region and the axial leakage flux inside the stator core. For the case of the core back leakage flux the following search coils were used: pancake, three-dimensional system and cylindrical, for the axial leakage flux inside the core printed search coils inserted in the stator core between laminations (figures 2.8).

The pancake search coil consists of 30 turns of 46 SWG enamelled wire, encapsulated in araldite, multi-layer, with a small thickness of 0.08mm, having an external diameter of 9.2mm. The three-dimensional system was composed of three individual search coils, each one having 10 turns of 44 SWG enamelled wire. Each individual search coil is located at one plane in a three-dimensional orthogonal system with a common centre point, multi-layer, with an external diameter of 12mm, mounted in a unique rod. The cylindrical search coil consists of 3780 turns of 42 SWG, wound as a multi-layer solenoid, having a cylindrical form with 15mm high and 19mm of basis diameter. The printed

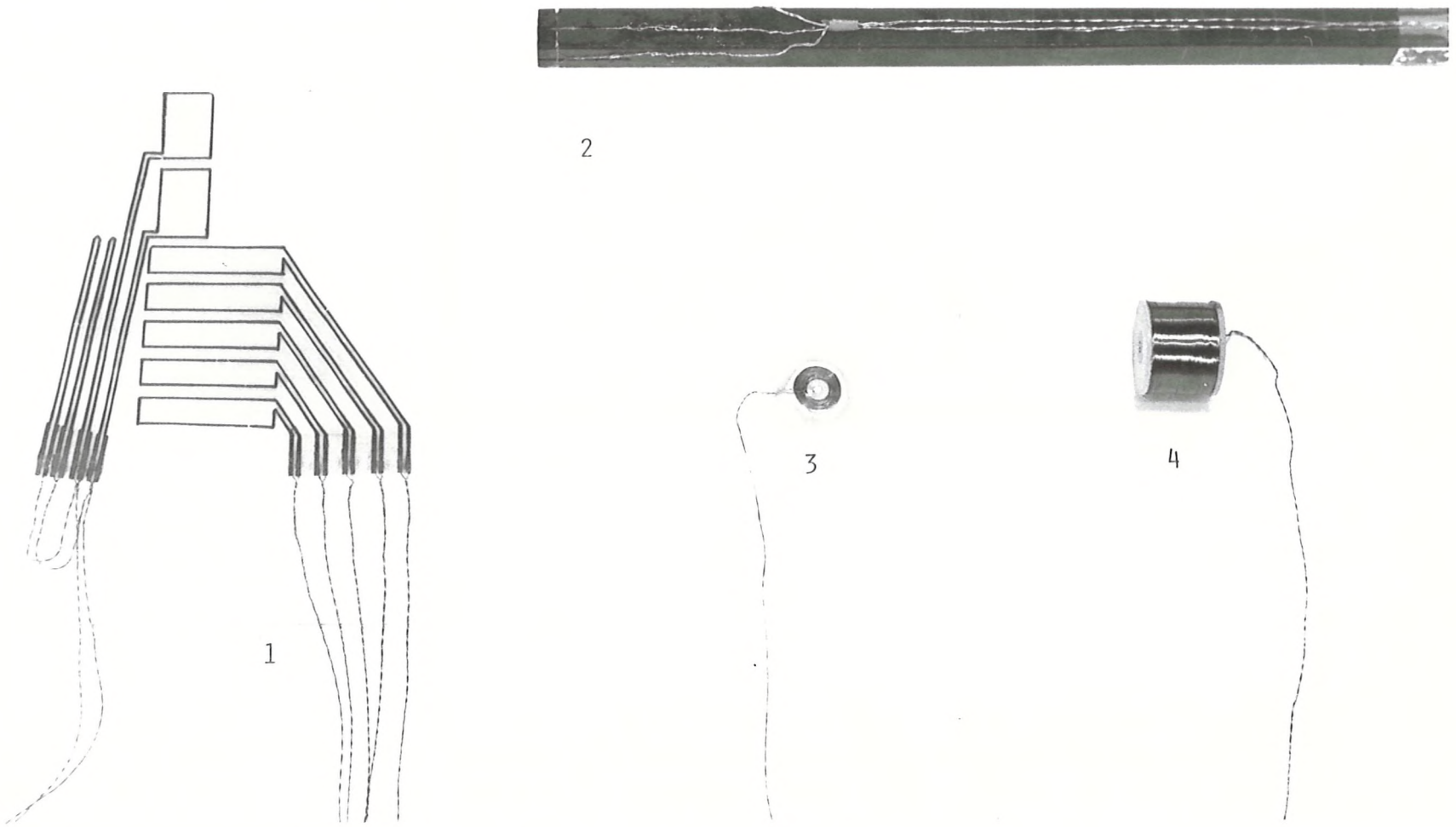

Fig. 2.8: Search coils: Printed (1) three-dimensional system (2), pancake (3) and chyindrical (4).

search coil has a square form, with an area equal to $1.5 \times 10^2 mm^2$, and has a small thickness to avoid undesirable disturbance in the inter-lamination gap. The printed search coils were distributed in the laminations as shown in figure 2.8.

The advantage of the pancake search coil lies in the fact that it has a small diameter and it is thin enough to be put close to any surface and has a reasonable signal. The three-dimensional system has the advantage of easing the simultaneous measurements of the three components of the leakage flux and assures the orthogonality between the three search coils planes. However, this system is relatively insensitive, giving a relatively small signal. The cylindrical search coil gives a large signal far greater than the others, but has bigger dimensions. This search coil measures the field component crossing axially at its centre.

It is important to use search coils having the minimum area possible since it is desirable to measure local leakage flux density at various points in the core back in order to establish the more troublesome sites. Actually when a flux is measured using a search coil the average value of the fluxes crossing its area is obtained. Therefore, if the search coil has a large area it can camouflage some considerable information about local values because it gives the average value. Of course, technologically the search coil area is limited by the necessity of having signals good enough to assure that its level is much bigger than any noise level that could distort the results.

There is a necessity of ensuring that each search coil is positioned correctly, i.e. each one needs to have its main plane perpendicular to the flux lines of the desired leakage flux component. If that does not happen the measurements can be influenced by another

component not under consideration. This can be minimised by a well designed mechanical arrangement.

The search coils were calibrated in order to identify accurately the leakage flux in each region considered. An experimental relationship between the RMS value of the search coil terminal voltage and the inducing flux has been established for each search coil in order to assure a more accurate measurement of the absolute value of the leakage flux. Only in the case of the printed search coils has this relationship been determined theoretically since it was the easiest way, considering its simpler configuration.

The RMS values of the voltages of the signals obtained from the search coil terminals were measured after both a convenient amplification and filtering in a range of frequency 1 to 1kHz. Both operational amplifier integrator and a differential high gain amplifier were used. Both the leakage flux components and its corresponding voltage waveforms were observed on an oscilloscope. Some leakage flux components signals were tape recorded and fed into a computer in order to get the Fourier analysis. To avoid the distorting effects of stray pick-ups the search coils were twisted, which has proved to be effective.

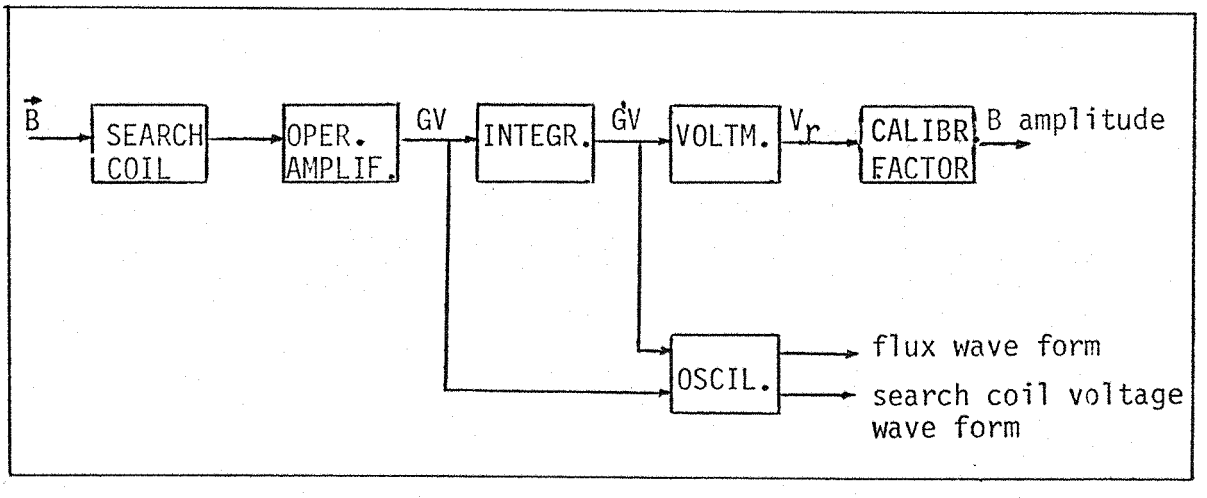

Fig.2.7: Measurement diagram

2.2.4 Coordinate Reference System

The cylindrical coordinate system (r, z, θ) was used for both the synchronous machine and the model with stationary rotor. The cylindrical coordinate system is located at the centre of the stator core back surface, as shown in figure 2.9. In the case of the model with stationary rotor, the smaller stator core back surface has been chosen.

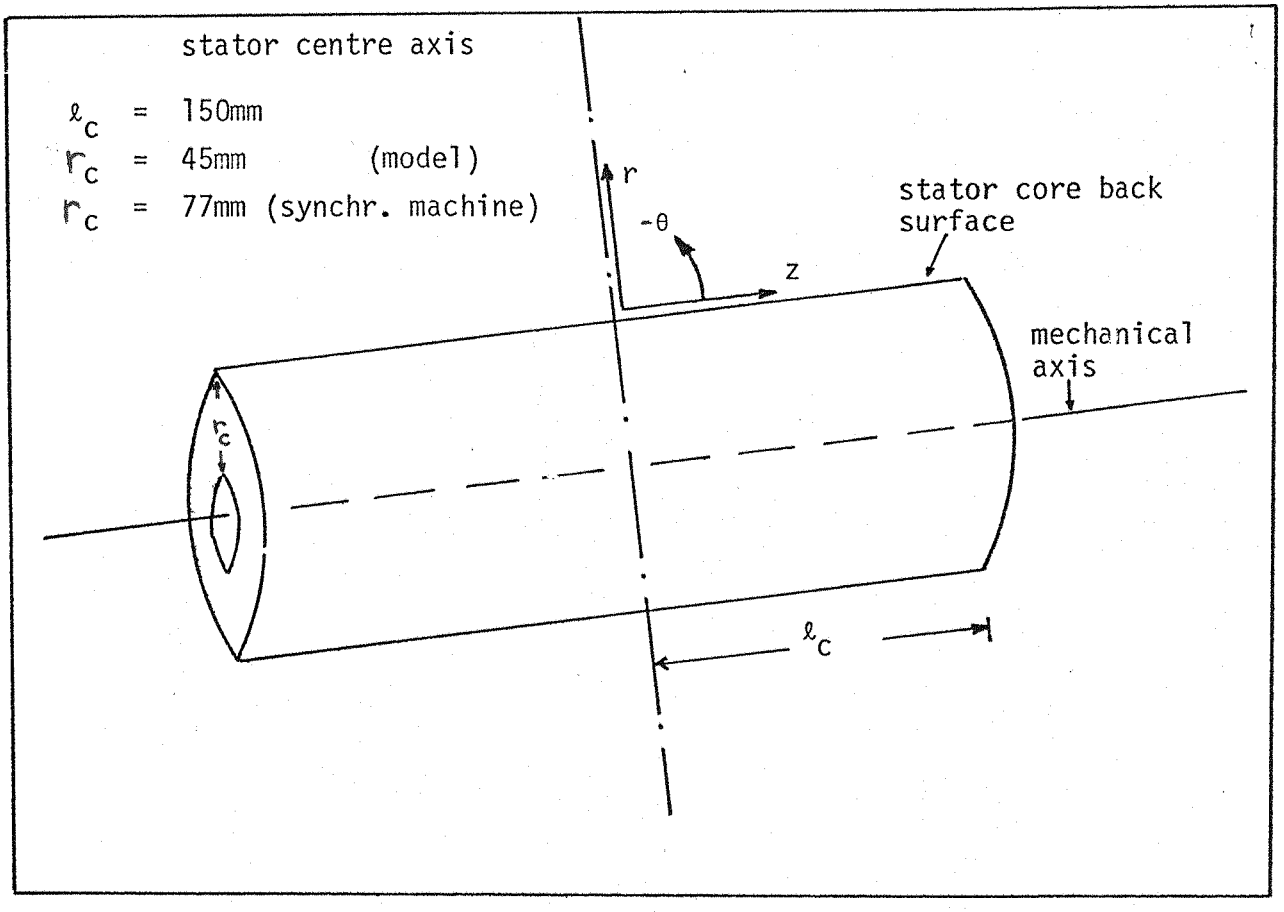

Fig. 2.9: The reference cylindrical co-ordinate system.

CHAPTER THREE

ELECTROMAGNETIC SOURCES OF STATOR CORE BACK LEAKAGE FLUX

3.1 DESCRIPTION

The stator core back leakage flux can be analysed and calculated by means of its electromagnetic sources.[19,46,48,49] These sources consist of magnetic polarity and conduction currents. The magnetic polarity sources are chiefly located on iron surfaces in the machine body and the conduction current sources are established by currents flowing in the conducting materials. Both of these types of source can be classified either as implicit or explicit sources.

The explicit sources are the distributed currents in both the stator and rotor windings which can be calculated from the machine rating and dimensions. If there are permanent magnets of known polarity in the device these would also be explicit sources.

The implicit sources depend on the explicit sources and on each other. They consist of polarity on soft magnetic materials[50-53] and of eddy currents[54-56] in conducting materials. In a synchronous machine all of the magnetic sources are implicit as well as the eddy current sources. It means that most of the sources are mutually related.

The method of the sources has been used by Tavner[49] to calculate the axial leakage flux penetrating the stator core front. The advantage of this method is that it makes it possible to analyse the leakage flux behaviour in terms of its individual causes. Therefore the first step is to recognise and to separate the various possible sources according to their relative importance. Once the sources have been surveyed it is possible to isolate the most troublesome ones in

order to minimise their undesirable effects.

To calculate the strength of the sources it is necessary to know the machine construction and the excitation currents. The distance between the source and the region where the leakage flux is under observation is relevant to the contribution of each source to the total leakage flux. The influence of elements of magnetic surface polarity and of current elements decreases with the square of the distance.[57-60] The closer the source to a considered region the more important is its contribution to the leakage flux at that region. Therefore a particular source can be considered negligible relatively to one specific problem but can be of great importance for another one. Local effects are generally due to local sources.

The total leakage flux at the stator core back of synchronous machines is obtained by the vector sum of the effects of the individual sources. The sources can be divided into main and secondary (smaller) ones. The main sources are shown in figure 3.1 and can be listed as follows:

- overhang currents (H_4)
- bore polarity (H_3)
- polarity on disc surfaces at core front (H_2)
- polarity on back of core (H_1).

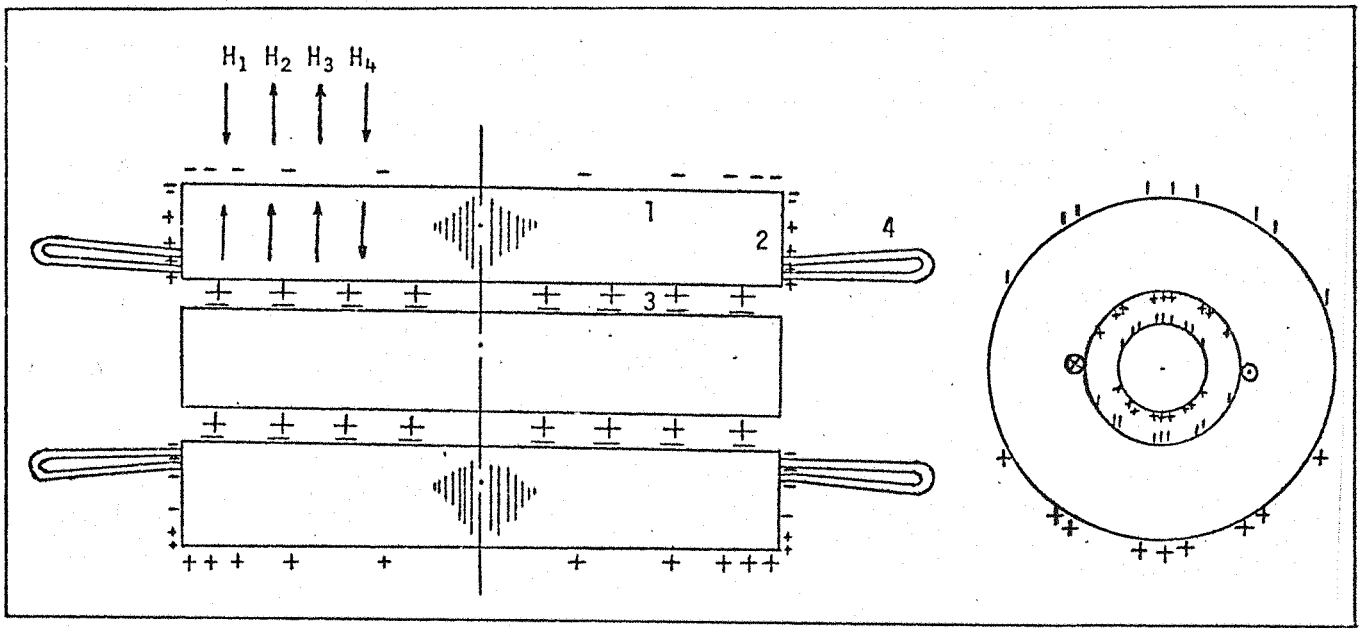

Fig. 3.1: The main electromagnetic sources of stator core back leakage flux

The secondary sources generally present a small contribution to the stator core back leakage flux. Their effects on the leakage flux distribution are localised ones. Some of the secondary sources can be listed as follows:

- volume polarity in the stator core interior
- polarity on building bars
- polarity on cooling duct surfaces
- eddy currents in the plane of the laminations
- eddy currents in the back of the laminations
- eddy currents in the end plates
- eddy currents in the screening plates
- eddy currents in the building bars.

3.2 OVERHANG CURRENTS

3.2.1 Considerations on Design Particularities

The winding overhang is defined as the part of the winding that is not used to induce useful electromagnetic force, in other words it is that part of the winding which is not surrounded by the machine active iron. The overhang shape varies according to the design of a particular machine. The most common stator winding designs used in electrical machines are: concentric, diamond, conical and helical, as shown in figure 3.2. The rotor winding shape predominantly observed in large machines is of concentric geometry.

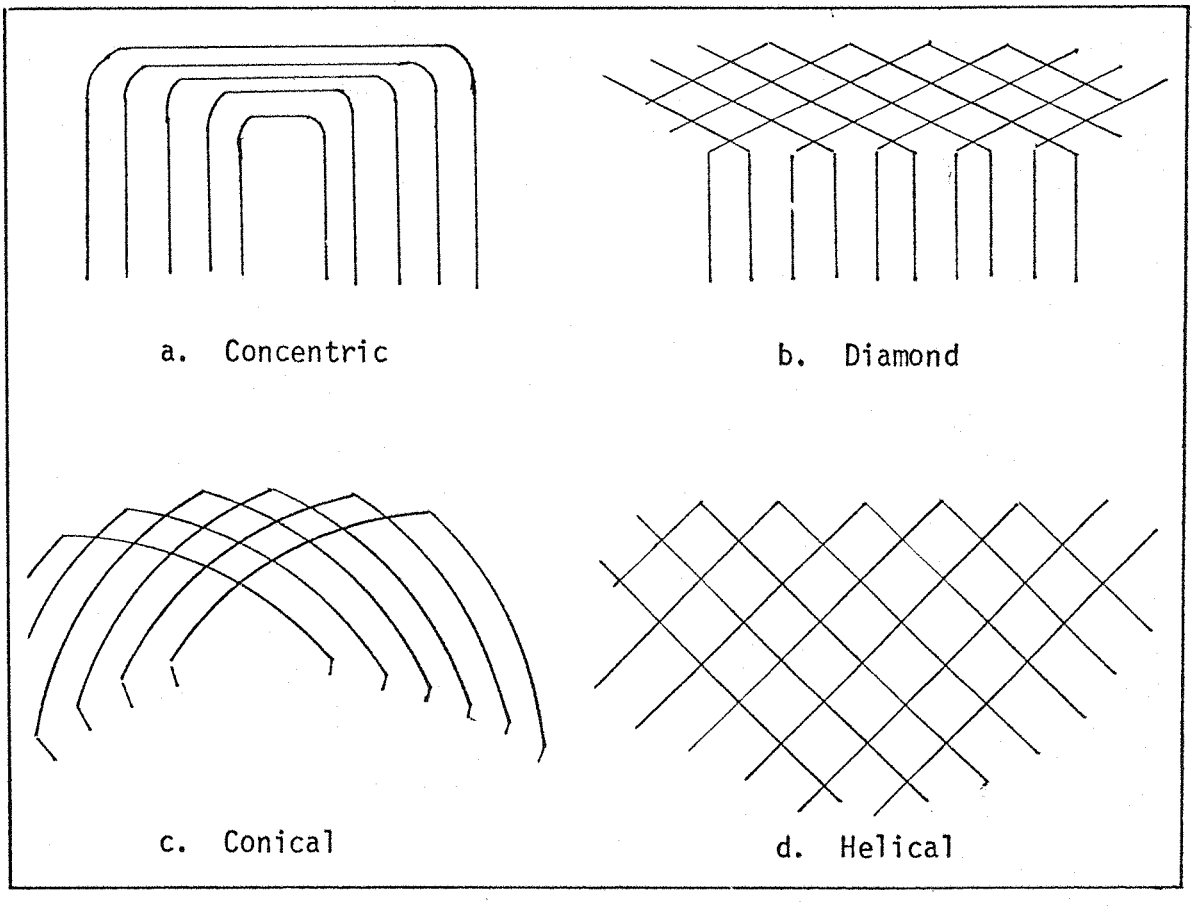

Fig. 3.2: Different shapes of winding

The overhang in the common synchronous machines is composed of the end winding section and the straight part of the winding that

is outside the active iron body. The helical winding has no straight part. In most of the literature presented in this subject there is no emphasis in the distinction between the overhang and the end winding. Actually the end winding is the part of the overhang that has the responsibility of transferring the excitation current from one side to another side of the conductors. There is a large number of end windings, directly related to the number of conductors. Generally the end winding length is much greater than the length of the non-active straight part, although it is much smaller than the active straight part of the winding. In superconducting generators the stator winding has no[61-63] straight part and the end winding coincides with the overhang. But it is still valid that either the end winding or the overhang length is much smaller than the active length of the stator winding. There may, however, be two different points of view among the electrical machine researchers with respect to the helical end winding specification. One view is based on the idea that the whole helical winding should be considered as end winding being a particular case of diamond winding with no straight part. The other point of view is that the stator winding has no end winding. All these implifications are brought about in order to simplify the mathematical treatment of the field established by the overhang. In any of the windings the end winding nose is generally very small and is located at a distant position from the stator core.

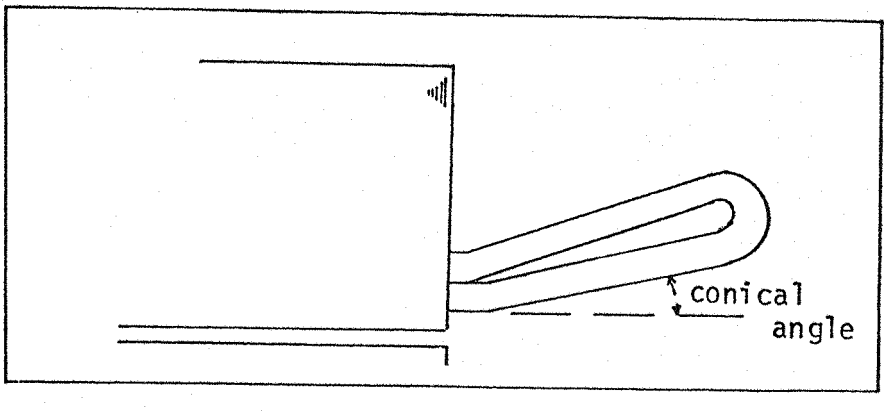

Fig. 3.2: A typical stator winding overhang

3.2.2 Overhang Effects on the Leakage Flux

When either the concentric, the diamond or the conical winding is used there is a sudden change on the excitation current path from the winding active part to the overhang zone. On the other hand the helical winding provides a gradual and smooth transformation between the active length and the overhang part of the winding. This can be an important point in favour of the helical winding since it avoids the presence of an acute step in the winding configuration at the ends of the stator core. This advantageous condition is not presented by the other windings. Mainly in terms of external leakage flux distribution close to the stator core this property of the helical winding can minimize the leakage flux effects. It is due to the fact that the excitation current path is not going to be dramatically changed at the core end zone when helical winding is present. However, the conventional windings present a much smaller axial field along their active length.[20]

The contribution of the overhang source to the leakage flux at the stator core back depends very much on both its shape and geometry as well as on excitation current. The increase in the excitation current due to the constant increase in the generator ratings has been determined a more salient effect of the overhang on the leakage flux distribution.

The relative position between the overhang and the stator core front surface plays an important rule in the determination of the overhang participation on the distribution of leakage flux. It is also important the relative position between the overhang and the stator core back surface. Both the core front and the back surfaces are determined by the stator length and its inner and outer radii.

To identify the winding overhang position it is necessary to

pay special attention to the winding shape and particularly to the winding parameters such as: cone angle, chording angle and length of the overhang. It is also necessary to emphasise the overhang component parts, specifying separately the length of both the end winding and the non-active straight part when a conventional winding is used.

Ashworth and Hammond[13] and Lawrenson[21] have studied the effects of the winding parameters on the field produced by the overhang at the stator core front. The cone angle of the stator winding can modify the distribution of leakage flux. The utilisation of a smaller cone angle can decrease the axial leakage flux at the stator core front. The radial component is increased close to the bore region and decreased at the core back region when the cone angle is decreased.[13,16,21] This is expected that bigger cone angles can have an increased effect on the stator core back leakage flux. That is intuitively explained by the fact that when bigger cone angles are used the overhang body is closer to the core back surface causing a more accentuated effect.

Therefore it is general practice to adopt small cone angles since their effectiveness in diminishing the loss in the core clamping plates has also been proved.[16] However, the reduction of the cone angle is mainly controlled by the length of the mechanical axis of the generator which is desirable to be made as short as possible for mechanical reasons. It is also controlled by the electric insulations requirements.

The cone angle of one winding is equal to zero when this winding can be wrapped by a cylinder envelope. In most of the present day synchronous machines it does not happen and the normal cone angle is about thirty degrees.[21] The superconducting generators are expected to have a stator helical winding which has a zero cone angle. That is so due to the fact that it is desirable to construct the stator winding

as an independent body that can be inserted later on the core bore. It is also desirable to maintain the stator winding surface as close as possible to the stator core inner surface in order to obtain an air gap as small as possible. Actually the surfaces of both the active and the overhang parts of the helical winding are maintained parallel to both the stator core and the rotor surfaces.

The chording angle is dependent on the pole pitch and as a general rule is made smaller than a pole pitch. The conventional synchronous generators use the fractional or short chording pitch. The arrangements on the chording angle help to minimise the effects of the harmonics and make the losses smaller.[4,15,64]

The length of the non-active straight part can also modify the leakage flux distribution at the core back.[21] Actually the core back leakage flux can be increased when longer non-active straight parts are present. Both the radial and circumferential components of the overhang field are increased close to the stator core when the non-active straight part has a longer length. The winding nose has a negligible effect on the core back leakage flux. It is explained by its small size and because of its relative distant position from the core surfaces.

The total length of the overhang also has an interference on the core back leakage flux distribution. The longer the overhang total length, the bigger is its effect on the core back leakage flux. The effects of the overhang length on the leakage flux distribution at the stator core have also been pointed out by Tavner et al.[20] The increased amount of core back leakage flux due to longer overhangs is explained by the greater spreading of leakage flux path. The longer path produced by the longer overhangs makes it possible that a greater amount of leakage flux links the stator core back surface.

3.3 BORE POLARITY

The bore polarity is located on the iron surfaces of the air gap region of the synchronous machines. The bore polarity is originated by the main field in the air gap which magnetises both the inner stator surface and the outer surface of the rotor body. Since the air gap field necessarily penetrates one surface after it has left the other, both surfaces are magnetised in the opposite way when a fixedradial direction is considered. The intensity of magnetisation is the same for both surfaces in small air gaps. That therefore means that both the inner surface of the stator core and the outer surface of the rotor body form a concentric cylindrical double layer of magnetic pole distribution. The bore polarity can be represented by a concentric cylindrical magnetic dipole distribution as presented in figure 3.4.

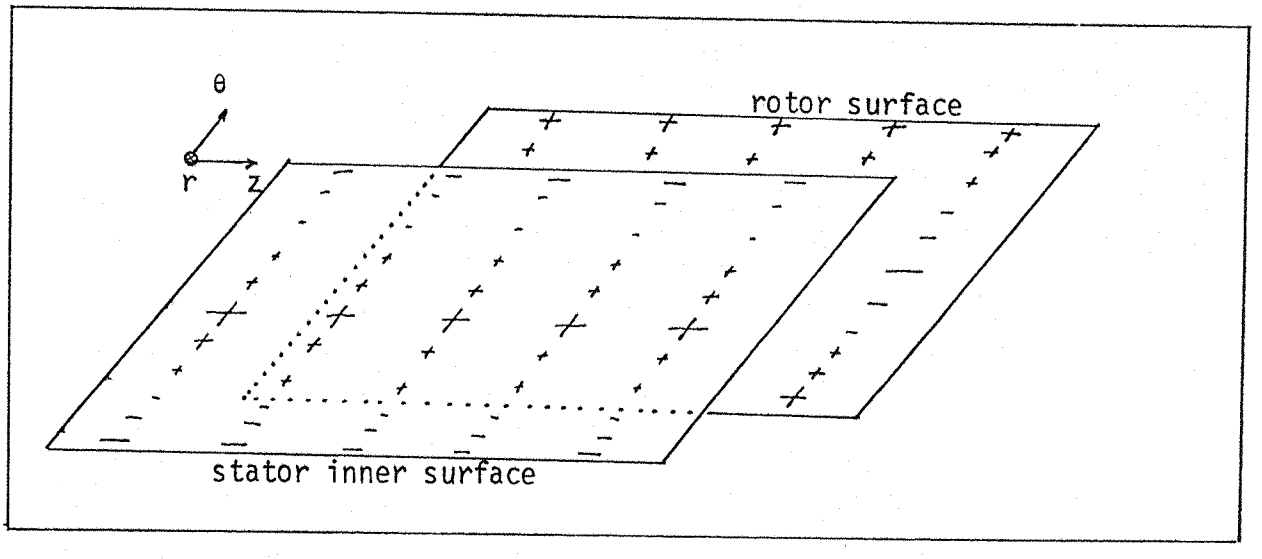

Fig. 3.4: Development of the bore polarity surface

The mathematical relationship between a single surface polarity at the bore and the radial component of the air gap flux is given by[50,51]

$$\frac{\uparrow H_{r_i} \quad \text{iron}}{\uparrow H_{r_{ag}} \quad \text{air gap}} \quad \text{(iron/air interface)}$$

$$n.(H_i - H_{ag}) = \frac{p^*}{\mu_o} \tag{3.1}$$

but we have

$$n.H_i = H_{r_i}$$

$$n.H_{ag} = H_{r_{ag}}$$

$$H_{r_i} = \frac{1}{\mu_o \mu_r} B_{r_i}$$

$$H_{r_{ag}} = \frac{1}{\mu_o} B_{r_{ag}}$$

Therefore equation (3.1) becomes

$$\frac{1}{\mu_r} B_{r_i} - B_{r_{ag}} = p^* \tag{3.2}$$

But the normal component of the magnetic flux density is continuous at the stator bore surfaces.

$$B_{r_i} = B_{r_{ag}} = B_r$$

Therefore equation (3.2) becomes

$$B_r \left(1 - \frac{1}{\mu_r} \right) = p^* \tag{3.3}$$

For usual stator cores with high permeability equation (3.3) can be written as

$$B_r \simeq p^*.$$

The bore polarity is an implicit source, therefore its distribution along the air gap depends on both the synchronous machine geometry and the excitation currents. The air gap dimension plays an important rule in the determination of the bore polarity. The smaller the air gap, the bigger the bore polarity strength for a constant excitation current. The bore polarity is also increased with the

increase in the excitation current for a given air gap.

The contribution of the bore polarity to the leakage flux at the stator core back is greatly dependent on the ratio between the machine bore and the stator core back radii. The deeper the stator core the smaller are the effects of the bore polarity on the core back leakage flux. Actually it could be explained by the fact that the stator core back region is taken away from the bore polarity source when deeper cores are present. That is always important to bear in mind that the bore polarity, being a magnetic source, has its effects weakened when more distant places are considered.

The bore polarity source in synchronous machines is a function of both time and space.[4,64,65] This is a sinusoidal function of the time since the synchronous machine has a magnetising air gap field which varies sinusoidally in time. The spatial variation of bore polarity in synchronous machines can be considered in two different directions: axial and circumferential. Therefore it becomes very important to have available the main field's spatial distribution. In most of the synchronous machines the air gap field is constant in the axial direction. Special considerations apply in the end region of the air gap where the main field is affected by the presence of the end windings and special mechanical arrangements. The magnetic pole concentration at the bore end regions is diminished by specially shaping the stator core corners.[66] If the corners are made either by steps or with a round shape, the magnetic surface polarity at the bore ends presents a smaller intensity. The different types of end windings produce different effects in the distribution of the bore polarity at the end region of the air gap. The bore polarity varies sinusoidally in the circumferential direction and depends on the number of poles. The pole pitch determines the bore polarity pitch in such a way that

the number of pairs of poles is equal to the number of pairs of magnetic pole distribution at both the inner surface of the stator and the rotor surface.

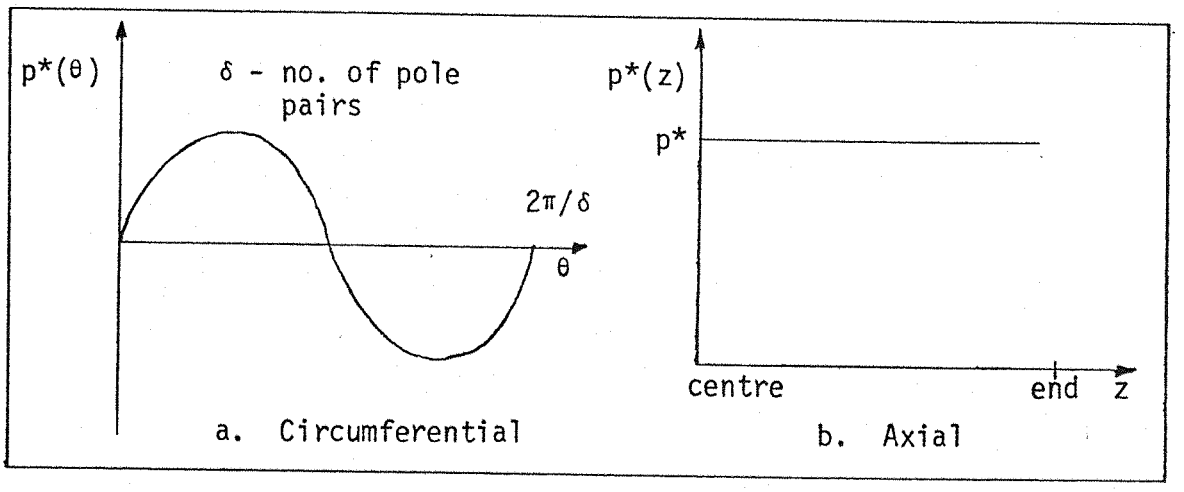

Fig. 3.5: Intensity of the core bore surface polarity

The superconducting synchronous machine has a stator helical winding, therefore a different distribution of bore surface polarity is expected in the axial direction.[63] That is imposed by the fact that the radial magnetising field varies when a fixed axial direction is considered. The distribution of core bore surface polarity along the axial direction is shown in figure 3.6. The bore polarity still presents a sinusoidal variation against the circumferential direction.

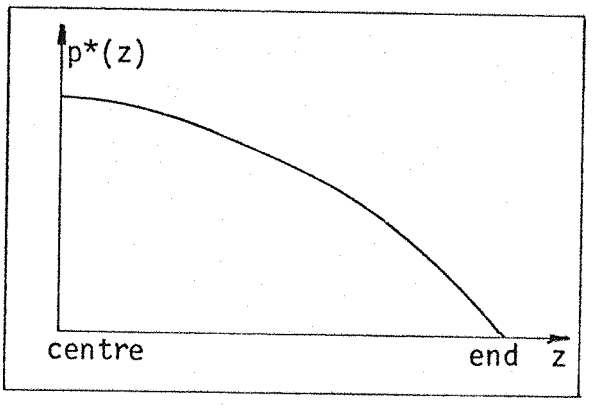

Fig. 3.6: Axial variation of the core bore surface polarity due to presence of helical winding

The distribution of surface polarity at the stator core bore varies with the different types of operations: on load and open and short circuits. When the synchronous machine is operating on short circuit there is practically no core bore surface polarity.[38] That negligible bore polarity is due to the existence of an air gap field waveform with a large harmonic content. Actually, if there were no harmonic in the air gap field it should be equal to zero. The open circuit operation presents a sinusoidal bore polarity distribution in the circumferential direction and a constant value of bore polarity intensity along a fixed axial direction. The same happens with the bore polarity distribution when the synchronous machine is on load condition. Although when the axial direction is under consideration it is always necessary to bear in mind the existence of the end regions. On load operation it is necessary to pay special attention to the power factor. The magnetic polarity intensity at the stator bore varies with the synchronous machine power factor. A leading power factor produces an increased leakage flux effect.

3.4 POLARITY ON DISC SURFACES AT CORE FRONT

The polarity on disc surfaces at the core front is located in the external surface of the stator core end region. This surface polarity is also an implicit source since it rests at the surface of a soft magnetic material.[49-52] Therefore the surface polarity on disc at the core front is dependent on both the geometry and size of the synchronous machines as well as on the excitation currents. This surface polarity is intimately related to the flux penetrating[49] perpendicularly the stator core front. It is necessary to establish the distribution of the axial leakage flux in both the circumferential and the radial directions at the core front in order to determine the

polarity on disc surfaces. The mathematical demonstration of the equality between the core front pole distribution and the axial leakage flux is the same as shown in section 3.3. It is just necessary to substitute the radial component of the main flux by the axial component of the leakage flux and consider the magnetic poles at the core front.

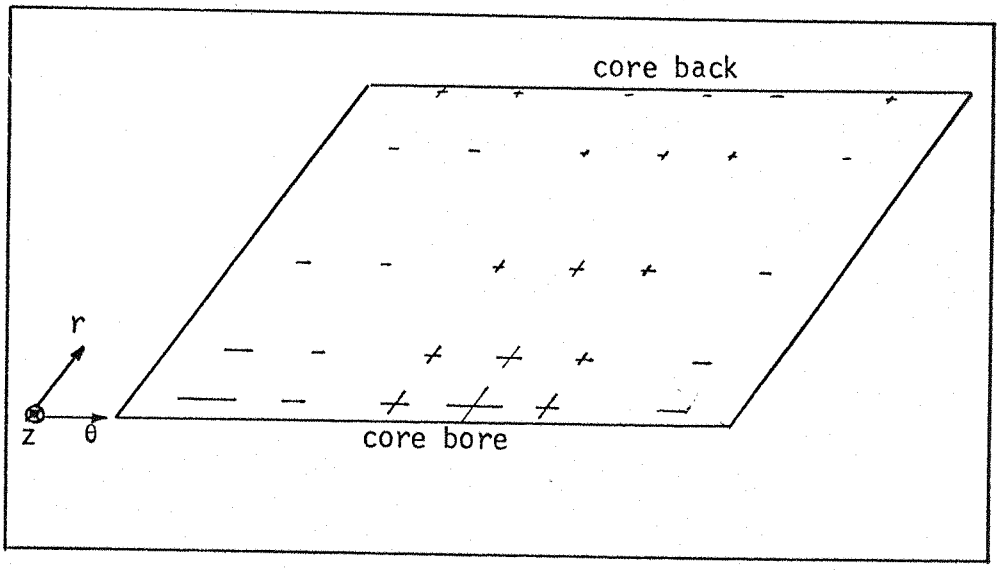

Fig. 3.7· Development of the polarity on disc surfaces at core front

The core front polarity is smaller than the bore polarity due to the different magnetising fields causing each one respectively. The magnetising field at the bore polarity is much bigger than the polarity on disc surfaces at the core front since the first one is placed in the air region where the largest field is produced. Actually it is desirable, in the synchronous machine, to have a bore surface polarity as big as possible while the polarity on disc surfaces at the core front is required to be as small as possible. The bigger the intensities of the polarity at the core front surface, the more troublesome are the effects brought about at the end regions of synchronous machines. The increased intensities produce an increased heating effect at the core ends that can lead to undesirable hot spots.

The disc surface polarity at the core front is bigger than the stator core back surface polarity. The magnetic pole distribution at the stator core front presents a significant interference on the stator core back leakage flux distribution. That interference is more accentuated at the end zones of the stator core back. Actually the interference is dependent on the ratio between both the inner and the outer stator radii as well as on its length. At deeper stator cores the polarity on disc surfaces has an increased effect on the core back leakage flux distribution. The effects of the polarity on disc surfaces are less accentuated when longer stator cores are used. Actually in both cases the effects are greatly concentrated at the end zones of the core back. Therefore it can be noticed that the distribution of leakage flux at the core back is also dependent on both the intensity of the magnetisation and the area where the magnetic poles are spread at the core front.

The magnetisation of the core front surface in the synchronous machines is made smaller by the existence of laminated core with high permeability laminations. It would be much greater if the core was not built up of laminations. The axial permeability of the stator core plays an important part in the intensity of the disc surface polarity at the core front. If the permeability is constant all over the magnetic core the polarity is distributed just at its surfaces. That is not the case of the real synchronous machine. In a real machine the effective axial permeability of a compact core is substituted by an equivalent volume permeability having a much smaller value. It is much smaller due to the presence of non-conductive gaps between adjacent laminations. The axial permeability of a laminated stator core is given as a function of the stacking factor (γ) and the relative permeability of the laminations (μ_r) by the expression below:[10]

$$\mu_z = \frac{\mu_r}{\mu_r - \gamma(\mu_r - 1)}$$

Therefore both the core stacking factor and the lamination permeability can modify the magnetisation of the core front surface. The smaller the core stacking factor, decreased is the intensity of the disc surface polarity at the core front.

An external way to vary the core front surface polarity is by fitting conducting screening plates. The screening plates are generally made of either copper or aluminium. These good conducting plates have the responsibility of turning the magnetising field obstructing its penetration in the core front. Actually an ideal screening plate at the core front diverts the field from the axial to the radial direction making it parallel to the plane of the laminations. That effect can be more effective if the screening plates are laminated.

The rolling direction of the laminations can determine regions of different permeability.[67] If the laminations are aligned the distribution of magnetic poles presents a non-smooth variation along the circumferential direction. The regions of the stator core front of small permeabilities are expected to be more intensively magnetised, therefore present higher surface polarity intensities.

The winding overhang is also essential to the distribution of surface polarity at the stator core front.[13,16,20,21] The surface polarity is reduced by reducing the cone angle of the winding. The cone angle can also determine the region where the surface polarity changes sign at the core front region. The smaller the cone angle, the more distant from the core bore occurs the change of polarity sign. Therefore, for the helical windings used in superconducting synchronous machines it is expected that the change of sign happens closer to the stator core back region.

3.5 SURFACE POLARITY ON THE STATOR CORE BACK

The surface polarity on the stator core back is intimately related to the radial leakage flux either entering or leaving the stator core back surface. The radial leakage flux at the stator core back is approximately equal to the pole strength at the core back surface if the permeability is high. It can be shown mathematically in the same way as the bore polarity in section 3.3.

The core back surface polarity makes a small contribution to the axial leakage flux distribution at the core front. This contribution is negligible at the region close to the core bore. On the other hand this surface polarity plays an important part in the determination of the leakage flux at the stator core back region.

The distribution of magnetic poles along the stator core back is not uniform. There is a higher concentration of magnetic poles at the end zone of the stator core back. This is explained by the fact that the end zones are under more intensive magnetising effects than the zones close to the centre of the generator. Actually the surface polarity intensity is a function of both the axial and circumferential directions as well as the time. In an ideal synchronous machine it varies sinusoidally with the time as well as with the circumferential position around the stator core back, and varies exponentially with the axial direction. Figure 3.8 considers the distribution of the surface polarity on the stator core back of a 2-pole synchronous machine.

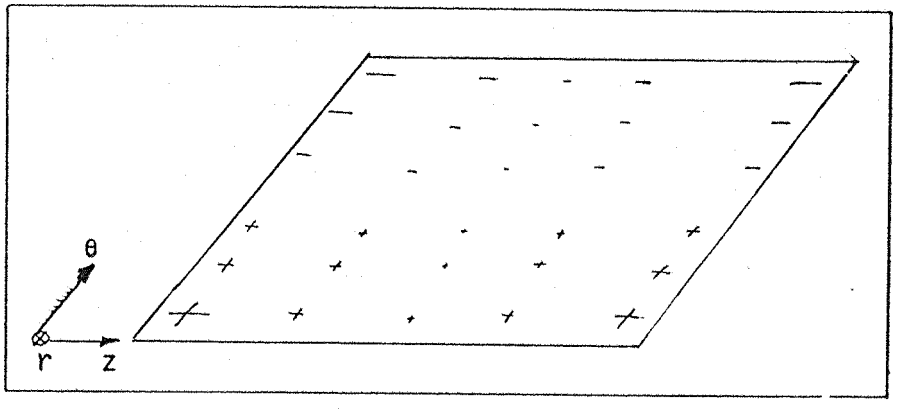

Fig. 3.8: Development of the surface polarity on the stator core back

The stator core back surface polarity is an even symmetrical distribution along the axial direction. The number of maxima and minima of the core back surface polarity at each instant depends on the number of poles of the synchronous machine. The values of the core back surface polarity decreases with the number of poles. The greater the number of poles, the smaller are the back polarity intensities. The greatest intensities of core back surface polarity are therefore present in a two pole synchronous machine.

The surface polarity at the core back varies with the machine geometry and dimensions and is increased with the enlarged excitation currents on the modern synchronous machines. The polarity on the back of the core has a predominant effect on the leakage flux at the stator core back. This effect is increased if the machine length is made great relative to the core diameter. Although at the end zones of the stator core back the other source effects are still present. For machines with a relatively large diameter compared with their length the surface polarity on the stator core back has a decreased effect on the distribution of the leakage flux.

The ratio between the axial and the transverse permeability of the stator core plays an important part on the evaluation of the core back leakage flux. The transverse permeability is dependent on the silicon steel permeability. The axial permeability is dependent on both the lamination permeability and on the interlaminar insulation gap. The greater the ratio between the transverse and the axial permeabilities, the smaller is the quantity of leakage flux that reaches the core back surface. It means a smaller surface polarity at the stator core back.

The stator core back surface polarity is increased by the presence of either aluminium or copper screening plates generally used at the core fronts of the synchronous machines. The screening plates

can divert the leakage flux from the core front surface to the back of the core. Actually these plates increase the radial component of the leakage flux, therefore producing a greater concentration of magnetic poles at the core back. Particularly at the end zones of the core back the surface polarity is largely increased by the action of the screening plates.

The saturation effects can also perturb the distribution of the surface polarity on the stator core back. These effects can increase the magnetisation of the core back surface producing therefore an increase in the core back leakage flux. This increase is more effective at the end zones of the core back, but the magnetisation effects propagate progressively to inner regions of the core back towards the centre of the stator.

The distribution of magnetic poles at the core back can be changed by the presence of radial ventilating ducts. These ducts can establish a higher concentration of magnetic poles in their surroundings. They can introduce crowded regions producing a variation of the surface polarity on the core back. A similar effect can be produced by the butt joints.[32-37] This effect can be attenuated by the utilisation of appropriate overlapping arrangements.

The overhang can also introduce a modification on the back of the core surface polarity.[18] A longer overhang causes a more intense value of surface polarity. The variation on the overhang length is mainly felt at the end zones of the core back. The variation of the cone angle of the overhang also changes the distribution of surface polarity on the core back. By increasing the cone angle the surface polarity is also increased. This can be explained by the fact that the magnetising field from the overhang is closer to the core back surface. When the overhang has longer straight parts it also[21]

produces an increment in the core back surface polarity. The longer the straight part, increased are both the radial and circumferential components of the field due to the overhang close to the stator core.

3.6 SECONDARY ELECTROMAGNETIC SOURCES

3.6.1 Volume Polarity

A volume of magnetic material can be magnetised by the action of a magnetic field that links its body. This magnetic field can establish two different kinds of magnetic pole distribution over the material. A spatial distribution of magnetic poles at the interior and a surface distribution on the outer surfaces. Therefore the field produced by that magnetic material can be composed of the sum of two different sources: the surface polarities and the volume polarity. The surface polarities have been previously discussed.

Hammond[51] has shown a mathematical calculation of the magnetic potential of a spatial distribution of magnetic poles departing from a simple dipole structure which is going to be outlined here.

$$V = k \left[\oint_S \frac{P^*.ds'}{r} - \iiint \frac{\nabla'.P^*}{r} dv' \right]$$

where

$$k = \frac{1}{4\pi\mu_o} .$$

But

$$H = -\nabla V.$$

Therefore

$$H = -\nabla k \left[\oint \frac{P^*.ds'}{r} - \iiint \frac{\nabla'.P^*}{r} dv' \right]$$

$$H = -k\nabla \left[\oint \frac{P^*.ds'}{r} - \iiint \frac{\nabla'.P^*}{r} dv' \right] \qquad (3.4)$$

where

$\oint\!\!\oint \frac{P^* ds'}{r}$ is the component of the magnetic field due to the magnetic surface polarities outside the magnetic material.

$\iiint \frac{\nabla' . P^*}{r} dv'$ is the contribution to the magnetic field due to the magnetic volume polarity inside the magnetic material.

Equation (3.4) presents both the surface and the volume polarities components. The dash (') indicates that the physical entity is related to the source coordinate system and not to the field coordinate system. The variations of the relative proportions of both components are dependent on both the mechanical and electromagnetic properties of the material, mainly the permeability and the geometry. In this section there is an interest in presenting the effects of the volume polarity on the stator core back leakage flux.

If an idealised solid magnetic material is considered the permeability would be constant all over its volume. Therefore the magnetic polarity would be totally distributed on its surfaces. But in a real synchronous machine the stator core is built up by laminations properly grouped which produce both volume and surface polarities. Therefore, although it is smaller than the surface polarities, the volume polarity is present in the stator core of a synchronous machine.

The existence of volume polarity is intimately related to the redistribution of axial leakage flux in the interior of the stator core.[16,19] Actually the volume polarity strength is dependent on the axial flux strength, permeability and the insulation gap between adjacent laminations. The permeability of the stator core varies from point to point and depends on saturation. Increased saturation

determines a smaller value of permeability. The insulation gap between adjacent laminations depends on the core pressure.[45,68] The bigger the interlaminar gap, increased is the volume polarity intensity. We have chosen to talk about interlaminar gaps instead of stacking factors because of the existence of non-uniform spacing between laminations. This irregular interlaminar gap can be caused by mechanical reasons as well as by radial ducts. When talking about stacking factors the localised effect caused by non-uniform interlaminar gaps can be masked because it is considered an average gap. Although both terms are closely related.

The mechanism of producing volume polarity is explained by the different intensity of magnetisation imposed by the axial leakage flux on the successive adjacent laminations. It is shown in figure 3.9.

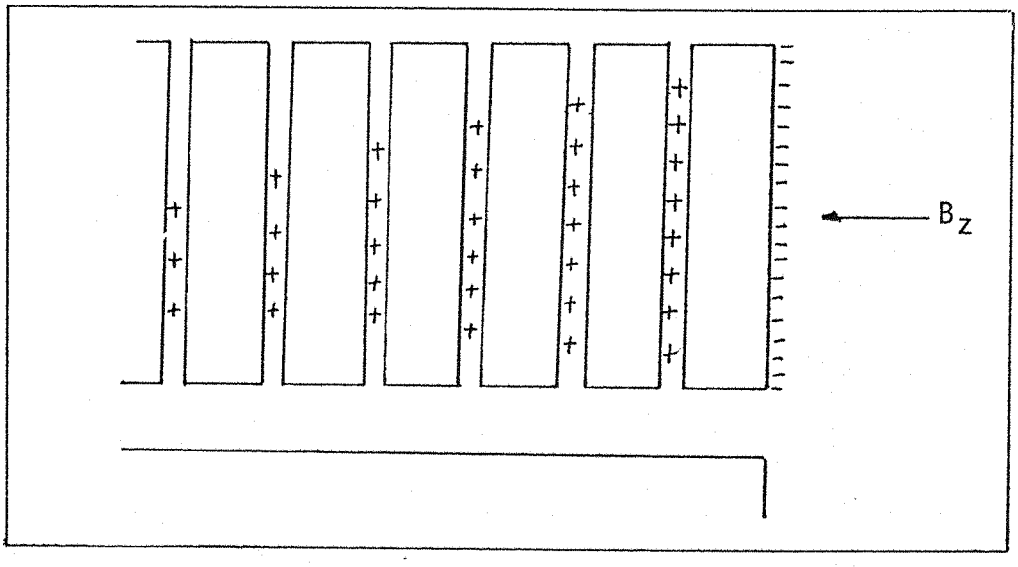

Fig. 3.9: Volume polarity in the stator core

When the axial flux is penetrating the successive layers of the synchronous machine stator core it has the possibility of diverting to two different directions. Part of the axial flux can be diverted either to circumferential or radial directions, while some can be maintained in the axial direction. Both the circumferential and radial

directions offer a path with a much larger permeability. Therefore once the axial leakage flux pierces the stator core it changes gradually to the direction of the plane of the laminations. This means that the different intensities of axial flux reach different layers of lamination. This originates a different level of magnetisation at the successive layers inside the stator core. The magnetic poles produced are distributed on the surface of the laminations since each lamination is a solid body. The group of surface distribution of magnetic poles in the interior of the stator core composes the volume polarity.

The volume polarity contributes a field in the axial direction that opposes the magnetising axial leakage flux that produces them. A more intensive axial leakage flux can establish a larger volume polarity and can produce a deeper volume polarity distribution inside the stator core. This effect can also be assisted by a decrease in the permeability. The dependence of the magnetic volume polarity on the permeability can be given mathematically. The magnetic field can be calculated by analogy with the electric field.[51] The electric field is associated with both the free charges and bound charges distribution. Actually the total charge distribution is given as the sum of both charges distribution ($\rho_{total} = \rho_{free} + \rho_{bound}$). But when considering the magnetic field, it cannot be associated with the part due to the free charges since there is no free magnetic poles in a magnetic material. Therefore in a magnetic material the total pole distribution is equal to the "bound" polarity distribution.

Electric material	Magnetic material
$\rho_{total} = \rho_{free} + \rho_{bound}$	$\rho^*_{total} = \rho^*_{bound} = \rho^*$ $(\rho^*_{free} = 0)$
$\rho_{total} = \varepsilon_0 \nabla . E$	$\rho^* = \mu_0 \nabla . H$

Electric material	Magnetic material
$\rho_{bound} = -\nabla.P$	$\rho^* = -\nabla.P^*$
$D = P + \varepsilon_0 E$	$B = P^* + \mu_0 H$
$D = \varepsilon_0 \varepsilon_R E$	$B = \mu_0 \mu_r H$
$\nabla.D = \rho_{free}$	$\nabla.B = 0$ (3.5)

Therefore, applying the divergence in the relationship (3.5)

$$\nabla.B = \nabla.(P^* + \mu_0 H)$$

$$0 = \nabla.P^* + \nabla.(\mu_0 H)$$

$$\nabla.(\mu_0 H) = -\nabla.P^*$$

$$\nabla.\left(\mu_0 \frac{B}{\mu_0 \mu_r}\right) = \rho^*$$

$$\nabla.\frac{B}{\mu_r} = \rho^*$$

$$\frac{1}{\mu_r}\nabla.B + B.\nabla\frac{1}{\mu_r} = \rho^*$$

$$B.\nabla\frac{1}{\mu_r} = \rho^*$$

When the permeability (μ_r) is constant, the divergence is zero, therefore the magnetic volume polarity is zero.

The distribution of the magnetic volume polarity has a higher concentration at the end regions of the stator core. Therefore the effects of that magnetic source on the leakage flux distribution is expected to be more effective at the core ends. The existence of radial ventilating ducts in the stator core can produce an increase in

the volume polarity around them. The radial ducts can introduce the volume polarity source to deeper regions at the stator core.

3.6.2 Eddy Currents

3.6.2.1 General

Any magnetic or non-magnetic conducting material crossed by a time varying field is subject to the effects of the induced eddy currents.[15,31,70] These effects are sometimes useful as in squirrel cage rotors of induction machines, induction furnaces, eddy currents brakes as well as in the solid body rotor of a synchronous machine providing either the starting torque or the damping effect depending on if it is operating as a motor or as a generator, respectively. They are undesirable in most electrical machines due to their contribution to core loss, distortion of the flux density and demagnetising effects.

The most common way used to diminish their troublesome effects is to construct laminated cores. The insulated laminations avoid the eddy current flowing in the axial direction of the stator core. Although both the radial and circumferential components of the eddy currents at the plane of the laminations are still present. These effects are dominant at the end regions of the stator core.

Eddy currents in a conducting material originate the skin effect phenomenon, whereby the crossing flux tends to crowd towards the surface region. Figure 3.10 shows the flux density distribution for different permeabilities, as well as for different lamination thickness.[71] The concentration of flux at the surface is dependent on electric, magnetic and mechanical properties of the laminations as well as on the crossing flux. Actually this concentration increases with the increase in electrical conductivity, magnetic permeability and thickness of the lamination. An increase in the frequency of the

crossing flux can also increase that concentration. This frequency is dictated by the main frequency in the case of a synchronous machine which is strictly constant.

In the case of the stator core of a synchronous machine it is necessary to consider two kinds of skin depth. Firstly the transverse skin depth which is dependent on the transverse permeability, and secondly the axial skin depth which is dependent on the axial permeability. Both depend on the same means frequency and the same lamination resistivity. Jacobs et al.[10] have suggested an axial permeability as a function of the core stacking factor and the relative permeability of the stator core lamination.

$$\delta_t = \left(\frac{1}{\pi f \partial \mu_o \mu_r} \right)^{\frac{1}{2}}$$

$$\delta_z = \left(\frac{1}{\pi f \partial \mu_o \mu_z} \right)^{\frac{1}{2}}$$

$$\mu_z = \frac{\mu_r}{\mu_r - \gamma(\mu_r - 1)}$$

δ_r - transverse skin depth

f - frequency

∂ - conductivity of the lamination

μ_o - permeability of the air

μ_r - relative permeability of the lamination (transverse)

μ_z - axial permeability of the stator core

γ - stacking factor.

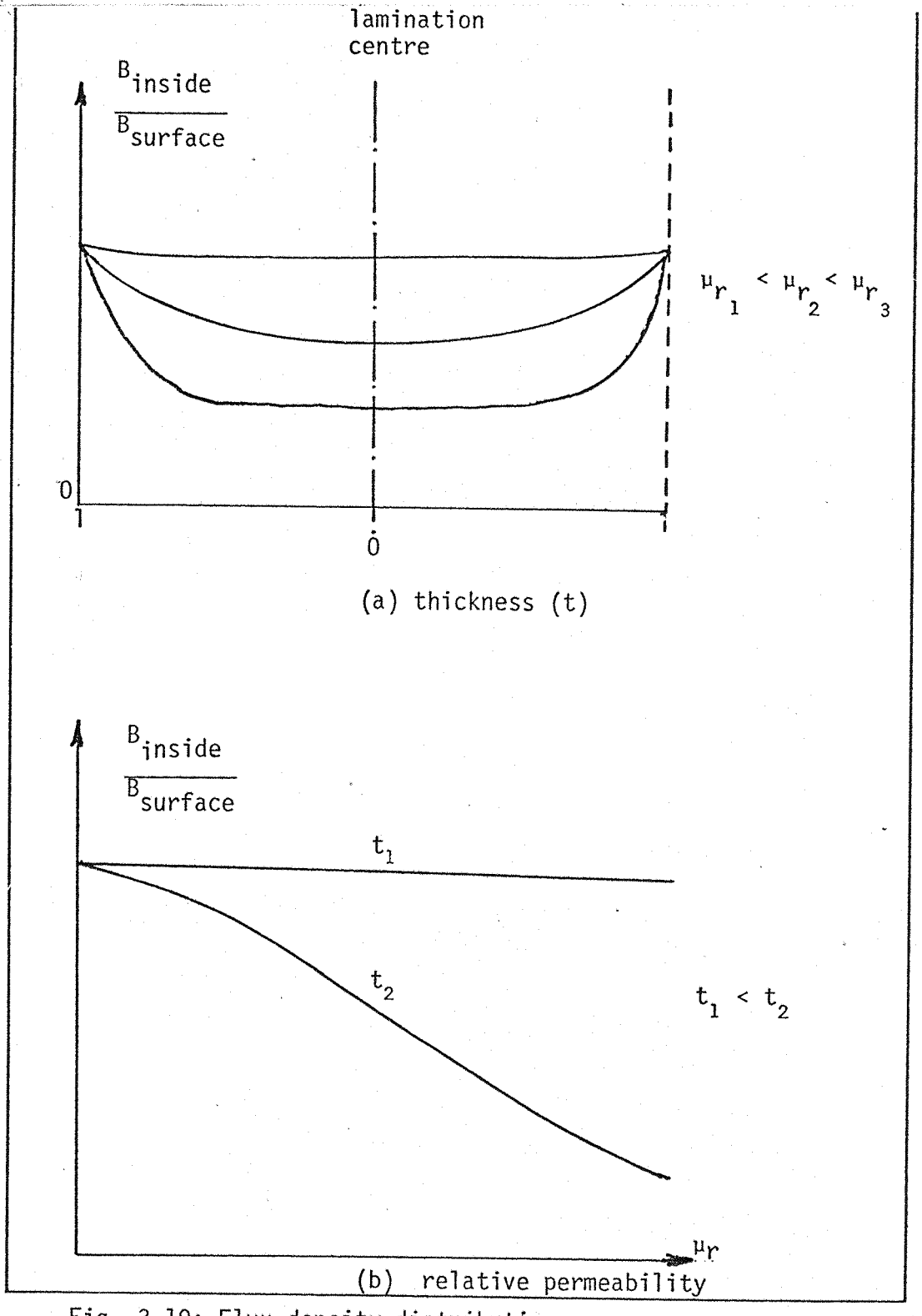

Fig. 3.10: Flux density distribution

3.6.1.B Eddy currents in the plane of the laminations

The axial component of the leakage flux at the core front of synchronous machines can induce eddy currents in the plane of the laminations.[31,40] These eddy currents circulating in the laminations create a field that opposes the field crossing the laminations which originated them. This opposition will be dependent on both the lamination depth and the resistivity of the silicon steel. For the case of stator cores

existing in the synchronous machines where the lamination depth is not negligible and the resistivity is not extremely high, the eddy currents are defined as inductance limited.[16,53]

Therefore the axial flux penetrating the stator core front is subject to a more accentuated action imposed by the inductance limited eddy currents. These effects are such that the axial leakage flux is diminished inside the stator core.

The eddy currents are confined to the plane of the lamination and have both radial and circumferential components. They are distributed in such a way that most of the eddy current density is found at the border of the lamination. The eddy current density far from the edges of the lamination is small. The circumferential component flowing close to the bore is expected to be equal to that flowing at the core back. Both the butt joints and lapping arrangements[35,36] can cause a disturbance in the eddy currents' path. They can reduce the reaction field imposed by the eddy currents against the axial leakage flux penetration into the stator core. A core with laminations composed of sectors is expected to present deeper axial leakage flux than that with entire laminations.

The electrical supply allows only a small variation in the main frequency during normal operation which permits us to say that the main frequency is constant. But in order to analyse the effects of eddy currents in the axial leakage flux penetration it is important to vary the frequency. The increase in the frequency of the inducing field causes an increase in the eddy currents' reaction. Therefore it is expected that less axial leakage flux penetrates the plane of the laminations. The effect of those eddy currents on the leakage flux distribution is stronger at the end zones of the stator core.

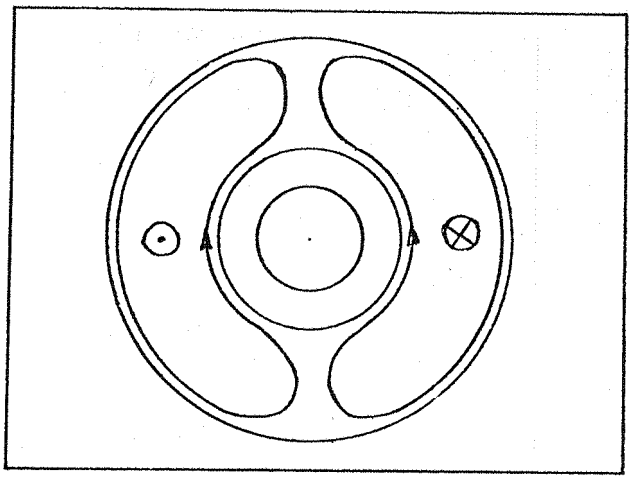

Fig. 3.11: Eddy currents in the plane of the laminations

3.6.2.C Eddy currents in the end plates

The eddy currents circulating in the end plates are similar to the eddy currents circulating in the plane of the laminations. The end plate eddy currents are also due to the axial leakage flux entering the stator core front. The effects caused by the eddy currents in the end plates are stronger than the other ones due to the fact that the end plates have a thickness greater than the laminations thickness.[72,73] Therefore they cause a larger concentration of axial leakage flux at both the stator core bore and the core back regions. This can produce a great heating loss at both regions. In order to minimise the undesirable effects of the eddy currents in the end plates in modern synchronous machines the end plates are made of non-magnetic material. The eddy currents' path is the same as shown in figure 3.11 for the eddy currents in the plane of the laminations. Therefore the end plate eddy current also presents only circumferential and radial components. It can therefore be suggested that these eddy currents have a tendency to increase the leakage flux at the stator core back mainly at the end zones of the core back.

3.6.2.D Eddy currents in the screening plates

The synchronous machines generally have at the core fronts screening plates made of either copper or aluminium. The screening

plates are intentionally placed at the front of the stator core end plate in order to protect both the end plates and the end laminations against the action of the axial leakage flux. The screening plates amplify the eddy currents reaction, allowing less flux to reach both the end plates and the laminations at the core end.[54-56]

The thickness of the screening plates plays an important part in the axial leakage flux behaviour. Actually the importance of the thickness is emphasised by the fact that both the frequency and the material conductivity are already established. The frequency is fixed by the electrical system and can generally be either fifty or sixty Hz. The material conductivity is wished to be as large as possible but it has already been achieved, in practical terms, with the use of either copper or aluminium. A screening plate that has a thickness greater than the effective skin depth presents an induced eddy current that is inductance limited. Therefore the screening plate does not allow the axial leakage flux to penetrate the stator core front region. The leakage flux in the air region of the stator core front sees the screening plate as an infinitely conducting and zero permeability component of the stator core. The screening plate diverts the axial component of the leakage flux to the radial direction close to the core. It can, therefore, increase the leakage flux at the stator core back.

The divertion of the leakage flux to the core back region is more effectively noticed at the end zones of the core back. Therefore the screening plate eddy current can cause a higher concentration of core back leakage flux at the stator core back end zones. Due to the relatively high eddy currents circulating in the screening plate, a high dissipation of heating close to the end regions of the stator core of large synchronous machines can be noticed.

3.6.2.E Eddy currents in the back of the laminations

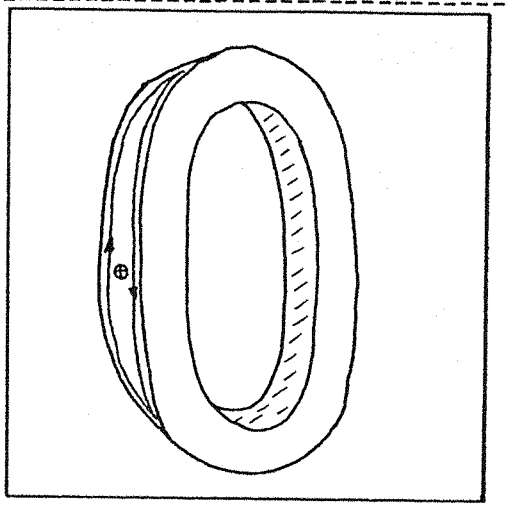

Fig. 3.12: Eddy currents in the back of the laminations

The back of the laminations can be subject to the action of eddy currents.[41] They are induced by the radial component of the stator core back leakage flux. These eddy currents present both the axial and the circumferential components. The circumferential component is larger than the axial one.

The eddy currents in the back of the laminations present a most noticeable effect at the end zones of the stator core back. At the centre zone the effect is expected to be very much smaller. Considering the small space where the eddy currents are distributed at the back of the laminations they are defined as resistance limited. Therefore they do not present a sensible reaction to the penetration of the radial leakage flux at the stator core back. Although these eddy current effects can be increased when the insulation between adjacent laminations is deteriorated, which can be explained by the fact that the damaged insulation can cause a short circuit between neighbouring laminations establishing a larger path to the eddy currents' circulation. Another important point is the electrical contact between each lamination and the building bars. That contact can also produce large eddy currents circulating at the stator core back of synchronous

machines. Therefore special care must be taken at the end zones of the core back where the leakage flux is more intensive.

3.6.B.F Eddy currents in the building bars

The building bars have the responsibility of maintaining as rigid as possible the stator core body.[45,68] This means that most of all the designers of synchronous machines try to obtain building bars able to support very high stresses. The building bar is made of solid magnetic material and the eddy currents are largely concentrated at the surfaces.[74,75] These eddy currents are induced by the core back leakage flux. Most of these eddy currents are induced by the radial component of the leakage flux at the stator core back.

The eddy currents in the building bars have both the axial and circumferential components. The axial component is the largest one. Their effects are expected to be very much localised at the vicinity of the building bars with special reference to the ends.

Again it is very important to determine the electrical contact between the building bars and the laminations in order to estimate the eddy currents' effects. The connections between the building bars also play an important part in the effects of these eddy currents on the core back leakage flux. If the building bars are short circuited with the laminations the core back leakage flux can induce eddy currents that can provide high temperatures at the core back.

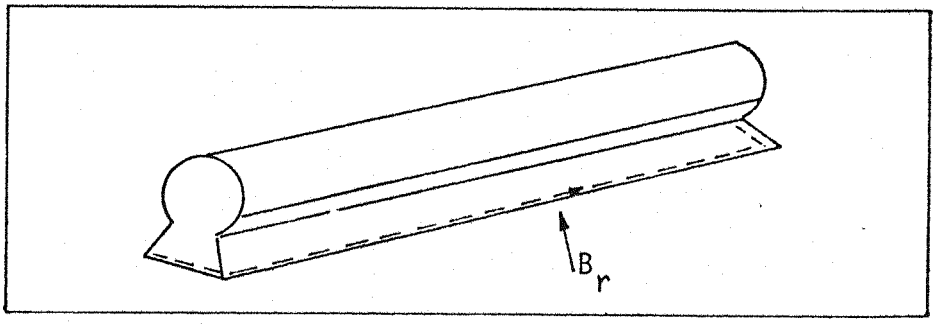

Fig. 3.13: Eddy currents in the building bars

3.6.C Surface Polarity on Building Bars

The building bars have all their magnetic poles distributed at the surfaces since it is a solid magnetic material.[49-52] The surface polarity distribution is determined by the radial component of the stator core back leakage flux. Therefore the distribution of the building bar surface polarity is not uniform along the building bar length. It presents a higher concentration at the ends.

The field established by the building bar surface polarity reinforces the field produced by the surface polarity at the stator core back in the air region and opposes it inside the stator core. The effects of that field is very concentrated at the regions around the building bars. They are more salient at the ends of the building bars.

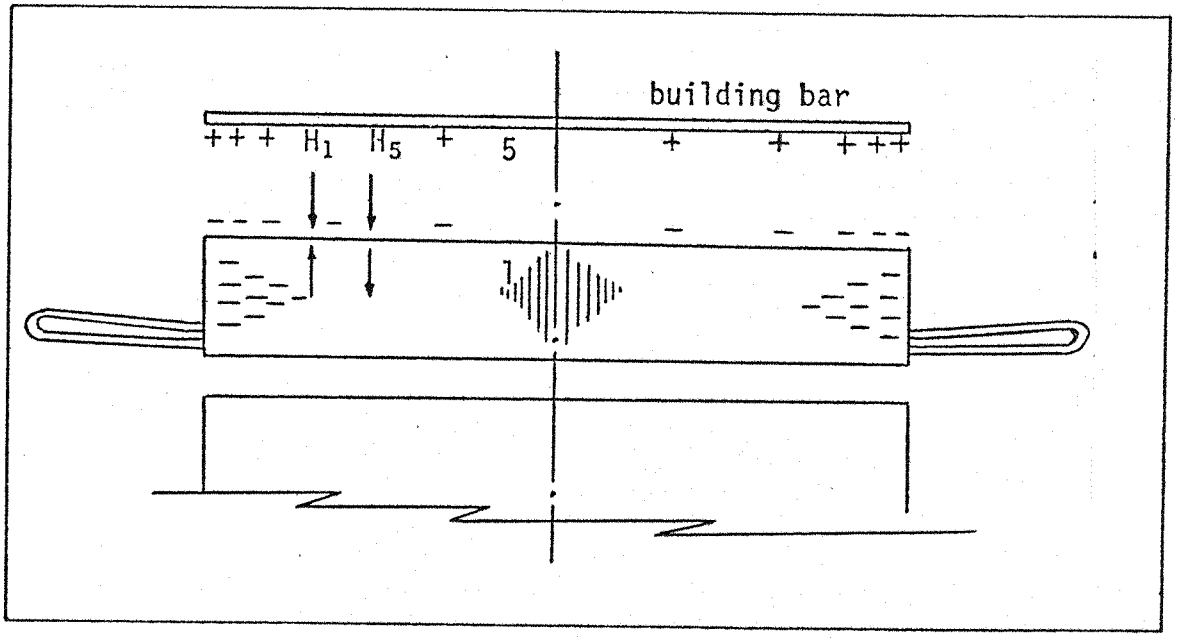

Fig. 3.14: Surface polarity on building bars (H_1 and H_5 are the fields due to the surface polarities on the back of the core and building bar, respectively

3.6.D Polarity on Cooling Duct Surfaces

The cooling systems of the stator core of synchronous machines can consist of radial and axial ducts.[4] The radial ventilating ducts can interfere with the distribution of magnetic poles at the stator

core back surface.[6-8,37,66] On the other hand the axial ventilating ducts can disturb the surface polarity distribution at the core front. Both of them produce a concentration of magnetic poles in the surrounding regions. This means that the leakage flux is increased in the regions around the ventilating ducts. Actually the radial ducts introduce double surface polarities inside the stator core along its length. The axial ducts produce double surface polarities at the stator core front of the synchronous machines. The polarity on cooling duct surfaces produces a rearrangement on the magnetic surface polarity inside the core.

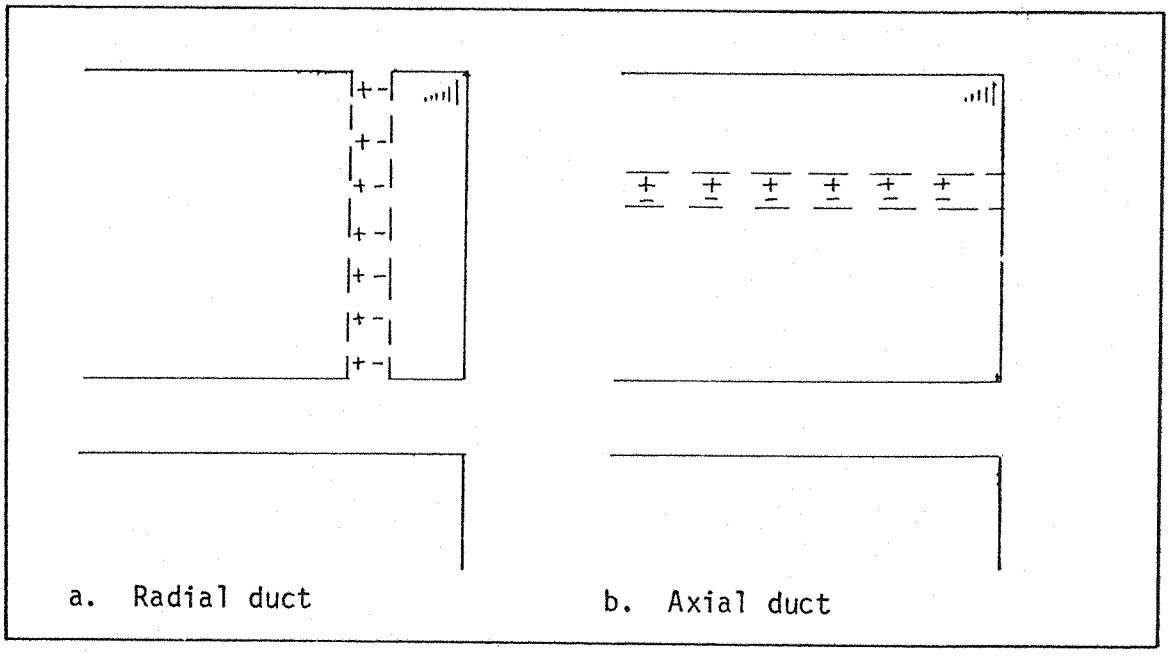

Fig. 3.15: Polarity on cooling duct surfaces

CHAPTER FOUR

MATHEMATICAL TREATMENT OF THE ELECTROMAGNETIC SOURCES OF STATOR CORE BACK LEAKAGE FLUX

4.1 PRELIMINARY DISCUSSIONS

The calculation of the leakage flux of synchronous machines has been subject to intensive research.[9-31] Although the researchers' attention has most of the time been directed to the axial leakage flux. Most of the methods used seek to obtain a complete solution to the problem. Whereas the method of sources examines the individual sources which produce the field. The method of sources has been described and used by Hammond[12,13,48,52] to calculate the magnetic field of the windings of synchronous machines. Tavner[49] has used this method to calculate the distribution of axial leakage flux at the stator core front of electrical machines. The Department of Electrical Engineering at Southampton University is still developing computational researches in order to use the method of sources to calculate leakage flux on electrical machines.

If one makes a comparison between the method of the sources and the method of electromagnetic fields it can be noticed that the first deals with integral equations, while the second one deals with differential equations. That emphasises the main reason why most of the experts on electrical machines have directed their attention towards the electromagnetic field method. That is due to the fact that more extensive progress has been made in the solution of differential equations by means of computer programs. Amongst the different techniques which have been used we can mention both the finite difference and the finite element techniques. Meanwhile the computational solutions of the integral equation solution has advanced less rapidly. The method

of sources has a restricted accuracy dependent on the necessary assumptions made about the magnetisation of the iron surfaces.

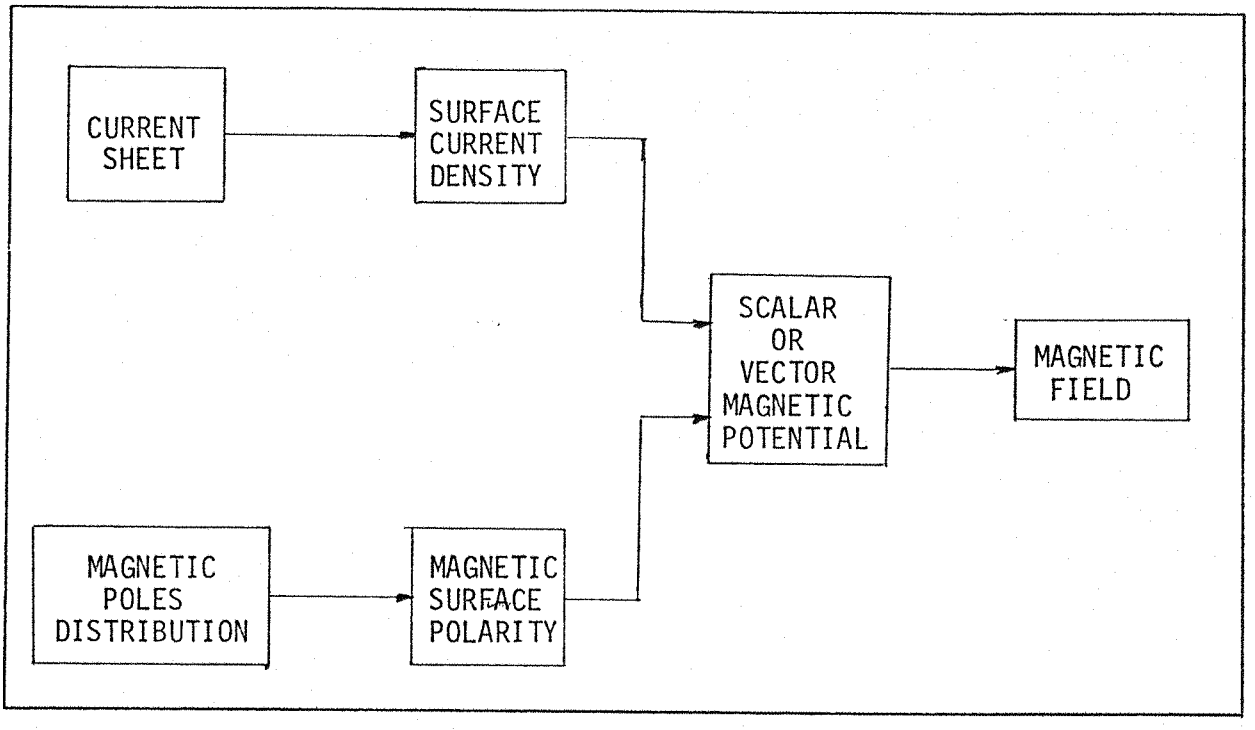

Fig. 4.1: Block diagram of magnetic field calculation by the method of sources

4.2 THE FIELD EQUATIONS

The calculation of the magnetic field due to the various electromagnetic sources can be obtained by means of either the magnetic vector potential or the magnetic scalar potential. The magnetic scalar potential solution needs only the magnitude of the physical quantity specified in a region of the space. However, the magnetic vector potential solution requires three independent numbers associated with each point over that region. Whenever possible it is wiser to deal with magnetic scalar potential considering that the solution can be more easily obtained. Although special care must be taken when using scalar magnetic potential to solve a problem. It is necessary to check its existence according to the kind of problem under analysis.

Considering the particularities of the problem it has been decided to use the magnetic vector potential to obtain the winding field and the magnetic scalar potential to find the field of the magnetic surface polarities.

4.2.1 Magnetic Vector Potential Solution

The relationship between the magnetic flux density and the magnetising force is:

$$B = \mu_o \mu_r H \tag{4.1}$$

The relationship between the magnetic flux density and the magnetic vector potential is:

$$B = \text{curl } A \tag{4.2}$$

Substituting (4.1) in (4.2) we have

$$H = \frac{1}{\mu_o \mu_r} \text{curl } A \tag{4.3}$$

In cylindrical coordinates we have

$$H = \frac{1}{\mu_o \mu_r} \begin{vmatrix} \frac{\mu_r}{r} & \mu_\theta & \frac{\mu_z}{r} \\ \frac{\partial}{\partial r} & \frac{\partial}{\partial \theta} & \frac{\partial}{\partial z} \\ A_r & r A_\theta & A_z \end{vmatrix}$$

Therefore the three components of the magnetic field are:

$$H_z = \frac{1}{\mu_o \mu_r} \left[\frac{A_\theta}{r} + \frac{\partial A_\theta}{\partial r} - \frac{1}{r} \frac{\partial A_r}{\partial \theta} \right] \tag{4.4}$$

$$H_\theta = \frac{1}{\mu_o \mu_r} \left[\frac{\partial A_r}{\partial z} - \frac{\partial A_z}{\partial r} \right] \tag{4.5}$$

$$H_r = \frac{1}{\mu_o \mu_r} \left[\frac{1}{r} \frac{\partial A_z}{\partial \theta} - \frac{\partial A_\theta}{\partial z} \right] \tag{4.6}$$

Equations (4.4), (4.5) and (4.6) form an equation system with three unknowns. Therefore once the three components of the magnetic vector potential are determined the magnetic field components can also be determined.

For rotational but solenoidal field we have:

$$\text{curl } H = J \tag{4.7}$$

$$\text{div } B = 0 \tag{4.8}$$

Substituting (4.7) in (4.3) we have

$$\text{curl } H = \text{curl} \left(\frac{1}{\mu_o \mu_r} \text{curl } A \right) = J$$

$$\therefore \text{curl } H = \frac{1}{\mu_o \mu_r} \text{curl curl } A = J$$

$$\therefore \frac{1}{\mu_o \mu_r} (\text{grad div } A - \nabla^2 A) = J \tag{4.9}$$

But the vector potential is defined to have a divergence equal to zero, therefore

$$\text{div } A = 0 \tag{4.10}$$

Substituting (4.10) in (4.9) we have

$$\nabla^2 A = -\mu_o \mu_r J \qquad \text{(Poisson's equation)} \qquad (4.11)$$

The current density J can be given in cylindrical coordinates as

$$J = J_r \hat{r} + J_z \hat{z} + J_\theta \hat{\theta}$$

But if we consider a cylindrical winding of a synchronous machine the radial component of the current density is equal to zero. Both the axial and the circumferential components can be expressed as a function of both the axial and circumferential positions, the time and the number of pair poles, and are ninety electrical degrees out of phase. The pair pole number determines the number of current patterns.

Therefore,

$$J_r = 0$$

$$J_z = f_1(z, p\theta, t)$$

$$J_\theta = f_2(z, p\theta, t) \qquad (4.12)$$

Although both the axial and the circumferential components can be also expressed as a product of functions as given below

$$J_z = J_z(z) \cdot e^{-jp\theta}\, e^{-j\phi} \qquad (4.13)$$

$$J_\theta = J_\theta(z) \cdot e^{-jp\theta}\, e^{-j(\phi - \pi/2)} \qquad (4.14)$$

The axial and circumferential are interrelated by the imposition of continuity of current. Therefore,

$$\text{div } \underline{J} = 0 \quad \text{(at the conductor surface where } r = R_w).$$

In cylindrical coordinates we have:

$$\frac{1}{R_w} \frac{\partial}{\partial r} (R_w J_r) + \frac{1}{R_w} \frac{\partial}{\partial \theta} J_\theta + \frac{\partial}{\partial z} J_z = 0 \qquad (4.15)$$

Substituting the expressions (4.12), (4.13) and (4.14) in the expression (4.15) we have

$$\frac{1}{R_w}\frac{\partial}{\partial\theta} \quad J_\theta(z)\, e^{-jp\theta}\, e^{-j(\phi - \pi/2)} \quad = \quad -\frac{\partial}{\partial z}\left[J_z(z)\, e^{-jp\theta}\, e^{-j\phi} \right]$$

$$\therefore \quad J_\theta(z) \quad = \quad -\frac{R_w}{p}\frac{\partial}{\partial_z} J_z(z) \qquad (4.16)$$

The expression (4.16) shows that in cylindrical windings the circumferential current is proportional to the axial current partial derivative relatively the axial direction.

Therefore the three components of the magnetic vector potential can be obtained by the current density components. The current density components can be determined by means of current sheets as presented in section 4.3.1. The current density components are functions of Fourier coefficients that depend on the machine geometry and excitation current which are known.

A sequence has, therefore, been established which starts from the known machine geometry and excitation current to determine the current density. Once the current density has been determined it is possible to calculate the magnetic vector potential. Finally it allows the calculation of the magnetic field. This sequence could be shortened if we get the expression for the magnetic field as a function of the Fourier coefficients. Therefore, considering that the current density is represented by a series of current sheets given in section 4.3.1. and using the expressions (4.4), (4.5), (4.6) and (4.11), it is possible to obtain the expressions for three components of the magnetic field as a function of the Fourier coefficients and machine dimensions as given in the references 12, 13 and 49.

The components' magnetic field expressions for the region $r > R_w$ are:

axial component of the magnetic field

$$H_z = -\frac{R_w}{r} e^{-jp\theta} e^{-j\phi} \sum_{n=odd} \frac{n\pi r}{4(R_w + l_w)} I'_1\left(\frac{n\pi R_w}{4(R_w + l_w)}\right) K_1\left(\frac{n\pi r}{4(R_w + l_w)}\right) b_n \sin\frac{n\pi z}{4(R_w + l_w)} \quad (4.17)$$

circumferential component of the magnetic field

$$H_\theta = \frac{R_w}{2r} jpe^{-jp\theta} e^{-j(\phi - \pi/2)} \sum_{n=odd} \frac{n\pi r}{4(R_w + l_w)} \left\{ \left[I_o\left(\frac{n\pi R_w}{4(R_w + l_w)}\right) K_o\left(\frac{n\pi r}{4(R_w + l_w)}\right) - I_2\left(\frac{n\pi r}{4(R_w + l_w)}\right) K_2\left(\frac{n\pi r}{4(R_w + l_w)}\right) \right] b_n + 2I_1\left(\frac{n\pi R_w}{4(R_w + l_w)}\right) K'_1\left(\frac{n\pi r}{4(R_w + l_w)}\right) a_n \right\} \cos\frac{n\pi z}{4(R_w + l_w)} \quad (4.18)$$

radial component of the magnetic field

$$H_r = \frac{R_w}{2r} e^{-jp\theta} e^{-j\phi} \sum_{n=odd} \left\{ 2I_1\left(\frac{n\pi R_w}{4(R_w + l_w)}\right) K_1\left(\frac{n\pi r}{4(R_w + l_w)}\right) a_n + \frac{n\pi r}{4(R_w + l_w)} \left[I_o\left(\frac{n\pi r}{4(R_w + l_w)}\right) K_o\left(\frac{n\pi r}{4(R_w + l_w)}\right) + I_2\left(\frac{n\pi R_w}{4(R_w + l_w)}\right) K_2\left(\frac{n\pi r}{4(R_w + l_w)}\right) \right] b_n \right\} \cos\frac{n\pi z}{4(R_w + l_w)} \quad (4.19)$$

4.2.2 Magnetic Scalar Potential Solution

For an irrotational and solenoidal field the equations are:

$$\text{div } H = 0 \tag{4.20}$$

$$\text{curl } H = 0 \tag{4.21}$$

$$H = -\text{ grad } V \tag{4.22}$$

$$\text{grad } V \equiv \frac{\partial V}{\partial r}\hat{r};\ \frac{1}{r}\frac{\partial V}{\partial \theta}\hat{\theta};\ \frac{\partial V}{\partial z}\hat{z} \tag{4.23}$$

$$H = H_r \hat{r} + H_\theta \hat{\theta} + H_z \hat{z} \tag{4.24}$$

Therefore, considering the expressions (4.22), (4.23) and (4.24) we have

$$H_r = -\frac{\partial V}{\partial r} \tag{4.25}$$

$$H_\theta = -\frac{1}{r}\frac{\partial V}{\partial \theta} \tag{4.26}$$

$$H_z = -\frac{\partial V}{\partial z} \tag{4.27}$$

Therefore equations (4.20), (4.21) and (4.22) allow us to obtain the three components of the magnetic field as a function of the magnetic scalar potential. We must, therefore, determine the scalar potential.

Applying the divergence at both sides of the equation (4.22) we have:

$$\text{div } H = -\text{ div grad } V \tag{4.28}$$

Substituting (4.15) in (4.23) we have

$$\nabla^2 V = 0 \quad \text{(Laplace's equation)} \tag{4.29}$$

In cylindrical coordinates equation (4.29) is given by:

$$\frac{\partial^2 V}{\partial r^2} + \frac{1}{r}\frac{\partial V}{\partial r} + \frac{1}{r^2}\frac{\partial^2 V}{\partial \theta^2} + \frac{\partial^2 V}{\partial z^2} = 0 \qquad (4.30)$$

The solutions of equation (4.30) are of the form:

$$V \alpha \begin{bmatrix} \cos q z \\ \sin q z \end{bmatrix} \begin{bmatrix} I_p(qr) \\ K_p(qr) \end{bmatrix} e^{\pm jp\theta}$$

Therefore the appropriate solutions of equation (4.30) can be found after considering the boundary conditions at the surface of either the tube of polarity on the annular discs of polarity as well as the magnetisation of both surfaces given in section 4.3.2. However, once the magnetic scalar potential has been determined it is possible to calculate the three components of the magnetic field using the expressions (4.25), (4.26) and (4.27). The magnetic scalar potential expressions have already been derived[12,19] and are going to be outlined here.

For the bore polarity we have:

$$V = \frac{R_{si} - R_r}{\mu_o} \cos(\omega t - p\theta - \phi) \sum_{n=odd} \frac{n\pi R_{si}}{4(R_{si} + l_c)} I'_1\left(\frac{n\pi R_{si}}{4(R_{si} + l_c)}\right)$$

$$c_n K_1\left(\frac{n\pi r}{4(R_{si} + l_c)}\right) \cos \frac{n\pi r}{4(R_{si} + l_c)} \qquad (4.31)$$

Therefore substituting (4.31) into (4.25), (4.26) and (4.27) we can get the expressions for the magnetic field components:

radial component

$$H_r = \frac{R_{si}(R_r - R_{si})}{\mu_o} e^{-jp\theta} e^{-j\phi} \sum_{n=odd} \left(\frac{n\pi}{4(R_{si} + l_c)}\right)^2 c_n$$

$$I'_1\left(\frac{n\pi R_{si}}{4(R_{si}+l_c)}\right)K'_1\left(\frac{n\pi r}{4(R_{si}+l_c)}\right)\cos\frac{n\pi z}{4(R_{si}+l_c)} \qquad (4.32)$$

circumferential component

$$H_\theta = \frac{R_{si}(R_{si}-R_r)}{\mu_o} jpe^{-jp\theta}\, e^{-j\phi} \sum_{n=odd} \frac{1}{r}\frac{n\pi}{4(R_{si}+l_c)} c_n$$

$$I'_1\left(\frac{n\pi R_{si}}{4(R_{si}+l_c)}\right)K_1\left(\frac{n\pi r}{4(R_{si}+l_c)}\right)\cos\frac{n\pi z}{4(R_{si}+l_c)} \qquad (4.33)$$

axial component

$$H_z = \frac{R_{si}(R_{si}-R_r)}{\mu_o} e^{-jp\theta}\, e^{-j\phi} \sum_{n=odd} \left(\frac{n\pi}{4(R_{si}+l_c)}\right)^2 c_n$$

$$I'_1\left(\frac{n\pi R_{si}}{4(R_{si}+l_c)}\right)K_1\left(\frac{n\pi r}{4(R_{si}+l_c)}\right)\sin\frac{n\pi z}{4(R_{si}+l_c)} \qquad (4.34)$$

For the polarity on disc surfaces at the core front we have:

$$V = \frac{R_c}{\mu_o}\cos(\omega t - p\theta - \phi) \sum_{n=1}^{\infty} \frac{1}{\lambda_n} J_1\left(\frac{\lambda_n r}{2R_c}\right) e^{-\frac{\lambda_n z}{2R_c}}\, d_n \qquad (4.35)$$

Therefore, substituting (4.35) into (4.25), (4.26) and (4.27) we can obtain the magnetic field components:

radial component

$$H_r = -\frac{1}{2\mu_o} e^{-jp\theta}\cdot e^{-j\phi} \sum_{n=1}^{\infty} J_1\left(\frac{\lambda_n r}{2R_c}\right) e^{-\frac{\lambda_n z}{2R_c}}\, d_n \qquad (4.36)$$

circumferential component

$$H_\theta = \frac{R_c}{2\mu_o r} jpe^{-jp\theta}\, e^{-j\phi} \sum_{n=1}^{\infty} J_1\left(\frac{\lambda_n r}{2R_c}\right) e^{-\frac{\lambda_n z}{2R_c}} \frac{1}{\lambda_n} d_n \qquad (4.37)$$

axial component

$$H_z = \frac{1}{2\mu_o} e^{-jp\theta} e^{-j\phi} \sum_{n=1}^{\infty} J_1\left(\frac{\lambda_n r}{2R_c}\right) e^{-\frac{\lambda_n z}{2R_c}} d_n \qquad (4.38)$$

For the polarity on the stator core back we have:

$$V = \frac{R_c}{\mu_o} \cos(\omega t - p\theta - \phi) \sum_{n=odd} I_1\left(\frac{n\pi R_c}{4(R_c + l_c)}\right) \cdot f_n$$

$$K_1\left(\frac{n\pi r}{4(R_c + l_c)}\right) \cos \frac{n\pi r}{4(R_c + l_c)} \qquad (4.39)$$

Therefore, substituting (4.41) into (4.25), (4.26) and (4.27) we can get the magnetic field components:

radial component

$$H_r = -\frac{R_c}{\mu_o} e^{-jp\theta} e^{-j\phi} \sum_{n=odd} \frac{n\pi}{4(R_c + l_c)} I_1\left(\frac{n\pi R_c}{4(R_c + l_c)}\right) f_n$$

$$K'_1\left(\frac{n\pi r}{4(R_c + l_c)}\right) \cos \frac{n\pi z}{4(R_c + l_c)} \qquad (4.40)$$

circumferential component

$$H_\theta = \frac{R_c jp}{\mu_o} e^{-jp\theta} e^{-j\phi} \sum_{n=odd} \frac{1}{r} I_1\left(\frac{n\pi R_c}{4(R_c + l_c)}\right) f_n$$

$$K_1\left(\frac{n\pi r}{4(R_c + l_c)}\right) \cos \frac{n\pi z}{4(R_c + l_c)} \qquad (4.41)$$

axial component

$$H_z = \frac{R_c}{\mu_o} e^{-jp\theta} e^{-j\phi} \sum_{n=odd} \frac{n\pi}{4(R_c + l_c)} I_1\left(\frac{n\pi R_c}{4(R_c + l_c)}\right) f_n$$

$$K_1\left(\frac{n\pi r}{4(R_c + l_c)}\right) \sin \frac{n\pi z}{4(R_c + l_c)} \qquad (4.42)$$

Therefore it can be seen from the field component expressions that it is necessary to determine the coefficients c_n, d_n and f_n. The calculations of those coefficients are shown in section 4.3.2.

4.3 ANALYTICAL REPRESENTATION

Both the explicit current and the implicit magnetic sources can be represented analytically.[19] The implicit magnetic sources can be represented either by cylindrical tubes or annular discs of magnetic surface polarity.[49] Both the tubular and the annular disc polarities are determined as functions of the machine dimensions and the explicit sources. The tubular polarity is set up as an infinite series of tubes in the axial direction, therefore it can be represented by Fourier series. The annular disc polarity is set up as an infinite succession of annulus in the radial direction, therefore it can be represented by Fourier-Bessel series.

The explicit current sources can be represented by a set of axial, radial and circumferential current sheets.[12,13] The current sheets are represented by a Fourier series expanded in the axial direction. If the winding is cylindrical it is just necessary to consider both the axial and the circumferential current sheets in order to obtain the magnetic field.[20] But when the winding is conical, it is also necessary to consider the radial current sheet. It is necessary to consider separately each different kind of winding. In order to simplify the mathematical calculations just the cylindrical windings are analysed.

4.3.1 Winding Current Sheet Representation

The winding is separated into two main component parts: the active part and the overhang. Both two parts are analysed separately. They are analysed by means of Fourier series.[76,78] Hammond[12] has suggested a value for the period equal to $4(R_w + l_w)$ which is going to be used here. That value is such that a minimum number of Fourier terms can be used in order to obtain an accurate field calculation and it guarantees a negligible mutual interference between the adjacent current sheets in the series.

4.3.1.A Active part

4.3.1.Aa Active part parallel to the machine axis

The active length of both the concentric and the diamond windings are parallel to the machine axis. Therefore they have the same shape when represented by a Fourier series. They just have the axial current sheet which is constant in the axial direction. The circumferential current density is equal to zero since it is proportional to the partial derivative of the axial component in the axial direction.

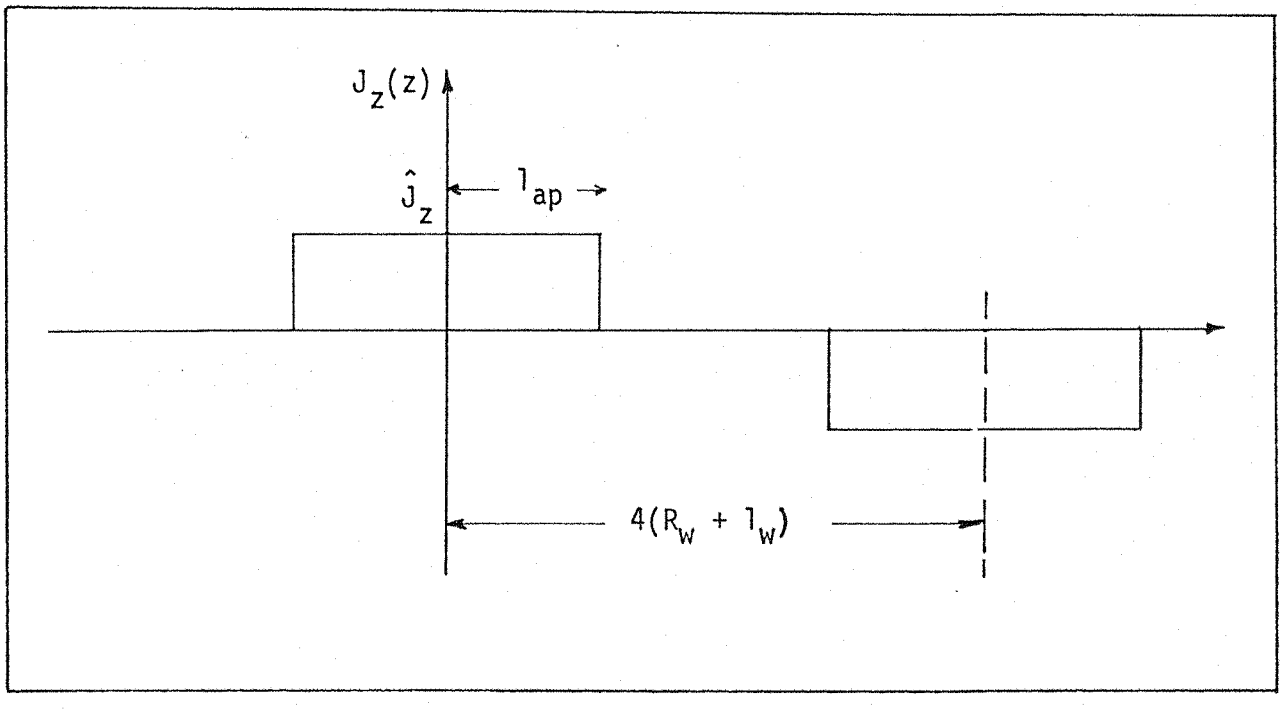

We have

$$J_z(z) = \hat{J}_z \quad \text{in the interval} \quad 0 \leq z \leq l_{ap}$$

$$J_z(z) = 0 \quad \text{in any other interval in the semi-period.}$$

Since $J_z(z)$ is an even function the Fourier expansion is just given as a sum of cosines.

$$J_z(z) = \sum_{n=\text{odd}} a_n \cos \frac{n\pi z}{4(R_w + l_w)} \tag{4.43}$$

where

$$a_n = \frac{1}{R_w + l_w} \int_0^{l_{ap}} \hat{J}_z \cos \frac{n\pi z}{4(R_w + l_w)} \, dz$$

$$\therefore \quad a_n = \frac{4}{n\pi} \hat{J}_z \sin \frac{n\pi}{4(R_w + l_w)} l_{ap} \tag{4.44}$$

where the value of $\hat{J}_z$ is given by:

$$\hat{J}_z = \frac{3pNK_cK_d}{\pi R_w} I$$

Therefore, substituting the value of a in the equation (4.43) we can obtain $J_z(z)$.

4.3.1.Ab Active part with helical distribution

The helical winding has both axial and circumferential current sheets. The axial current density varies cosinuosidally along the axial direction. On the other hand, the circumferential current density varies sinusoidally along the axial direction. Therefore the axial and the circumferential current densities are even and odd functions respectively. The maxima of the axial and the circumferential

densities occur at the centre and at the edge of the winding respectively. When one has a maximum value the other one has a minimum.

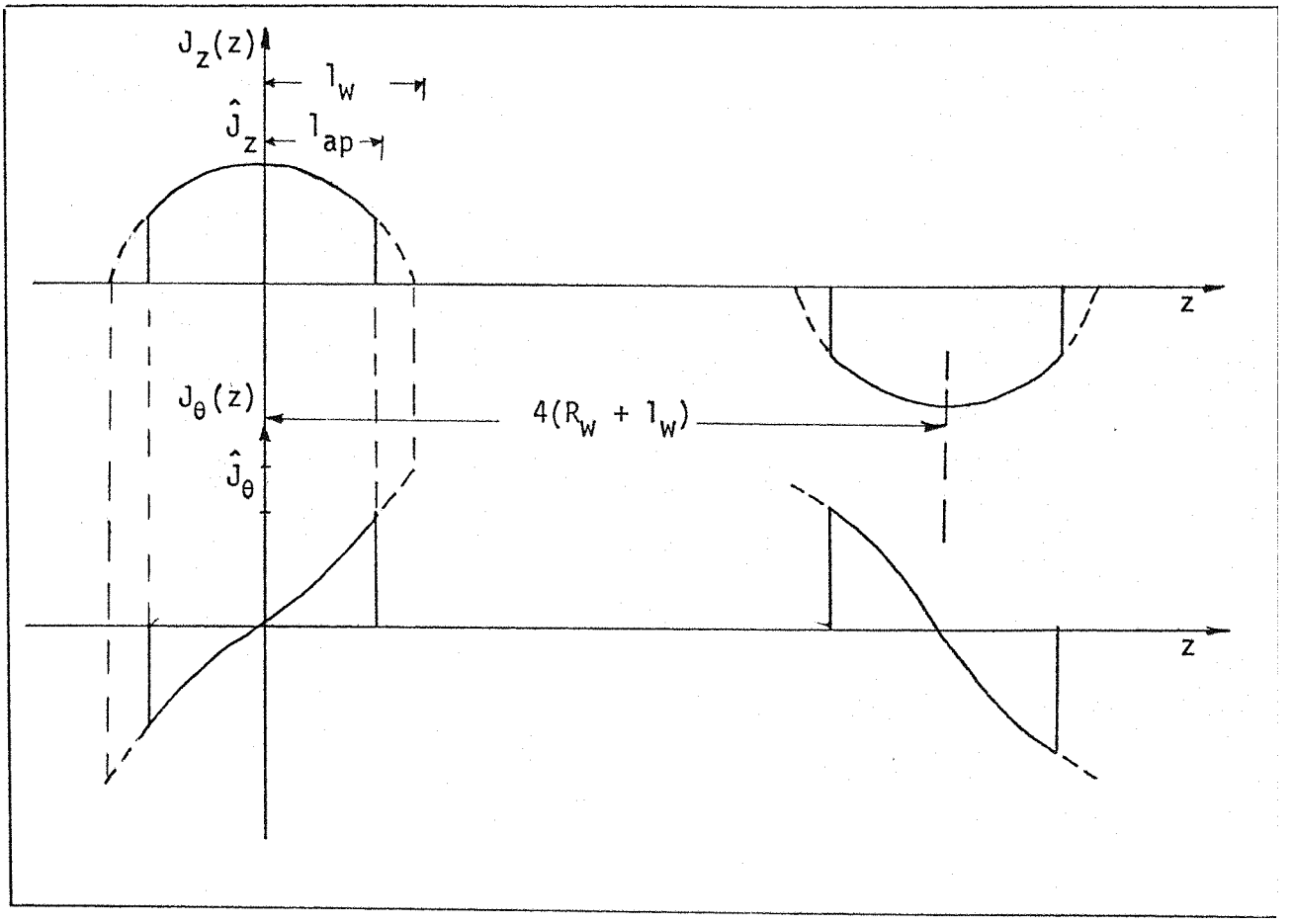

We have

$$J_z(z) = J_z \cos \frac{\pi z}{2l_w} \quad \text{in the interval} \quad 0 \leqslant z \leqslant l_{ap}$$

$$J_z(z) = 0 \quad \text{at any other interval in the semi-period.}$$

$$J_\theta(z) = J_\theta \sin \frac{\pi z}{2l_w} \quad \text{for the interval} \quad 0 \leqslant z \leqslant l_{ap}$$

$$J_\theta(z) = 0 \quad \text{for any other interval in the semi-period.}$$

$\hat{J}_\theta$ can be given as a function of J_z, as shown below.

We have the expression (4.16) which relates $J_\theta(z)$ to $J_z(z)$, therefore

$$J_\theta(z) = -\frac{R_w}{p}\frac{\partial}{\partial z} J_z(z)$$

$$\therefore \hat{J}_\theta \sin\frac{\pi z}{2l_w} = -\frac{R_w}{p}\frac{\partial}{\partial z}\left(\hat{J}_z \cos\frac{\pi z}{2l_w}\right)$$

$$\therefore \hat{J}_\theta = \frac{\pi R_w}{2pl_w}\hat{J}_z$$

Therefore we can get a_n

$$a_n = \frac{\hat{J}_z}{R_w + l_w}\int_0^{l_{ap}} \cos\frac{\pi z}{2l_w}\cos\frac{n\pi z}{4(R_w + l_w)}\,dz$$

$$\therefore a_n = \frac{\hat{J}_z}{2(R_w + l_w)}\left\{\int_0^{l_{ap}} \cos\left[\left(\frac{R_w + (1 - n)l_w}{4l_w(R_w + l_w)}\right)\pi z\right]dz + \right.$$

$$\left. + \int_0^{l_{ap}} \cos\left[\left(\frac{R_w + (1 + n)l_w}{4R_w + (R_w + l_w)}\right)\pi z\right]dz\right.$$

$$\therefore a_n = \frac{2l_w}{\pi}\hat{J}_z\left[\frac{1}{R_w + (1 - n)l_w}\sin\left(\frac{R_w + (1 - n)l_w}{4l_w(R_w + l_w)}\right)\pi l_{ap} + \right.$$

$$\left. + \frac{1}{R_w + (1 + n)l_w}\sin\frac{R_w + (1 + n)l_w}{4l_w(R_w + l_w)}\pi l_{ap}\right] \qquad (4.45)$$

Therefore $J_z(z)$ can be obtained after substituting the value of a_n in equation (4.43).

The circumferential current density, $J_\theta(z)$, can be obtained in a similar way and is given by

$$J_\theta(z) = \sum_{n=\text{odd}} b_n \sin\frac{n\pi z}{4(R_w + l_w)} \qquad (4.46)$$

For this particular case b_n can be given by

$$b_n = \frac{\hat{J}_\theta}{R_w + l_w} \int_0^{l_{ap}} \sin \frac{\pi z}{2l_w} \sin \frac{n\pi z}{4(R_w + l_w)} \, dz$$

$$\therefore \quad b_n = \frac{R_w}{2pl_w(R_w + l_w)} \hat{J}_z \left\{ \int_0^{l_{ap}} \left[\cos\left(\frac{R_w + (1 - n)l_w}{4l_w(R_w + l_w)} \right) \pi z \right] dz + \right.$$

$$\left. + \int_0^{l_{ap}} \left[\cos\left(\frac{R_w + (1 + n)l_w}{4l_w(R_w + l_w)} \right) \pi z \right] dz \right.$$

$$\therefore \quad b_n = \frac{R_w}{p} \hat{J}_z \left[\frac{1}{R_w + (1 - n)l_w} \sin \frac{R_w + (1 - n)l_w}{4l_w(R_w + l_w)} \pi l_{ap} + \right.$$

$$\left. + \frac{1}{R_w + (1 + n)l_w} \sin \frac{R_w + (1 - n)l_w}{4l_w(R_w + l_w)} \pi l_{ap} \right] \qquad (4.47)$$

Therefore $J_\theta(z)$ can be obtained after substituting the value of b_n in equation (4.43).

4.3.1.B Overhang

4.3.1.Ba Concentric winding

The concentric winding overhang has both the axial and the circumferential current sheets. They are even and odd functions respectively. Again it is necessary to calculate the coefficients a_n and b_n in order to obtain $J_z(z)$ and $J_\theta(z)$ respectively.

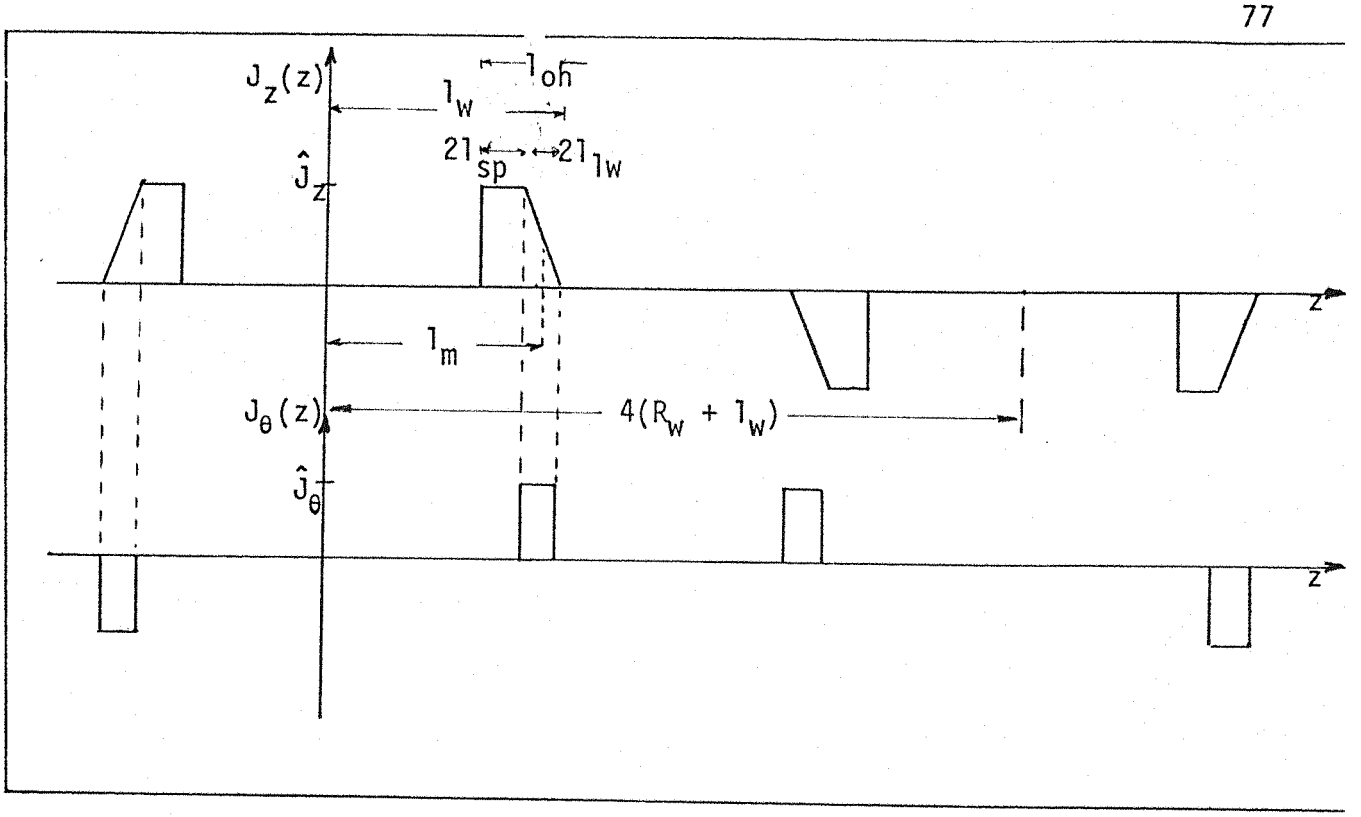

In order to simplify the mathematical calculations, 'l_m' is going to be defined as the distance between the end winding middle point and the centre of the winding.

We have

$$J_z(z) = \hat{J}_z \quad \text{in the interval} \quad (l_m - l_{lw}) - 2l_{sp} \leqslant z \leqslant l_m - l_{lw}$$

$$J_z(z) = \hat{J}_z \frac{l_w - z}{2l_{lw}} = \hat{J}_z \frac{l_m + l_{lw} - z}{2l_{lw}} \quad \text{in the interval}$$

$$l_m - l_{lw} \leqslant z \leqslant l_m + l_{lw}$$

$$J_z(z) = 0 \quad \text{at any other interval in the semi-period.}$$

$$J_\theta(z) = \hat{J}_\theta \quad \text{in the interval} \quad l_m - l_{lw} \leqslant z \leqslant l_m + l_{lw}$$

$$J_\theta(z) = 0 \quad \text{at any other interval in the semi-period.}$$

$\hat{J}_\theta$ can be given as a function of $\hat{J}_z$, as shown below.

From expression (4.16) we have

$$J_\theta(z) = -\frac{R_w}{p}\frac{\partial}{\partial_z} J_z(z)$$

$$\therefore \quad \hat{J}_\theta = \frac{R_w}{2p l_w}\hat{J}_z \tag{4.48}$$

The coefficients a_n and b_n can be calculated in a similar way that was used in the item before.

$$a_n = \frac{1}{R_w + l_w}\left[\int_{(l_m - l_{lw}) - 2l_{sp}}^{l_m - l_{lw}} \hat{J}_z \cos\left(\frac{n\pi z}{4(R_w + l_w)}\right)dz + \right.$$

$$+\int_{l_m - l_{lw}}^{l_m + l_{lw}} \hat{J}_z \frac{l_m + l_{lw}}{2l_{lw}} \cos\left(\frac{n\pi z}{4(R_w + l_w)}\right)dz -$$

$$\left.-\int_{l_m - l_{lw}}^{l_m + l_{lw}} \hat{J}_z \frac{1}{l_{lw}} \cdot z \cos\left(\frac{n\pi z}{4(R_w + l_w)}\right)dz\right]$$

$$a_n = \frac{4}{n\pi}\hat{J}_z\left[\frac{4(R_w + l_w)}{n\pi}\sin\frac{n\pi(l_w - l_{lw})}{4(R_w + l_w)}\sin\frac{n\pi l_{lw}}{4(R_w + l_w)} - \right.$$

$$\left. - \sin\frac{n\pi(l_w - l_{oh})}{4(R_w + l_w)}\right] \tag{4.49}$$

The coefficient b_n is given by the expression:

$$b_n = \frac{1}{R_w + l_w}\int_{l_m - l_{lw}}^{l_m + l_{lw}} \hat{J}_\theta \sin\frac{n\pi z}{4(R_w + l_w)}\,dz$$

Resolving the expression above and substituting the value of

$\hat{J}_\theta$ given by (4.48) we have:

$$b_n = \frac{4R_w}{npl_w} \hat{J}_z \sin \frac{n\pi(l_w - l_{lw})}{4(R_w + l_w)} \sin \frac{n\pi l_{lw}}{4(R_w + l_w)} \qquad (4.50)$$

Therefore both the axial and the circumferential current densities can be found substituting a_n and b_n in the expressions (4.43) and (4.46) respectively.

4.3.1.Bb Diamond winding

The diamond winding overhang has both axial and circumferential current densities. They also are even and odd functions respectively.

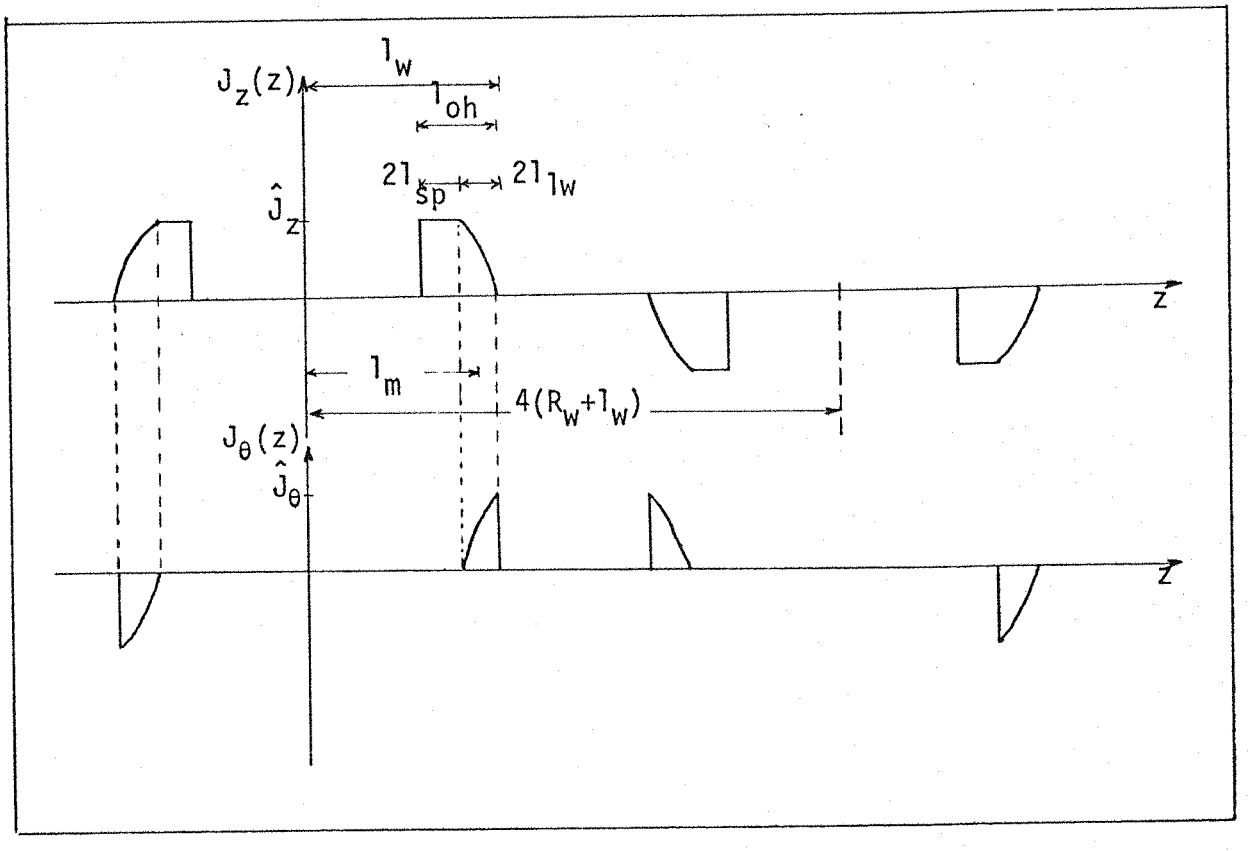

Again, a distance 'l_m' between the middle point of the end winding and the winding centre is going to be used to simplify the mathematical calculations. Now it is important to consider the angular

pitch (α) of the end winding in order to present the correct sinusoidal variation of the currents along the end winding. Therefore we have

$$J_z(z) = \hat{J}_z \quad \text{in the interval} \quad (l_m - l_{lw}) - 2l_{sp} \leq z \leq l_m - l_{lw}$$

$$J_z(z) = \hat{J}_z \frac{1}{\sin\alpha} \sin \frac{l_m + l_{lw} - z}{2l_{lw}} \quad \text{in the interval}$$

$$l_m - l_{lw} \leq z \leq l_m + l_{lw}$$

$$J_z(z) = 0 \quad \text{at any other interval in the semi-period.}$$

Since

$$J_\theta(z) = -\frac{R_w}{p} \frac{\partial}{\partial z} J_z(z)$$

we have

$$J_\theta(z) = \frac{R_w}{2l_w p \sin\alpha} \hat{J}_z \cos \frac{l_m + l_{lw} - z}{2l_{lw}} \quad \text{in the interval}$$

$$l_m - l_{lw} \leq z \leq l_m + l_{lw}$$

$$J_\theta(z) = 0 \quad \text{at any other interval in the semi-period.}$$

Therefore

$$a_n = \frac{1}{R_w + l_w} \left[\int_{(l_m - l_{lw}) - 2l_{sp}}^{l_m - l_{lw}} \hat{J}_z \cos\left(\frac{n\pi z}{4(R_w + l_w)}\right) dz + \right.$$

$$\left. + \int_{l_m - l_{lw}}^{l_m + l_{lw}} \hat{J}_z \frac{1}{\sin} \sin \frac{l_m + l_{lw} - z}{2l_{ls}} \cos\left(\frac{n\pi z}{4(R_w + l_w)}\right) dz \right]$$

Resolving the expression above we have:

$$a_n = 4\hat{J}_z \left\{ \left[\frac{n\pi l_{lw}^2}{2\alpha(R_w + l_w) + n\pi l_{lw}^2} + \frac{1}{n\pi} \right] \sin \frac{n\pi(l_w - 2l_{lw})}{4(R_w + l_w)} - \right.$$

$$- \frac{1}{n\pi} \sin \frac{n\pi(l_w - l_{oh})}{4(R_w + l_w)} + \left[\frac{8\alpha l_{lw}(R_w + l_w)}{2\alpha(R_w + l_w) + n\pi l_{lw}^2} \right] - \frac{1}{\sin\alpha} \cdot$$

$$\left. \cdot \left[\cos \frac{n\pi l_w}{4(R_w + l_w)} + \cos\alpha \cos \frac{n\pi(l_w - 2l_{lw})}{4(R_w - l_w)} \right] \right\} \qquad (4.51)$$

Now to calculate b_n we have the expression:

$$b_n = \frac{1}{R_w + l_w} \int_{l_m - l_{lw}}^{l_m + l_{lw}} \frac{R_w}{2l_w p \sin\alpha} \hat{J}_z \cos\left(\frac{l_m + l_{lw} - z}{2l_{lw}} \right) \cdot$$

$$\cdot \sin\left(\frac{n\pi z}{4(R_w + l_w)} \right) \cdot dz$$

$$\therefore b_n = \frac{2R_w l_{lw}}{l_w p \sin\alpha} \hat{J}_z \left\{ \cos \frac{l_m + l_{lw}}{2l_{lw}} \left[\frac{1}{n\pi l_{lw} + 2(R_w + l_w)} \cdot \right. \right.$$

$$\cdot \sin\left(\frac{n\pi l_{lw} + 2(R_w + l_w)}{4l_{lw}(R_w + l_w)} \cdot l_m \right) \cdot \sin\left(\frac{n\pi l_{lw} + 2(R_w + l_w)}{4l_{lw}(R_w + l_w)} \cdot l_w \right)$$

$$+ \frac{1}{n\pi l_{lw} + 2(R_w + l_w)} \cdot \sin\left(\frac{n\pi l_{lw} - 2(R_w + l_w)}{4l_{lw}(R_w + l_w)} \cdot l_m \right) \cdot$$

$$\left. \cdot \sin\left(\frac{n\pi l_{lw} - 2(R_w + l_w)}{4l_{lw}(R_w + l_w)} \cdot l_{lw} \right) \right] +$$

$$+ \sin \frac{l_m + l_{lw}}{2l_{lw}} \left[\frac{1}{n\pi l_{lw} - 2(R_w + l_w)} \cdot \right.$$

$$\cdot \sin\left(\frac{n\pi l_{lw} - 2(R_w + l_w)}{4l_{lw}(R_w + l_w)} \cdot l_m\right) \cdot \cos\left(\frac{n\pi l_{lw} - 2(R_w + l_w)}{4l_{lw}(R_w + l_w)} \cdot l_w\right)$$

$$+ \frac{1}{n\pi l_{lw} + 2(R_w + l_w)} \cdot \sin\left(\frac{n\pi l_{lw} + 2(R_w + l_w)}{4l_{lw}(R_w + l_w)} \cdot l_m\right) \cdot$$

$$\cdot \cos\left(\frac{n\pi l_{lw} + 2(R_w + l_w)}{4l_{lw}(R_w + l_w)} l_w\right)\Bigg]\Bigg\}$$

4.3.1.B.c Helical winding

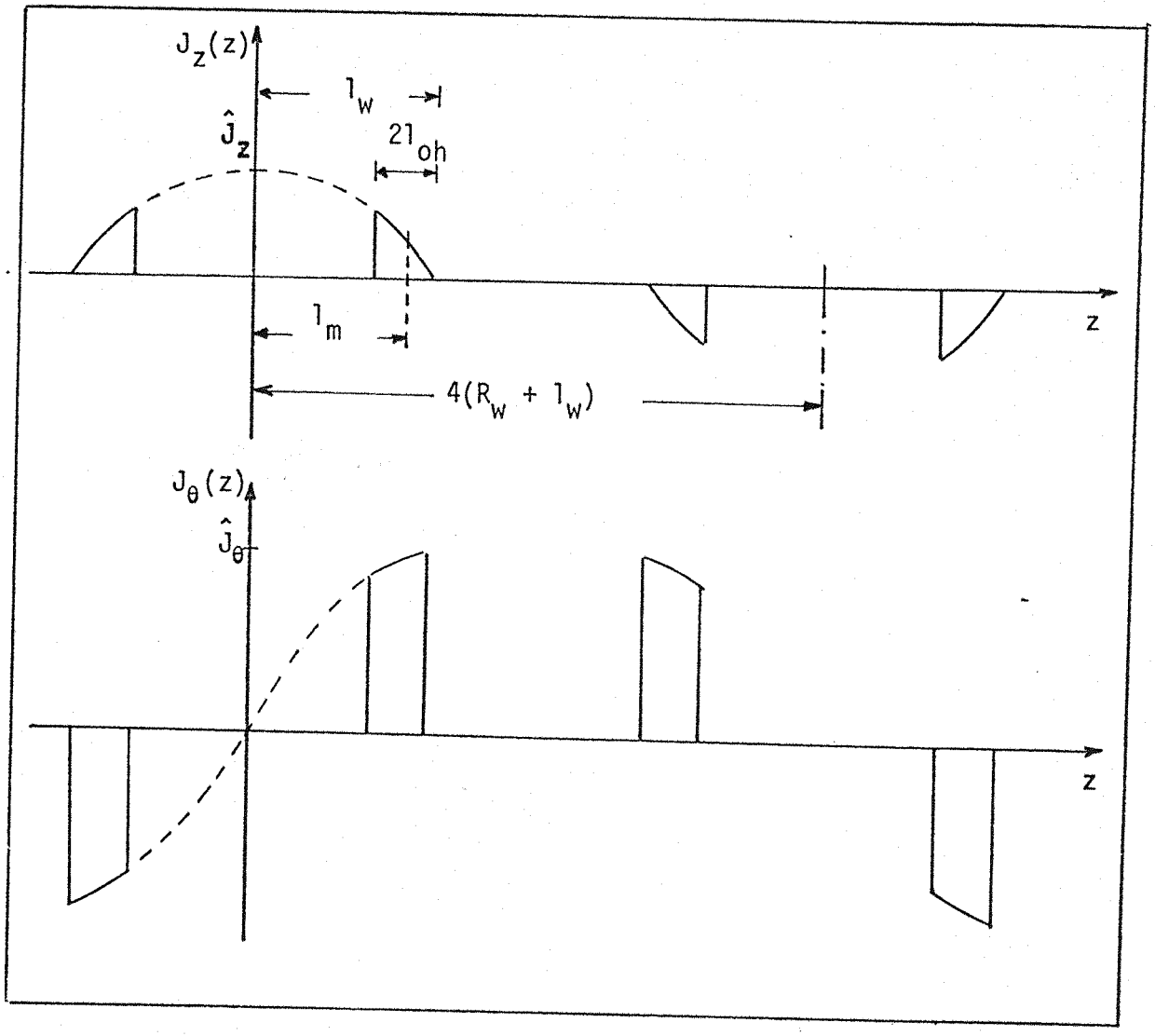

We have

$$J_z(z) = \hat{J}_z \cos \frac{\pi z}{2l_w} \quad \text{in the interval} \quad l_m - l_{oh} \leq z \leq l_m + l_{oh}$$

$$J_z(z) = 0 \quad \text{at any other interval in the semi-period.}$$

$$J_\theta(z) = \frac{\pi R_w}{2pl_w} \hat{J}_z \sin \frac{\pi z}{2l_w} \quad \text{in the interval} \quad l_m - l_{oh} \leq z \leq l_m + l_{oh}$$

$$J_\theta(z) = 0 \quad \text{at any other interval in the semi-period.}$$

Therefore

$$a_n = \frac{1}{R_w + l_w} \int_{l_m - l_{oh}}^{l_m + l_{oh}} \hat{J}_z \cos \frac{\pi z}{2l_w} \cos \frac{n\pi z}{4(R_w + l_w)} dz$$

Resolving the expression above, we have:

$$a_n = \frac{2l_w}{\pi} \hat{J}_z \left\{ \frac{1}{R_w + (1 - n)l_w} \left[\sin \frac{R_w + (1 - n)l_w}{4l_w(R_w + l_w)} (l_w - l_{oh})\pi - \right. \right.$$
$$\left. - \sin \frac{R_w + (1 - n)l_w}{4l_w(R_w + l_w)} l_{oh}\pi \right] + \frac{1}{R_w + (1 + n)l_w}$$
$$\left. \left[\sin \frac{R_w + (1 - n)l_w}{4l_w(R_w + l_w)} (l_w - l_{oh})\pi - \sin \frac{R_w + (1 - n)l_w}{4l_w(R_w + l_w)} l_{oh}\pi \right] \right\}$$

(4.53)

In a similar way we can find b_n from the expression below:

$$b_n = \frac{1}{R_w + l_w} \int_{l_m - l_{oh}}^{l_m + l_{oh}} \frac{\pi R_w}{2pl_w} \hat{J}_z \sin \frac{\pi z}{2l_w} \sin \frac{n\pi z}{4(R_w + l_w)} dz$$

Therefore

$$b_n = \frac{R_w}{p}\hat{J}_z\left\{\frac{1}{R_w + (1-n)l_w}\left[\sin\frac{R_w + (1-n)l_w}{4l_w(R_w + l_w)}(l_w - l_{oh})\pi + \sin\frac{R_w + (1-n)l_w}{4l_w(R_w + l_w)}l_{oh}\pi\right] + \frac{1}{R_w + (1+n)l_w}\left[\sin\frac{R_w + (1-n)l_w}{4l_w(R_w + l_w)}(l_w - l_{oh})\pi + \sin\frac{R_w + (1-n)l_w}{4l_w(R_w + l_w)}l_{oh}\pi\right]\right\} \quad (4.54)$$

Therefore both the axial and the circumferential current densities can be calculated after substituting a_n and b_n in equations (4.43) and (4.46) respectively.

4.3.1 Tubular and Annular Disc Magnetic Surfaces

The bore surface polarity is set up as a finite series of two concentric cylindrical tubes of magnetic pole distribution. The stator core back is set up as a finite series of single cylindrical tubes of magnetic pole distribution. Both are represented by Fourier series. The stator core front surface polarity is represented by an infinite number of concentric annular discs of magnetic pole distribution. That is represented by a Fourier-Bessel series.[76-80] The number of magnetic pole patterns is determined by the number of pole pairs of the synchronous machine.

4.3.2.A Bore polarity

Both the inner (rotor surface) and the outer (stator internal surface) tubular surfaces have a magnetic pole distribution proportional to the radii of both the rotor and the internal part of the stator. When the air gap is small, both surfaces will have similar intensities

of opposite signs considering that the permeabilities are high. The magnetic polarity distribution is assumed constant along the axial direction. The end effects are neglected in order to simplify the mathematical analysis. The bore magnetic polarity is shown in figure 3.4. The magnetic polarities on the outer and inner tubular surfaces are respectively:

$$P^*_{si} = F_{si}(z, p\theta, t) \quad \text{and}$$

$$P^*_{r} = F_{r}(z, p\theta, t)$$

But both the surface polarities vary sinusoidally with both the time and the circumferential direction. Therefore we can write:

$$P^*_{si} = p^*_{si}(z) \cdot e^{-jp\theta}\, e^{-j\phi}$$

$$P^*_{r} = p^*_{r}(z) \cdot e^{-jp\theta}\, e^{-j\phi}$$

Therefore it is necessary to determine p^*_{si} and p^*_r and it can be done by Fourier expansion. The period is similar to that suggested by Hammond.[12]

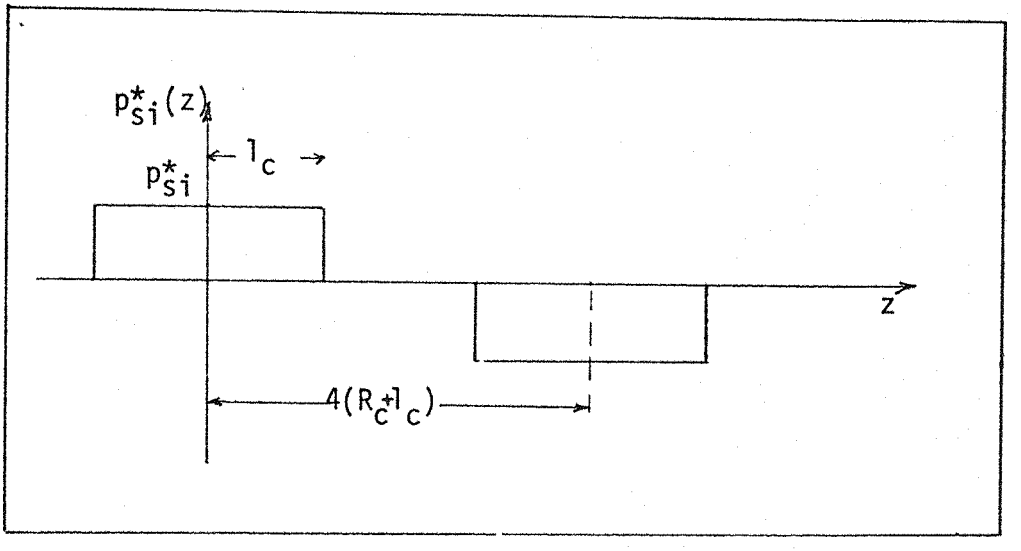

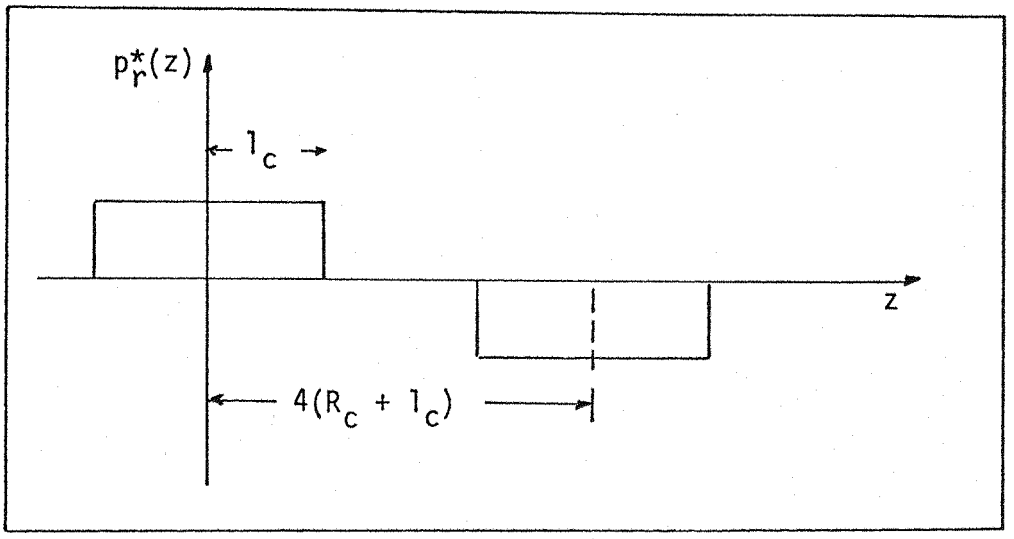

We have:

$$p_{si}^*(z) = P_{si}^* \quad \text{for} \quad 0 \leq z \leq l_c$$

$$p_{si}^*(z) = 0 \quad \text{for any other interval in the semi-period.}$$

$$p_r^*(z) = P_r^* \quad \text{for} \quad 0 \leq z \leq l_c$$

$$p_r^*(z) = 0 \quad \text{for any other interval in the semi-period.}$$

But the magnetic polarities on both the stator inner surface and the rotor surface are related to the respective radial flux density on each surface, as shown in section 3.3. Therefore

$$P_{si}^* = B_{R_{si}} \tag{4.55}$$

$$P_r^* = B_{R_r} \tag{4.56}$$

The radial flux densities in both the rotor and the inner stator surfaces are related by the expression

$$B_{R_r} = B_{R_{si}} \frac{R_{si}}{R_r} \tag{4.57}$$

Therefore substituting the values of B_{R_r} and $B_{R_{si}}$ given in expressions (4.55) and (4.56) into (4.57), we have

$$p_r^* = \frac{R_{si}}{R_r} p_{si}^*$$

Therefore we can write

$$p_{si}^*(z) = \sum_{n=odd} c_n \cos \frac{n\pi z}{4(R_c + l_c)}$$

$$p_r^*(z) = \frac{R_{si}}{R_r} \sum_{n=odd} c_n \cos \frac{n\pi z}{4(R_c + l_c)}$$

where

$$c_n = \frac{1}{R_c + l_c} \int_0^{l_c} p_{si}^* \cos \frac{n\pi z}{4(R_c + l_c)} dz$$

$$c_n = \frac{1}{R_c + l_c} p_{si}^* \sin \frac{n\pi z}{4(R_c + l_c)} \qquad (4.58)$$

Therefore substituting the value of c_n given by expression (4.47) into the expressions (4.32), (4.33) and (4.34) we can get the three components of the magnetic field due to the bore polarity.

4.3.2.B Polarity on disc surfaces at the core front

The magnetic pole distribution at the stator core front surface varies with the radial direction. It has a sinusoidal variation with both the time and the circumferential direction. That surface polarity is represented by an infinite series of concentric annular discs distributed in the same plane z. The Fourier-Bessel[79,80] expansion is utilised and the Bessel functions of first order and first kind are used to determine the core front surface polarity. The period considered is the same suggested by Tavner[49] since it guarantees a negligible interference between adjacent discs. We have that the magnetic polarity at the stator core front is given by:

$$P^*_{cf} = p^*_{cf}(r)\, e^{-jp\theta}\, e^{-j\phi}$$

Therefore it is necessary to find $p^*_{cf}(r)$ which can be done by a Fourier-Bessel expansion

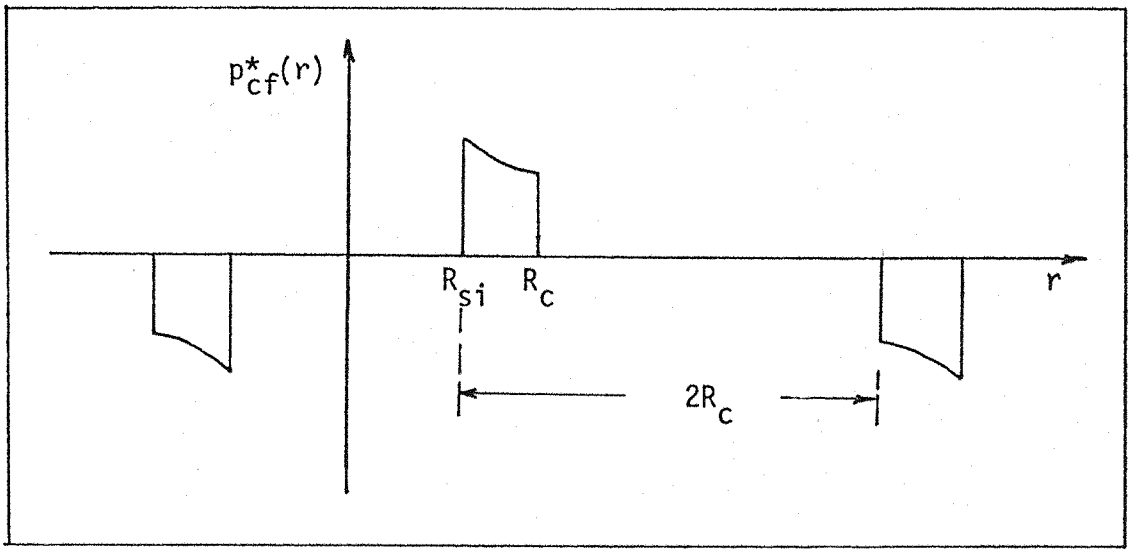

Therefore from Churchil[76] page 163 and Kreisig[77] page 143, we can write

$$p^*_{cf}(r) = d_1 J_1\left(\frac{\lambda_1 r}{2R_c}\right) + d_2 J_1\left(\frac{\lambda_2 r}{2R_c}\right) + \ldots$$

$$p^*_{cf}(r) = \sum_{n=1}^{\infty} d_n J_1\left(\frac{\lambda_n r}{2R_c}\right)$$

where the coefficient d_n is given by

$$d_n = \frac{2}{(2R_c)^2 J_2^2\left(\lambda_n \frac{2R_c}{2R_c}\right)} \int_{R_{si}}^{R_c} r\, J_1\left(\lambda_n \frac{2R_c}{2R_c}\right) p^*_{cf}(r)\, dr$$

$$\therefore \quad d_n = \frac{1}{2R_c^2 J_2^2(\lambda_n)} \int_{R_{si}}^{R_c} r\, J_1(\lambda_n) p^*_{cf}(r)\, dr \qquad (4.59)$$

where λ_n are the roots of the Bessel function J_1 for n = 1, 2, 3, ...

Therefore the value of d_n given by expression (4.59) allows us to calculate the three components of the magnetic field given by expressions (4.36), (4.37) and (4.38).

4.3.2.C Surface polarity on the stator core back

The magnetic pole distribution on the stator core back surface is not constant along the core length. Therefore it can be represented by a series of tubular surfaces with non-uniform magnetisation periodic in z. It can also be represented by a Fourier expansion. Therefore we can also write:

$$p^*_{cb} = p^*_{cb}(z)\, e^{-jp\theta}\, e^{-j\phi}$$

where $p^*_{cb}(z)$ can be determined as follows:

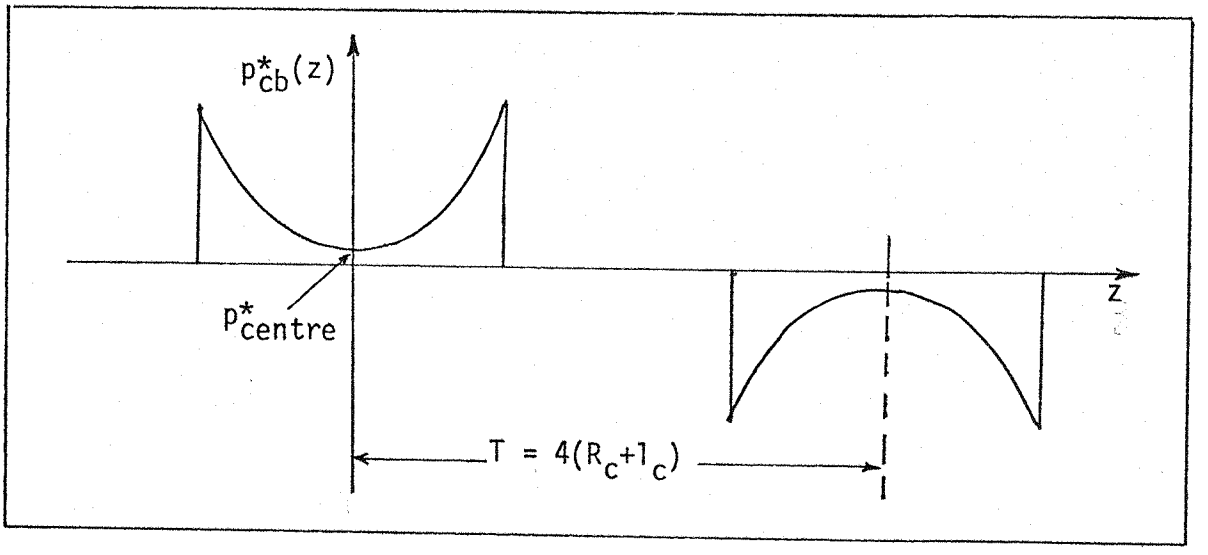

Therefore in order to simplify the calculations we assume a simple exponential variation of the core back surface polarity along the core length

$$p^*_{cb}(z) = p^*_{centre}\, e^{kz} \quad \text{for} \quad 0 \leq z \leq l_c$$

where k is dependent on the machine geometry.

$$p^*_{cb}(z) = 0 \quad \text{for any other interval in the semi-period.}$$

Therefore

$$p^*_{cb}(z) = \sum_{n=odd} f_n \cos \frac{n\pi z}{4(R_c + l_c)}$$

where:

$$f_n = \frac{1}{R_c + l_c} \int_0^{l_c} p^*_{centre}\, e^{kz} \cos \frac{n\pi z}{4(R_c + l_c)}\, dz$$

$$\therefore \quad f_n = \frac{p^*_{centre}}{R_c + l_c} \cdot \frac{e^{kl_c}}{k^2 + \left(\frac{n\pi}{4(R_c + l_c)}\right)^2} \cdot \left[\cos \frac{n\pi l_c}{4(R_c + l_c)} + \right.$$

$$\left. + \frac{n\pi}{4(R_c + l_c)} \cdot \sin \frac{n\pi l_c}{4(R_c + l_c)} \right] \qquad (4.60)$$

Therefore this expression for f_n allows us to obtain the magnetic field components due to the surface polarity at the stator core back after substitution into the formulae (4.40), (4.41) and (4.40).

CHAPTER FIVE

LEAKAGE FLUX AT THE STATOR CORE BACK OF THE SYNCHRONOUS MACHINE UNDER SHORT CIRCUIT CONDITIONS

5.1 GENERAL

The short circuit operation is determined by a symmetric short circuit applied to the stator winding terminals before exciting the synchronous machine. The field current is gradually increased in order to obtain the desirable value of short circuit current.

During short circuit conditions the synchronous machine contains practically no flux in the air gap and with the short circuit around the level of the normal operating current the internal flux is smaller than the steady state operation flux. Actually the field mmf must just be large enough to overcome the opposing stator mmf and to generate an emf for circulating the short circuit current in the stator windings.[4]

The short circuit characteristic gives the relationship between the stator current (stator mmf) and the field current (field mmf) when the stator windings are symmetrically short circuit and the machine is running at normal speed (figure 2.1).

Because the flux is small the saturation effect in the iron core at short circuit operation is negligible and the short circuit characteristic of the synchronous machine is a straight line, which would not be so far guaranteed by a very high short circuit current, at normal speed, which would imply in a high correlated field current and a consequent leakage flux that could produce saturation.

In practical machines the stator winding mmf waveform is close to a sinusoidal one, but actually this waveform is composed of fundamental and harmonic components.[38] The harmonics of the field mmf

are not overcome by correlative parts in the stator mmf, therefore the resultant air gap flux waveform has a large harmonic content, as shown in figure 5.1. In a real case the air gap flux is not equal to zero due to the existence of harmonics.

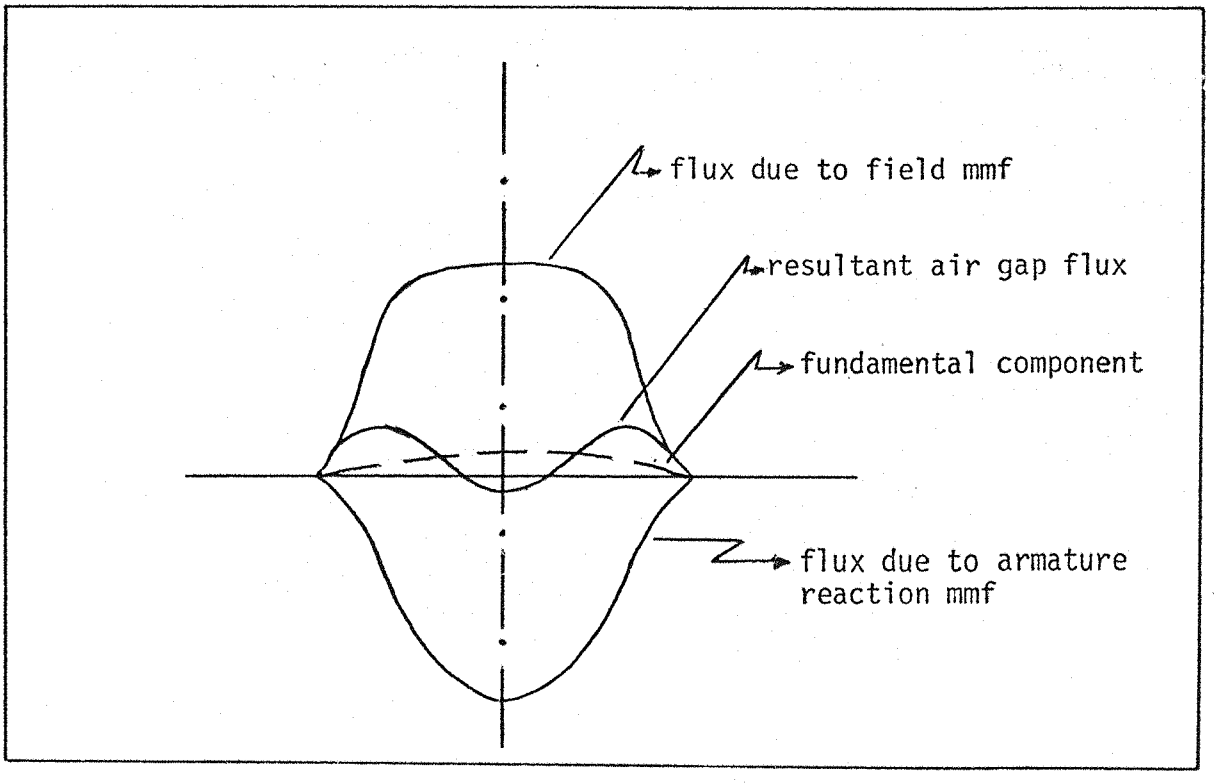

Fig.5.1: Short circuit airgap flux and mmf

The salient pole synchronous machine has large third harmonic mmf components due to the saliency contribution which has no counterpart in the stator mmf. Therefore there exists a troublesome harmonic air gap flux. The harmonics in the air gap flux waveform increase the iron losses observed in the stator core and teeth since they establish an alternating flux in the stator that has three times the fundamental frequency.

Under short circuit operation the field in the synchronous machine end region depends on the combination of the opposing stator winding mmf and rotor windings mmf. The losses are directly linked to the value of flux density in each particular site. The stator winding

shape is of substantial importance in the determination of the distribution of leakage flux when the synchronous machine is operating on short circuit conditions.

5.2 THE CONTRIBUTION OF MAGNETIC SOURCES

The various magnetic sources of core back leakage flux have been discussed in Chapter Three. Under short circuit conditions, the magnetic field in the air gap of the synchronous machine is practically equal to zero. Actually a very small air gap magnetic field could be expected to exist due to harmonics caused by the rotor system. Although since both the stator and rotor iron surfaces of a synchronous machine have a high permeability the surface polarities at both surfaces are equal to the radial components of the flux density crossing the surfaces, as shown in section 3.3. Therefore, there are very small distributions of magnetic poles at the core bore surfaces which are expected to have a larger concentration at the edges. Consequently the magnetic surface polarity at the stator bore makes a negligible contribution to the leakage flux at the stator core back and there is no air gap fringing flux.

On the other hand, the overhang contribution to the core back leakage flux is of fundamental importance since the overhang current produces the magnetic field that magnetises the iron surfaces. The effects of the current amplitude are presented in section 5.3.3. The intensity of magnetisation of both the core front and core back surfaces are also dependent on both the shape and geometry of the overhang. The magnetic field equations for the overhang are shown in Chapter Four. Both the surface polarities at the core front and core back are implicit sources and have an important interaction due to their relative positions. In the laboratory synchronous machine used

in the investigations no magnetic screen was used, therefore, the distribution of magnetic poles at the core front has a larger intensity than if the magnetic screen was present.[66] The secondary electromagnetic sources discussed in Chapter Three have a very small effect on the core back leakage flux. The volume polarity is localised at the ends of the synchronous machine. The eddy current effects were small since the stator core was built up by iron laminations and no magnetic screen was used at the core fronts. Therefore during the short circuit operation the most important sources are: the overhang current, the polarity on disc surfaces at the core front and the polarity at the back of the core.

5.3 LEAKAGE FLUX DISTRIBUTION

The distribution of leakage flux was examined in the space surrounding the stator core back surface. Actually the three components of leakage flux were surveyed around the core back region and their variations against both the axial and radial directions were investigated. The overhang current effects on the leakage flux distribution are presented.

5.3.1 Variation of the Leakage Flux Along the Stator Core Back Length

The leakage flux distribution along the stator core back length of the synchronous machine is not a uniform one. The edges of the stator core back have a concentration of leakage flux greater than the centre zone. This phenomenon is explained by the fact that the edges of the core back are closer to the magnetic sources than the centre region. The closer a magnetic source is to a region the bigger is the magnetic field produced by that source at that region.

Actually the effects of elements of either current or magnetic surface polarity sources vary inversely with the square of the distance between those elements and the region under consideration.[51] Figure 3.1 shows the main sources of core back leakage flux and confirms the fact that the main magnetic sources are closer to the edges of the core back region.[46]

An ideal synchronous machine must have symmetry between each half side of the stator core back region. Therefore the leakage flux intensities at each half side are equal in an ideal machine. This is not followed by the laboratory machine used seeing that it has no mechanical, electrical and magnetic symmetry. Consequently the two edges of the core back do not have the same leakage flux intensities.

Figure 5.3a shows the variation of the radial component of the leakage flux density along the stator core back length for different short circuit currents. The radial leakage flux intensity at the core back edges is greater than at the centre zone. Figure 5.3b also shows the variation of the radial component along the core back length. But in this case a more distant region from the core back surface is considered. The intensity of radial leakage flux is still bigger at the edges of the core back. Although in figure 5.3b the curves are flatter than those presented in figure 5.3a.

The variation of the axial component of leakage flux density along the stator core back length is shown in figure 5.4. The axial component also has a higher value at the edges. The intensity of the axial leakage flux at the centre zone of the core back is equal to zero. Figure 5.5 shows the variation of the circumferential component of leakage flux density along the length of the core back. Again the highest intensity is found to be at the core back edges. The curves of the circumferential component are flatter than both the axial and

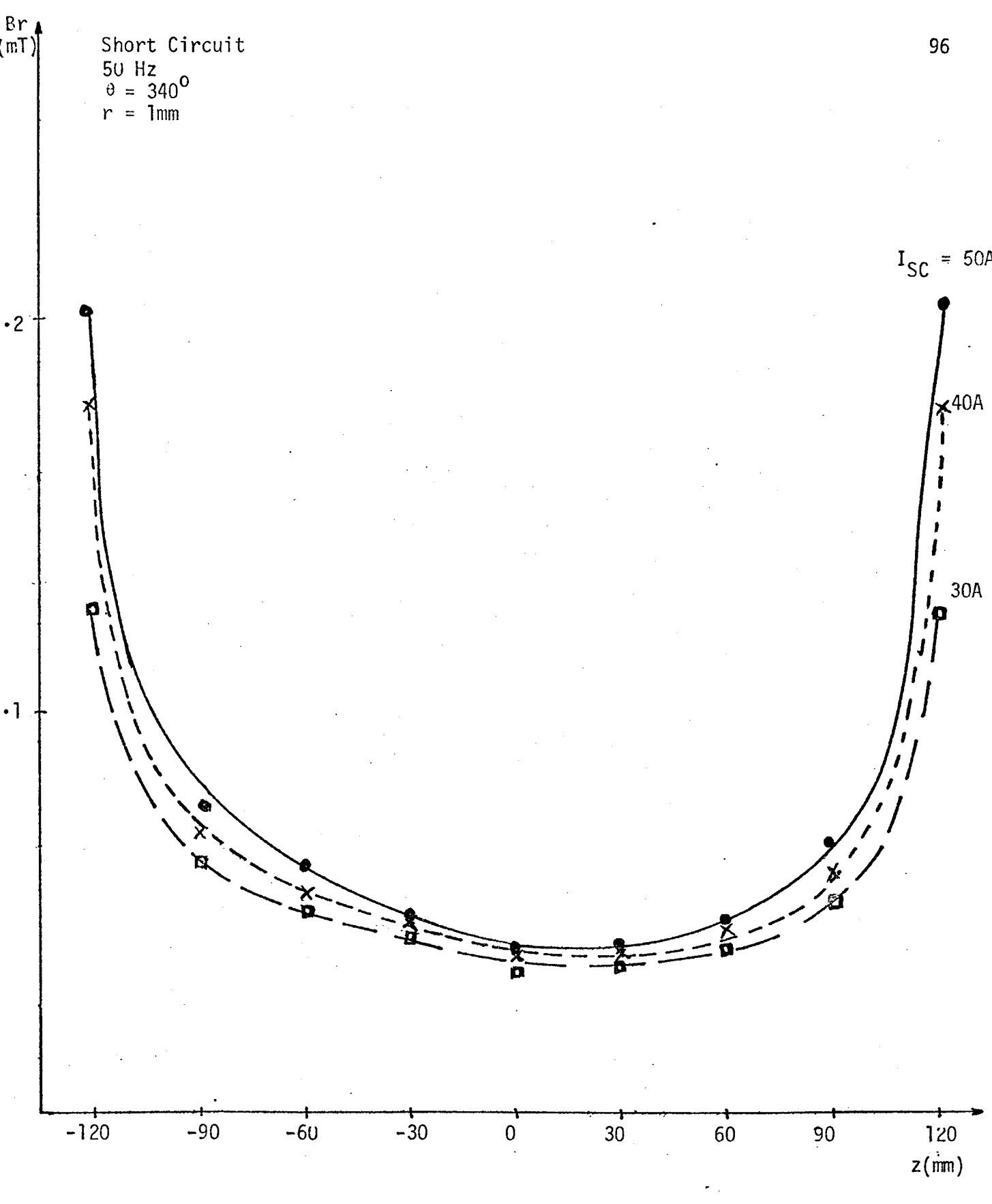

Fig. 5.3.a: Variation of the radial leakage flux density along the stator core back length.

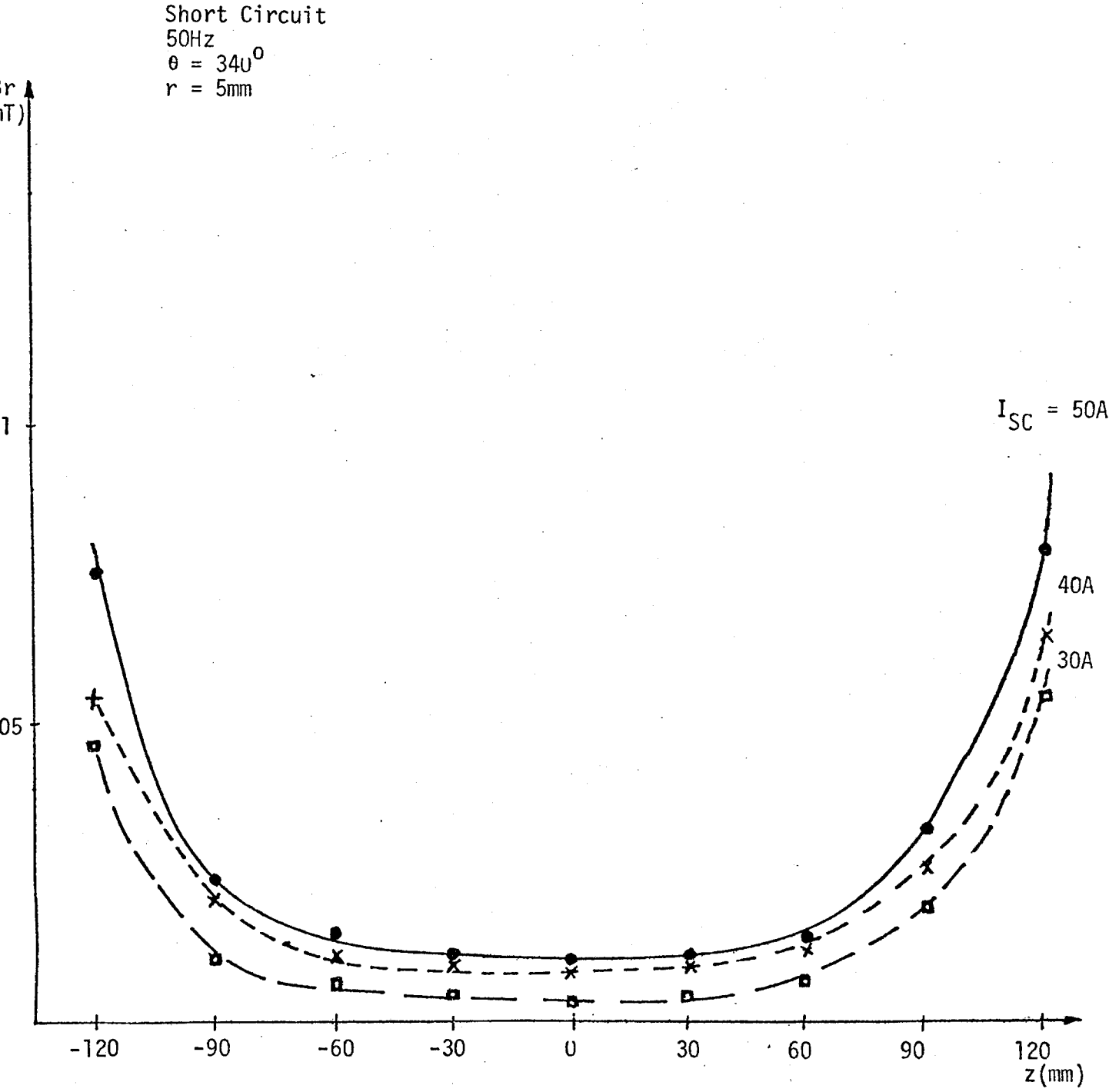

Fig. 5.3.b: Variation of the radial leakage flux density along the stator core back length.

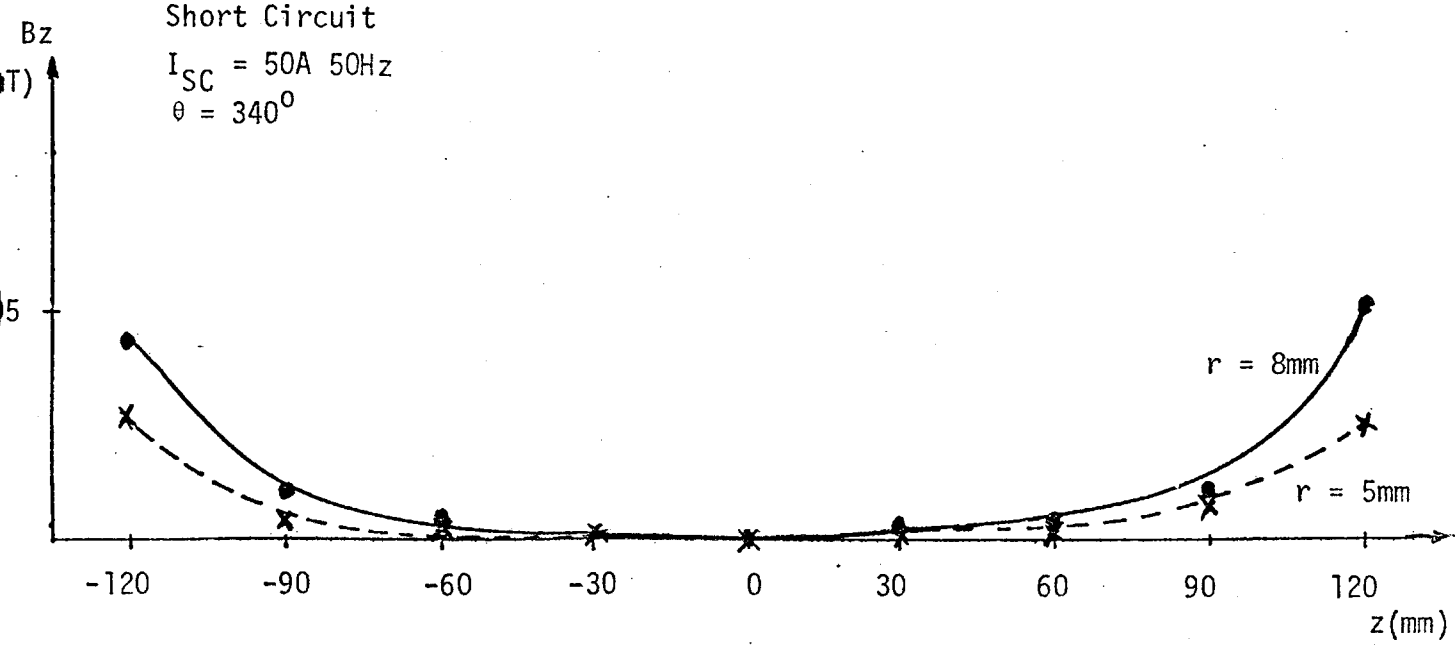

Fig. 5.4: Variation of the axial leakage flux density along the stator core back length.

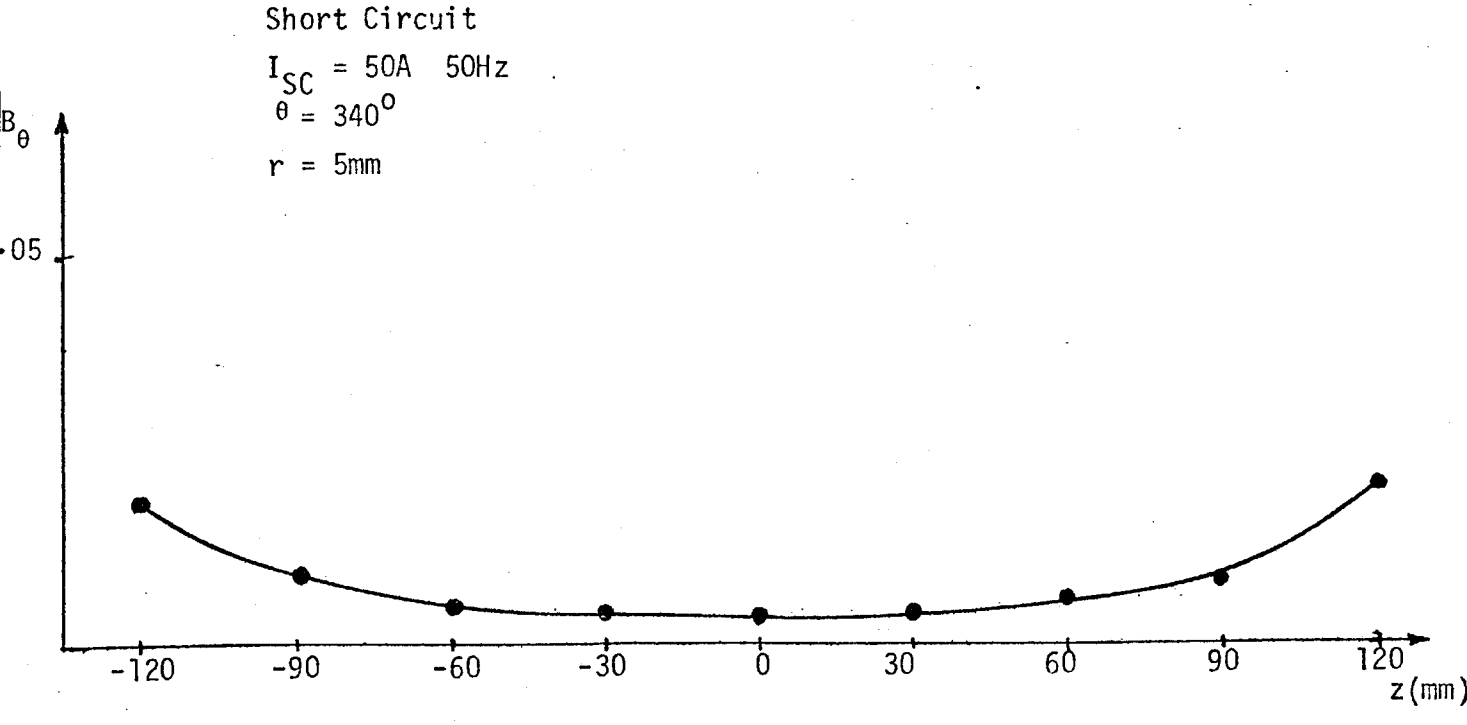

Fig. 5.5 : Variation of the circumferential leakage flux denstiy along the stator core length.

radial components. This phenomenon can be explained by the fact that most of the magnetic sources have a tendency to divert the core back leakage flux either to the radial or axial directions. Although the surface polarity at the core back can also contribute with a leakage flux in the circumferential direction, as shown in figure 5.2.

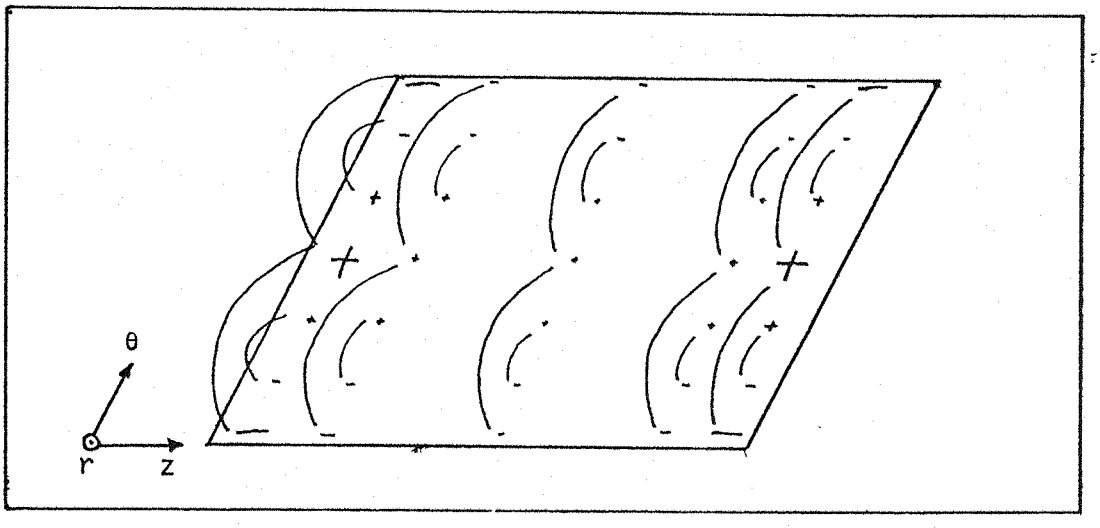

Fig. 5.2: Circumferential leakage flux produced by the surface polarity at the back of the core

5.3.2 Variation of the Leakage Flux With the Distance From the Stator Core Back Surface

The leakage flux diminishes with the distance from the stator core back surface. Figure 5.7 shows the variation of the radial component of the core back leakage flux density against the distance from the stator surface at both the edges and the centre regions. The radial component decreases sharply with the distance from the core back surface, indicating that its biggest concentration is at the surface. Actually, at the surface of the stator core back most of the leakage flux is practically composed of the radial component.

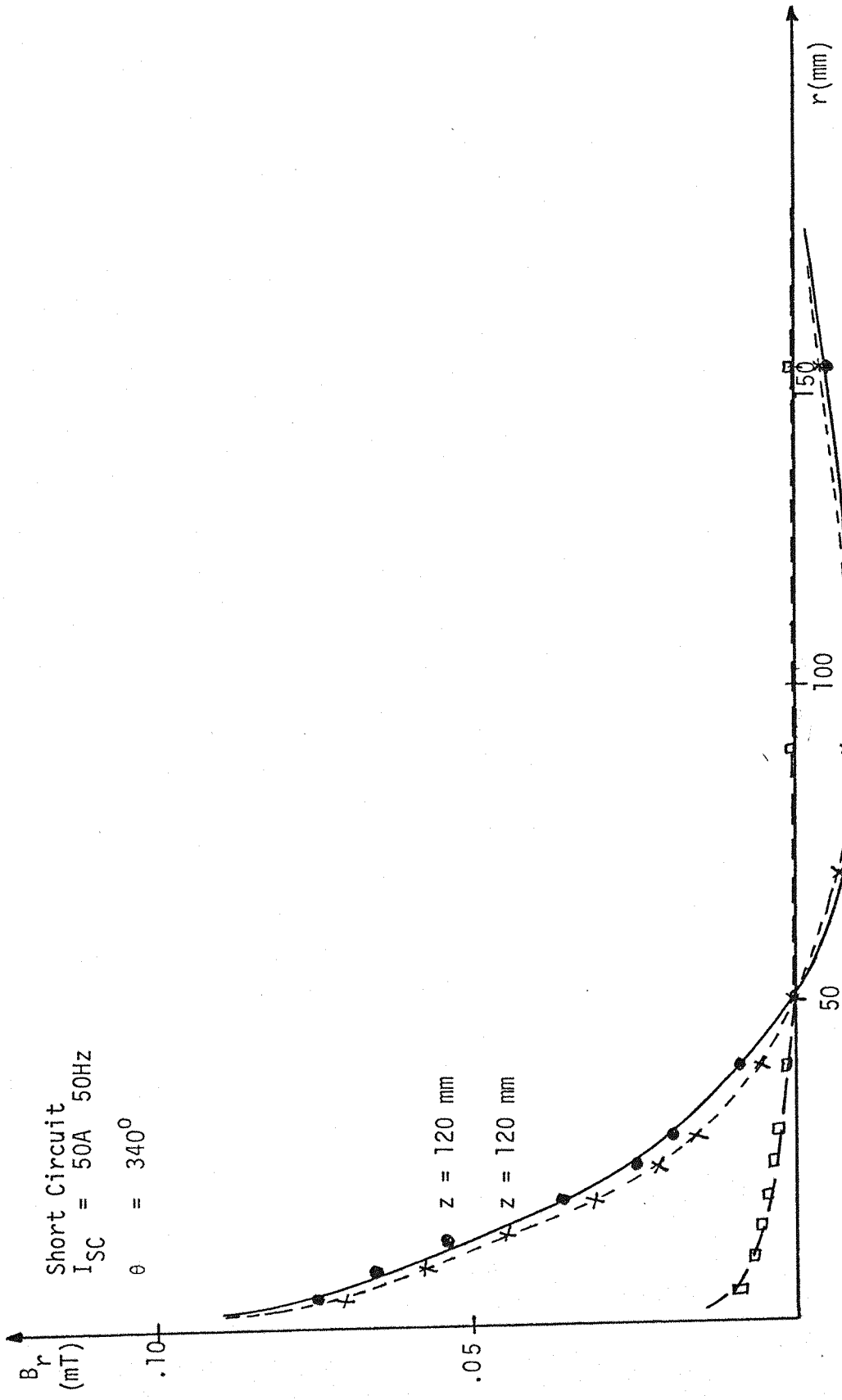

Fig. 5.7: Variation of the radial leakage flux density against the distance from the stator core back surface.

Supposing a solid stator core with a constant and infinite permeability with every line of flux emerging from the air to the core or from the core to the air, should get perpendicular to the iron surface which would be an equipotential surface. The relationship between the angles of incidence and refraction in the iron/air interface has been described by several authors on electromagnetism.[50,51,57-60] Figure 5.6 shows the boundary conditions at the interface iron/air.

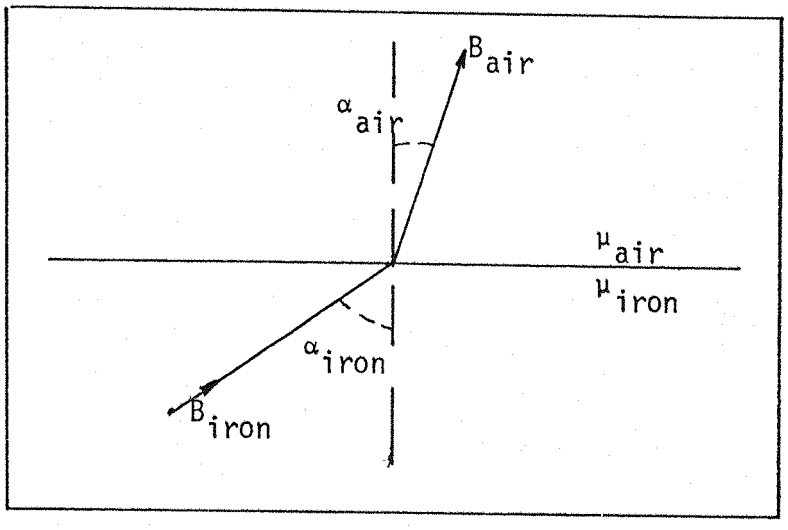

Fig. 5.6: Boundary conditions at the interface iron/air

Therefore the angles of incidence and refraction in the iron/air interface are given by:

$$\tan \alpha_{air} = \frac{1}{\mu_{r_{iron}}} \cdot \tan \alpha_{iron} \qquad (5.1)$$

where $\mu_{r_{iron}}$ is the relative permeability of the iron.

Consider a solid iron with a uniform and very high permeability, the value of $\mu_{r_{iron}}$ tends to infinity ($\mu_{r_{iron}} \to \infty$) therefore $\tan \to 0$ $\therefore$ $\alpha_{air} = 0^{o}$, which means that the flux line is perpendicular to the iron surface at the interface iron/air.

In an ideal case of uniform and infinite permeability, the flux line is perpendicular to the iron plane independently of the angle that the flux line has with the iron surface inside the iron, which is shown by equation (5.1) when $\mu_{r_{iron}} \to \infty$ is substituted. As the permeability decreases to small values the angle α_{air} passes to be also dependent on α_{iron}.[51] In a real case of laminated stator core machines the angle α_{air} will not be exactly equal to 90^{o} and will vary along the stator core length depending on saturation levels of each considered region as well as on the stacking factor. Therefore both the axial and circumferential components have their amplitudes increased. When the stacking factor is very high both axial and circumferential leakage flux components are small at the stator core back surface.

Figure 5.7 shows that at the edges of the core back the radial leakage flux first decreases sharply, then becomes negative, reaches a minimum and finally tends to zero as the distance is continuously increased. The sharp decrease of the leakage flux is due to the fact that the strength of the sources field decreases with the square of the distance. The total leakage flux at the stator core back is determined by the vector sum of the individual contribution of the sources. The sources do not produce magnetic fields with the same directions. The surface polarity source at the core back has the predominant contribution to the leakage flux at regions close to the core back surface. But compared with the other main magnetic sources the core back surface polarity has the smallest distribution of magnetic poles. The fact that the radial leakage flux becomes negative is explained by its change of direction which is opposite to the direction previously presented by the radial component with positive amplitude. The flux component caused by the surface polarity at the core back decreases more rapidly than those components caused by other main

sources. Therefore the radial leakage flux has a minimum value and afterwards tends to zero. At the centre region of the stator core back the radial leakage flux decreases straightforward because the surface polarity at the core back has the predominant effect even at regions more distant from the core back surface. That phenomenon is more expressive if the synchronous machine has a very long stator core.

Figure 5.8 shows the variation of the axial component of the leakage flux density against the distance from the stator core back surface. The axial leakage flux at the stator core edges initially increases, then reaches a maximum value and finally tends to zero when the distance is continuously increased. The increase in axial leakage flux component with the distance is explained by the diversion of the radial component into the axial direction. That phenomenon is particular of the leakage flux at regions close to the stator core back surface. Therefore the axial component of leakage flux density reaches a maximum and starts to decrease because the magnetic sources contributions become smaller with larger distances. At the centre of the stator core back the axial leakage flux is equal to zero.

Figure 5.9 shows the circumferential leakage flux density component variation with the distance from the stator core back surface. The circumferential component of the leakage flux has a smoother variation with the radial distance from the core back surface. This is explained by the fact that there is a tendency of the core back leakage flux of linking the end regions of the stator where the largest sources are located. Although it has been shown before in figure 5.2 that there is also a circumferential leakage flux that links the core back regions. The greatest part of them is due to the surface polarity at the core back. The circumferential component also has an initial

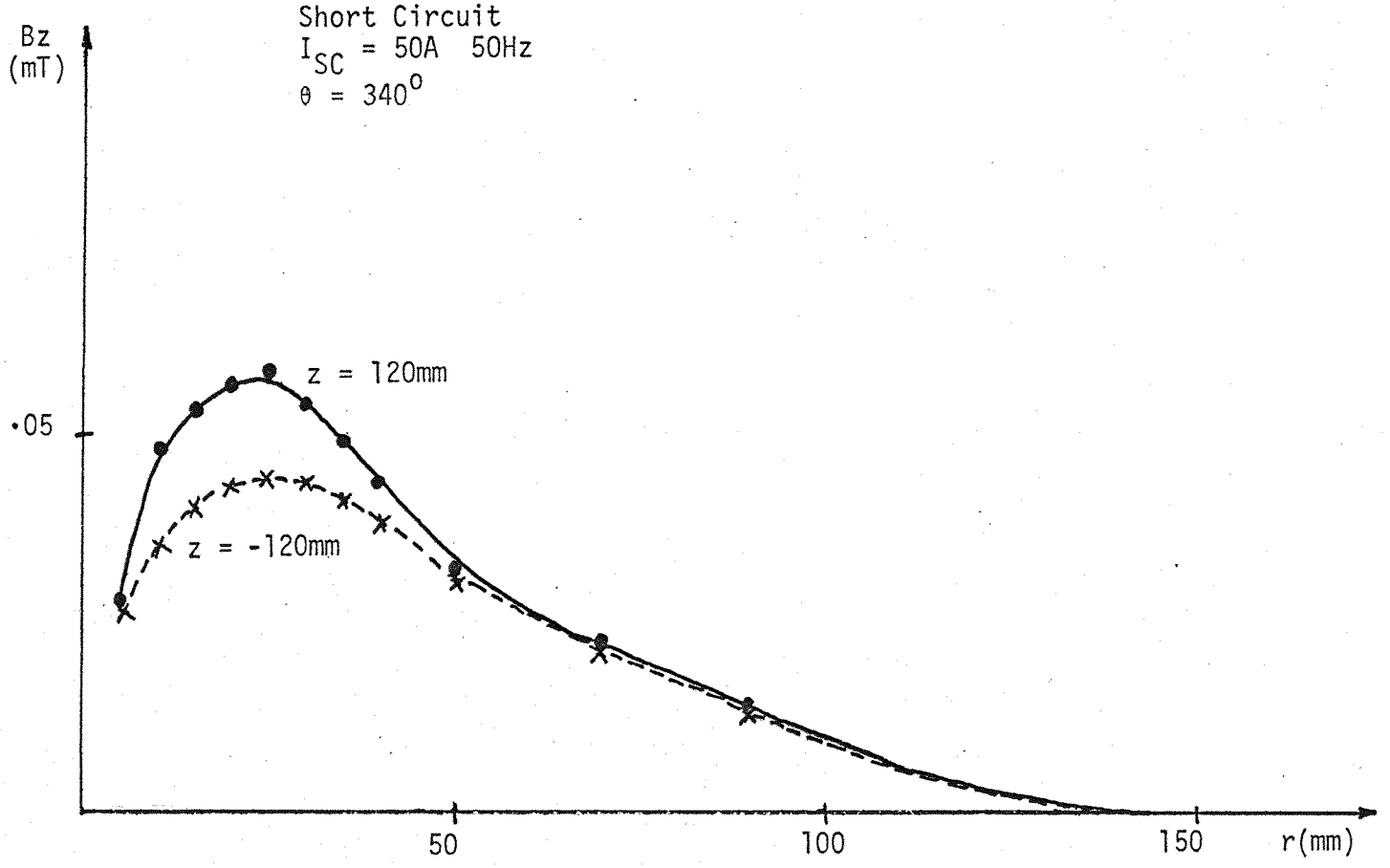

Fig. 5.8: Variation of the axial leakage flux density against the distance from the stator core back surface.

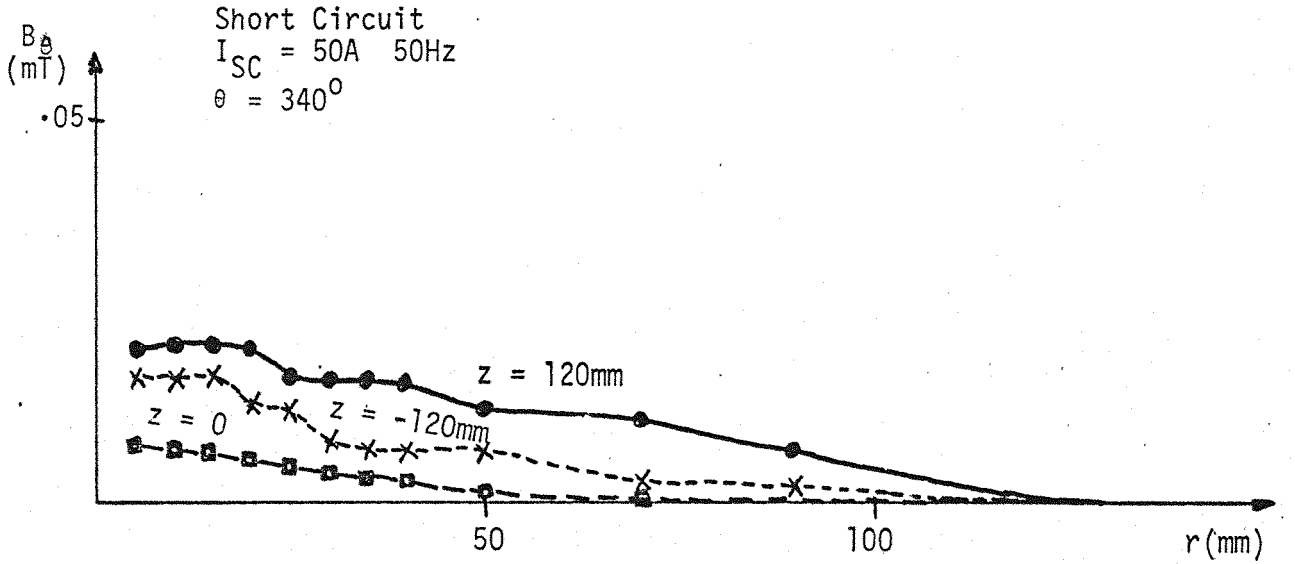

Fig.5.9: Variation of the circumferential leakage flux density against the distance from the stator core back surface.

increase due to radial leakage flux component that is diverted to the circumferential direction. The circumferential component of leakage flux is not equal to zero at the centre of the stator core back.

5.3.3 Effects of the Overhang Current

When the synchronous machine is operating on short circuit the overhang current (short circuit current) increases or decreases with the field current at constant frequency, as shown before in Chapter Two (figure 2.1). The leakage flux increases with the increase in the overhang current. That is in agreement with the field equations presented in section 4.3.1 of Chapter Four, for the different shapes of overhang.

The increase of leakage flux with the overhang current is not the same along all the stator length. The leakage flux at the stator core back edges have a greater increase than at the centre regions of the core back because the edges are closer to the overhang sources.

The distributions of magnetic poles at both surfaces at the stator core back and the stator core front are increased with the increase on the overhang current. Therefore an increase in the explicit source causes an increase in the implicit sources, which means greater leakage flux. This fact emphasises that the increase in the power output of synchronous machines achieved by the increase in the winding current can establish larger leakage flux at the stator core back.

Both figure 5.10a and figure 5.10b show the variation of the radial leakage flux density against the overhang current during the short circuit operation at both the edges and the centre of the stator core back. The first figure considers points closer to the stator core back surface than the second one. In both figures the effects on the

leakage flux distribution are more prominent at the edges of the core back. Figure 5.11 shows the variation of the axial component against the overhang current during short circuit conditions. The circumferential leakage flux component has a similar effect at both the edges and the centre regions caused by the overhang current. The circumferential component is less affected by the variation on the overhang current than the other two components.

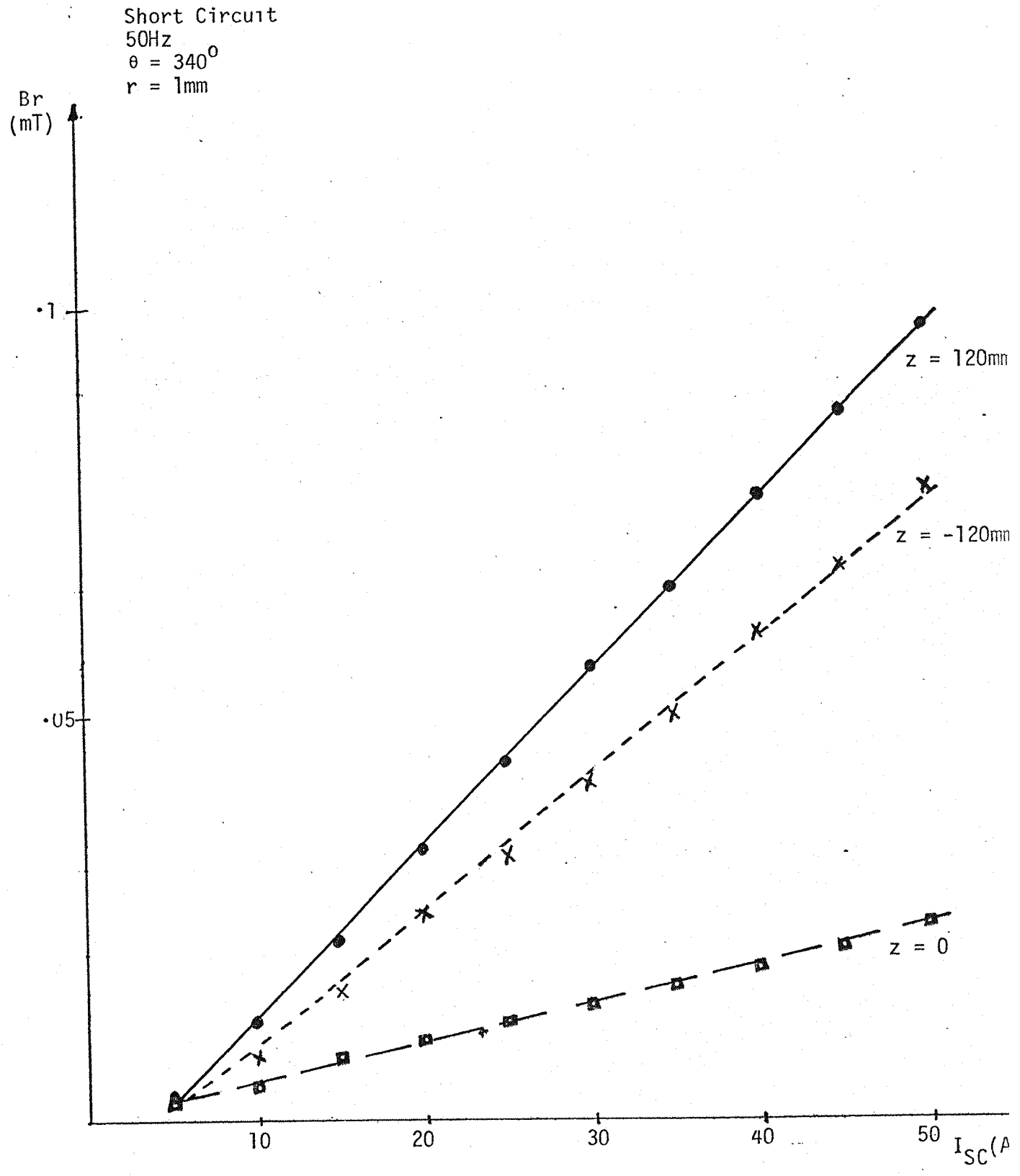

Fig. 5.10.a:Variation of the radial flux density against the short circuit current.

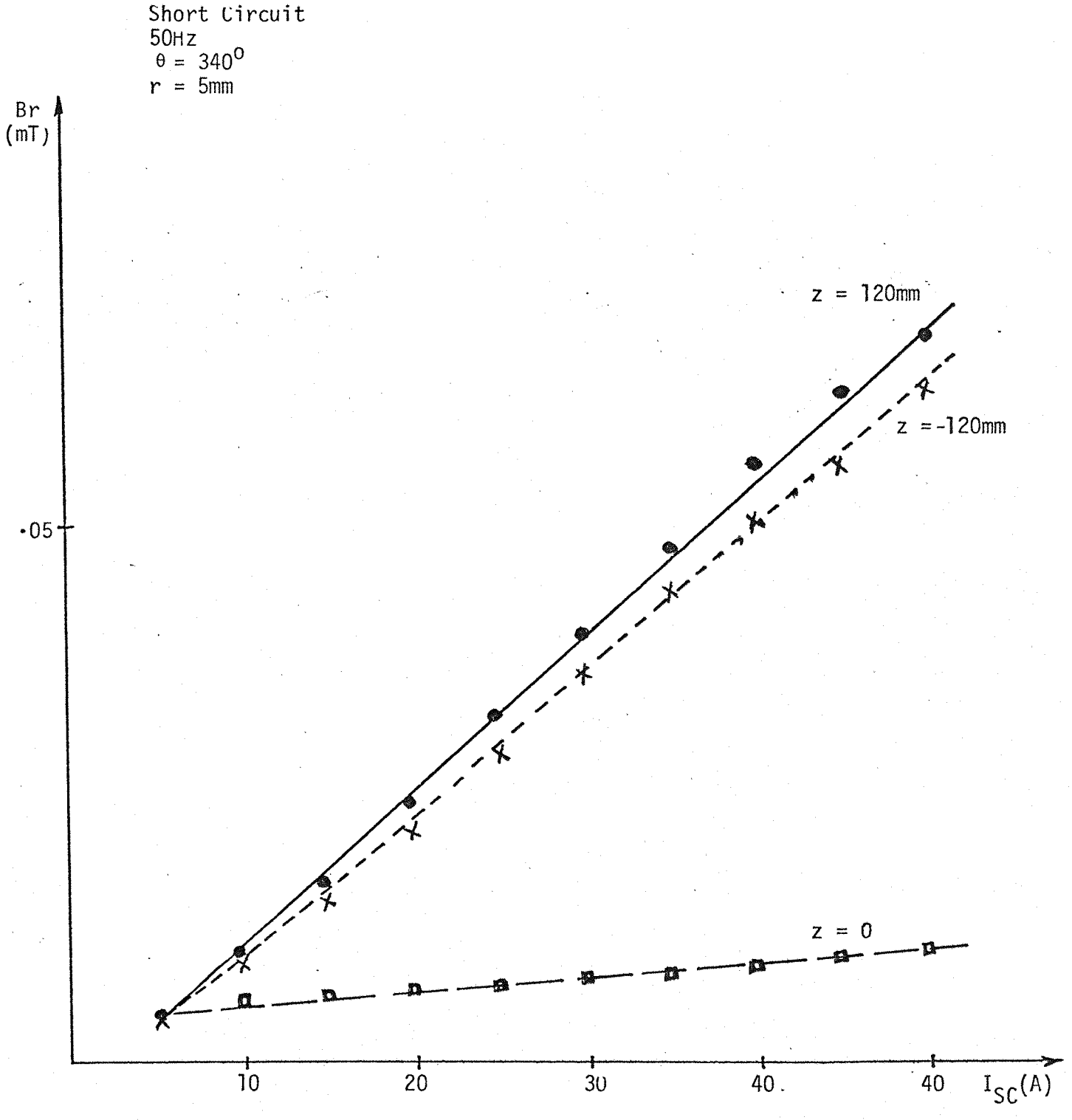

Fig. 5.10.b: Variation of the radial leakage flux density against the short circuit current.

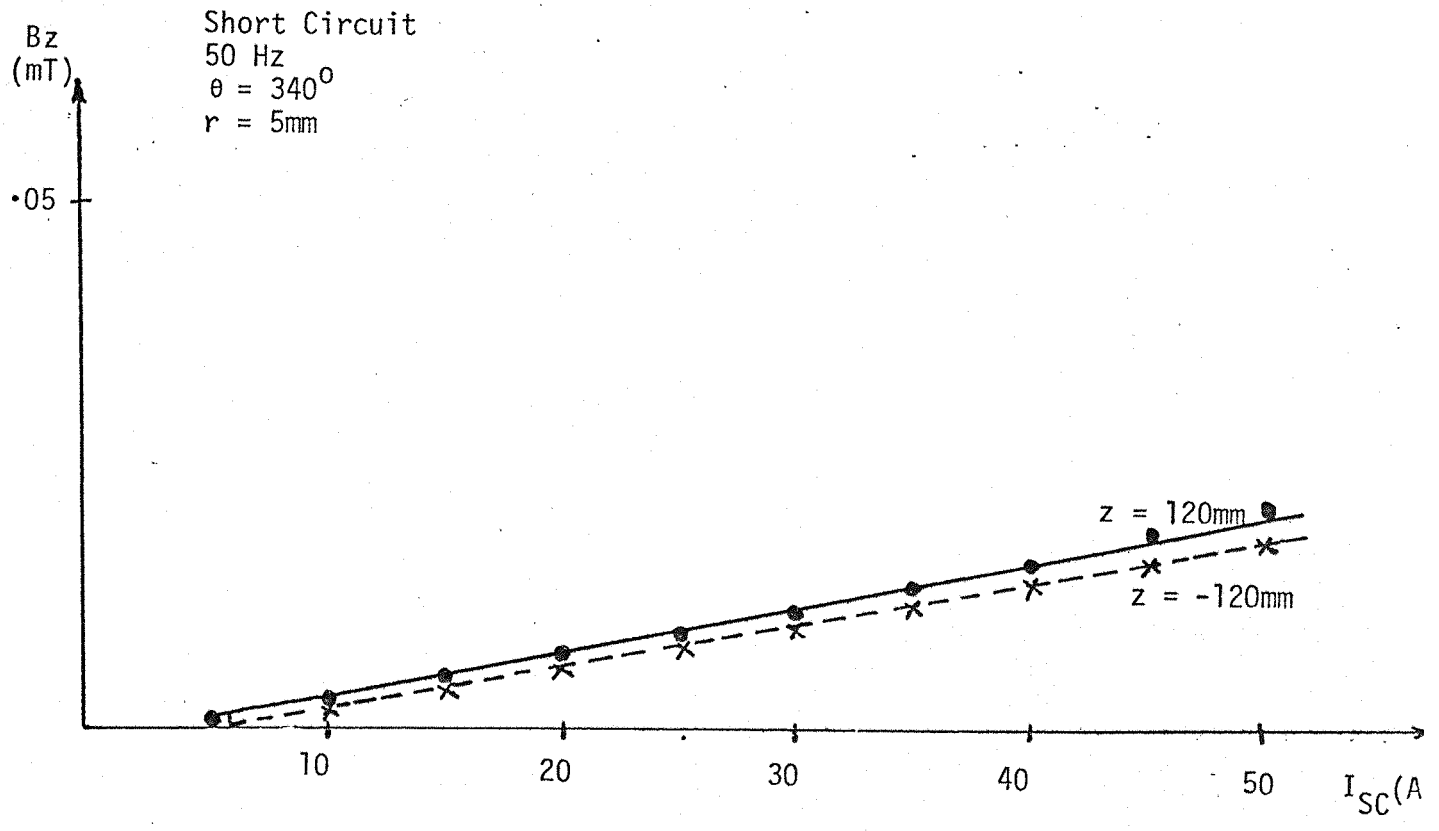

Fig. 5.11: Variation of the axial leakage flux density against the short circuit current.

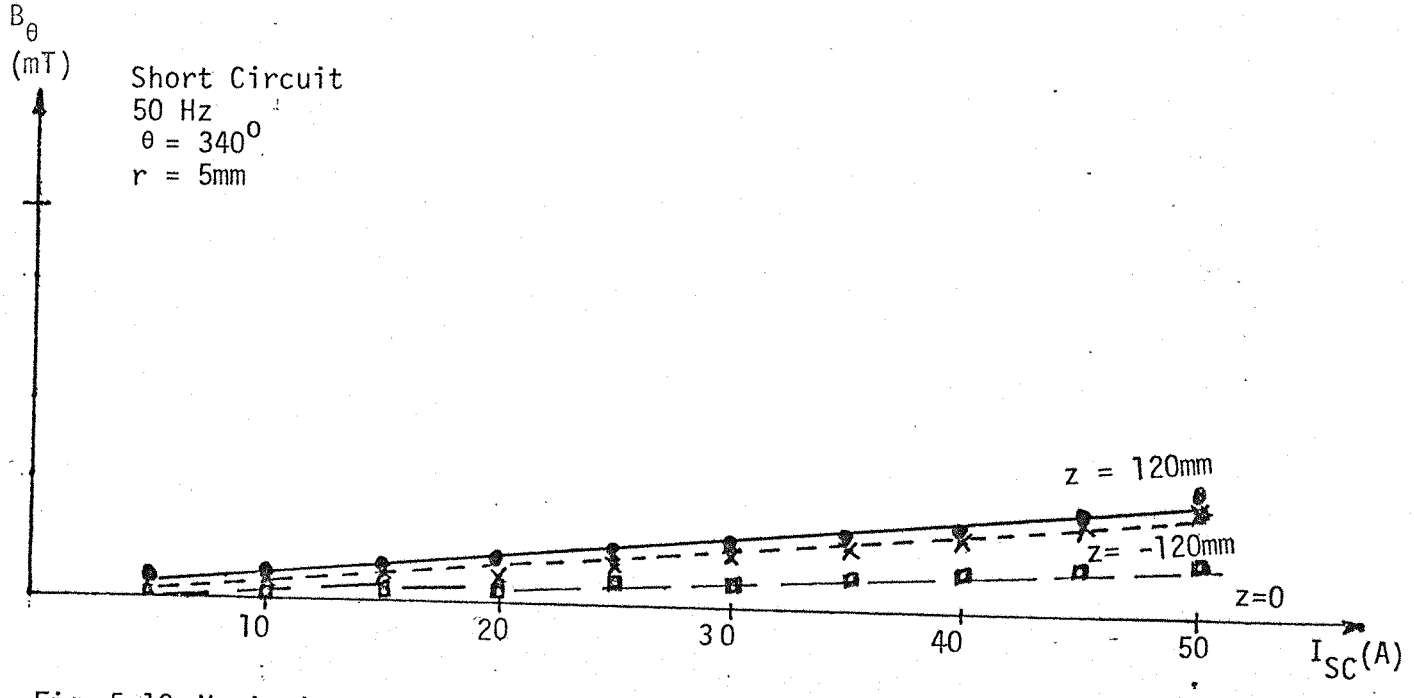

Fig. 5.12: Variation of the circumferential leakage flux density against the short circuit current.

CHAPTER SIX

LEAKAGE FLUX AT THE STATOR CORE BACK OF THE SYNCHRONOUS MACHINE UNDER OPEN CIRCUIT CONDITIONS

6.1 GENERAL

The synchronous machine is operated under open circuit conditions when the stator winding terminals are disconnected and the field winding excited by a d.c. current with the rotor rotating at a constant speed. The stator windings carry no current during open circuit operation. Then there is no armature reaction which means that it is only necessary to supply a driving torque to overcome the opposing torque due to windage and friction in order to generate an emf in the stator winding. In open circuit conditions the flux of the synchronous machine is determined by the field mmf.[64] Assuming that the rotor is driven at a constant angular speed, which means constant frequency, the alternating induced emf is proportional to the flux linking the stator windings.

The open circuit characteristic gives the relationship between the open circuit voltage, at normal speed, and the field excitation (figure 2.1). The open circuit operation is used to determine both the losses caused by the flux required to produce rated open circuit voltage and saturation effects when the machine has constant main frequency. The relationship between the open circuit voltage and the field current would be a complete straight line if there was no saturation effect.

In an ideally designed machine, the flux distribution round the air gap is sinusoidal, but in practice, it actually has a trapezoidal waveform.[81] Another important fact to be noticed in real machines is that the windings are distributed in slots causing

disturbances in the air gap flux density accentuating its space harmonics components which impose time harmonics together with the fundamental in the alternating emf.

In order to simplify the analysis of the leakage flux at the stator core back the air gap is considered to be crossed by a radial flux distributed sinusoidally both in space and time.[82]

6.2 THE CONTRIBUTION OF THE MAGNETIC SOURCES

Since the stator windings carry no current during the open circuit operation the overhang source does not have any contribution to the core back leakage flux. On the other hand, the bore surface polarity source is present because of the air gap magnetic flux crossing the core bore. Therefore both the stator and rotor surfaces at the core bore are magnetised by the action of the main air gap magnetic field. That does not happen when the synchronous machine is operating in short circuit conditions, as discussed in Chapter Five. The main sources of core back leakage flux during open circuit conditions are: bore polarity, polarity on disc surfaces at the core front and polarity on the back of the core. All of those sources are implicit and interact between themselves. Those sources are shown in figure 3.1.

Both the surfaces at the core front and at the core back are under the action of the fringing field caused by the air gap field. This fringing field can magnetise both the surfaces at the core front and the core back. Because the core front surface is closer to the core bore than the core back surface, it suffers a larger magnetising action from the fringing magnetic field. Therefore the magnetic pole distribution at the core front surface is greater than that at the stator core back surface. The zone of the core front surface closer to the core bore has a larger concentration of magnetic surface polarity.

The fringing field distribution at the ends of the stator core depends on both the shape and dimensions of the core bore. Howe[66] has studied the effects of various shapes of stator core ends on the distribution of the fringing field. The reduction of the magnetic surface polarity at the core front is the target. Since the largest concentration of magnetic poles occurs at the zone of the core front close to the bore, the first aim is to reduce the magnetic surface polarity at that place. This has been achieved with the utilisation of stator core ends made either stepped or rounded. Both the stepped and the rounded stator core ends divert the fringing flux away from the stator core zone close to the core bore. Actually those special arrangements at the stator core ends impose an increase in the flux path length diminishing the magnetising effects of the fringing flux close to the core bore region.

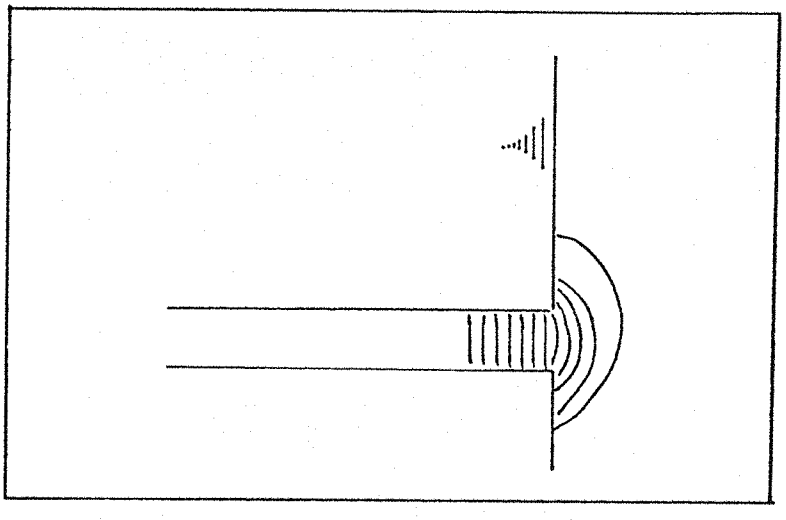

Fig. 6.1: Distribution of the fringing field at the end region of the stator core

The magnetic surface polarity at the core front can also be reduced with the utilisation of either aluminium or copper screens placed in front of the clamping plates. The screening plate imposes an impermeable barrier to the magnetic field and diverts the field from

the stator core front surface. Chapter Three presents a further discussion on the screening plates. Chapter Eight presents some figures which show the effects of the screening plates on the leakage flux.

Therefore, it can be noticed that either the special arrangements on the stator core ends or the magnetic screening plates cause an increase in the length of the magnetic flux path diverting the flux from the core front surface. This means that the effects of the leakage flux are minimised at some regions of the stator core but can be increased to other regions. Actually the magnetic flux diverted from the core front can reach the stator core back causing an enlargement in the magnetic surface polarity at the core back. Depending on the stator core depth the increase in the surface polarity at the core back can reach intensities much higher than those normally expected. Therefore the stator core back region can be under effects of larger leakage flux. Owing to the positions of the magnetic sources, the end zone of the stator core back is likely to have a higher concentration of magnetic poles.

The core back surface can also be magnetised by the main flux that passes through the stator core reaching the core back surface due to finite reluctance of the laminations. The main flux that reaches the stator core back is generally small and depends basically on both the stator core depth and the circumferential permeability of the stator core which is dependent on the size, shape, number and distribution of axial ventilating ducts, the size of laminations segments, the butt-joints and lapping arrangements, and the level of saturation imposed to the stator core. The main flux contributes with a circumferential leakage flux in the laminations at the stator core back and in an ideal synchronous machine it should

have a uniform distribution all over the stator core back length.

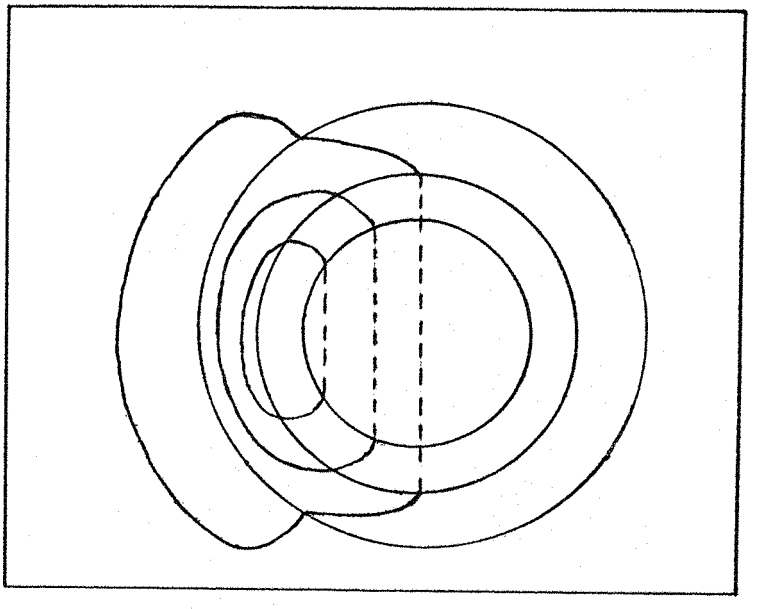

Fig. 6.2 : Main leakage flux at the stator core back

6.3 LEAKAGE FLUX DISTRIBUTION

The distribution of leakage flux was examined in the space surrounding the stator core back surface. The three components: axial, radial and circumferential, were investigated. The eddy current and the saturation effects on the leakage flux distribution are presented. The leakage flux distribution during open circuit operation has the same shape as that obtained in short circuit conditions.

6.3.1 Variation of the Leakage Flux Along the Stator Core Back Length

Also during the open circuit operation the distribution of leakage flux along the stator core back length of the synchronous machine is not uniform. Because the core back edges are closer to the main magnetic sources than the centre region they have a larger concentration of leakage flux.

The variation of the radial component of the leakage flux density at the stator core back against the position along the stator core length is shown in both figure 6.3a and figure 6.3b. The curves presented in both figures were obtained at different distances from the stator core back surface. The curve of figure 6.3a has larger intensities of leakage flux than those in figure 6.3b. That is explained by the fact that the region considered in the first figure is closer to the surface of the core back than that of the second figure; therefore, in figure 6.3a the plane of the measurements was closer to the electromagnetic sources of core back leakage flux. The magnetic surface polarity on the core back has the largest contribution to the core back leakage flux when the region is close to the surface of the core back. The magnetic polarity on disc surfaces at the core front, the bore polarity and the overhang current have a more pronounced effect at the edges of the stator core back than at the centre region. Therefore, because the main electromagnetic sources are closer to the edges than to the centre of the stator, the concentration of leakage flux at the core back end zone is higher than at the centre region, as shown by both figure 6.3a and figure 6.3b. Although figure 6.3b does not show the maximum intensity of the core back leakage flux occurring at the very end of the stator core back. The maximum intensity of leakage flux occurs in the inner regions because the contribution of the polarity on the back of the core at the edge region decreases sharply with the distance from the core back surface and the other main sources' contributions become more effective when more distant points are considered. Close to the corner of the stator core back the leakage flux tends to bend towards the stator core front region where most of the electromagnetic sources of leakage flux are located.

Figure 6.4 shows the variation of the axial leakage flux density component along the stator core length. Figure 6.4a shows

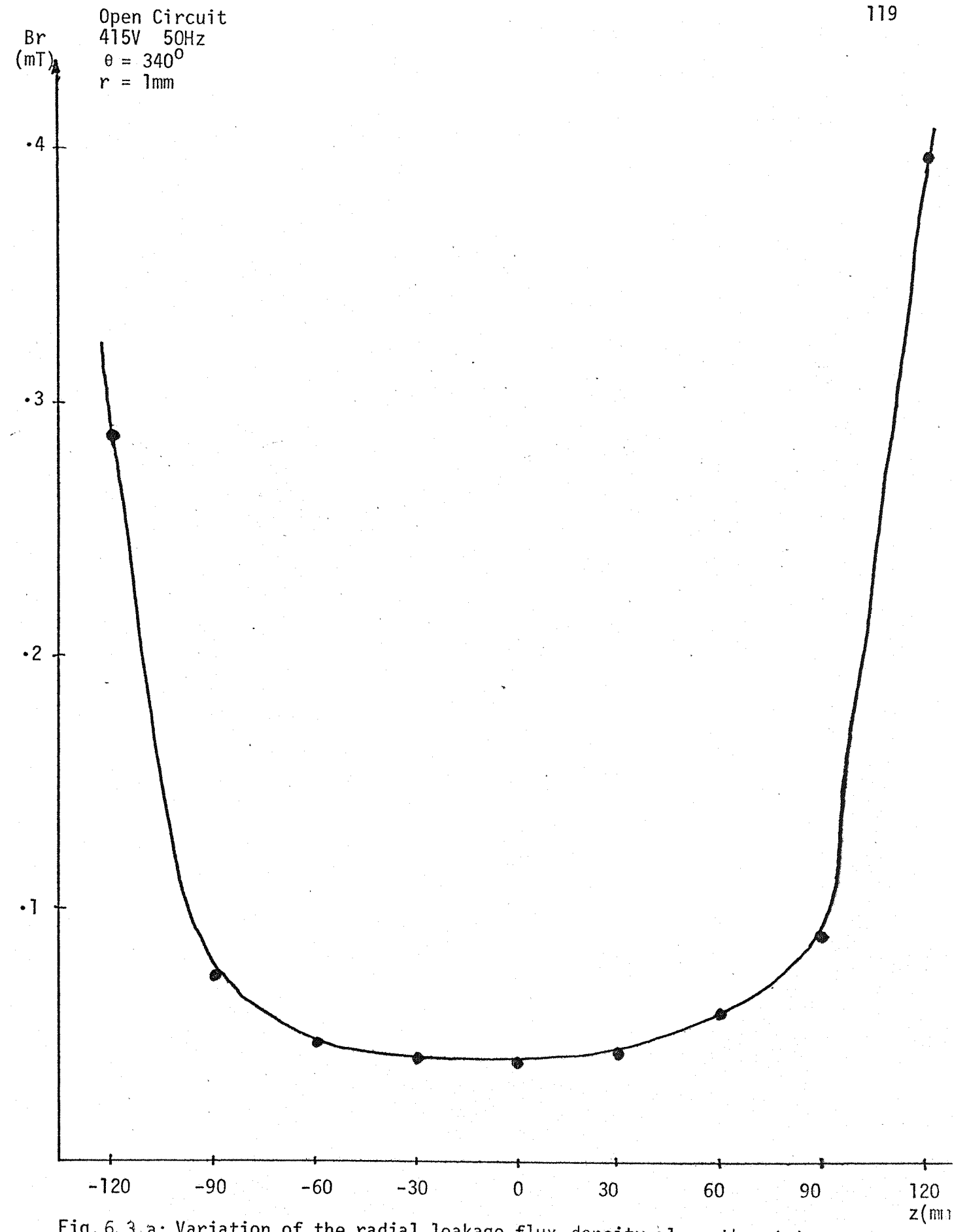

Fig. 6.3.a: Variation of the radial leakage flux density along the stator core back length.

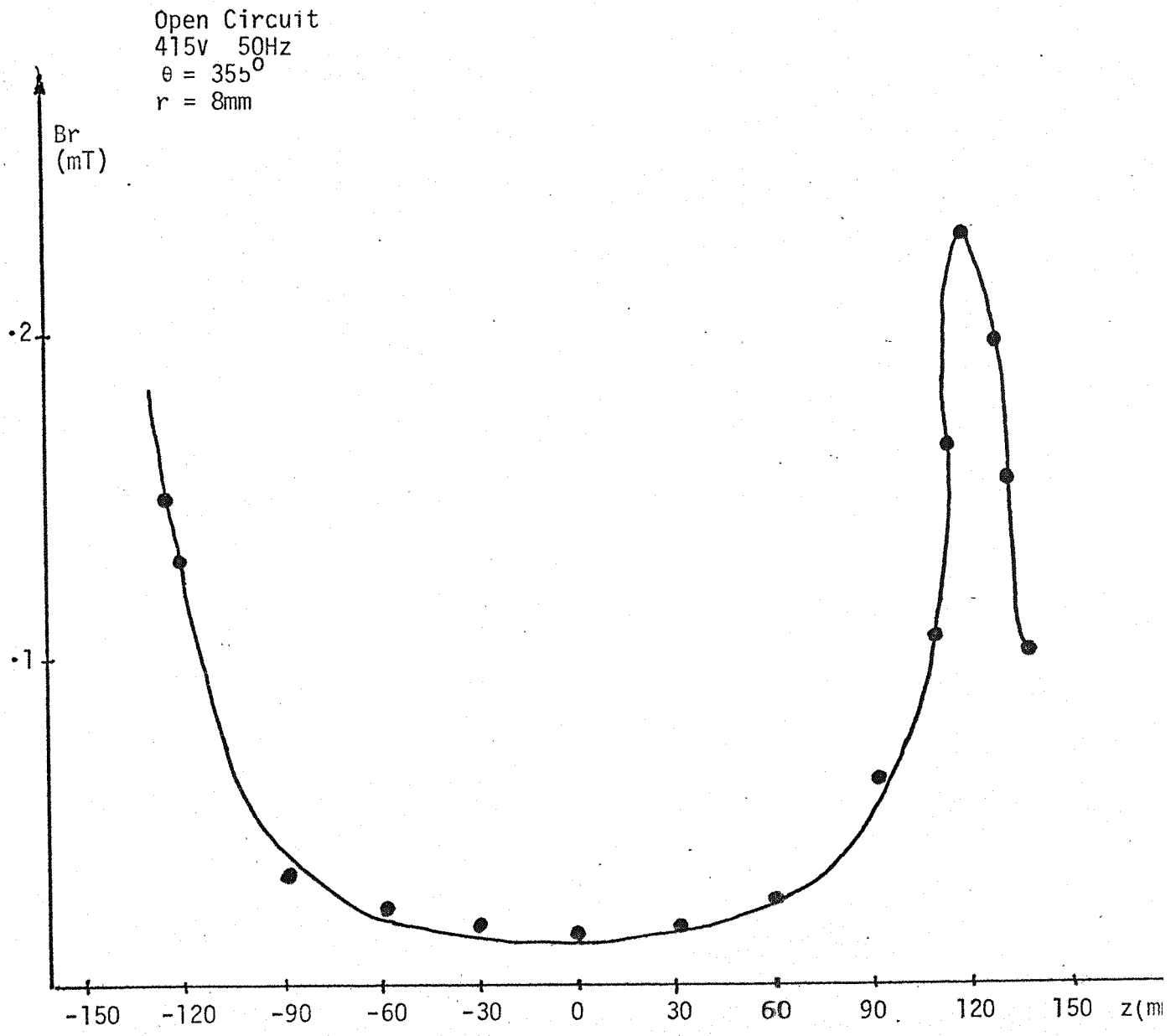

Fig.6.3.b: Variation of the radial leakage flux density along the stator core back length.

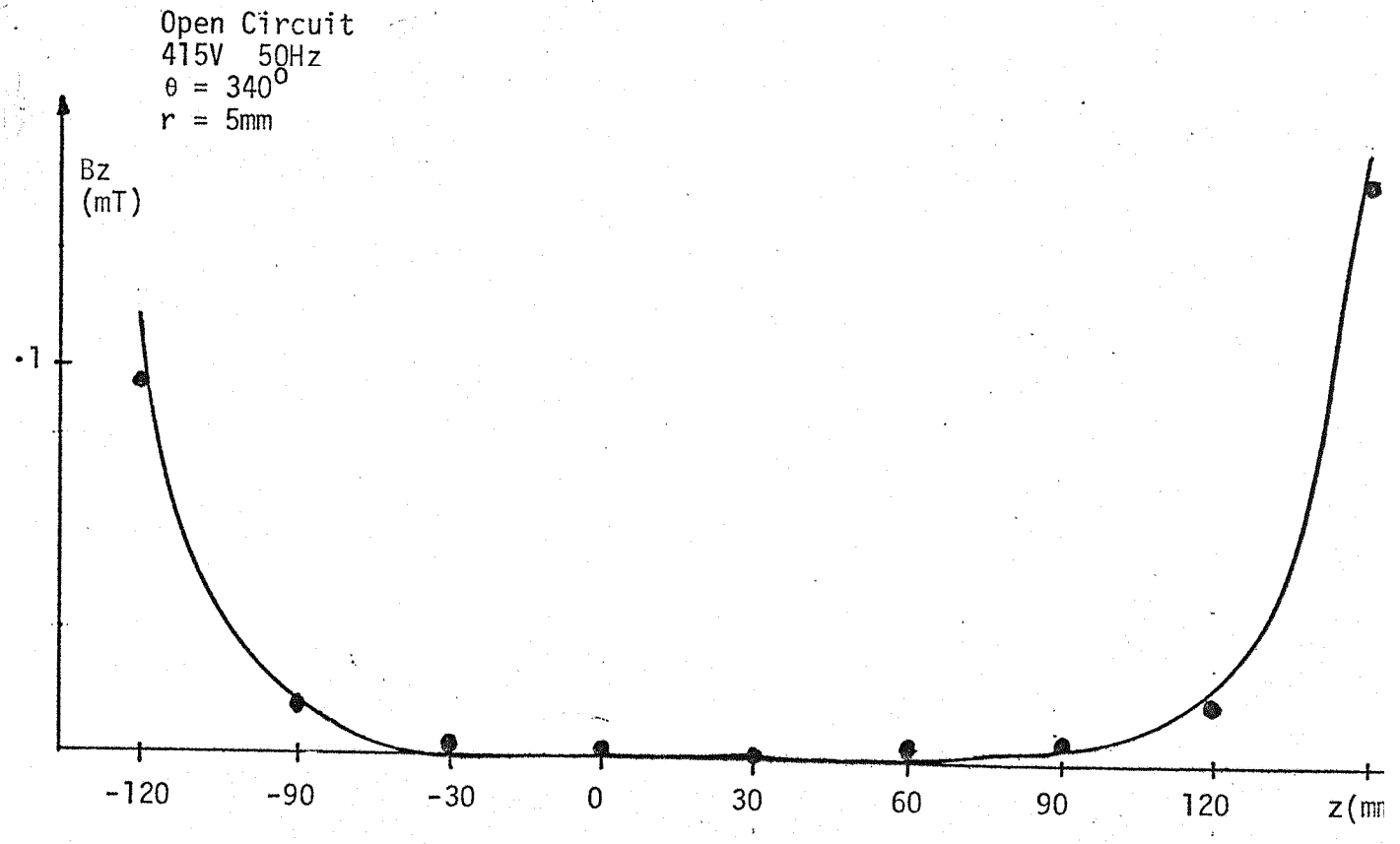

Fig.6.4.a: Variation of the axial leakage flux density along the stator core back length.

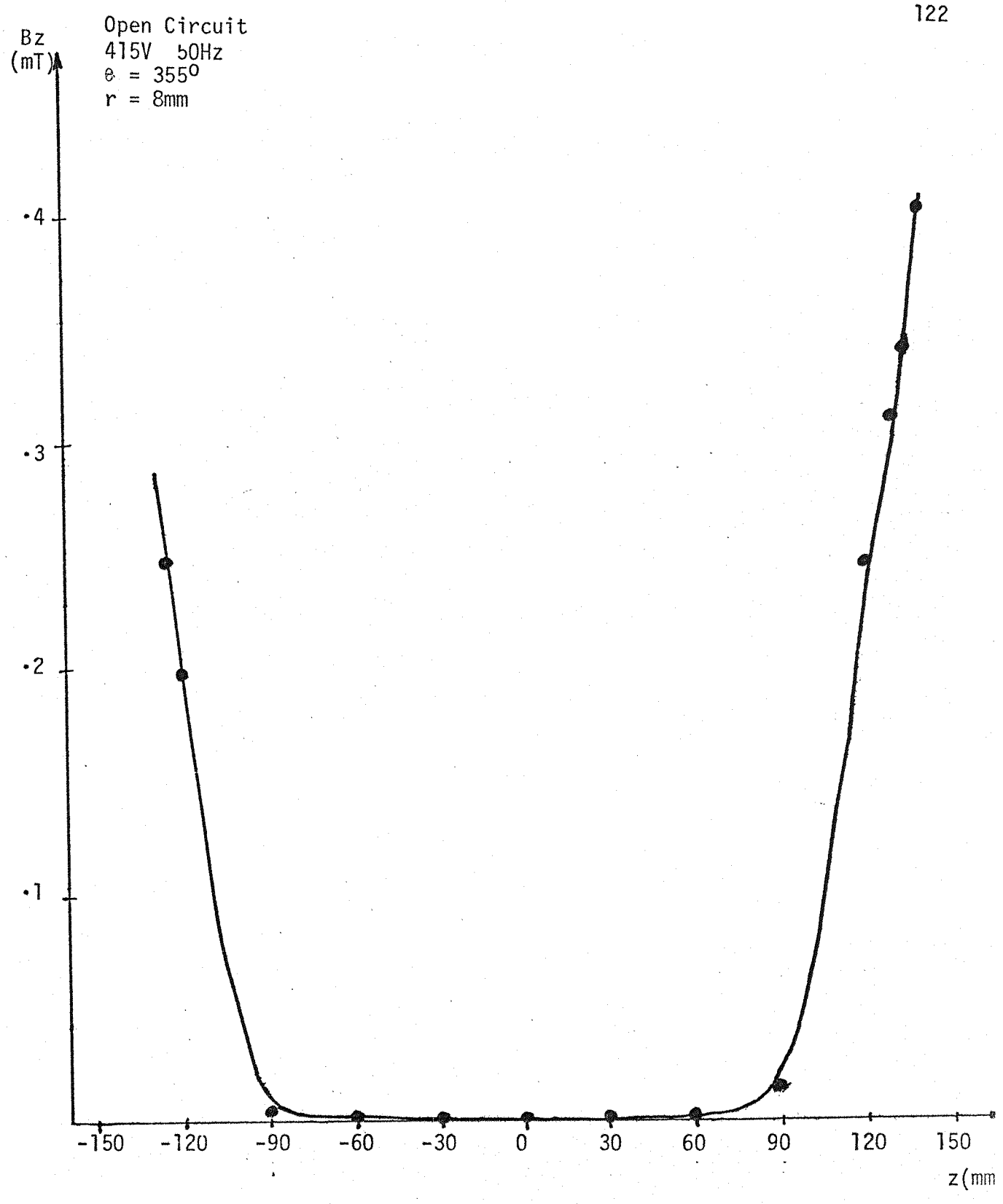

Fig.6.4.b: Variation of the axial leakage flux density along the stator core back length.

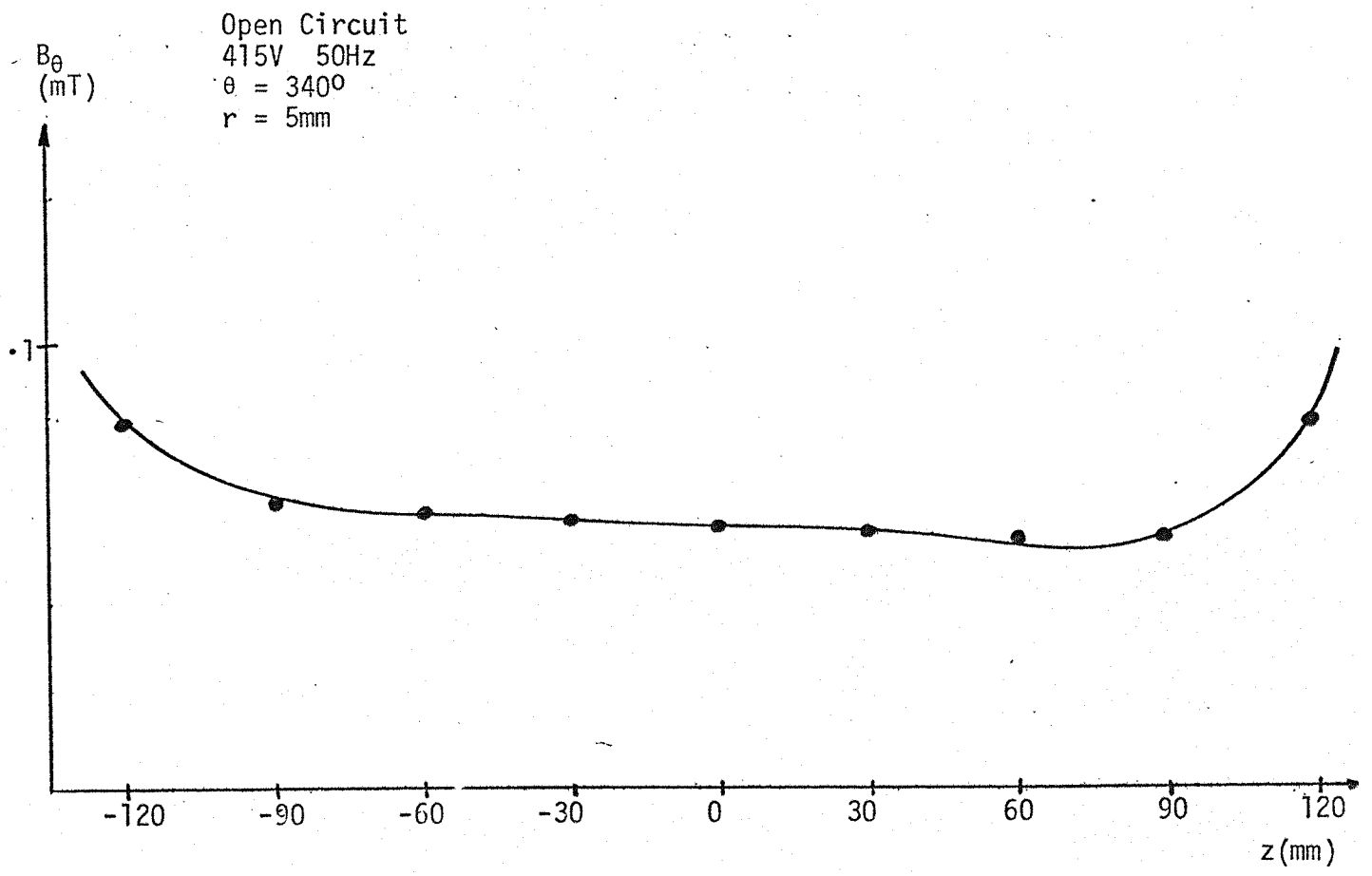

Fig.6.5.a: Variation of the circumferential leakage flux density against the open circuit voltage.

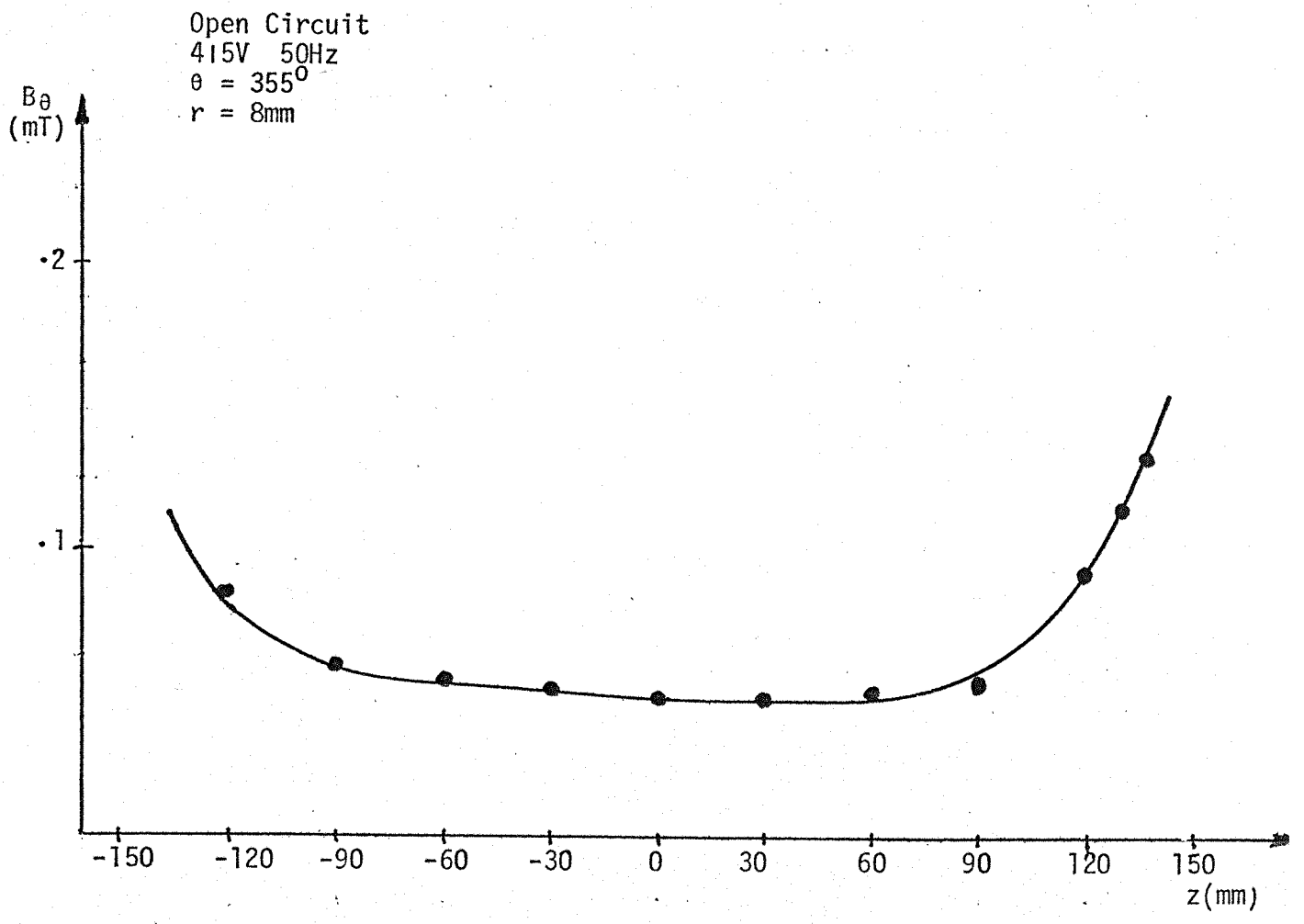

Fig.6.5.b: Variation of the circumferential leakage flux density along the stator core back length.

measurements at a plane (r, θ) closer to the surface of the core back than figure 6.4b. The axial leakage flux density is also expected to have a higher concentration at the edges of the stator core back because of the locations of the electromagnetic sources. That is confirmed by the curves in both figure 6.4a and figure 6.4b. The axial leakage flux component is equal to zero at the centre of the stator core back surface.

The circumferential component of the core back leakage flux also varies along the stator core length, as shown in figure 6.5a and figure 6.5b. Although this variation is smoother than both axial and radial component variations. That is explained by the tendency of the main electromagnetic sources to bend the core back leakage flux towards the stator core front. Therefore most of the core back leakage flux leaves the core back surface in the radial direction and changes to the axial direction in order to reach the core front region. It can also go in the opposite direction leaving the core front and reaching the core back. There is also a part of the core back leakage flux that circulates in the circumferential direction of the core back, as presented in section 5.3. The intensity of the circumferential component is also larger at the edges.

6.3.2 Variation of the Leakage Flux With the Distance From the Stator Core Back Surface

The radial component of the core back leakage flux decreases sharply with the distance from the stator core back surface, as shown in both figure 6.6a and figure 6.6b. The regions at the edges show a sharper decrease than the region at the centre of the stator core back because the surface polarity at the core back at the edges has a rating of decrease greater than those of the other main electromagnetic

sources. That happens because the relative decrease in the distance from the core back surface polarity is much bigger than the relative decrease in the distances from the other sources. Another reason is the fact that the surface polarity at the core back is the smallest of the main sources in absolute terms. Therefore at the edges of the stator core back the leakage flux is more rapidly changed to the axial direction by the action of the electromagnetic sources at the core front region of the synchronous machine. At the centre of the stator core back the radial leakage flux has a straightforward decrease and does not reach negative values because of the largely predominant influence of the polarity at the back of the core.

Figure 6.7a and figure 6.7b show the variation of the axial leakage flux density with the distance from the stator core back surface which is similar to that variation obtained during short circuit conditions; in other words, the axial component has an initial increase, reaches a maximum value and then decreases with the continuous increase in the distance. The axial flux at the centre of the core back is equal to zero.

Figure 6.8a and figure 6.8b show the variation of the circumferential component of the leakage flux against the radial distance from the core back surface which is also similar to that obtained when the machine was operating on short circuit.

Both the axial and the circumferential components of the leakage flux have a large intensity at the very end of the core back away from the surface because of the changing in direction of the radial leakage flux that leaves or penetrates the stator core back surface.

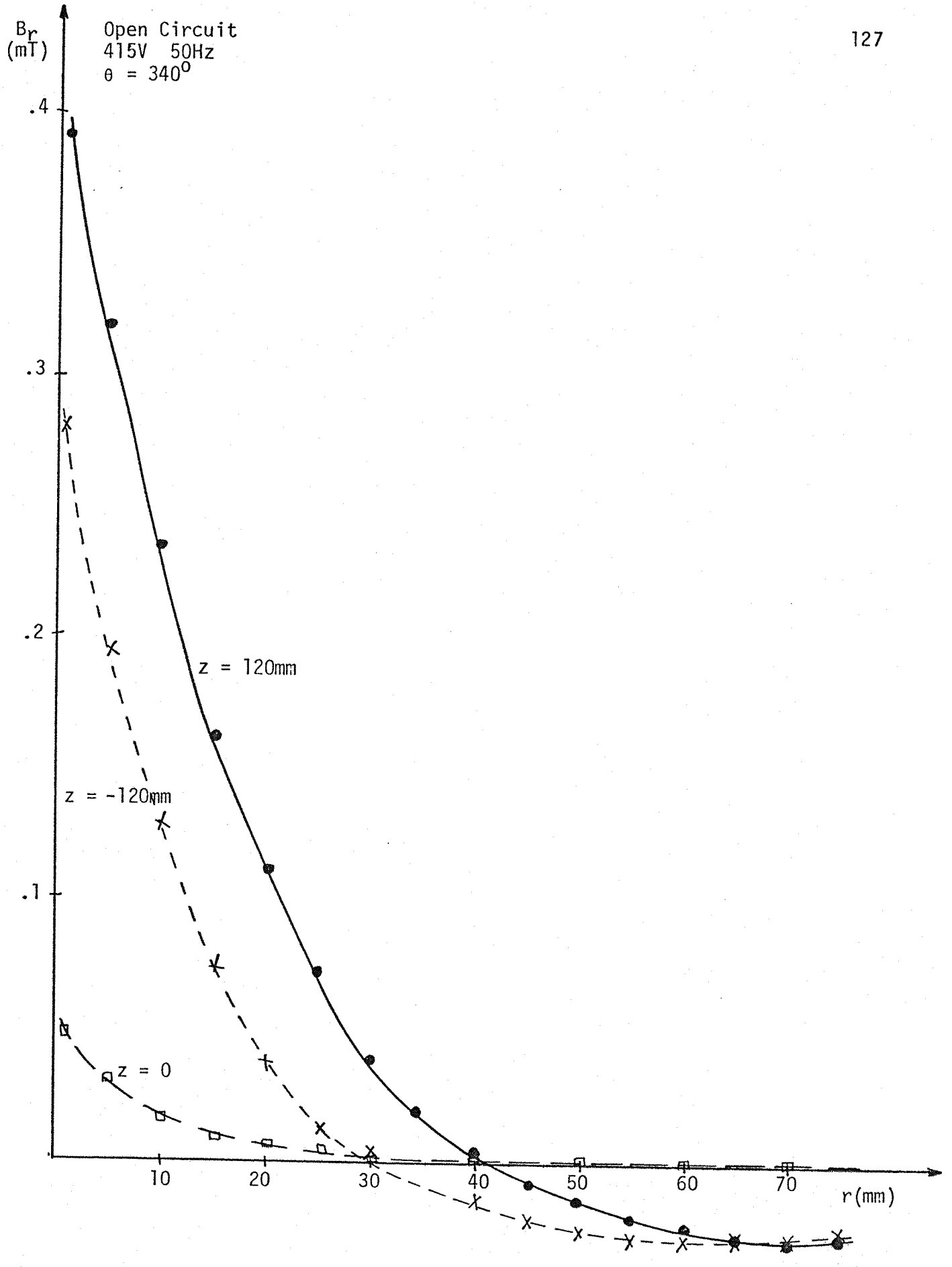

Fig. 6.6.a: Variation of the radial leakage flux density against the distance from the stator core back surface.

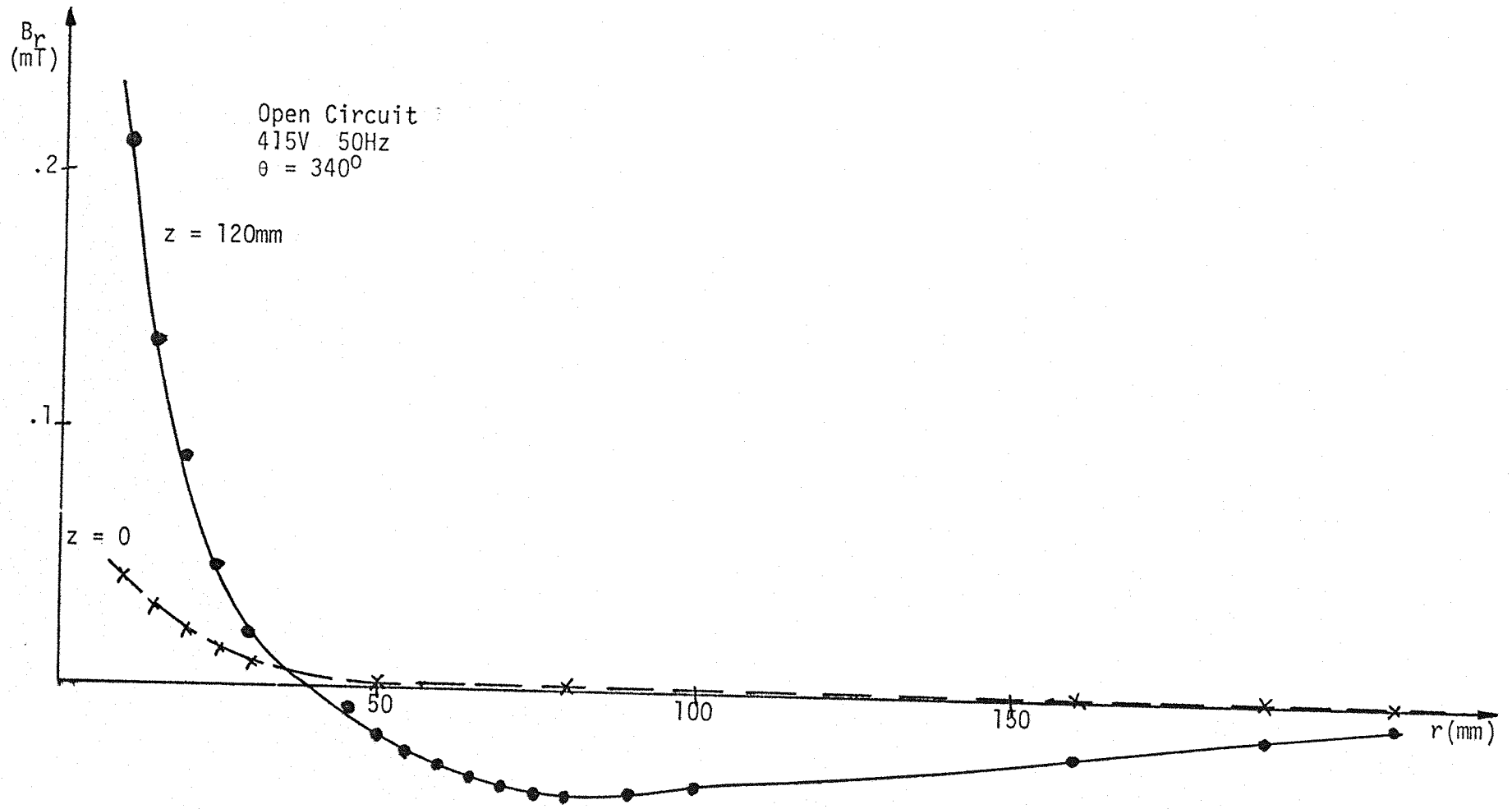

Fig. 6.6.b: Variation of the radial leakage flux density against the distance from the stator core back surface.

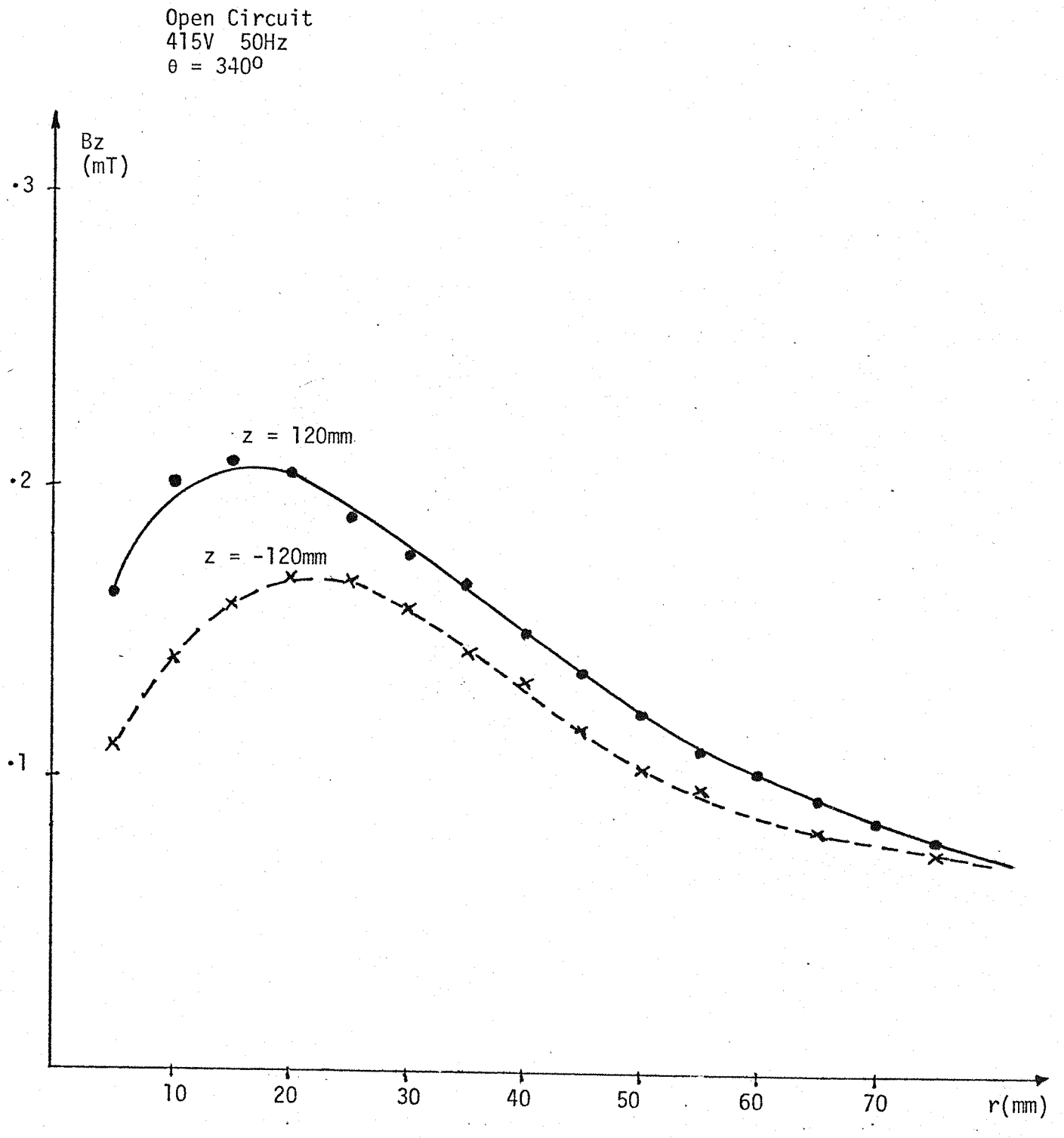

Fig. 6.7.a: Variation of the axial leakage flux density against the distance from the stator core back surface.

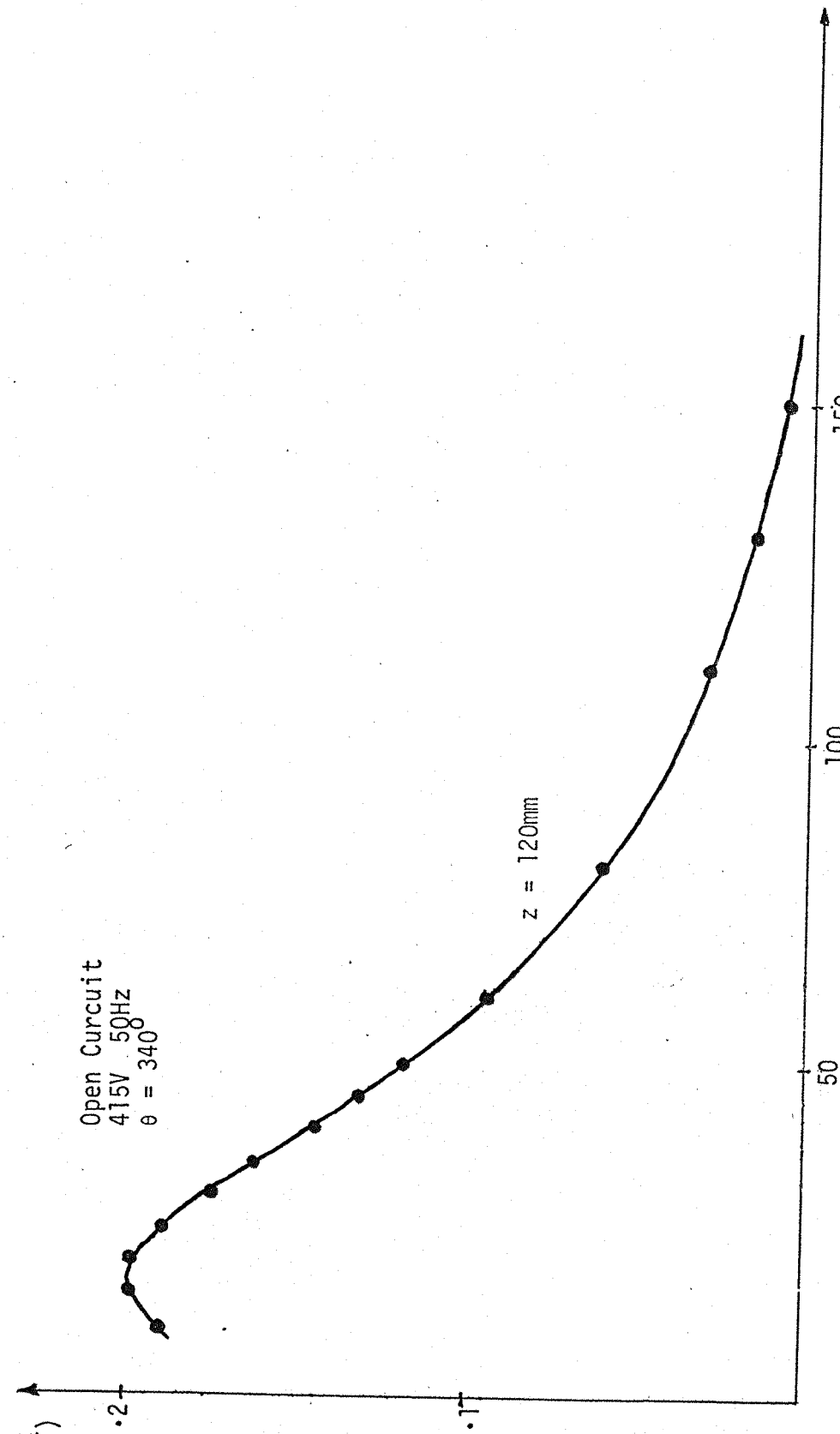

Fig.6.7.b: Variation of the axial leakage flux density against the distance from the stator core back surface.

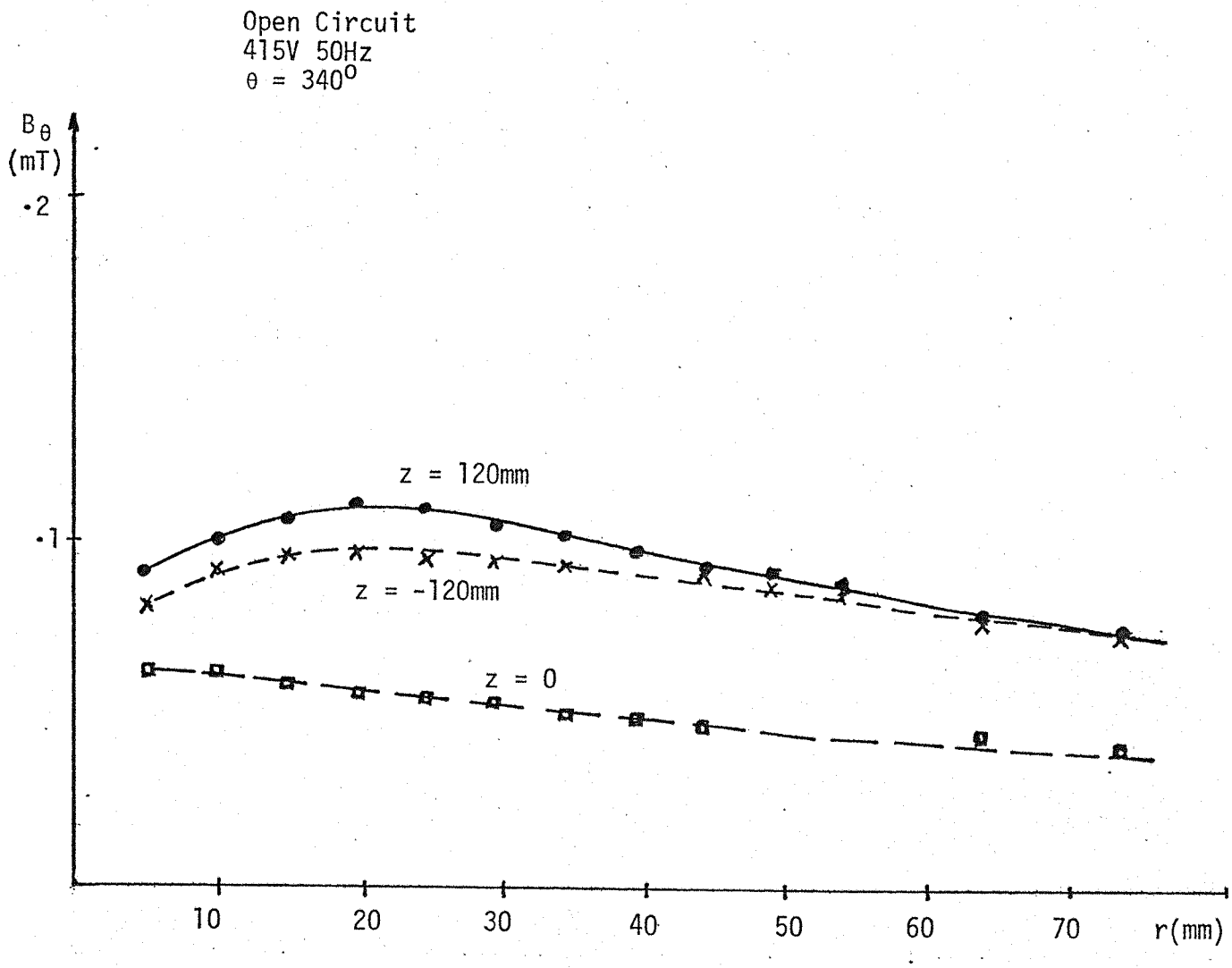

Fig.6.8.a: Variation of the circumferential leakage flux density against the distance from the stator core back surface.

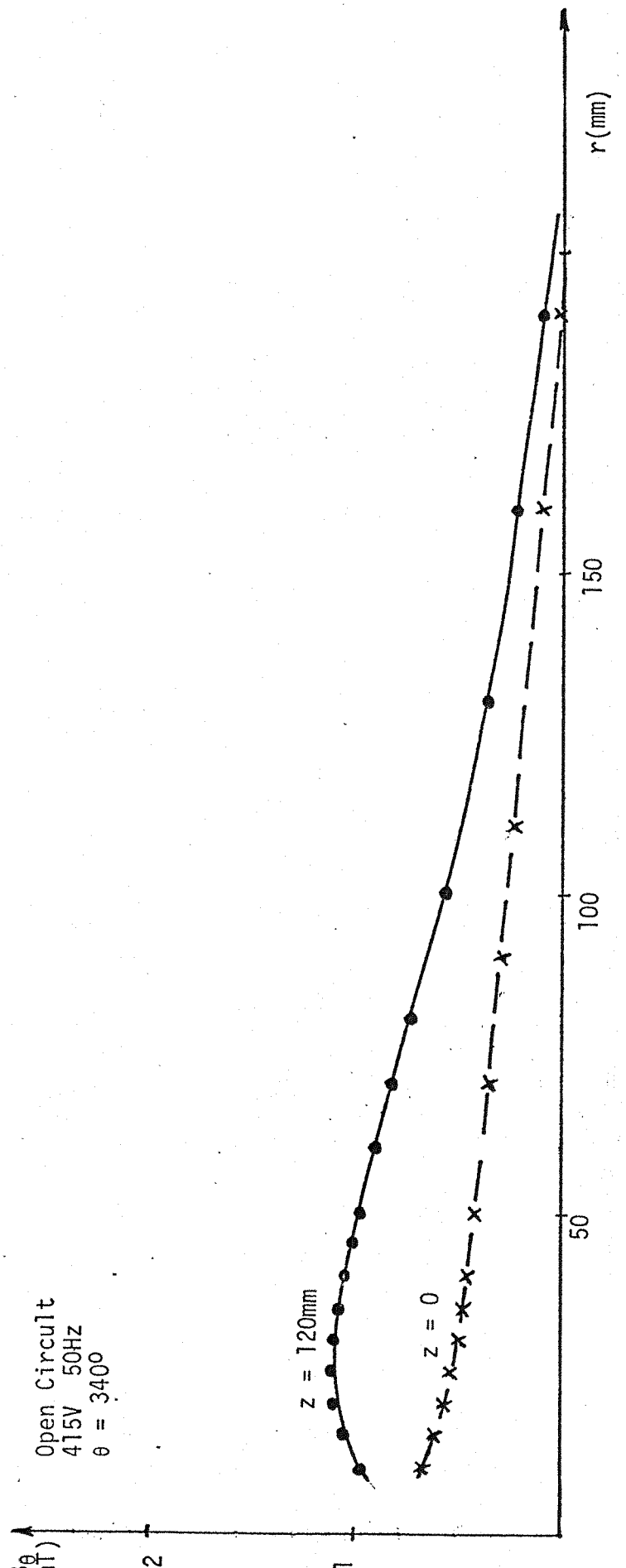

Fig.6.8.b: Variation of the circumferential leakage flux density against the distance from the stator core back surface.

6.3.3 Variation of the Leakage Flux Along the Circumferential Direction at the Stator Core Back

The main magnetic field produced in the air gap of the synchronous machine varies sinusoidally with the circumferential direction around the machine bore. This field also rotates with a constant frequency around the core bore. Therefore the main electromagnetic sources of an ideal machine produce a constant magnetic field component at the points situated at a constant distance from the back surface and at a fixed axial position around the core back. But, there still is a larger concentration of the leakage planes both closer to the surface and at the edge of the core back because the main electromagnetic sources are located close to the core back edge.

In a real synchronous machine the circumferential distribution of core back leakage flux is not the same as an ideal machine. That happens because the introduction of the mechanical structure and core supports, such as building bars, which have a localised effect and disturb the core back leakage flux distribution. Manufacturing imperfections, such as non-uniform gaps between laminations, can also affect the distribution of core back leakage flux introducing regions of larger concentration of leakage flux.

Figure 6.9 shows the variation of the radial component of the core back leakage flux around the circumferential direction. Because the laboratory synchronous machine does not have perfect symmetry and due to the existence of mechanical support which clamps the stator core laminations, the leakage flux does not have a smooth circumferential distribution. The existence of regions of larger leakage flux intensities can aggravate the situation, introducing points of larger concentration of temperature.

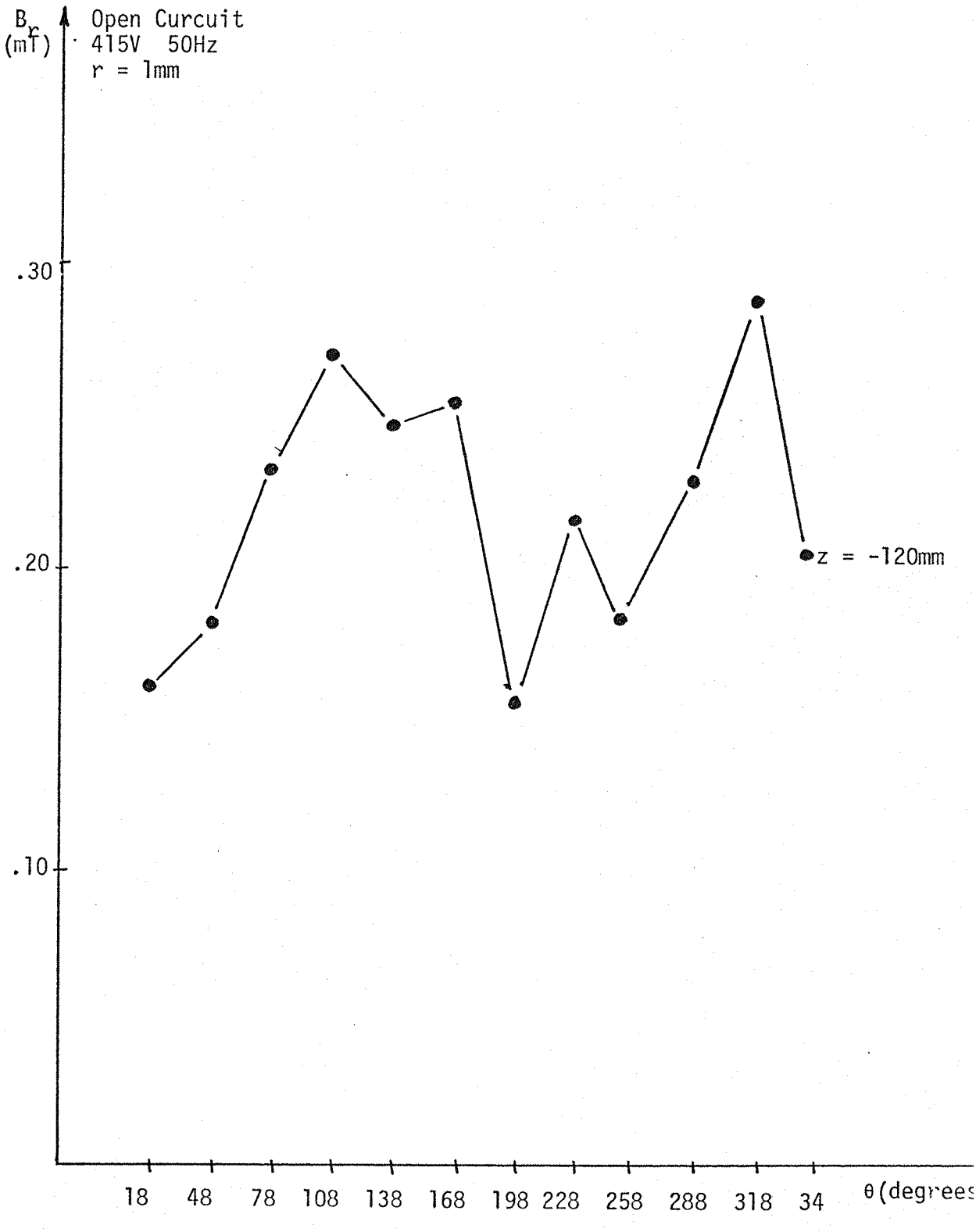

Fig. 6.9: Variation of the radial leakage flux density around the stator core back

6.3.4 Eddy Current Effects

In order to study the effects of eddy currents in the leakage flux distribution during open circuit conditions, the synchronous machine frequency was varied. Unfortunately the range of frequency was small due to limitations of the d.c. motor speed, mechanical vibrations and the maximum stator winding voltage admissible. The normal speed of the synchronous machine is 1500 RPM and the normal voltage is 415 volts. The stator core was not fitted with a screening plate. Therefore the effects of the eddy current in the distribution of leakage flux were not very significant. The eddy current effects discussed in Chapter Eight are more significant because of the use of a larger range of frequency and the presence of screening plates.

In the synchronous machine operating on open circuit, both the axial leakage flux inside the stator core and the radial leakage flux at the stator core back were analysed. Figure 6.10 shows the variation of the radial component of core back leakage flux density against the synchronous machine frequency. Both the centre and the end zones of the core back were analysed. The distribution of radial leakage flux at the centre region of the core back is not affected by the eddy current and the distribution at the end region is just slightly affected because of the relative weakness of the eddy current reaction imposed on the stator core. Figure 6.13 shows the variation of the axial leakage flux inside the stator core due to eddy current effects. Both different depths into the stator core and different positions relative to the plane of the laminations were considered. The locations of the search coils used to measure the axial leakage flux inside the stator core are shown in figure 6.12. The axial leakage flux inside the core is much larger in the area around the tooth edge than in the other areas when the lamination is close to the core end.

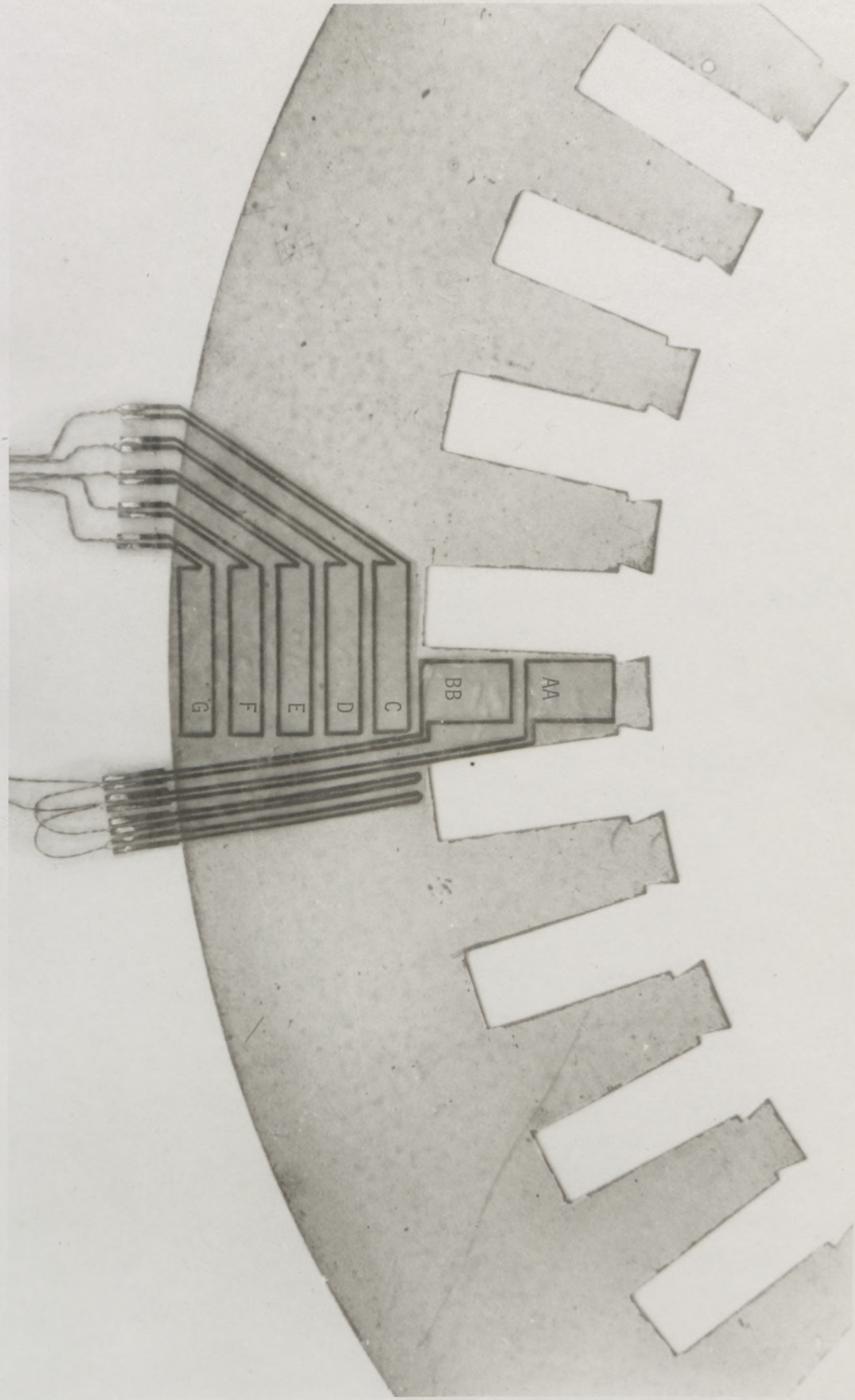

Fig. 6.12: Location of the printed search coils in the stator core laminations.

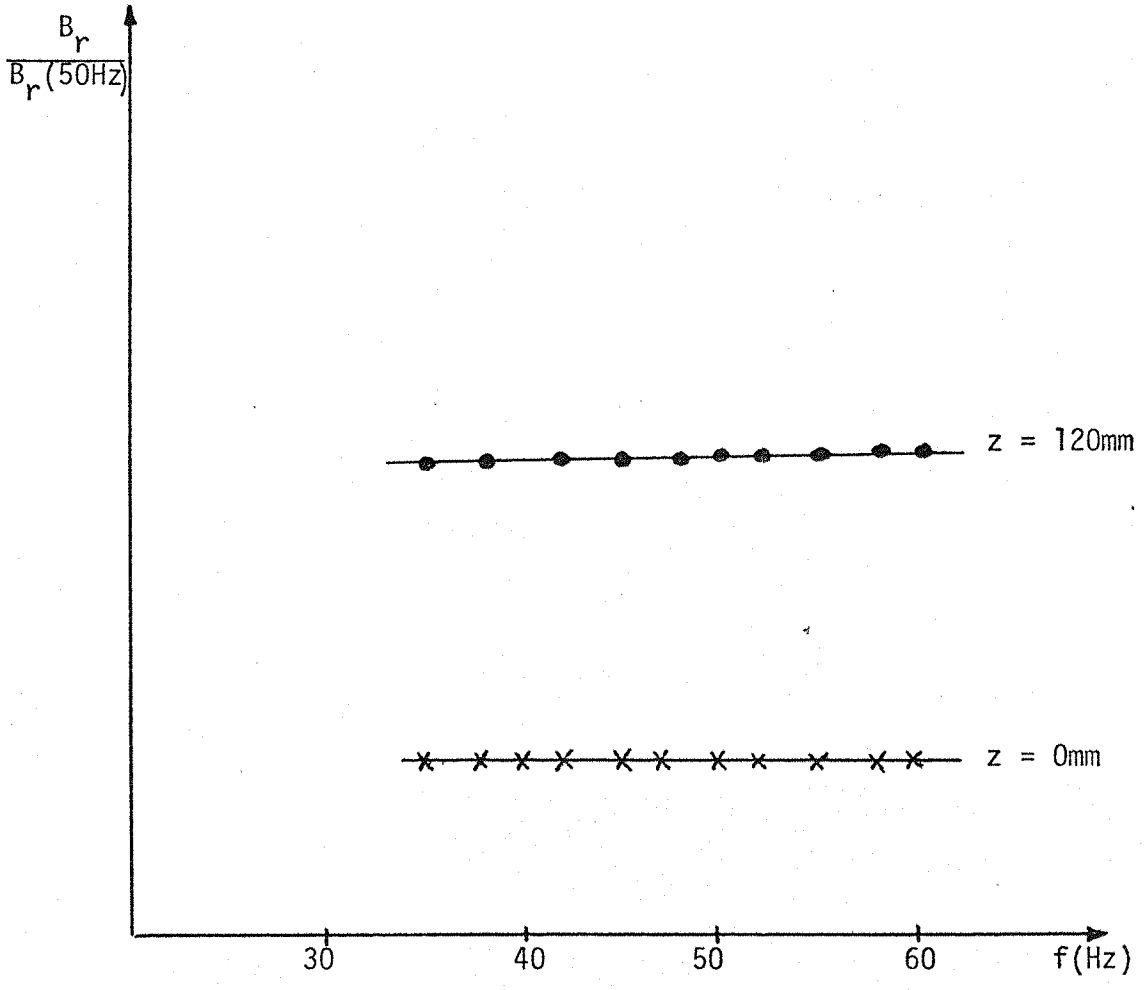

Fig. 6.10: Relative Variation of the radial component of the core back leakage flux density against the frequency

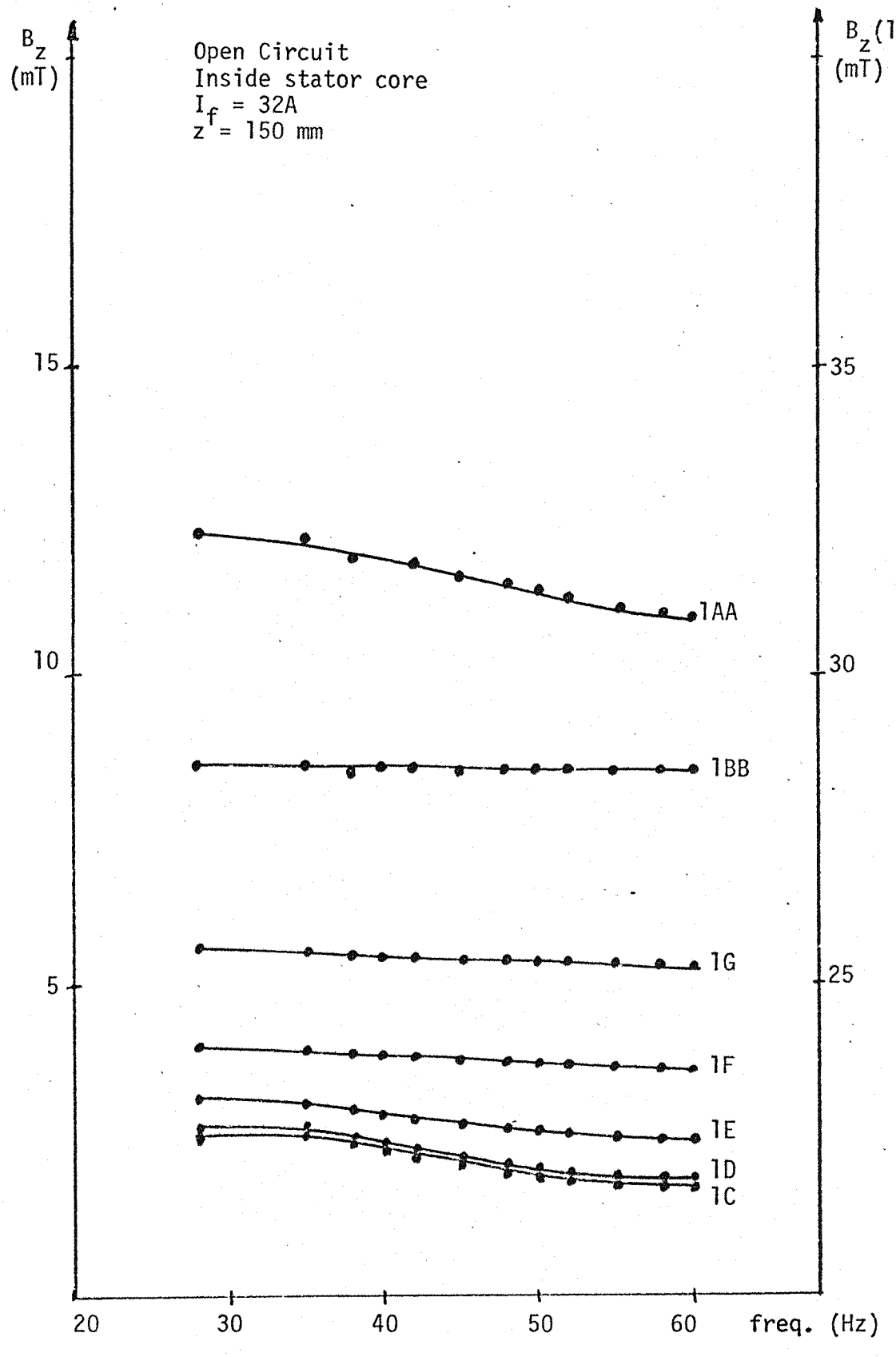

Fig.6.13.a : Variation of the axial leakage flux density against frequency.

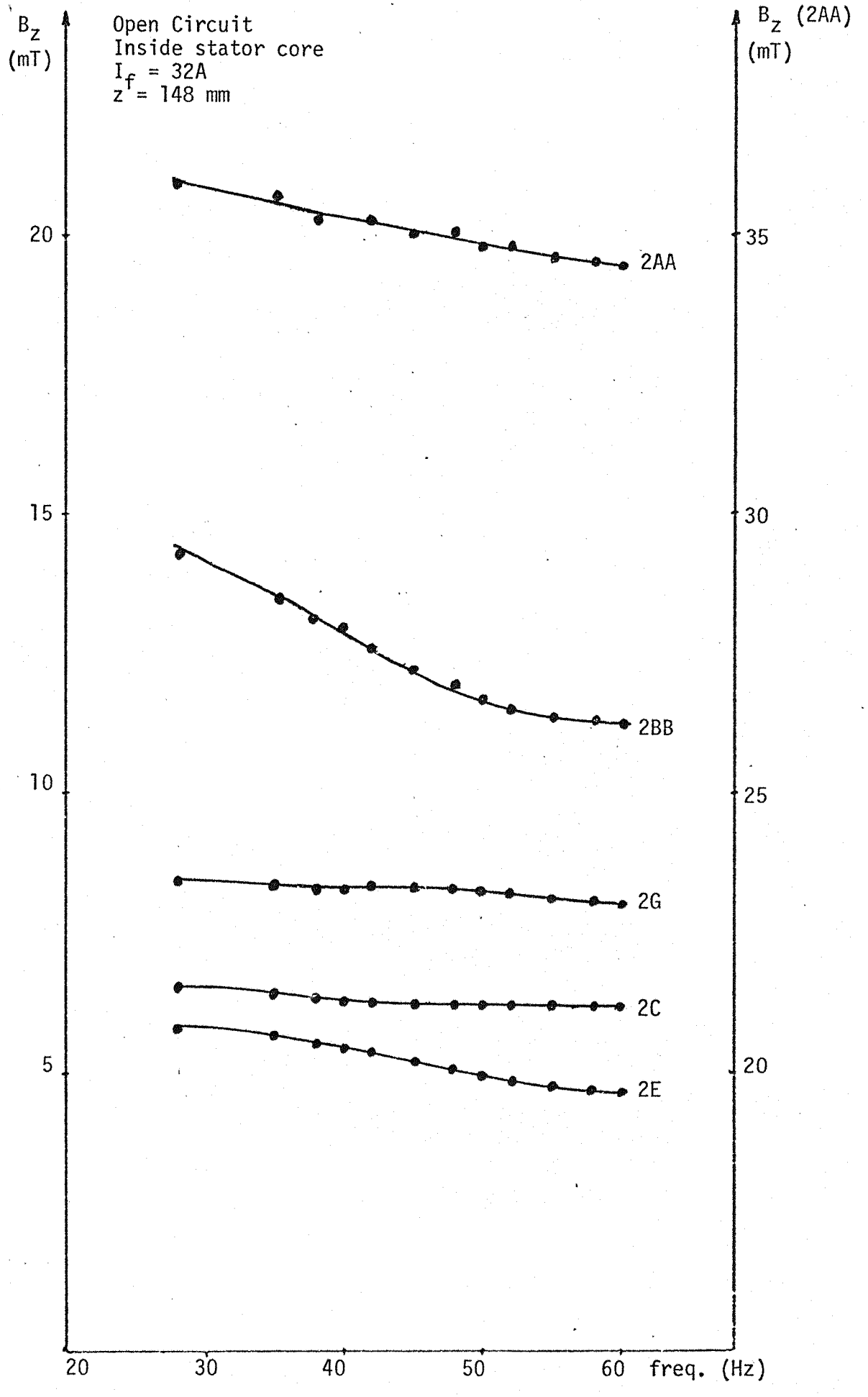

Fig.6.13.b: Variation of the axial leakage flux density against frequency.

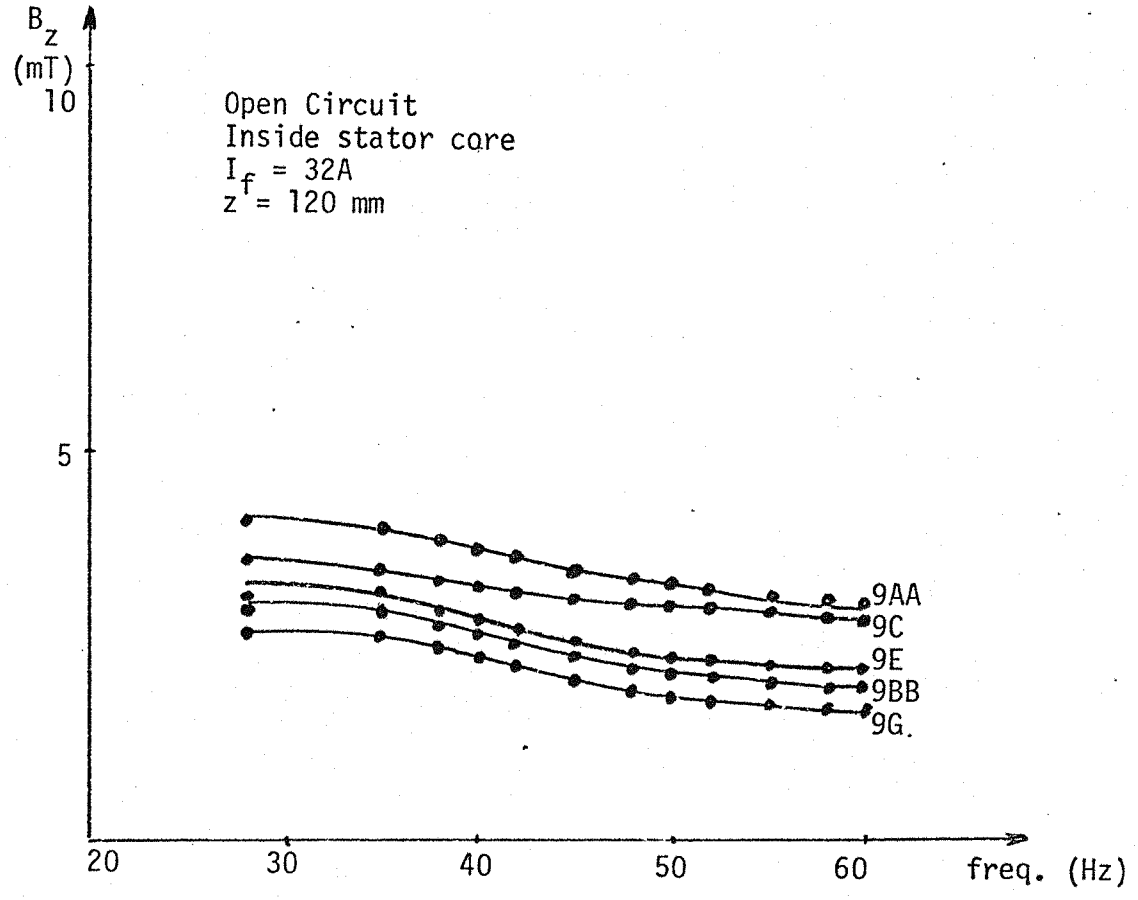

Fig.6.13.c : Variation of the axial leakage flux density against frequency.

For laminations deeper into the core the axial leakage flux has a much smoother distribution. Therefore the eddy current induced in the plane of the laminations does not have a uniform distribution and has the largest intensity in the area close to the tooth edge. The axial leakage flux distribution inside the stator core of the synchronous machine is modified by the action of the eddy currents. The eddy current circulating in the plane of the laminations produces a magnetic field that opposes the axial leakage flux. Actually the eddy current diminishes the quantity of axial leakage flux diverting this flux away from the stator core front. The phenomenon of diverting axial flux from the core front is of substantial importance to the distribution of leakage flux at the stator core back. The eddy current circulating in the lamination plane can increase the amount of leakage flux at the core back, mainly at the edge areas. That effect can become worse with the presence of screening plates at the stator core front. The eddy current circulating in the back of the laminations has a negligible effect on the core back leakage flux distribution because it is resistance limited.[54]

6.3.5 Saturation Effects

The synchronous machine has its performance affected by the magnetic saturation of its magnetic circuit because of the introduction of considerable non-linearities.[83] Both the main and the leakage flux can use the same magnetic circuit which could reduce the synchronous machine magnetising inductance by a significant increase in the armature leakage flux. The permeability at any point of the magnetic circuit is a function of the local flux density. A high concentration of flux means that the local saturation may become important even when the mean flux density is not too big.[65,84]

In an ideal machine it is expected that all flux densities are proportional to the currents producing them. This is disturbed in a real one by the presence of non-linearities caused by the action of saturation. When the currents increase to high values the leakage flux path can become saturated, altering the flux distribution and distorting the waveform. The open circuit test of synchronous machines shows the saturation effects in introducing non-linearities into the mutual flux, as shown in the curve V_{oc} x I_f (figure 2.1).

The saturation causes a decrease in the stator core permeability easing the penetration of the magnetic leakage flux towards the synchronous machine stator core. Therefore a larger distribution of magnetic poles is imposed on the surfaces of the stator core because of the presence of larger indúcing magnetic fields. That means that the intensity of the main electromagnetic polarity sources at the surfaces of the stator, such as bore, core front and back back, are increased when the synchronous machine is under saturation conditions. Therefore the leakage flux at the stator core back is increased with the saturation effects. The saturation can affect the distribution of either the core back leakage flux or the axial leakage flux inside the stator core. The axial leakage flux penetrating the stator core front reaches deeper laminations and has its amount increased by the saturation due to the decreased stator core permeability. The volume polarity source inside the stator core is also increased with the saturation and helps to reduce the amount of leakage flux penetrating the stator core. The volume polarity opposition to the axial leakage flux penetration is treated in detail in section 3.6.1.

Saturation can aggravate the existence of hotspots in the stator core of synchronous machines because a greater concentration of

leakage flux is imposed on the regions under more intensive saturation effects. The edge of the stator core back is under more severe conditions than the centre region because the edge has a larger density of leakage flux.

Figure 6.14 shows the variation of radial leakage flux density against the open circuit voltage at both the centre and edge zone of the core back and for different distances from the core back surface. The saturation intensity is increased with the increase of open circuit voltage when the synchronous machine has a constant frequency. Figure 6.14a shows the curves of the radial component closer to the back surface than figure 6.14b. As expected, the curves are not linear because of the presence of the saturation effects. The curves show that the saturation effect is greater at the edges of the stator core back than at the centre regions and the core back leakage flux is more intensively increased. That is explained by the fact that the surface polarity at the back of the core has a greater increase at the edge zone. Both edges of the stator core back have different values of leakage flux due to a lack of perfect symmetry of the synchronous machine, but both edges are affected in a similar way. The centre region of the core back starts to feel the saturation effects at higher voltages. Figure 6.14b shows the curves of the radial component for a region more distant from the back surface than figure 6.14a and also shows the variation of the radial component with the saturation at a zone closer to the very end of the core back. It is very important to notice that at the edge of the core back, at planes distant from the core back surface, the intensity of the radial leakage flux initially increases with the voltage, reaches a maximum and then decreases. That happens because the action of the saturation which rearranges the leakage flux distribution and imposes a higher

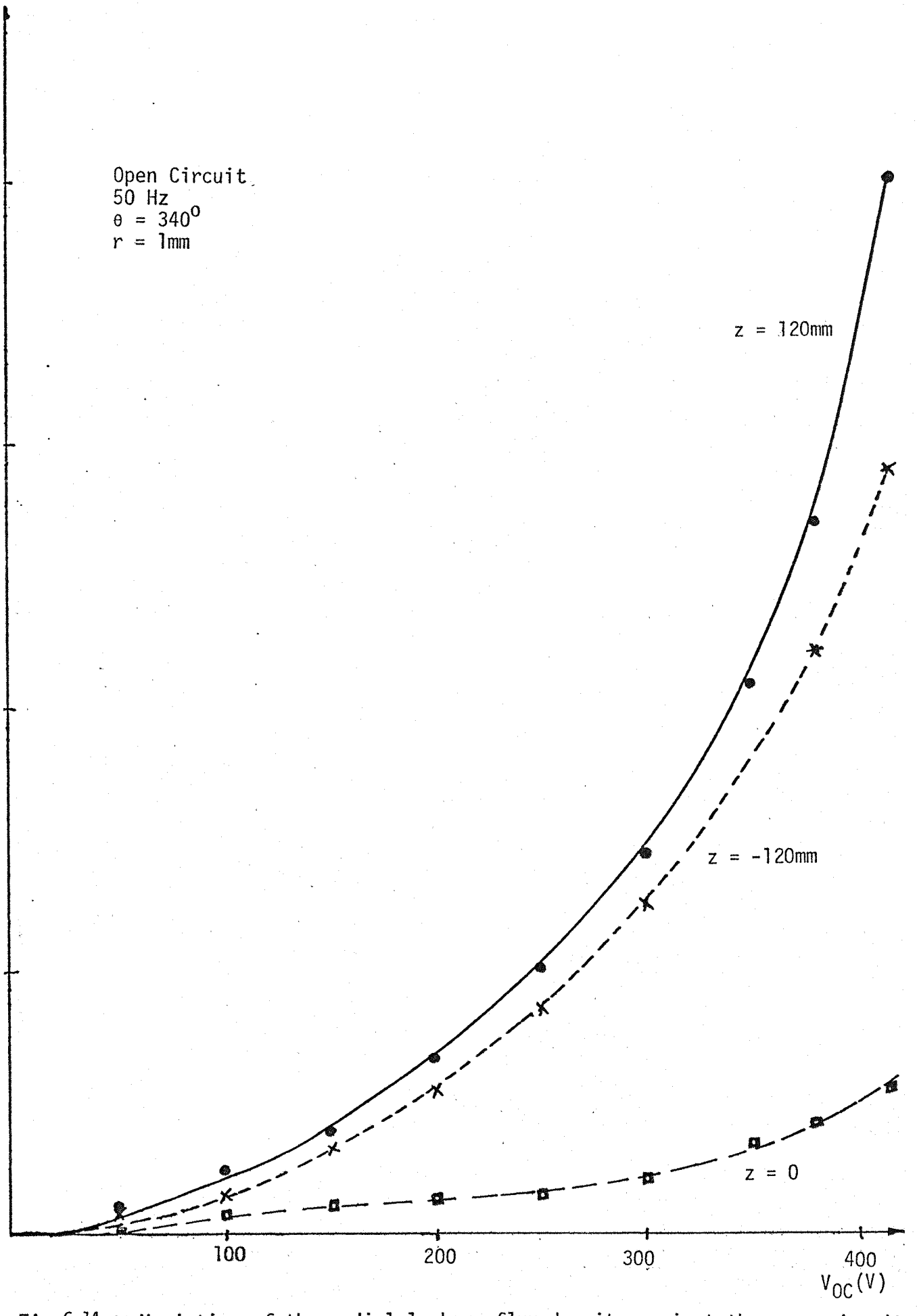

Fig.6.14.a: Variation of the radial leakage flux density against the open circuit voltage.

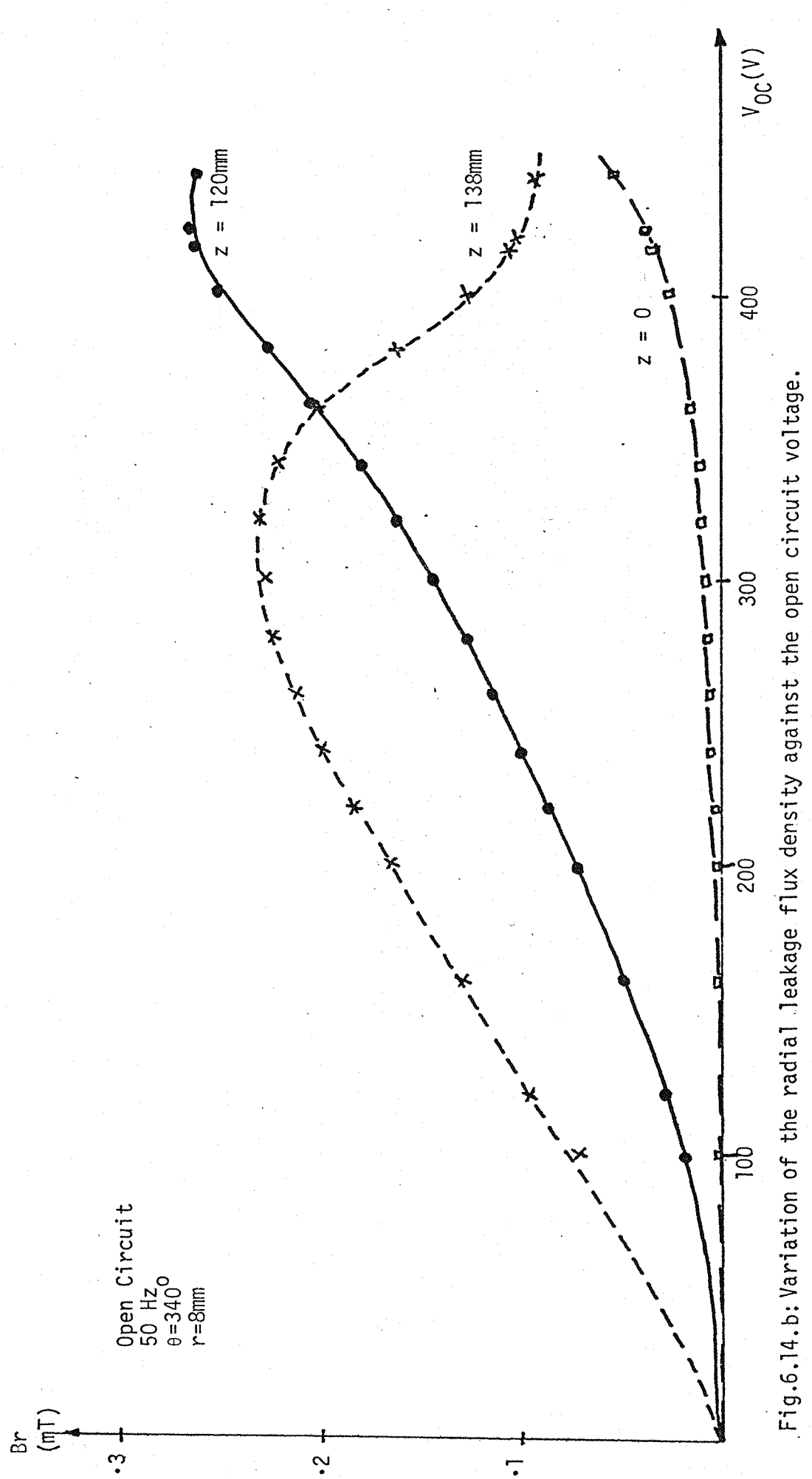

Fig.6.14.b: Variation of the radial leakage flux density against the open circuit voltage.

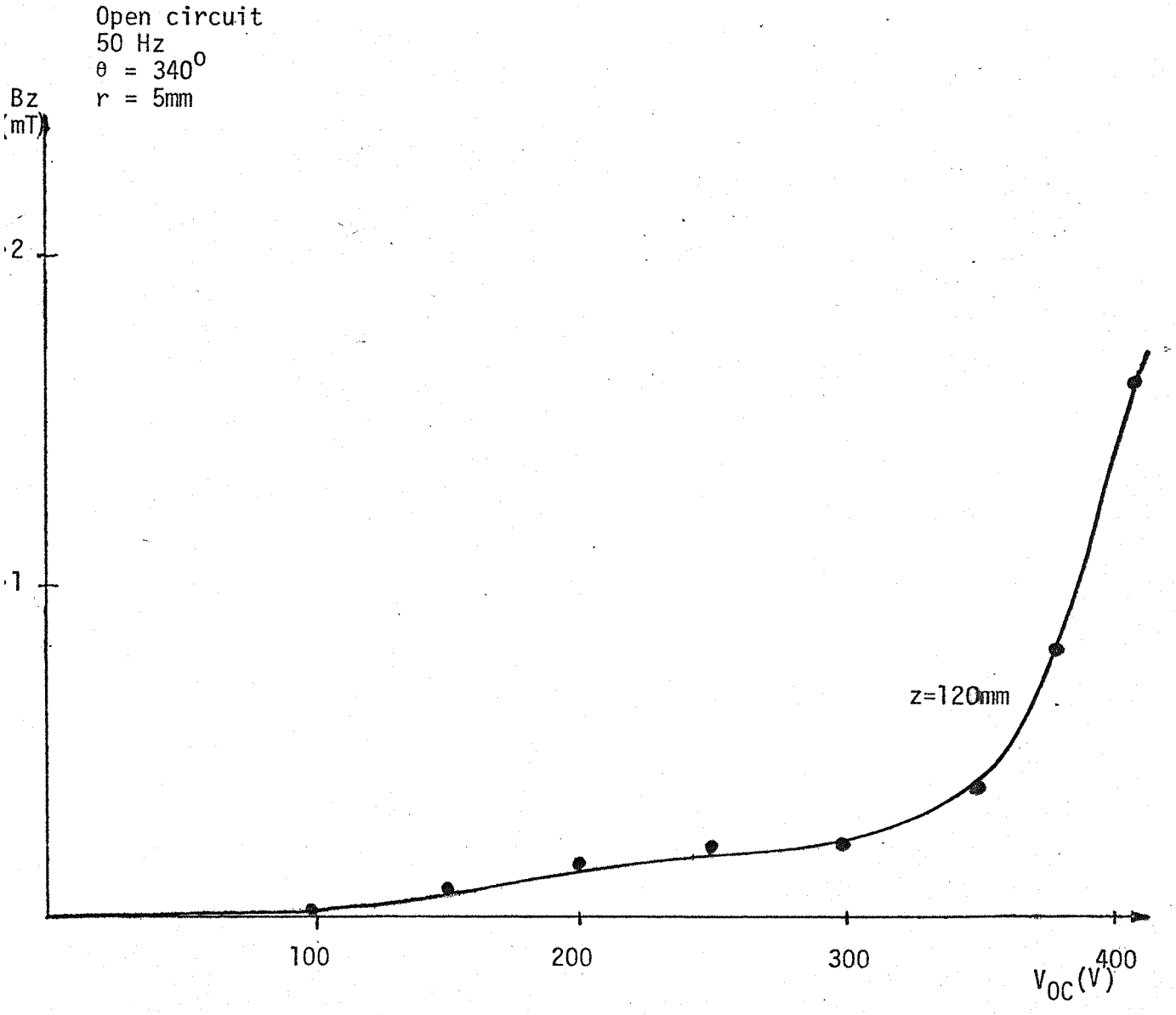

Fig. 6.15.a: Variation of axial leakage flux density against the open circuit voltage.

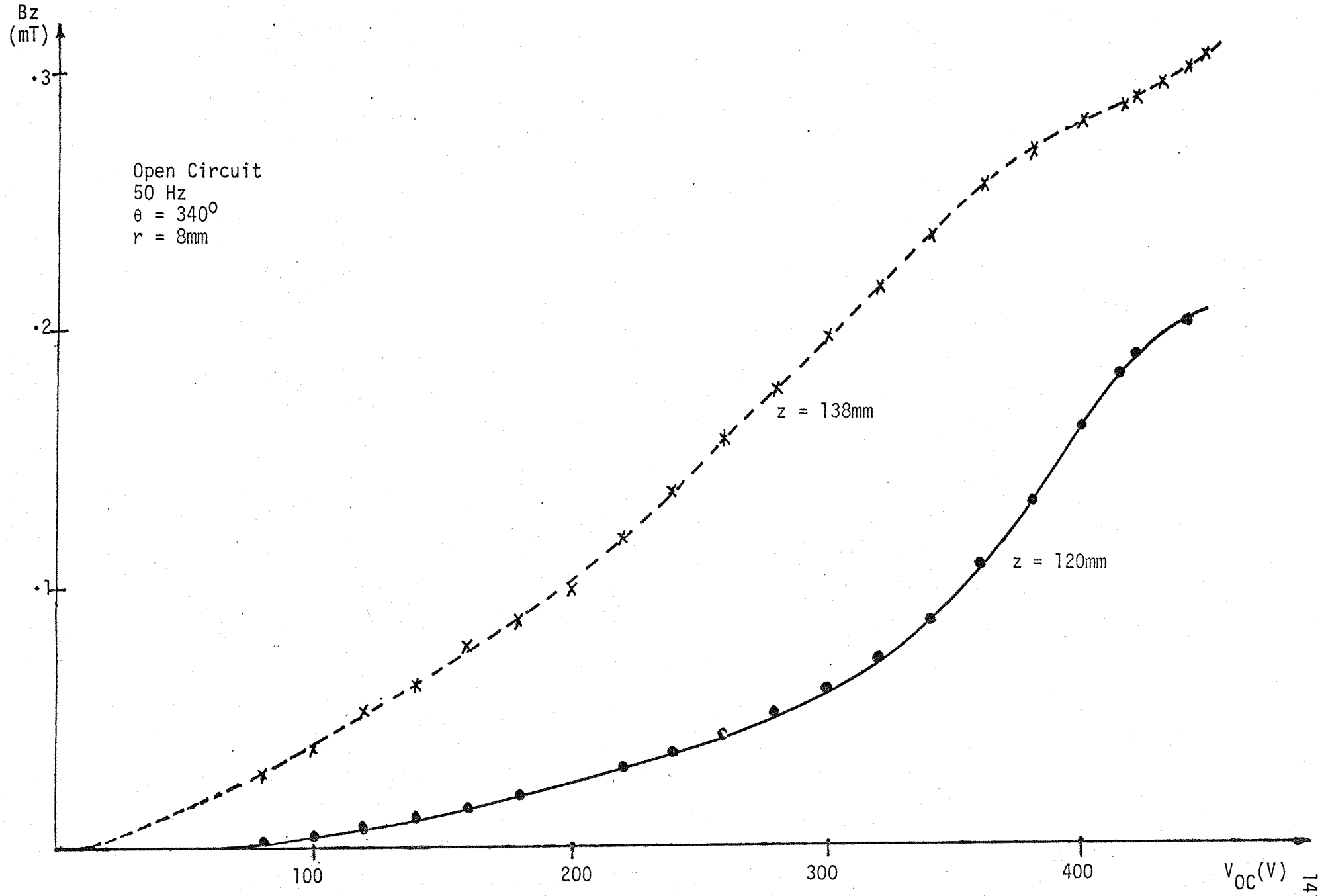

Fig.6.15.b: Variation of the axial leakage flux density against the open circuit voltage.

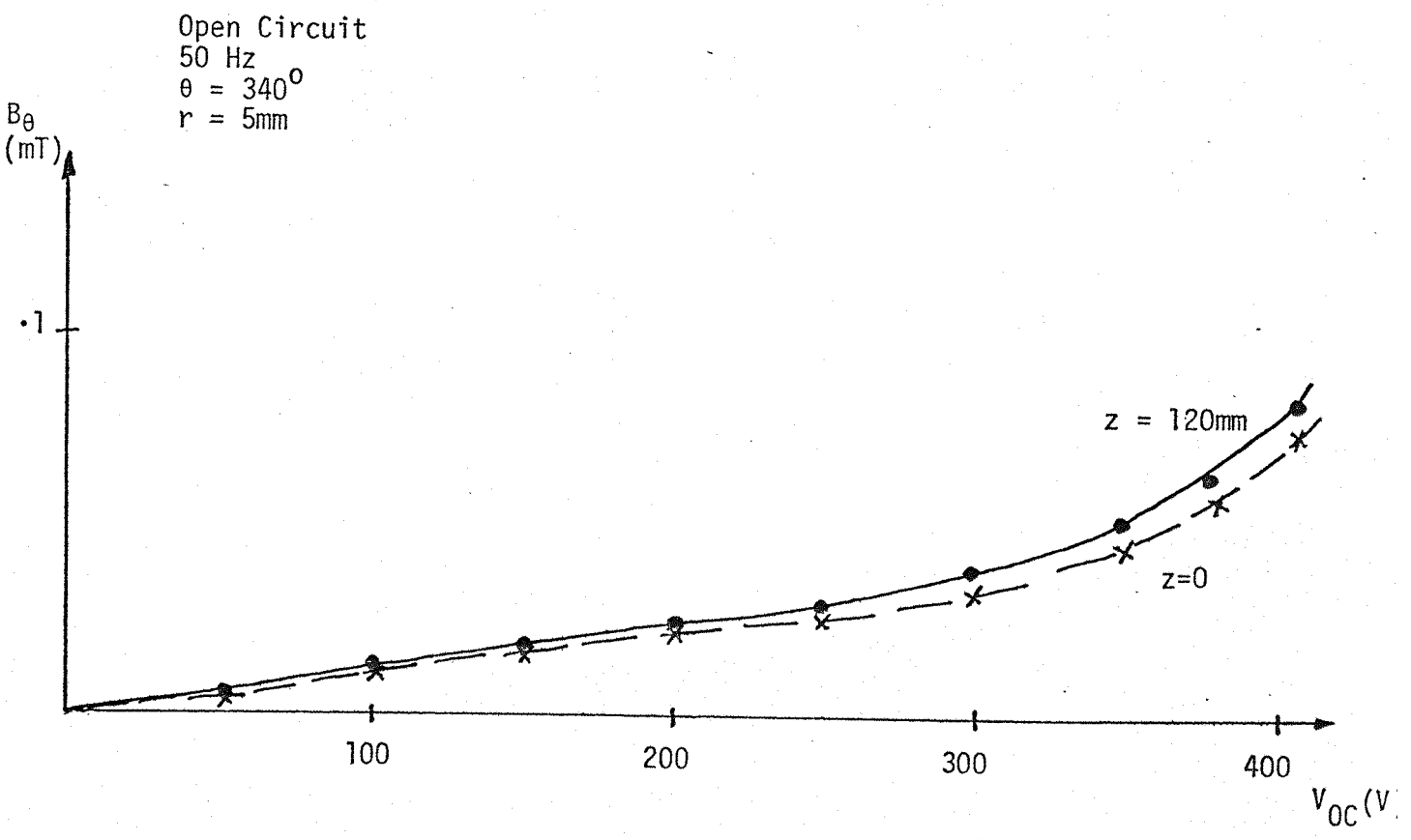

Fig.6.16.a: Variation of the circumferential leakage flux density against the open circuit voltage.

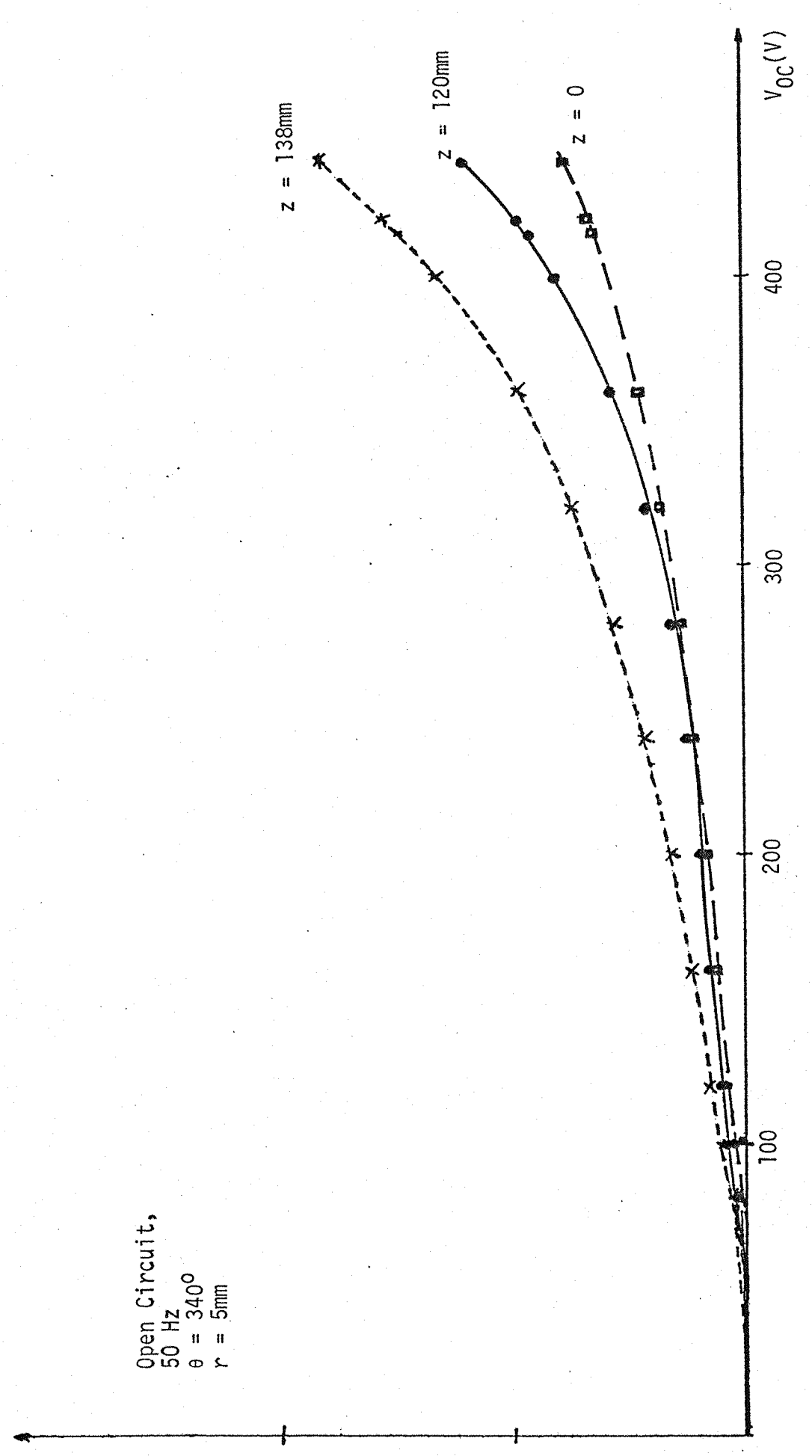

Fig.6.16b: Variation of the circumferential leakage flux density against the open circuit voltage.

concentration of core back leakage flux at the surface of the stator core back. This is also explained by the fact that the saturation causes a change in the direction of the radial component into either axial or circumferential directions, at planes distant from the core back surface.

The variations of both the axial and circumferential leakage flux density components with saturation are shown in figures 6.15 and 6.17, respectively. The curves show that the saturation effects cause an increase in both the axial and the circumferential components, even at a zone closer to the very end of the core back. That is in agreement with the theory of rearrangement in the distribution of leakage flux imposed by the saturation effect which diverts the radial component into either the axial or circumferential directions. Both the axial and the circumferential components are also more affected by the saturation at the edges of the stator core.

At short circuit operation the saturation effects are not present since the main flux is very small and the components of the core back leakage flux have a linear variation with the field current, as shown in section 5.3.3.

6.3.5.A Harmonics in the core back leakage flux due to saturation

Saturation can also cause distortion in the waveforms of the stator core back leakage flux increasing the magnitude of the odd harmonics.[83-87] The harmonics can cause losses in both the iron core and the copper and their effects can cause undesirable additional losses in the solid iron bodies. Therefore it is undesirable to have harmonics in the core back leakage flux because of the presence of the building bars. It is necessary to avoid harmonics having large magnitudes because they could also affect the interlaminar insulation

by increasing the dielectric stresses since the crest interlamination voltage may be higher for a distorted picked wave than for a sinusoidal wave with the same RMS value. With synchronous machines having building bars insulated from the stator core laminations, the presence of harmonics in the core back leakage flux can also damage the insulation between the building bars and the stator core laminations.

In order to estimate the presence of the harmonics in the core back leakage flux an analysis of the waveforms is required. Figures 6.17, 6.18 and 6.19 show the waveform, the fast Fourier transform (FFTA) and the power spectrum density (PSD) of the radial, axial and circumferential components, respectively, at both the end and the centre regions of the stator core back, for two different levels of saturation. The axial component is equal to zero at the centre region. The fast Fourier transform (FFTA) gives the contributions of the fundamental and the various harmonics to the leakage flux amplitude, and the power spectrum density (PSD) gives the distribution of the energy density in the magnetic field for the different harmonics.[88] From the figures mentioned above it can be noticed that the waveforms of the leakage flux components are more distorted when higher levels of saturation are imposed to the synchronous machine. The fast Fourier transform shows that the harmonics contribution to the leakage flux intensity becomes more accentuated when the saturation level is increased. Mainly the third and fifth harmonics are substantially increased relative to the fundamental when the saturation is more pronounced. The energy density also has a larger contribution of the third harmonic when the saturation level is higher. Although because the energy density is proportional to the square of the flux density the effects of the harmonics in the energy

density quantity are softened.

Definitions of the abbreviations presented in figures 6.17, 6.18 and 6.19 are given below.

BR - radial component of the core back leakage flux

BZ - axial component of the core back leakage flux

Bθ - circumferential component of the core back leakage flux.

OC - open circuit conditions

CR - centre region of the stator core back

ER - end region of the stator core back.

300V - open circuit voltage

415V - open circuit voltage.

(1) - leakage flux component waveform

(2) - fast Fourier transform (FFTA)

(3) - power spectrum density (PSD).

Vertical axis: amplitude

Horizontal axis, figure (1): time

figures (2) and (3): frequency (160Hz per division).

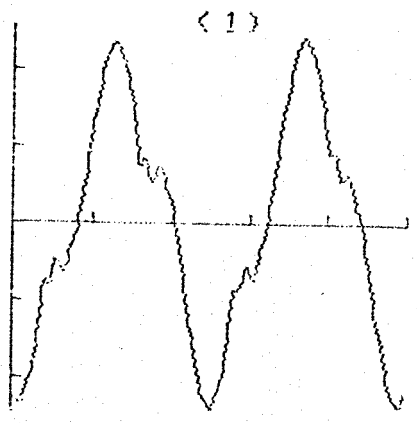

BR (OC, CR, 380V)

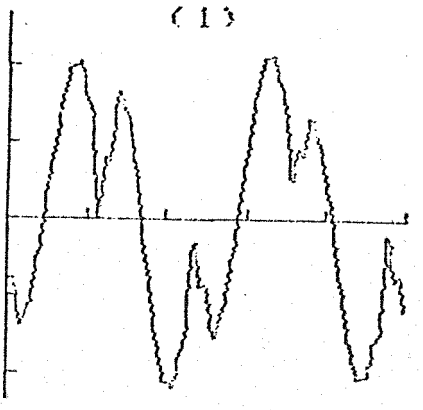

BR (OC, CR, 415V)

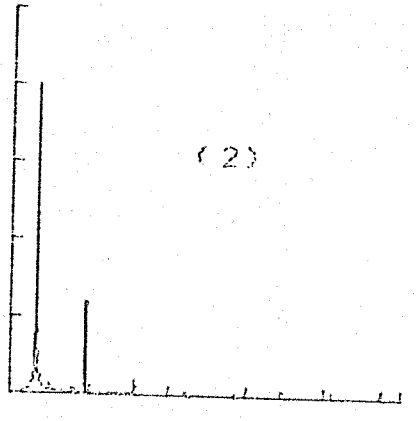

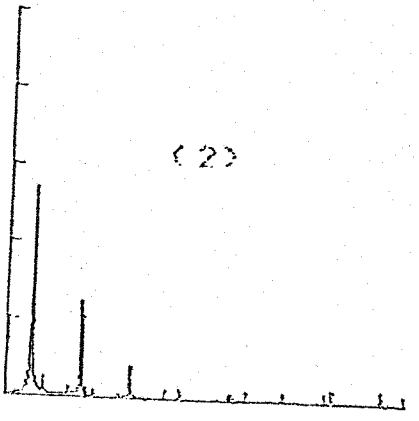

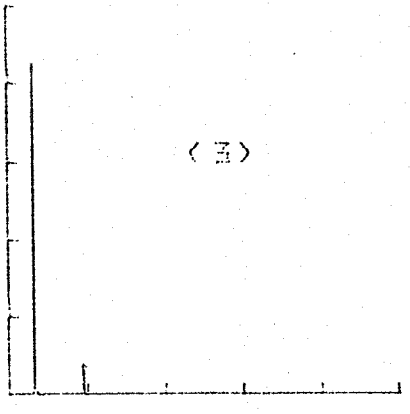

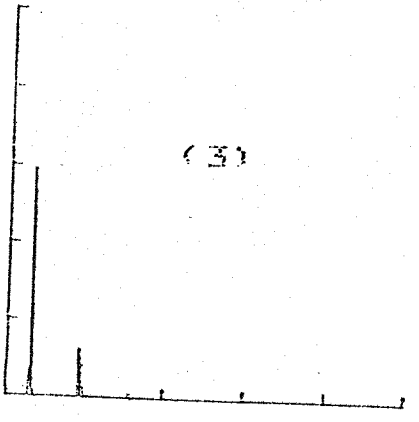

Fig. 6.17a: Radial leakage flux density (core back centre region).

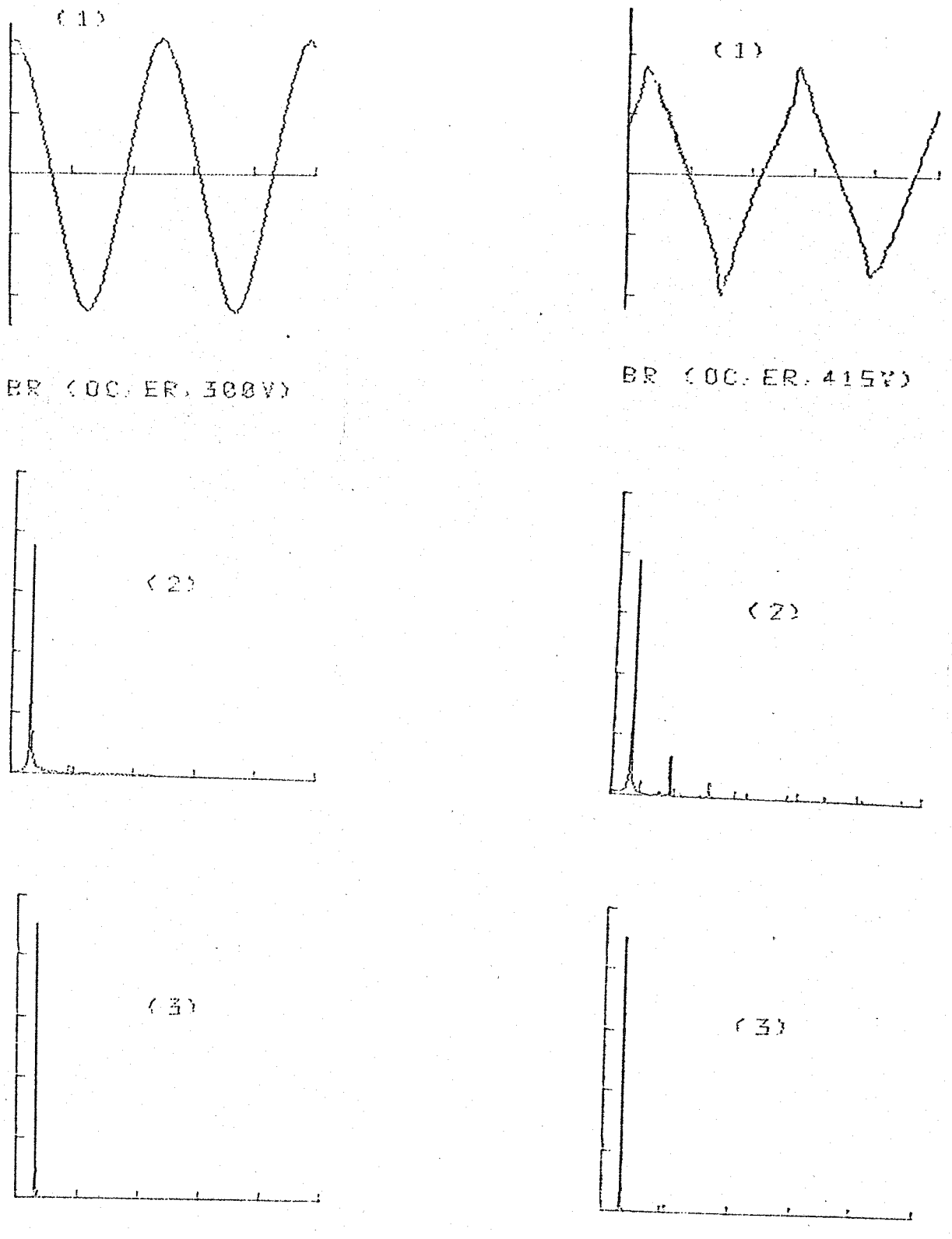

Fig. 6.17b: Radial leakage flux density (core back end region).

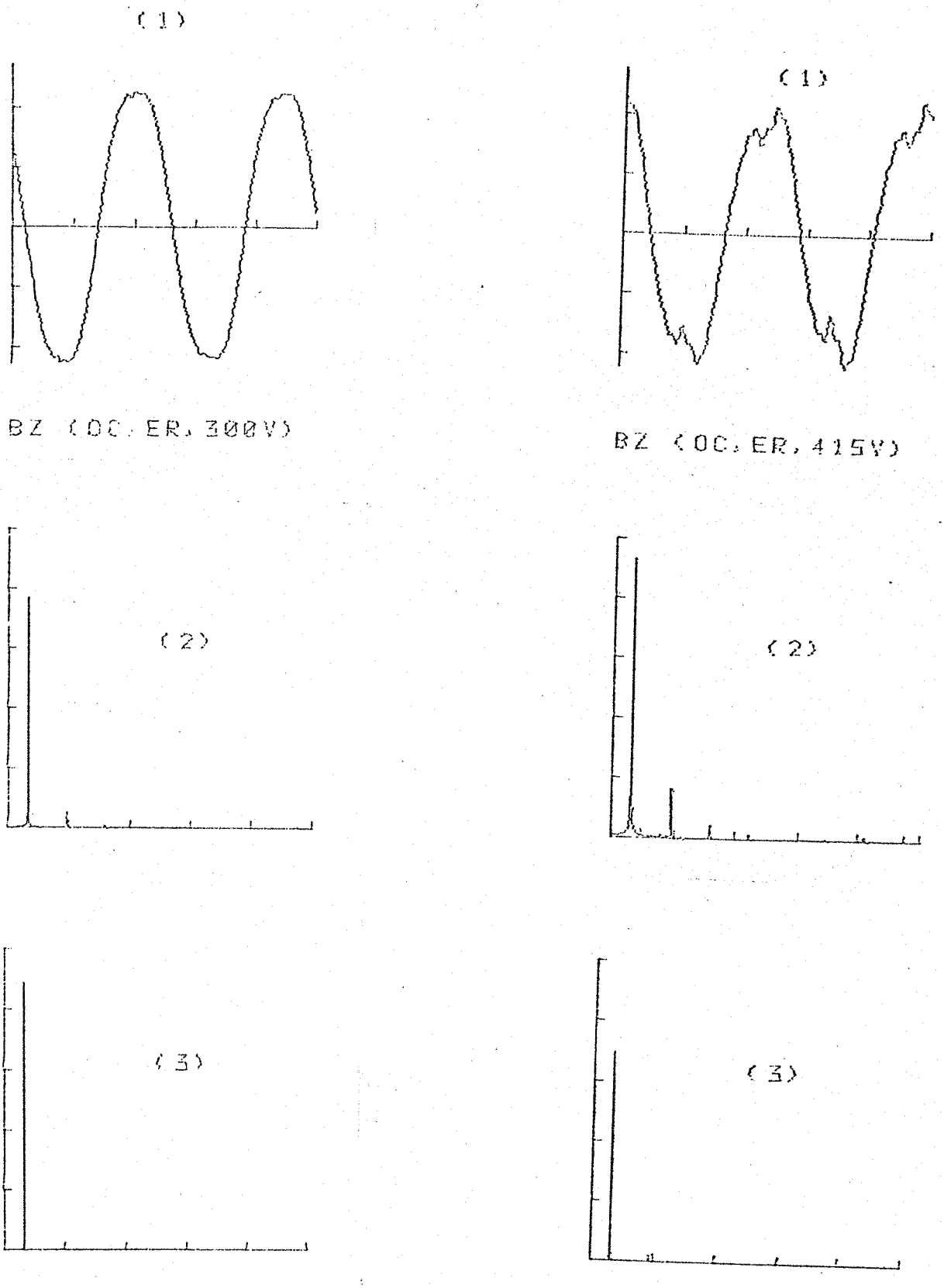

Fig. 6.18:Axial leakage flux density (core back end region).

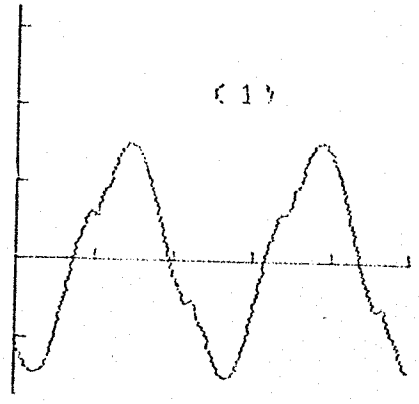

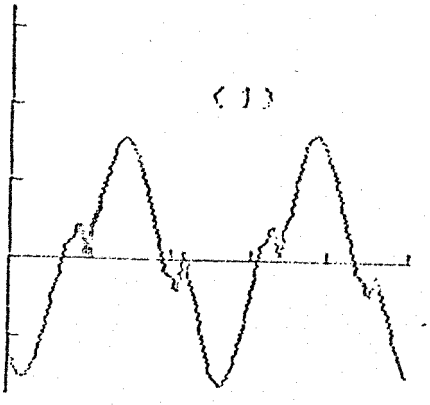

B0 (OC. CR. 300V)

B0 (OC. CR. 415V)

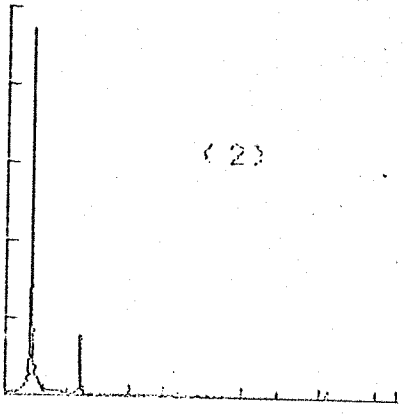

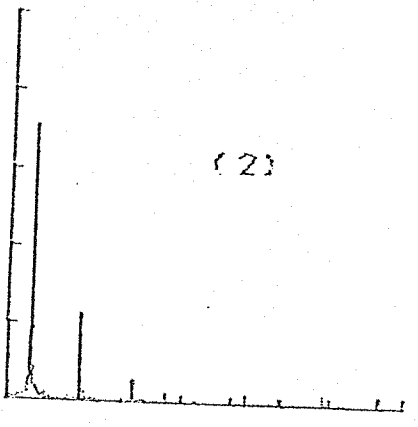

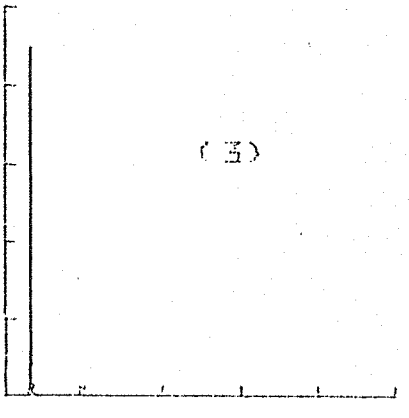

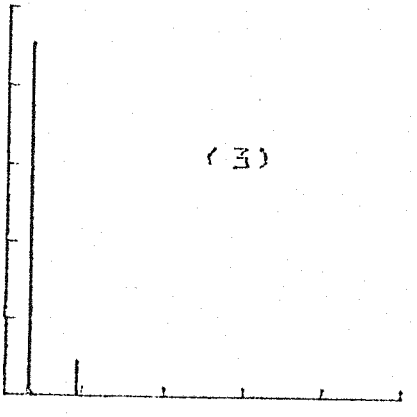

Fig. 6.19b: Circumferencial leakage flux density (core back centregion).

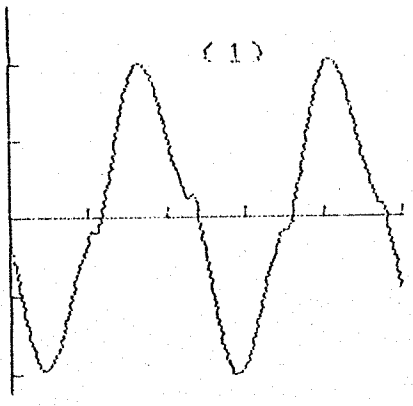

B2 (OC. ER. 300V)

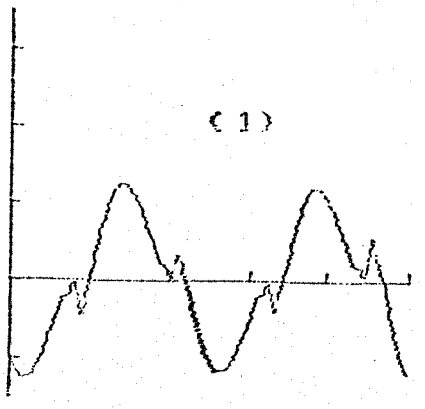

B0 (OC. ER. 415V)

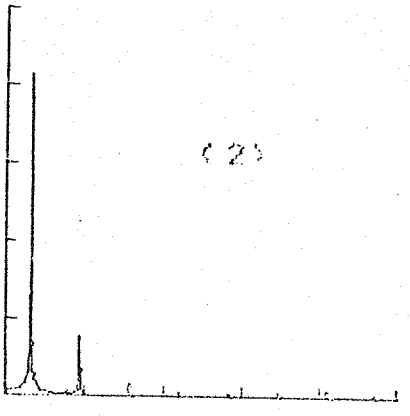

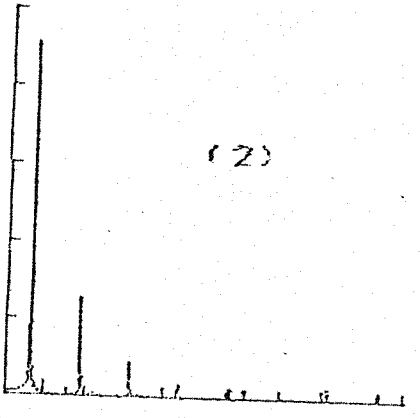

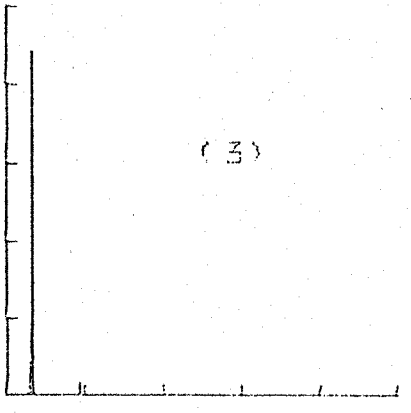

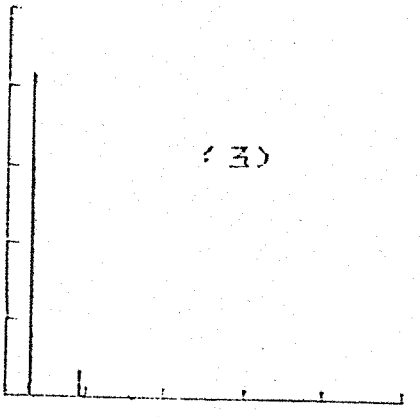

Fig. 6.19a: Circumferential leakage flux density (core back end region).

CHAPTER SEVEN

LEAKAGE FLUX AT THE STATOR CORE BACK OF THE SYNCHRONOUS MACHINE UNDER ON-LOAD CONDITIONS

7.1 GENERAL

When the synchronous machine was operating under on-load conditions the rotor winding was excited by a d.c. current, the rotor was driven at a constant speed by a d.c. motor and an a.c. current was induced in the stator winding (the synchronous laboratory machine was operated as a generator).

The synchronous machine field current was varied in such a way that the machine operated either at overexcited or at underexcited conditions. When the machine was overexcited the field current was higher than when the machine was underexcited. An overexcited synchronous machine delivers reactive power and an underexcited one consumes reactive power.[89] Actually most of the discussions presented are directed to the synchronous machine operating as a generator because the largest machines constructed up to now are the synchronous generators which are likely to have more accentuated effects caused by the core back leakage flux.

Knowledge of the power factor is very important to the determination of the distribution of leakage flux in the synchronous machine. The effects of different power factors on the heating produced at the stator core front have been discussed by several authors.[9,13,16,22,90-92] An increased effect of the axial leakage flux penetrating the stator core front is obtained when the synchronous generator is operating at leading power factor. The effects of the power factor in the distribution of leakage flux at the stator core back are presented in section 7.3.3.

7.2 THE CONTRIBUTION OF THE MAGNETIC SOURCES

Neither during short circuit nor during open circuit conditions are all of the main electromagnetic sources of core back leakage flux present. The magnetic surface polarity at the bore does not exist when the synchronous machine is operating in short circuit conditions and the overhang current is not present in open circuit operation, as discussed in Chapters Five and Six respectively. However, when the synchronous machine is at on-load conditions, all the main electromagnetic sources produce a magnetic field component which contributes to the leakage flux at the stator core back. In terms of electromagnetic sources the operation on-load condition can be considered as if both the short and the open circuit conditions were put together.

Richardson[90] shows that the leakage flux at the end region of the stator core may be obtained from the vector sum of the leakage fluxes due to both the stator and rotor windings. Because we are dealing with vector fields, not just the amplitudes of the flux components are necessary to calculate the total leakage flux at the core end, but also the phase angle between the components is essential. That phase angle is determined by the power factor of the synchronous machine. The leading power factor gives a greater intensity of core end leakage flux because the leakage flux component due to both the stator and rotor windings assist one another. However, at lagging power factor the leakage flux components due to both the stator and rotor windings are in anti-phase and are actually subtracting one another. A larger leakage flux at the core end produces larger magnetisation effects on the surfaces of the stator core. Therefore the magnetic surface polarities at both the core front and the core back are increased at leading power factor.

The bore polarity in an ideal machine is expected to have a uniform distribution of magnetic poles in the axial direction but, in practice the end of the bore has a larger concentration of magnetic poles. The magnetic surface polarity at the core front has a bigger intensity at the region close to the bore. The stator core back magnetic surface polarity has a greater intensity at the edge of the core back. Therefore the concentration of magnetic poles at the core surface can be more accentuated when the machine is operating at leading power factor and the contribution of the electromagnetic sources to the core back leakage flux can be increased. Actually a larger interaction between the electromagnetic sources is expected during the operation at leading power factor.

7.3 LEAKAGE FLUX DISTRIBUTION

The distribution of leakage flux around the stator core back surface was examined in terms of the axial, radial and circumferential components. The effects of the power factor on the leakage flux distribution are also presented.

7.3.1 Variation of the Leakage Flux Along the Stator Core Back Length

The results obtained when the synchronous machine was operating on-load come to confirm the shape of the distribution of the leakage flux along the stator core back length. Therefore, also on load conditions, the edge of the core back has a larger concentration of leakage flux than the centre region. The reason for that is the same as that presented in both short and open circuit operation: the edge is closer to the main electromagnetic sources than the centre of the core back. Although now both the overhang current and the bore polarity sources exist together.

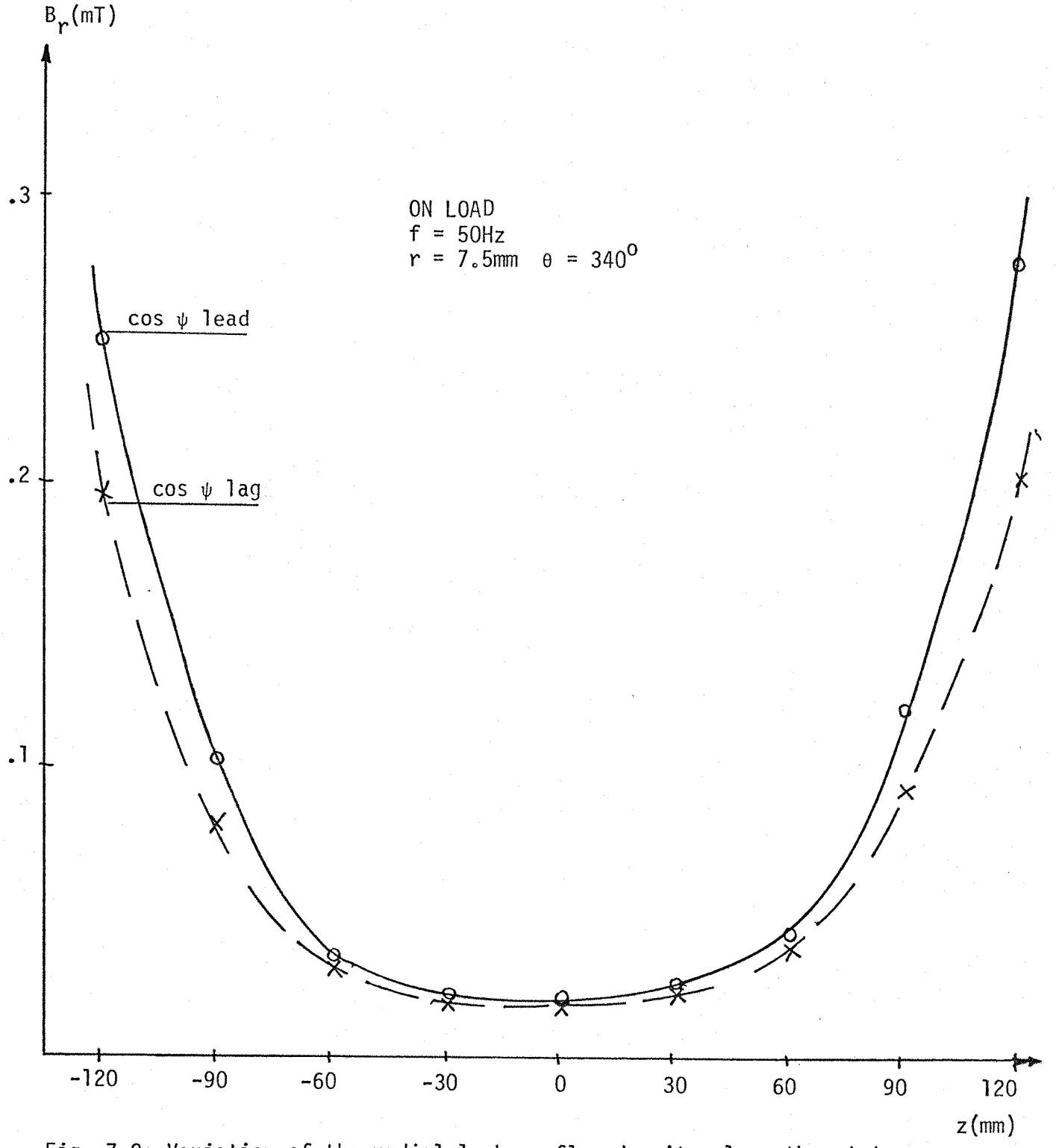

Fig. 7.2: Variation of the radial leakage flux density along the stator core back length.

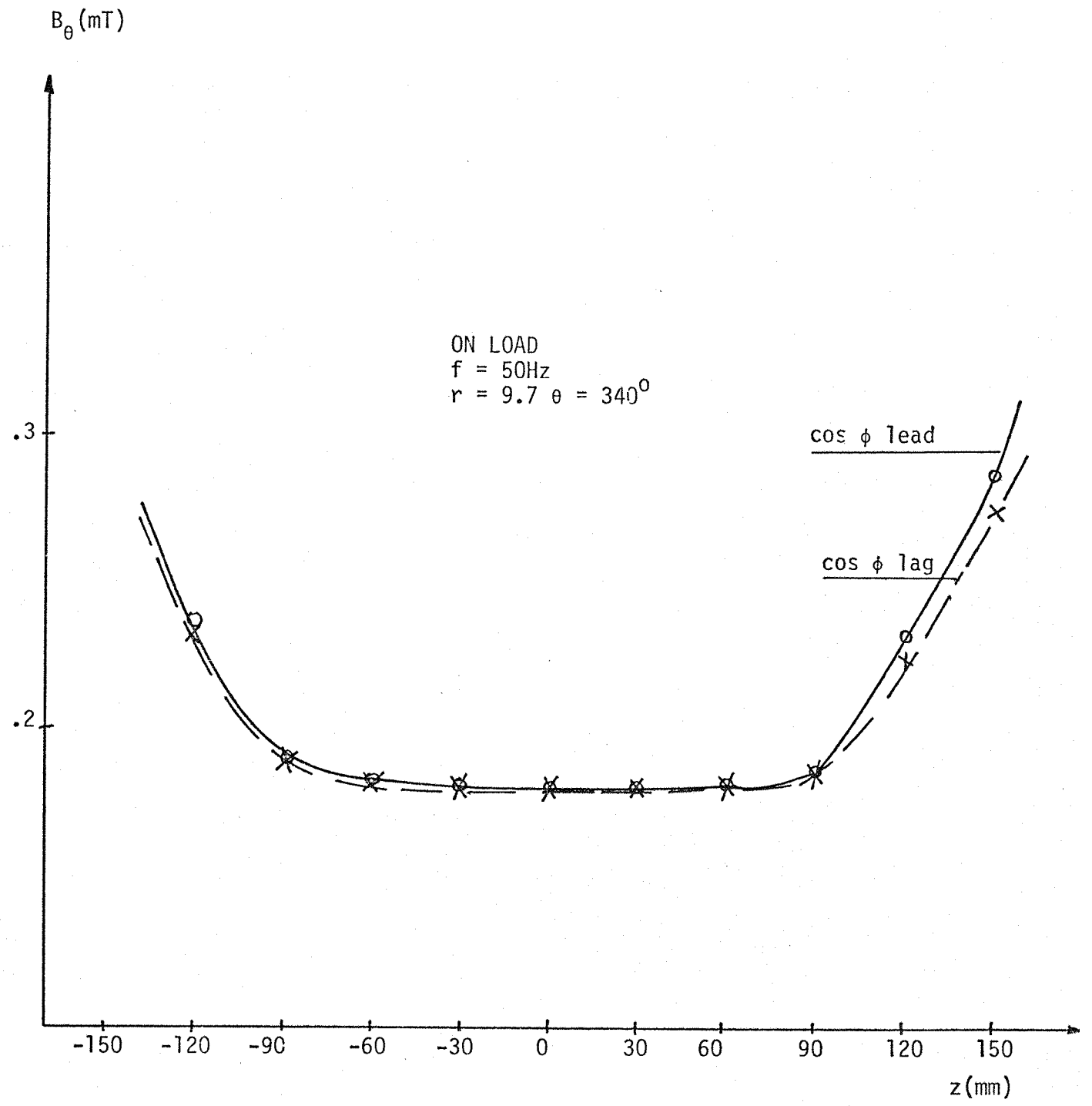

Fig. 7.3: Variation of the circumferential leakage flux density along the stator core back length.

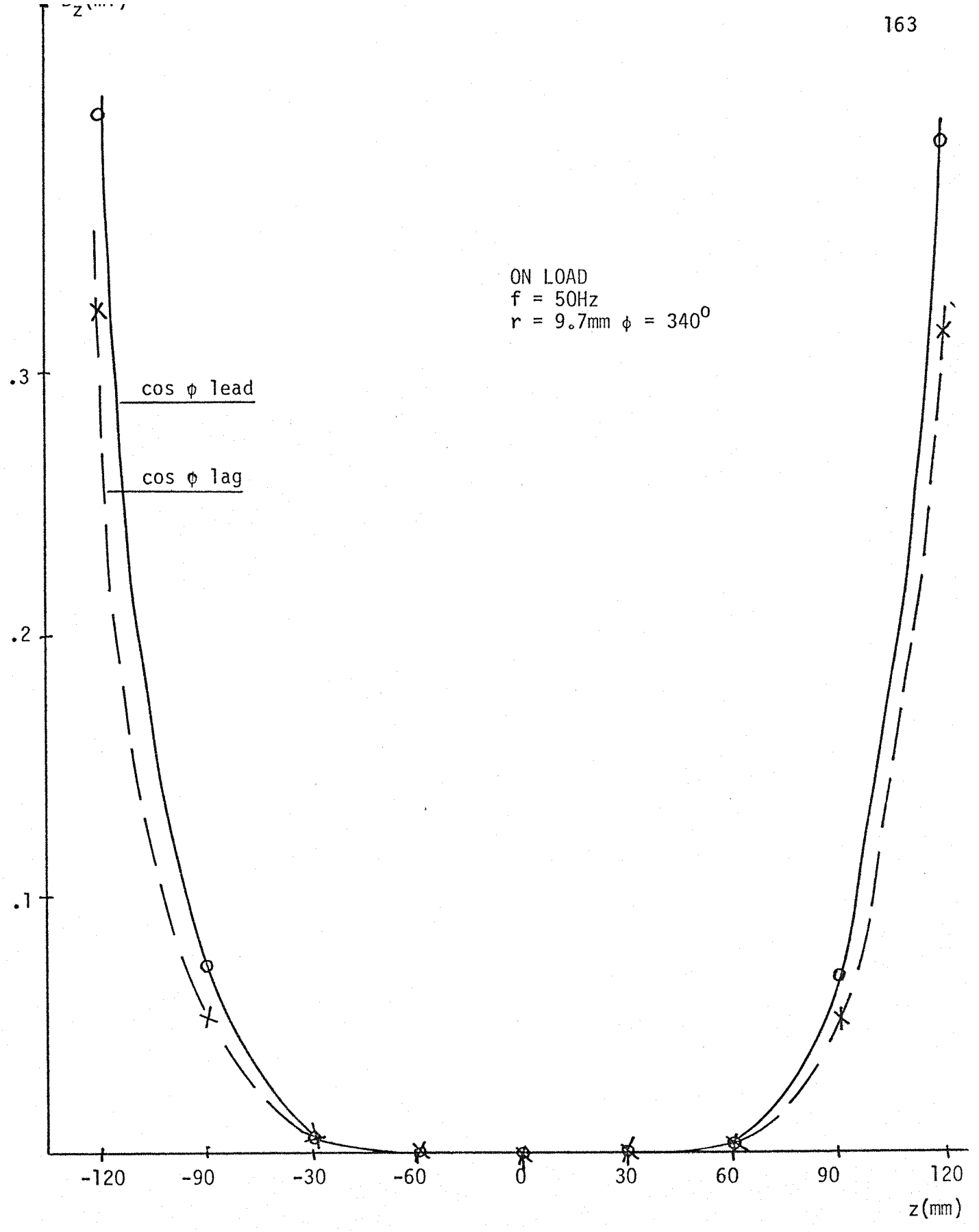

Fig. 7.4: Variation of the axial leakage flux deisnty along the stator core back length.

Figure 7.2 shows the variation of the radial component of core back leakage flux density along the core back length at both lagging and leading power factors. The curves at both power factors confirm the existence of a higher intensity of radial leakage flux at the edges of the core back. Figure 7.3 shows the variation of the axial component of the axial leakage flux density along the core back length for operations at lagging and leading power factors. The axial leakage flux at the centre of the core back is equal to zero. The axial leakage flux increases towards the edges of the stator core back at both power factors. The circumferential component of leakage flux density also varies along the stator core length, as shown by the curves in figure 7.4, at both lagging and leading power factors. Although the curves shown in figure 7.4 are flatter than those obtained for both the axial and radial components. The highest intensity of circumferential leakage flux also localises at the edge of the core back but the circumferential component at the centre region is different of zero. Further discussions about the distribution of the leakage flux along the core back length are presented in Chapters Five and Six.

7.3.2 Variation of the Leakage Flux With the Distance From the Stator Core Back Surface

The distribution of the core back leakage flux in the radial direction varies at the different planes (z, θ) over the stator core back region. The sharpest variation of core back leakage flux occurs at the edge of the stator core back and the greatest intensity of core back leakage flux is at the end surface of the core back.

The variation of the radial component of leakage flux against the distance from the stator core back surface is shown in figure 7.5. Several curves are shown at different axial positions

along the stator core back. The curves show that the radial leakage flux varies in a similar way to that obtained during both short and open circuit conditions, i.e. it has an initial decrease, changes direction, reaches a minimum and tends to zero when planes more distant from the back surface are considered. The several curves also show that the plane where the radial component changes direction is not the same for the different axial positions along the core back. Actually, when the distance from the core back surface is increased the direction of the radial component is first changed at the edge and successively towards the inner axial positions with the continuous increase in the distance. That phenomenon is due to the fact that the electromagnetic sources are closer to the edges and because the field components due to the main sources do not have the same direction, as shown in figure 3.1. In the air region of the core back both the overhang current and the surface polarity at the back of the core produce field components in the opposite direction of the field components produced by both the bore and core front polarities. The intensity of the field component varies inversely with the square of the distance between the source which produced the field and the point where the magnetic field is analysed. At the core back surface the polarity at the back of the core source produces the largest field component. Local effects are generally due to local sources. However, the intensity of the field component due to the polarity at the back of the core has a much larger decrease than the intensities of the components due to both the bore and core front polarity sources when the distance from the core back surface is continuously increased. Therefore, there is a distance from the core back surface where the field component due to both the polarity at the back of the core and the overhang current is smaller than the field component due to both

the bore and core front polarities. Then the total field changes the direction. Because the inner axial positions along the core back length have a larger influence from the polarity at the back of the core it is necessary to reach more distant planes in order to have a change in the radial leakage flux. Actually towards the centre of the core back the stator iron behaves as a screening body to the magnetic fields due to the core front region. With further increase in the distance the total leakage flux decreases because all the source contributions decrease. The curves in figure 7.5 show that the change of direction in the radial leakage flux at the core back first occurs at the axial position z = 120mm and then successively at z = 115, z = 105, z = 90 and z = 30mm.

Figure 7.6 shows the variation of the axial component of the leakage flux density against the distance from the core back surface at different axial positions along the stator core back. Again, as obtained during both the short and the open circuit, the axial leakage flux first increases, reaches a maximum and then decreases. That is explained by the changing of direction of radial leakage flux to the axial direction which causes an increase in the axial component of leakage flux. As discussed in sections 5.3 and 6.3, the leakage flux in the surface of the core back is predominantly in the radial direction. However, increasing the distance from the core back surface the axial component is initially increased up to a maximum value and then decreases with the continuous growth in the distance. The different axial positions along the stator core back do not reach the maximum at the same distance. A position closer to the edge of the core back reaches the maximum intensity at planes closer to the back surface than a position more distant from the edge, because both the bore and the core front polarities have an increased effect at the edge and

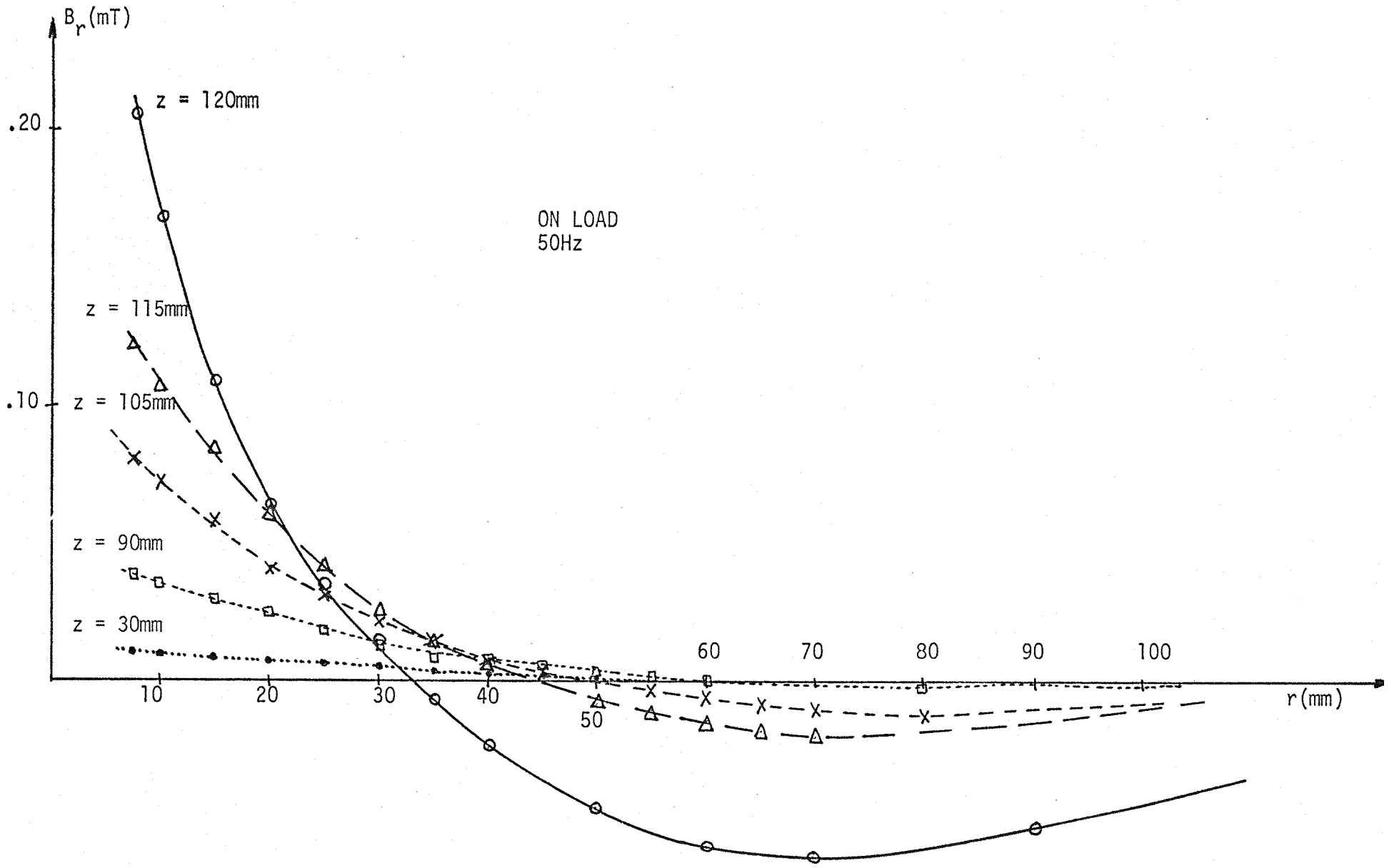

Fig. 7.5: Variation of the radial leakage flux density against the distance from the stator core back surface

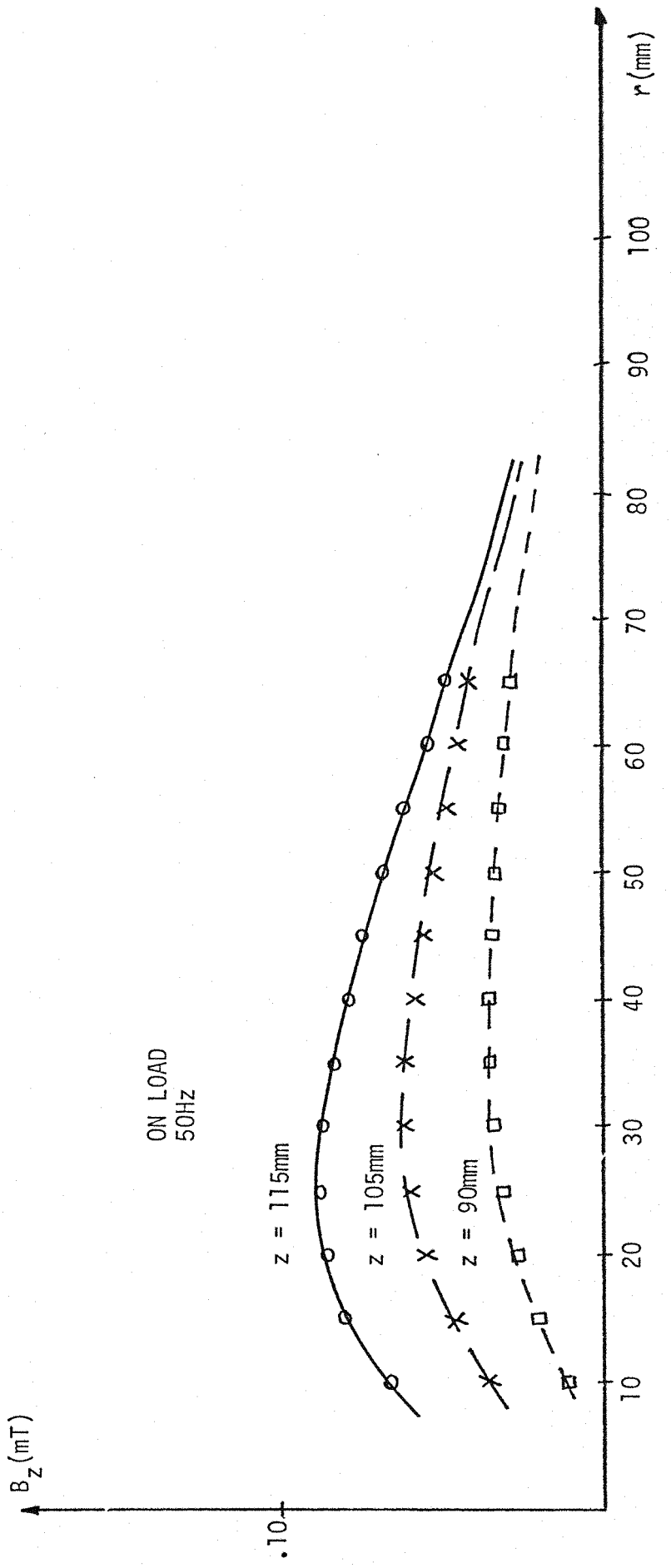

Fig. 7.6: Variation of the axial leakage flux density against the distance from the stator core back surface.

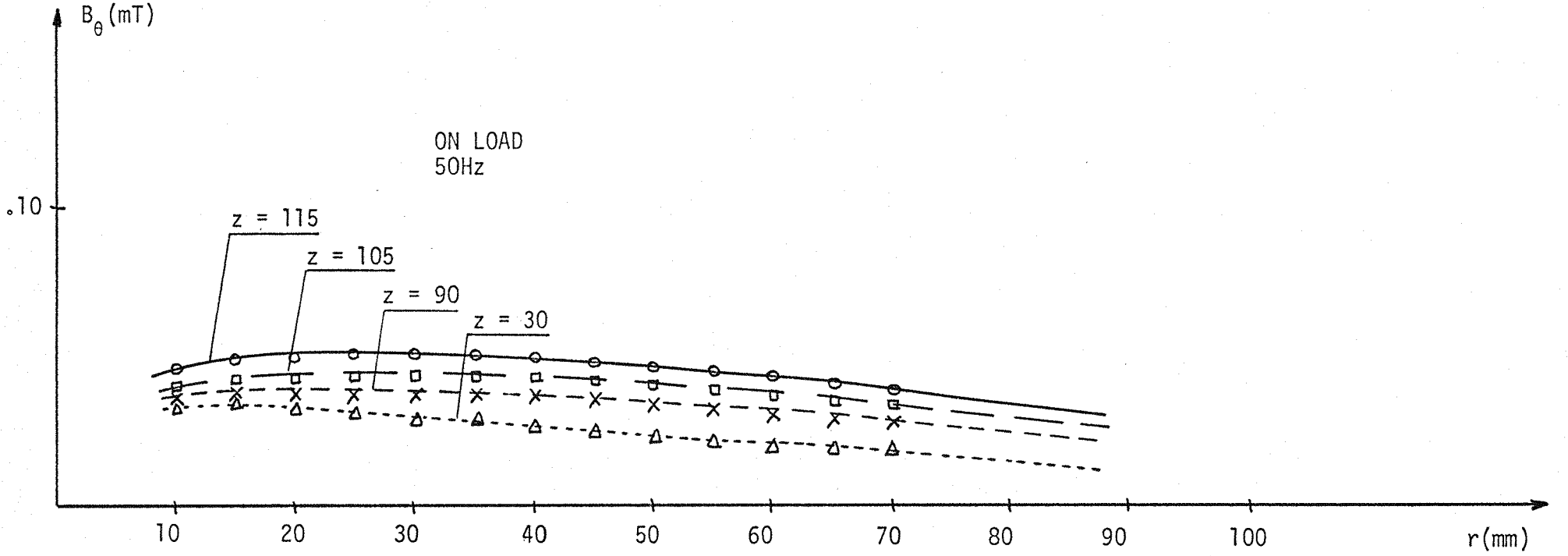

Fig. 7.7: Variation of the circumferential leakage flux density against the distance from the stator core back surface.

bend the core back leakage flux towards the stator front region.

Figure 7.7 shows the variation of the circumferential leakage flux density against the distance from the surface of the stator core back. This component also has curves similar to those obtained during both short and open circuit conditions. The circumferential leakage flux also shows an initial increase of magnitude due to the change of radial core back leakage flux into the circumferential direction. At the edge zone of the core back most of the leakage flux is changed to the axial direction due to the influence of the main sources at the core front region. Although at the centre region of the stator core back length a larger relative proportion of radial leakage flux is bent to the circumferential direction because of the weaker effects of the core front main sources. At the centre region the polarity at the back of the core has a more predominant effect. Further discussions are presented in both sections 5.3 and 6.3.

7.3.3 Power Factor Effects

The power factor can be defined either as leading or lagging depending on the stator current leading or lagging the voltage in the stator, respectively. For the synchronous machine operating as a generator, which is the case of the laboratory synchronous machine used in this thesis, the leading power factor defines the underexcited operation of the synchronous machine and the lagging power factor defines the overexcited operation. The opposite occurs if the machine is operated as a synchronous motor. The field current in the rotor winding is larger at overexcited conditions than at underexcited conditions. The synchronous machine delivers or consumes reactive power if it is operated overexcited or underexcited respectively.

The power factor plays an important role in the determination of leakage flux at the stator core end of the synchronous machine. Several authors have studied the effects of the power factor in the core end leakage flux. Ashworth and Hammond[13] show the variation of the core end leakage flux components with the power factor. Richardson[90] shows that the power factor modifies the temperature at the stator core front with either magnetic or non-magnetic end-rings, at various stator currents and at different hydrogen pressures. Mason et al.[91] show the variation of the core end-ring temperature with the power factor for both cases of magnetic and non-magnetic end-bell. Hawley et al.[22] present the variation of the stator end region temperature with the power factor. Stoll and Hammond[16] show the variation of the clamping-plate loss due to the power factor. Winchester[9] discusses the variation of the end tooth temperature with the power factor. Estcourt et al.[92] present the variation of the core front temperature with the power factor. There is a unanimous conclusion that the leakage flux at the stator core end causes a more severe effect when the synchronous generator is operating at leading power factor.

The leakage flux at the stator core back also varies with the power factor. The intensity of core back leakage flux is increased when the synchronous machine has a leading power factor. That is explained by the fact that the contributions of the main electromagnetic sources to the core back leakage flux are greater at leading power factor. It might seem strange that the main sources components are greater at leading power factor, when the field is underexcited. Although it must be recalled that the main electromagnetic sources are located at the end of the machine where the magnetising effect of the core end leakage flux is increased at leading power factor, as discussed in section 7.2.

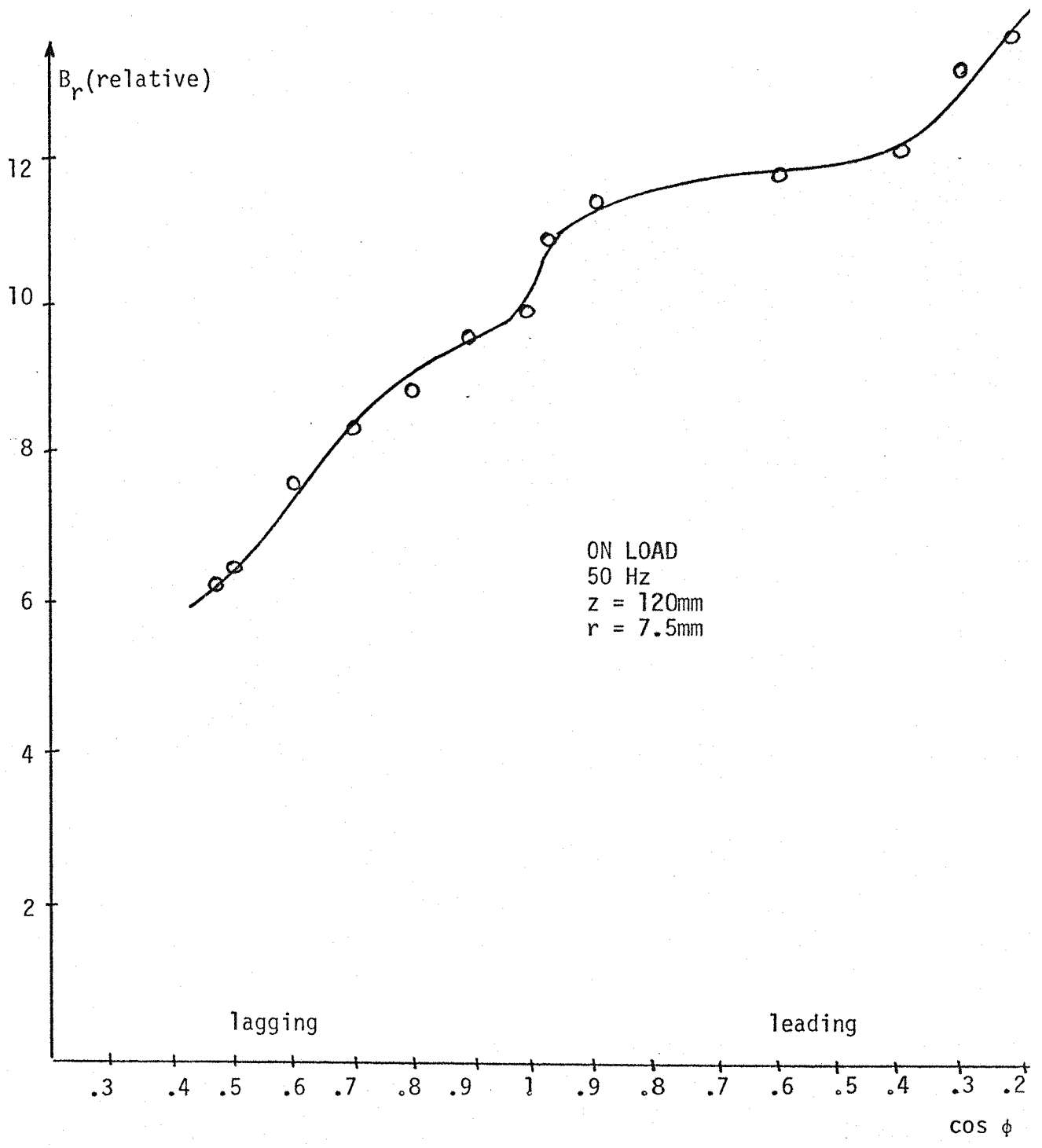

Fig. 7.8: Variation of the radial leakage flux density against the power factor.

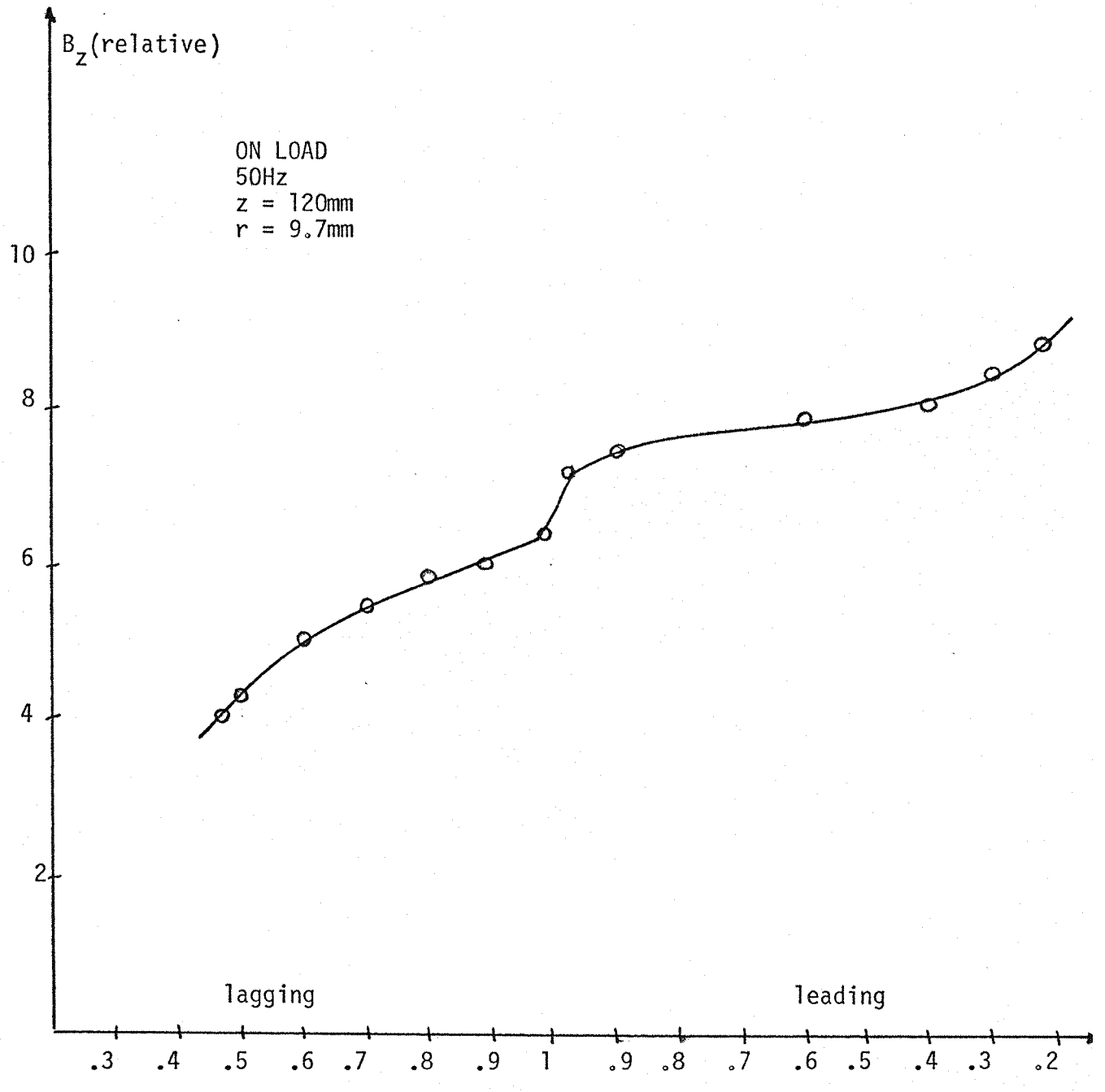

Fig. 7.9: Variation of the axial leakage flux density against the power factor.

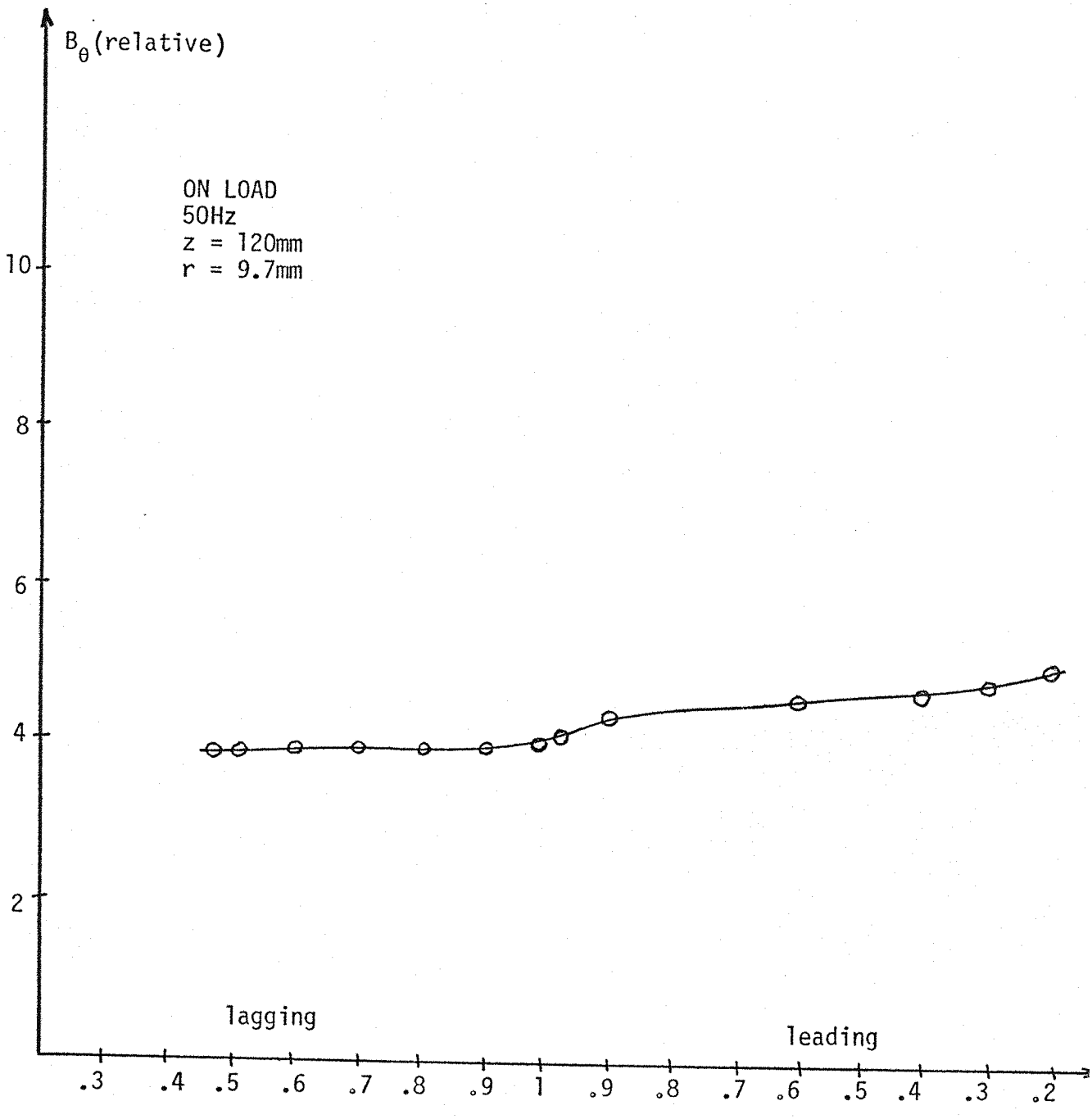

Fig. 7.10: Variation of the circumferential leakage flux density against the power factor.

The variations of the radial, axial and circumferential components of leakage flux at the stator core back with the power factor are shown in figure 7.8, figure 7.9 and figure 7.10 respectively. All the three components are increased when the synchronous machine is operating at leading power factor. A larger increment in the leakage flux is shown to occur at the edge of the stator core back.

7.3.3.A Harmonics in the core back leakage flux due to the power factor

The harmonics content in the leakage flux at the stator core back varies with the power factor. The magnitude of the odd harmonics is increased when the synchronous machine is operating at leading power factor. That is explained by the fact that the stator core is under more severe saturation conditions at leading power factor because of the greater leakage flux at the core end. The saturation causes distortion in the core back leakage flux waveforms producing larger odd harmonics, as discussed in section 6.3.5.A.

Figures 7.11 to 7.15 show the waveform, the fast Fourier transform and the power spectrum density for the radial, axial and circumferential components of leakage flux at both the edge and centre of the core back at both leading and lagging power factors. Those figures show that the components waveforms have a larger harmonic content at leading power factor, either at the centre or the edge of the core back. However, the increase in the odd harmonics magnitudes is more pronounced at the edge of the core back. The graphs of the fast Fourier transform[88] show an increase in the relative amplitudes of the odd harmonics obtained at leading power factor. Mainly both the third and the fifth harmonics show an increase in their amplitudes relative to the amplitude of the fundamental at leading power factor.

The graphs of the power spectrum density show that the third harmonic of the energy density in the magnetic field is increased at leading power factor.

Definitions of the abbreviations presented in figures 7.11 to 7.15.

BR - radial component of the core back leakage flux

BZ - axial component of the core back leakage flux

Bθ - circumferential component of the core back leakage flux.

LO - on-load conditions

CR - centre region of the stator core back

ER - end region of the stator core back.

IND - leading power factor

CAP - lagging power factor.

(1) - Leakage flux component waveform

(2) - Fast Fourier transform (FFTA)

(3) - Power spectrum density (PSD).

Vertical axis: amplitudes

Horizontal axis, figure (1): time

figures (3) and (3): frequency (160Hz per division).

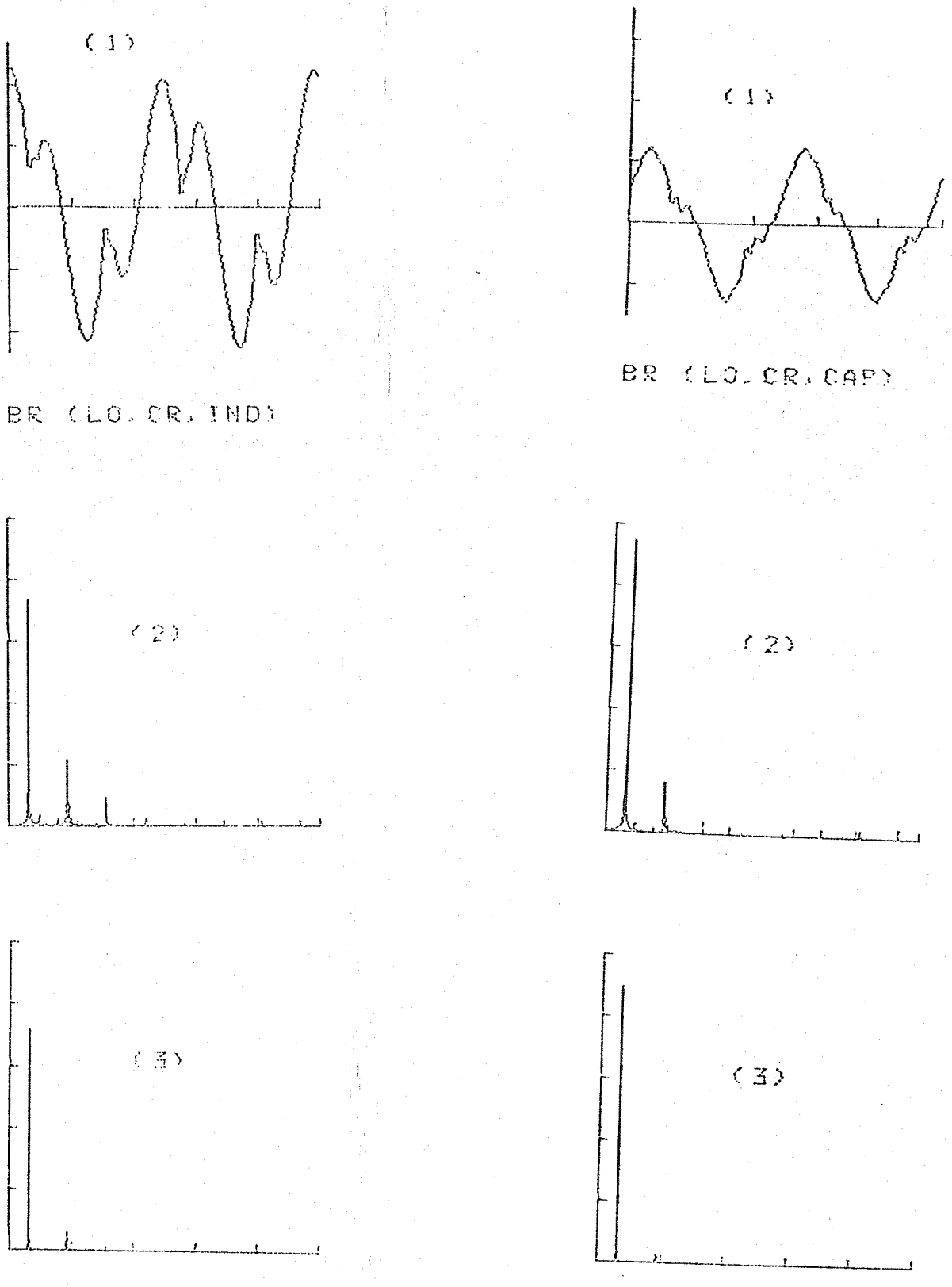

Fig. 7.11: Radial leakage flux density (core back centre region).

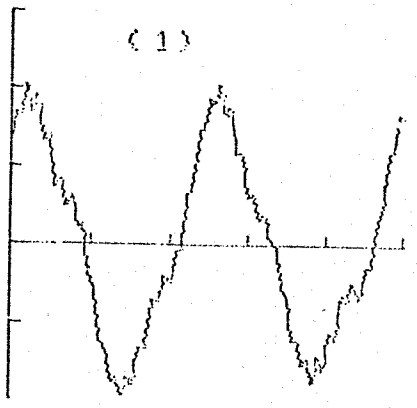

BR (LO, ER, IND)

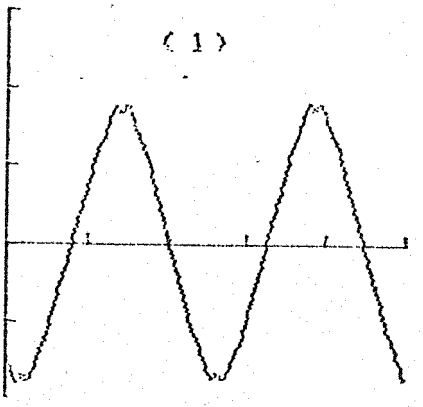

BR (LO, ER, CAP)

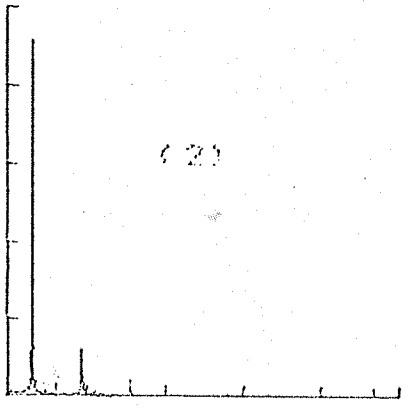

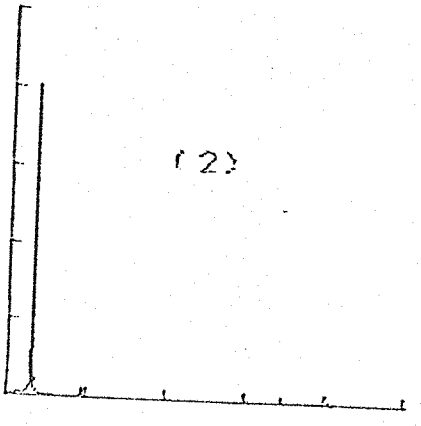

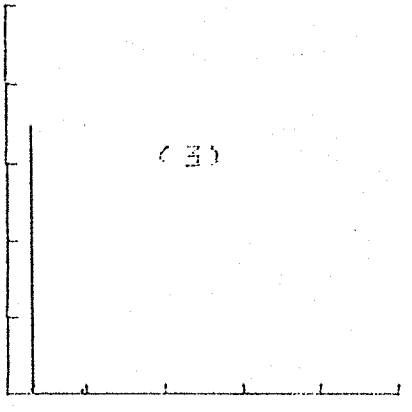

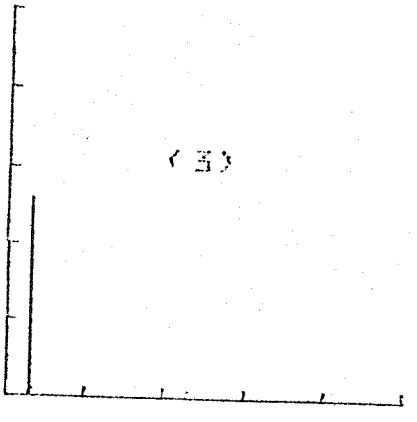

Fig. 7.12: Radial leakage flux density (core back end region).

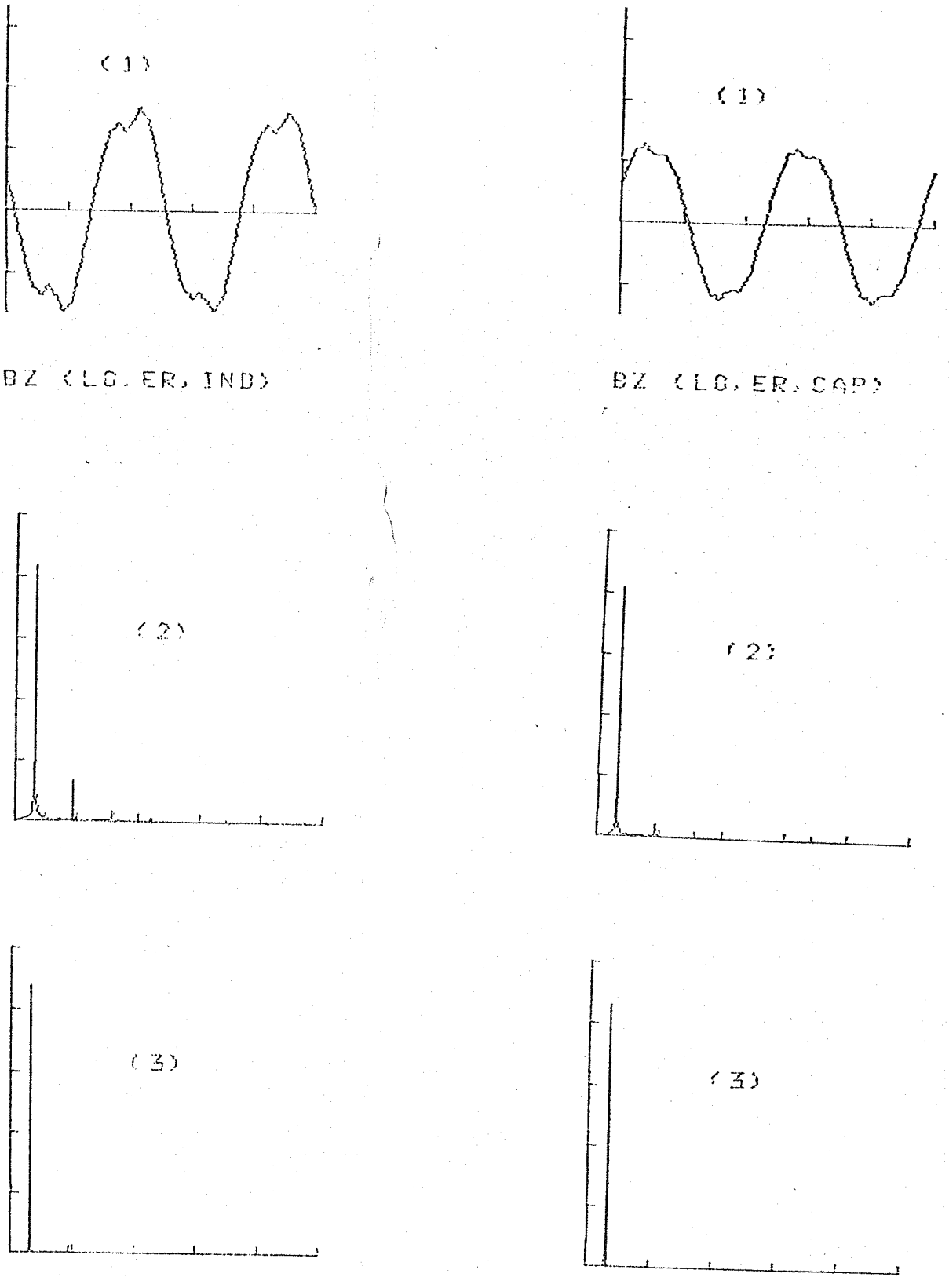

Fig. 7.13: Axial leakage flux density (core back end region).

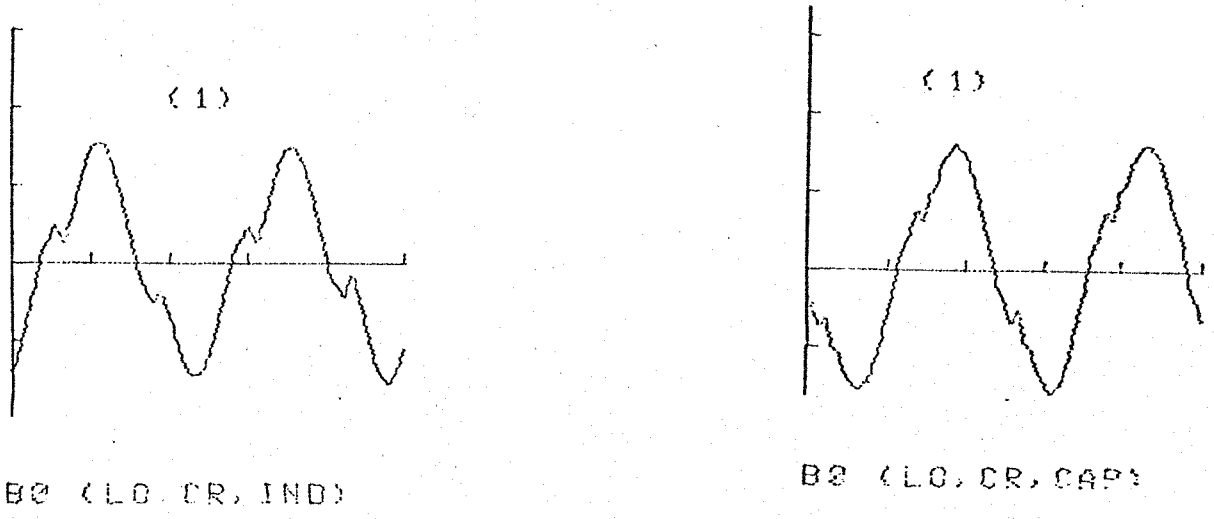

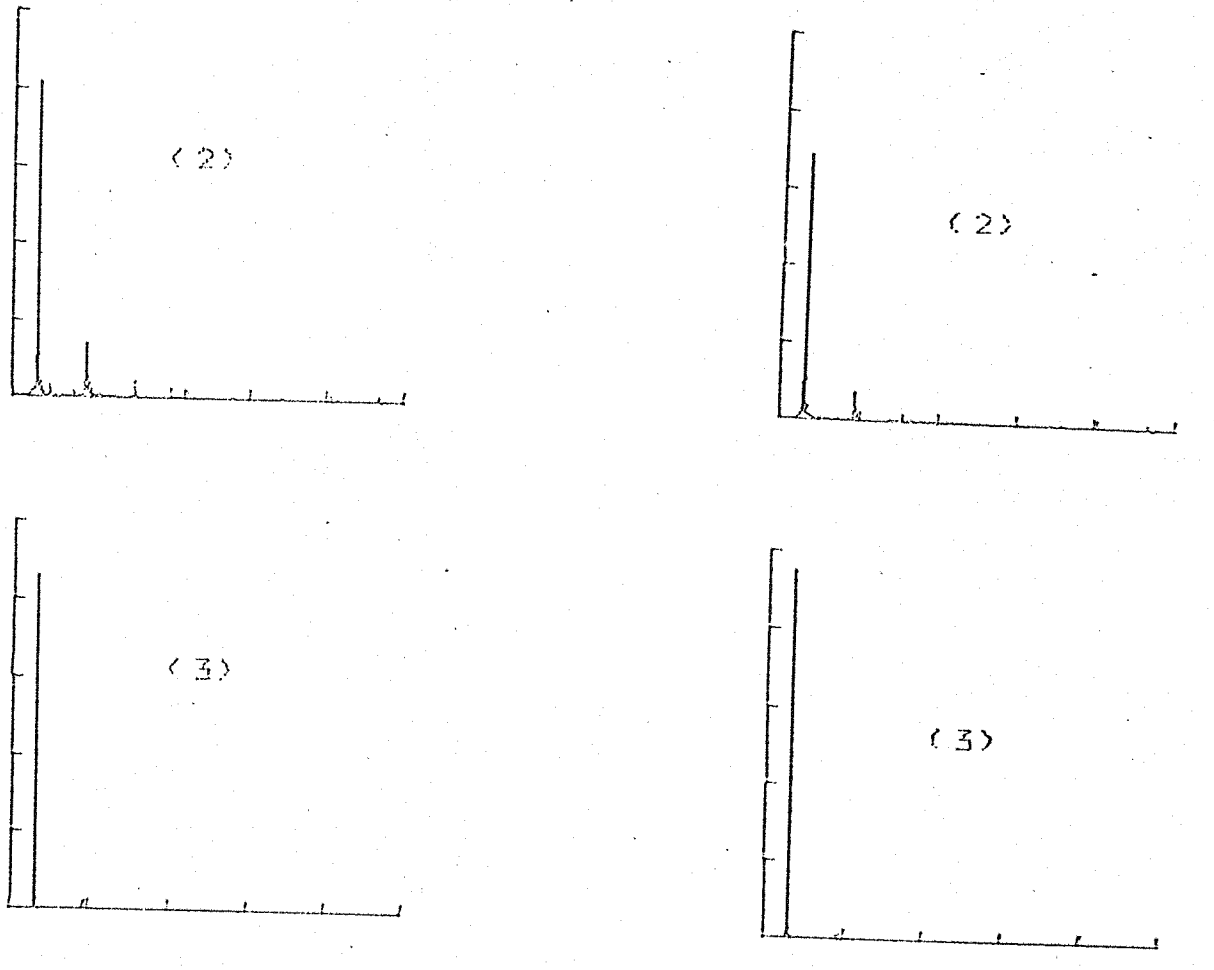

Fig. 7.14: Circumferential leakage flux density (core back centre region).

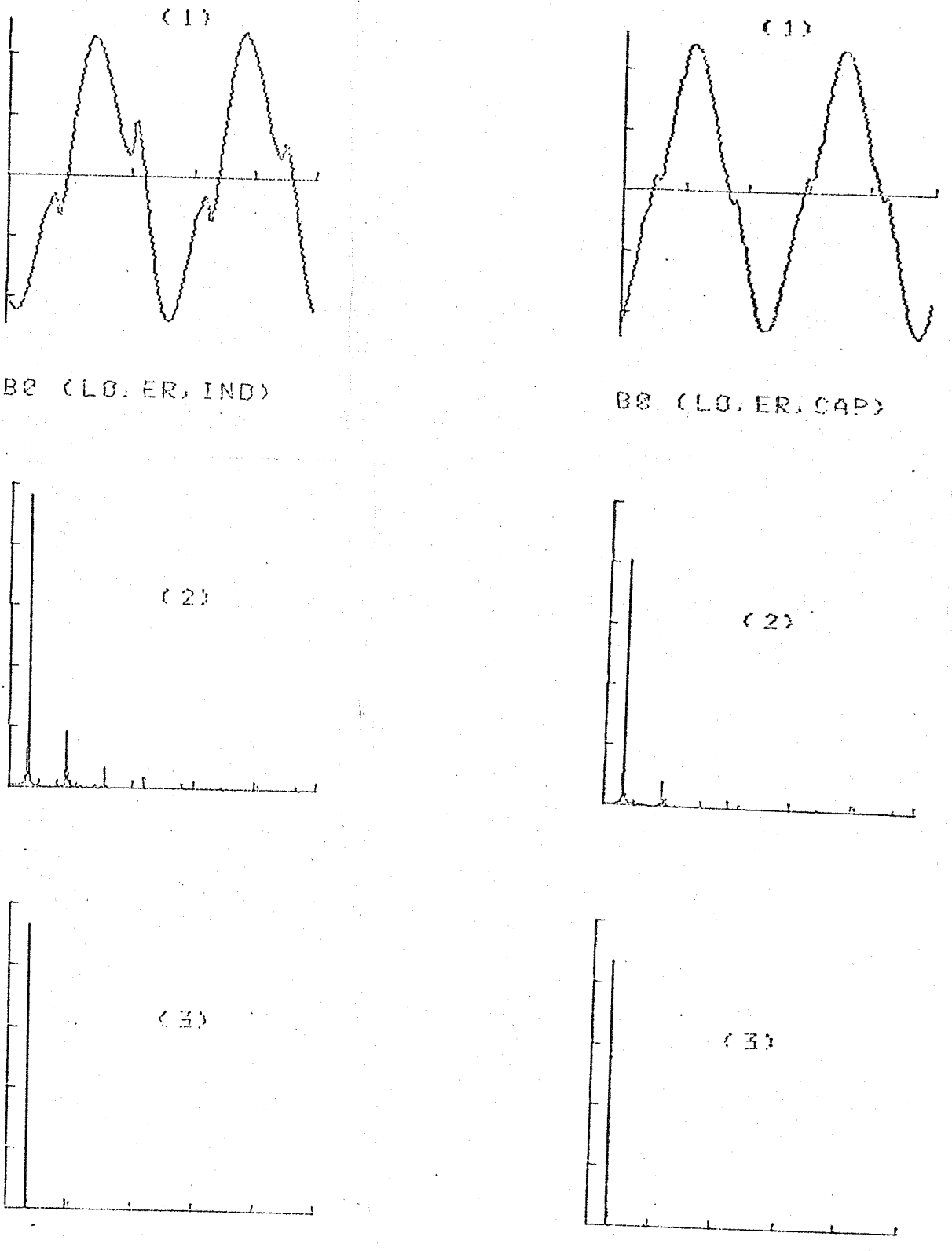

Fig. 7.15: Circumferential leakage flux density (core back end region)

CHAPTER EIGHT

EFFECTS OF DESIGN PARTICULARITIES ON THE DISTRIBUTION OF LEAKAGE FLUX AT THE STATOR CORE BACK OF THE SYNCHRONOUS MACHINE

8.1 GENERAL

The discussion presented in this chapter has as its main target to bring some light to the understanding of the effects of different design particularities on the distribution of core back leakage flux. The laboratory model presented in Chapter Two, in figure 2.6, was constructed in such a way that the effects of design particularities such as relative position between the rolling direction of the laminations, depth of the stator core, overhang length, air gap length, relative positions between both the stator and rotor cores, screening plates at the core front were investigated. Therefore, the discussion presented in this chapter is of particular importance to synchronous machine designers because the behaviour of the core back leakage flux is analysed for different geometries and dimensions of the synchronous machine.

The distribution of leakage flux at different radial, axial and circumferential positions along the stator core back is presented. Both the radial, axial and circumferential components of core back leakage flux were measured. Two different depths of stator core, 45mm and 70mm, and two different rotor diameters, 140mm and 225mm were utilised. The distribution of core back leakage flux was investigated for different combinations of those stator and rotor cores such as:

a) both smaller stator and rotor cores

b) both larger stator and rotor cores

c) smaller stator and larger rotor cores.

The distribution of leakage flux was also investigated for the cases:

d) smaller stator core without rotor

e) without the stator core and smaller rotor core

f) without both the stator and rotor cores (without any iron at all).

The stator winding has a diamond shape in order to enable the removal of the stator core laminations and also in order to make possible the variation of the length of the overhang. Two different depths of screening plate, 45mm and 70mm, were used in the stator core front when the eddy current effect was analysed. The effects of the overhang current in the distribution of leakage flux were also investigated.

The measurements were carried out with the stator core laminations packed in a randomised way. However, when the effect of rolling direction was investigated the stator core was built up with the laminations rolling direction aligned. The laminations were composed by one entire annular disc.

8.2 LEAKAGE FLUX DISTRIBUTION

8.2.1 Variation of the Leakage Flux Along the Stator Core Back Length

The distribution of the leakage flux along the stator core back of the model with stationary rotor is similar to the distribution obtained in the synchronous machine operating either on open and short circuits or on-load conditions. The edge of the stator core back has a larger concentration of leakage flux than the centre region. The reason for the higher intensity of leakage flux is also because of the positions of the main sources relative to the core back, as discussed

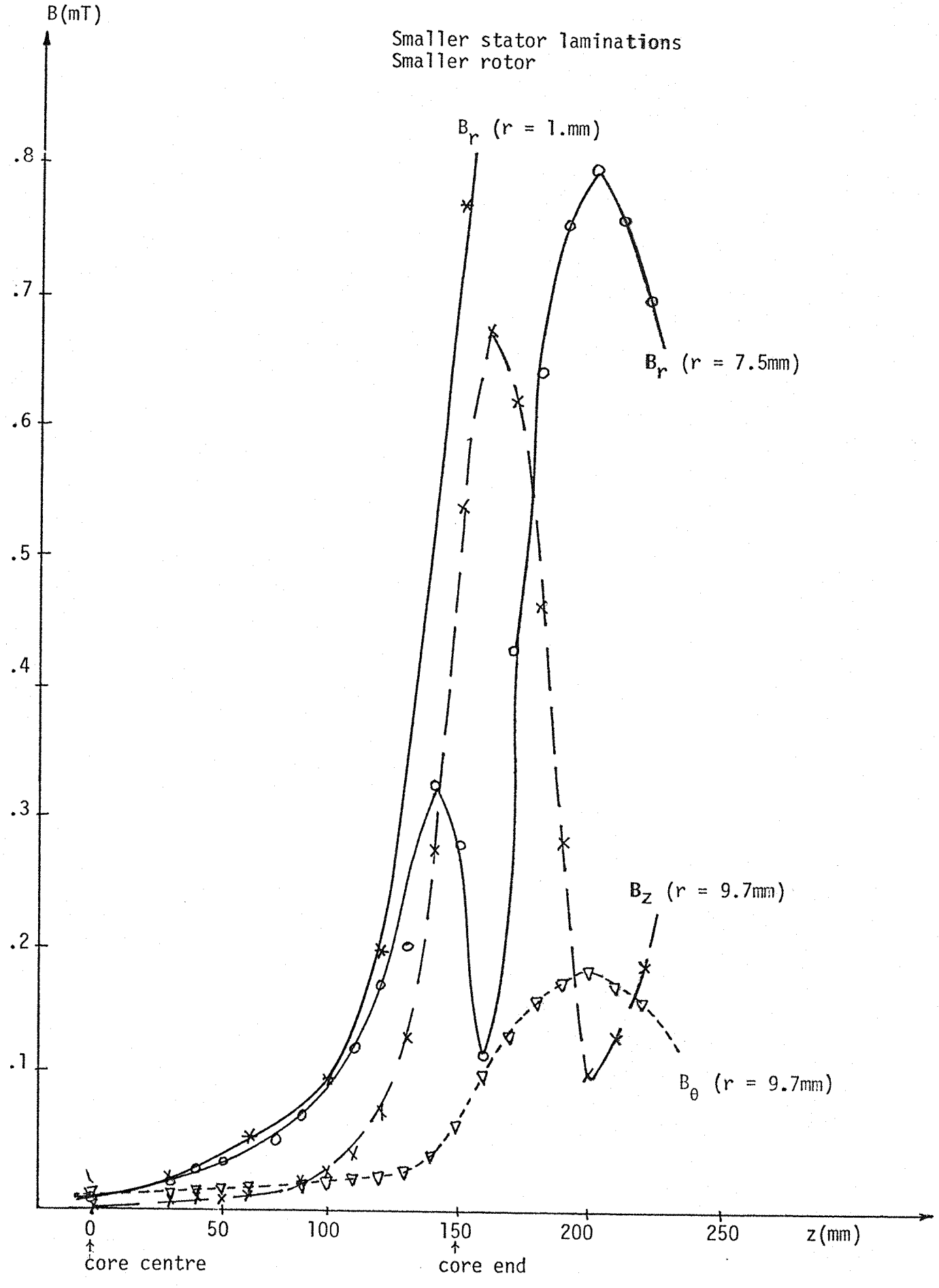

Fig. 8.1.a: Variation of the leakage flux density components along the stator core back length.

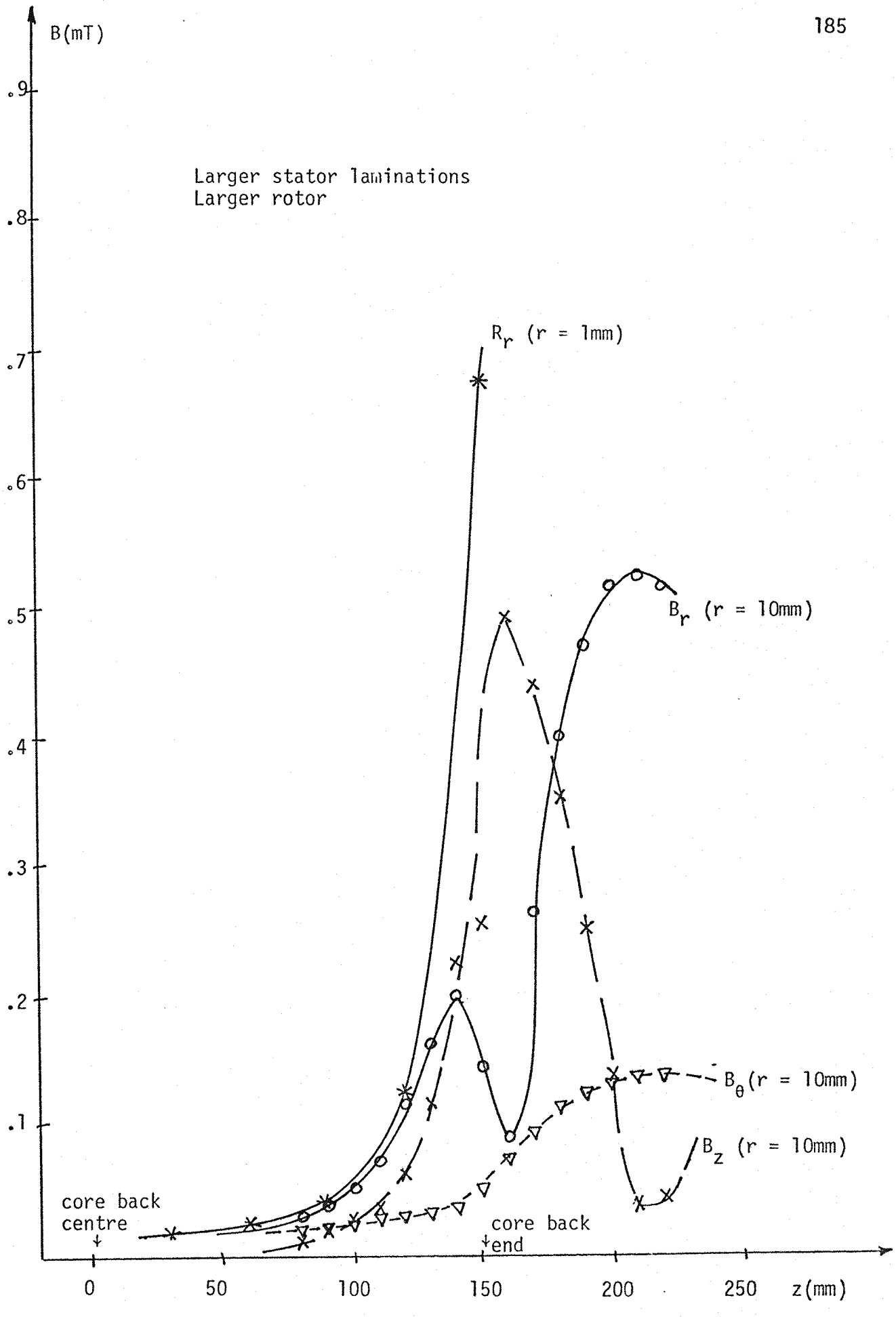

Fig. 8.1.b: Variation of the leakage flux density along the stator core back length.

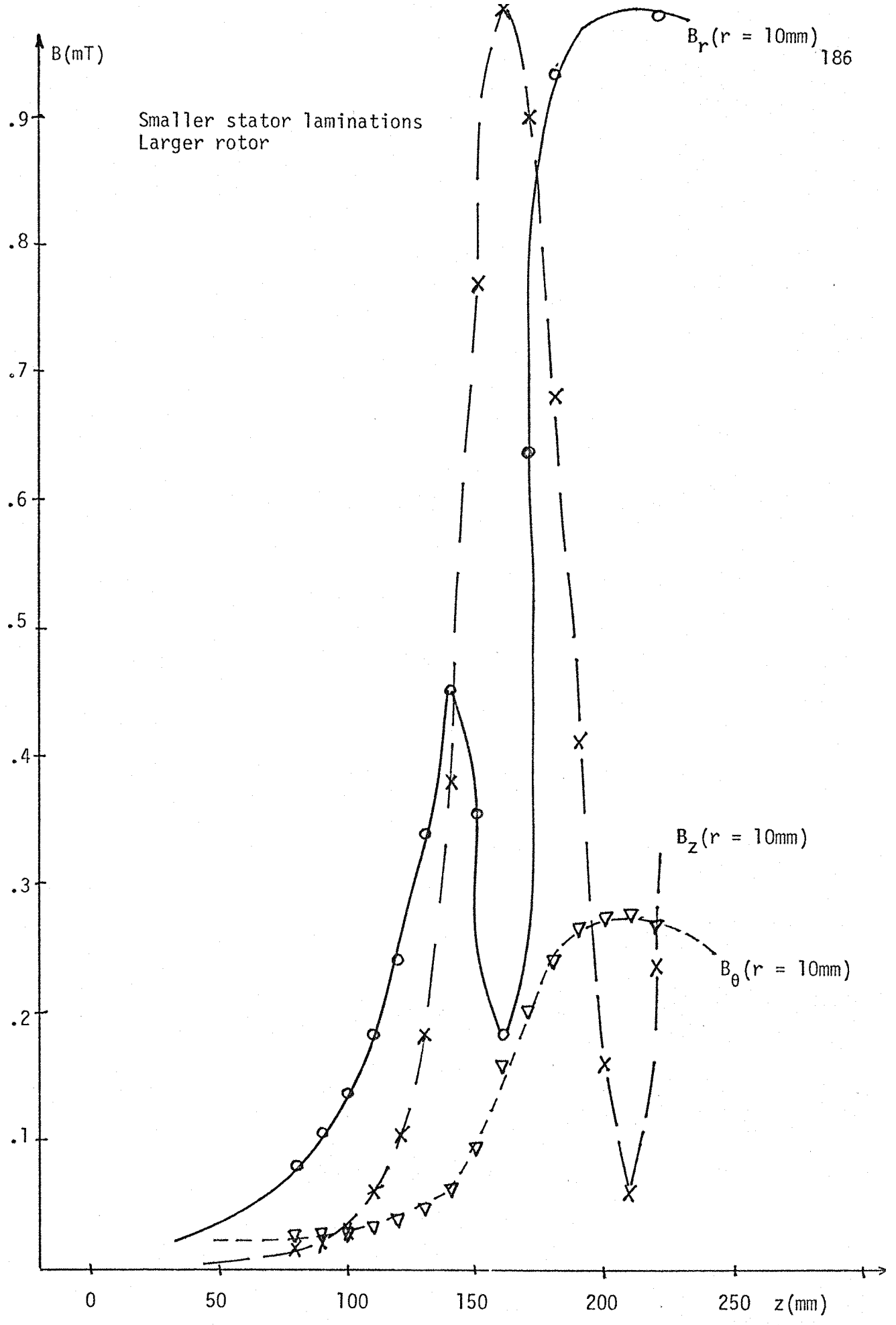

Fig. 8.1.c: Variation of the leakage flux density along the stator core back length.

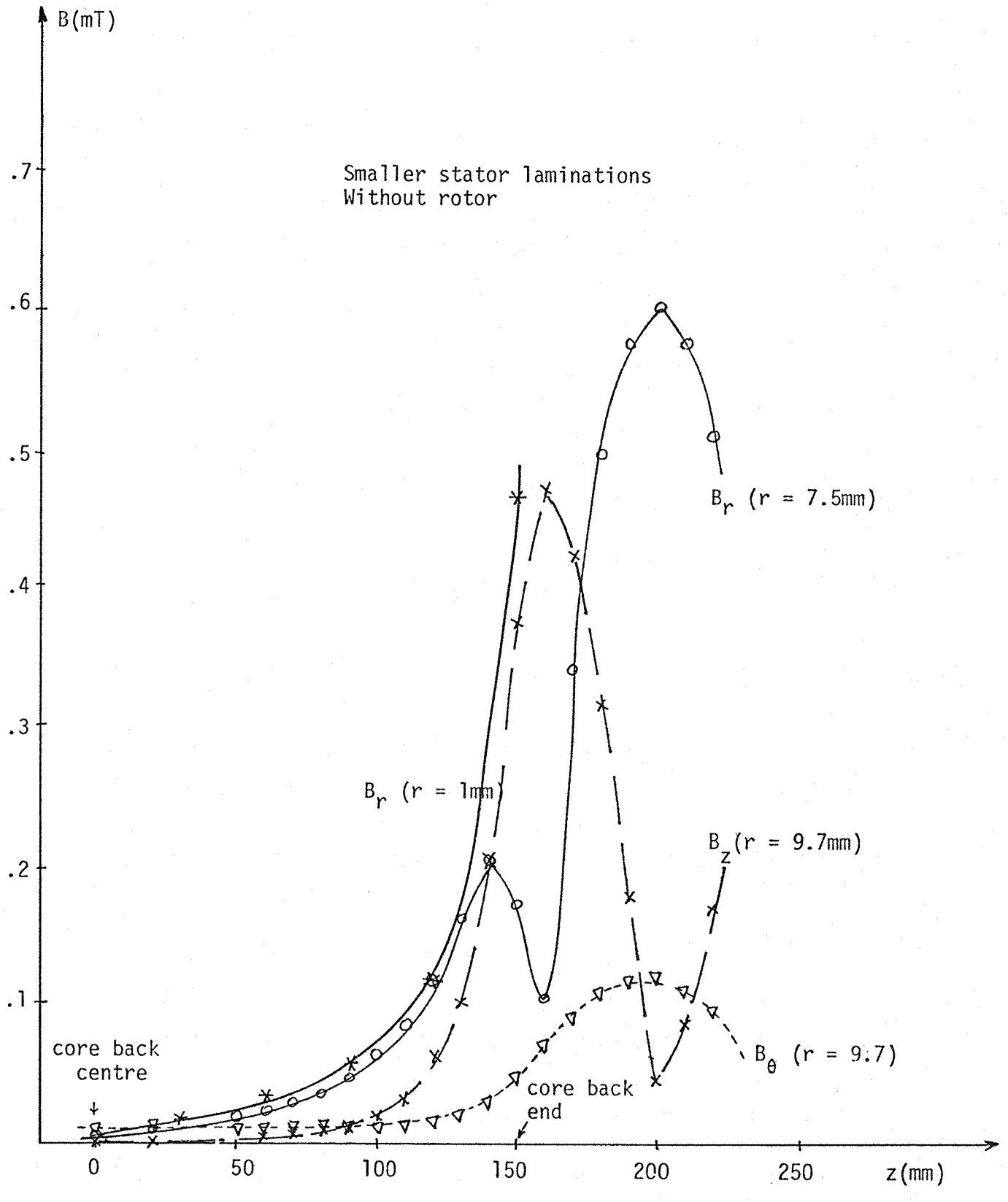

Fig. 8.1.d: Variation of the leakage flux density components along the stator core back length.

in detail in sections 5.3, 6.3 and 7.3. All the different combinations of stator and rotor cores show a larger concentration of leakage flux at the edge of the stator core back.

The variations of the radial, axial and circumferential components of the leakage flux along the stator core back, for different pairs of stator and rotor cores, are shown in figure 8.1 (a, b, c, d). The utilisation of different pairs of stator and rotor cores produces a modification in the intensities of the main electromagnetic sources located on the surfaces of the core. But it was not possible to isolate the surface polarities at the bore, stator front and stator core surfaces because they are implicit sources and interact with one another and also depend on the explicit overhang current source. In all the arrangements made in both the stator and rotor cores the overhang current was kept constant. Therefore, it is important to notice from figures 8.1 (a, b, c, d) that however the diameters of both stator and rotor cores were modified the core back leakage flux components are larger at the edge of the core back of the model.

8.2.2 Variation of the Leakage Flux With the Distance From the Stator Core Back Surface

The leakage flux varies with the distance from the surface of the stator core back of the model with stationary rotor in a similar way to the variation obtained in the laboratory synchronous machine operating either on short and open circuits or on-load.

The variations of the radial, axial and circumferential components of leakage flux against the radial distance from the core back surface are shown in figures 8.2, 8.3 and 8.4, respectively. Those figures show the variation of the intensity of the leakage flux

components at different positions along the stator core back. Also, different combinations of the larger and smaller cores of both the stator and rotor bodies are given in the figures mentioned before. Figures 8.5, 8.6 and 8.7 show the variation of the phase angle of the radial, axial and circumferential components, respectively; also at different positions along the core back and for different stator and rotor cores.

Further discussion about the variation of the leakage flux components with the distance from the back surface is given in sections 5.3.2, 6.3.2 and 7.3.2. The contributions of the main electromagnetic sources are also discussed. Figures 8.5, 8.6 and 8.7 confirm the theory of the sources contribution to the core back leakage flux. The phase angles of both the axial and circumferential components do not have a change of sign which means that both the axial and the circumferential components do not change direction. On the other hand, the phase angles of the radial leakage flux change sign which explains the reversal of direction in the radial component with the variation of the distance from the stator core back. The radial component phase angles have a reversal of sign at different distances from the core back surface for different axial positions along the stator core length. The phase angle of the radial component at a position closer to the edge of the core back changes the sign at a shorter distance from the surface of the core back than the phase angle at a position closer to the centre region. That means that the radial leakage flux changes its direction at a shorter distance from the edge surface of the core back. As explained in section 7.3.2 the change of sign in the radial component direction occurs at the distance where the field component due to both the bore and core front surface polarities is greater than that due to both the core back surface polarity and overhang current.

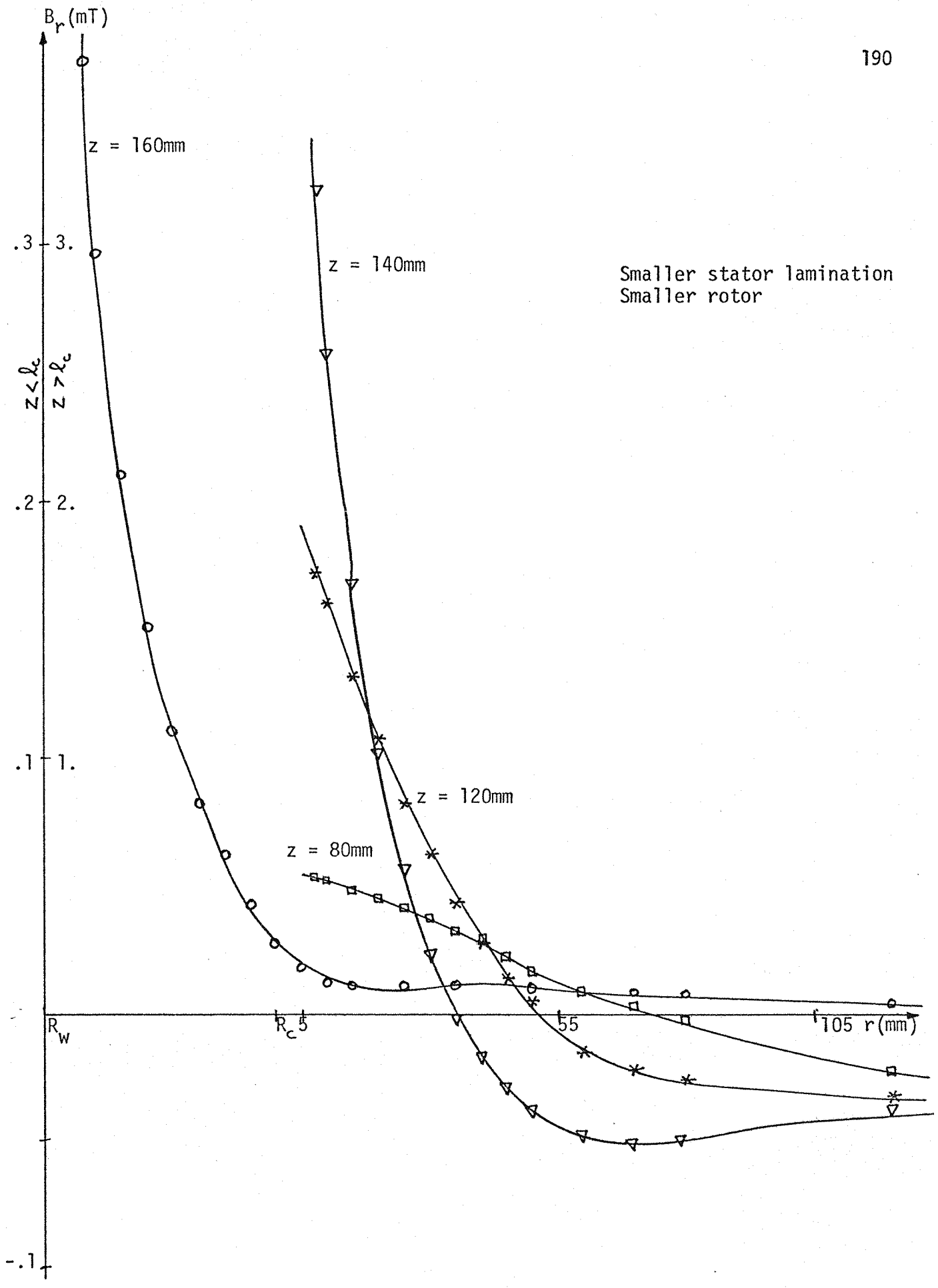

Fig. 8.2.a: Variation of the radial leakage flux density against the distance from the stator core back surface.

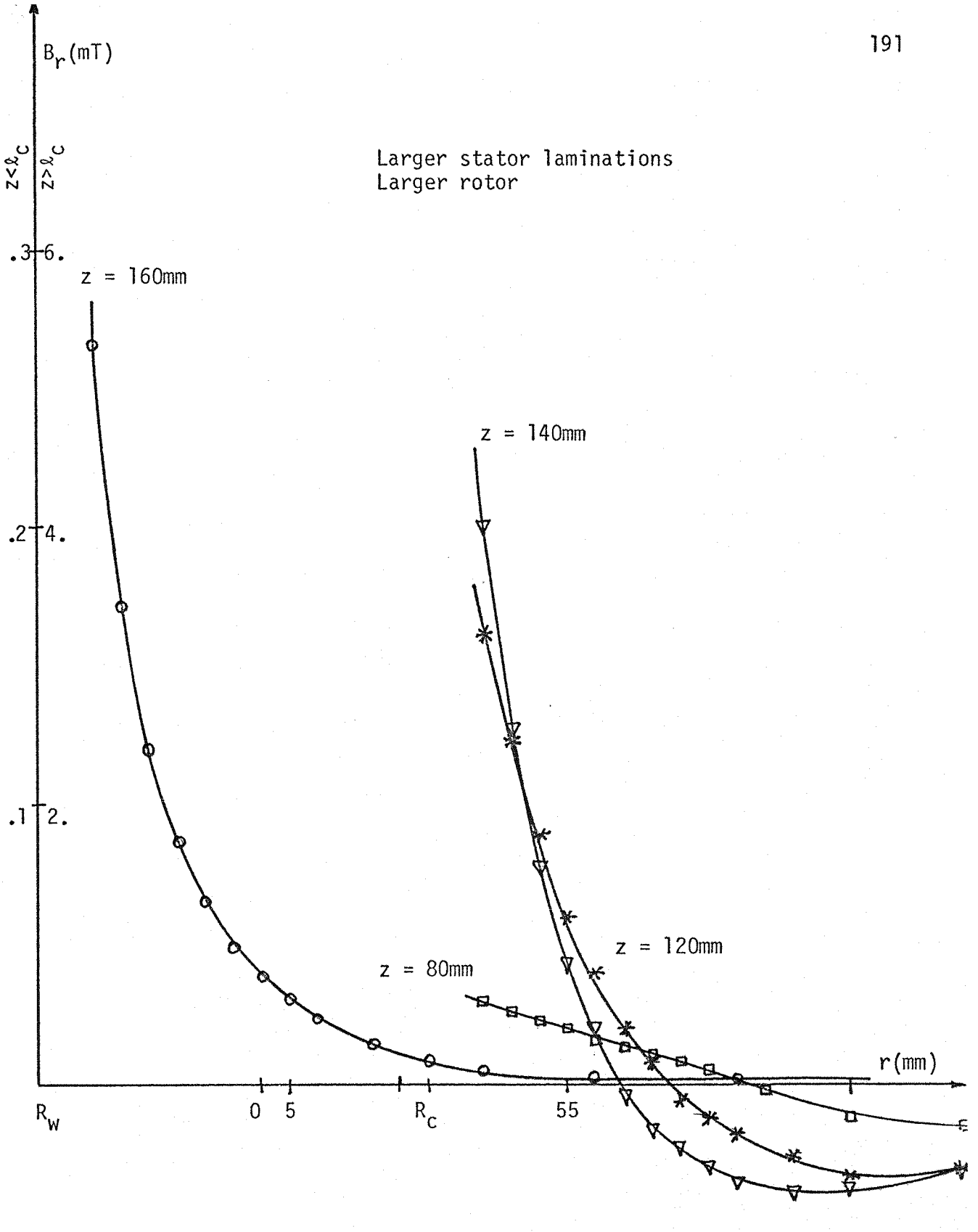

Fig. 8.2.b: Variation of the radial leakage flux density against the distance from the stator core back surface.

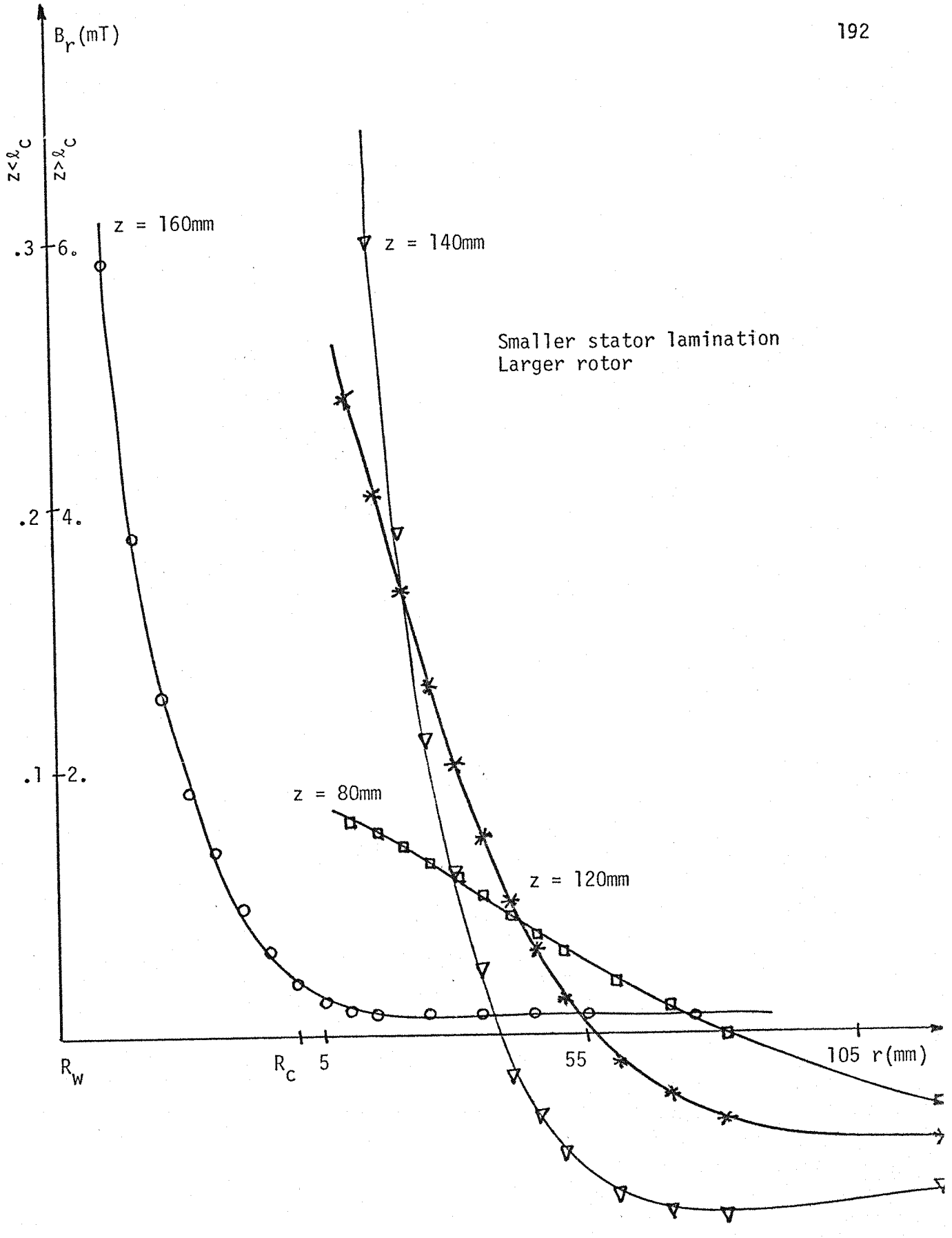

Fig. 8.2.c: Variation of the radial leakage flux density against the distance from the stator core back surface.

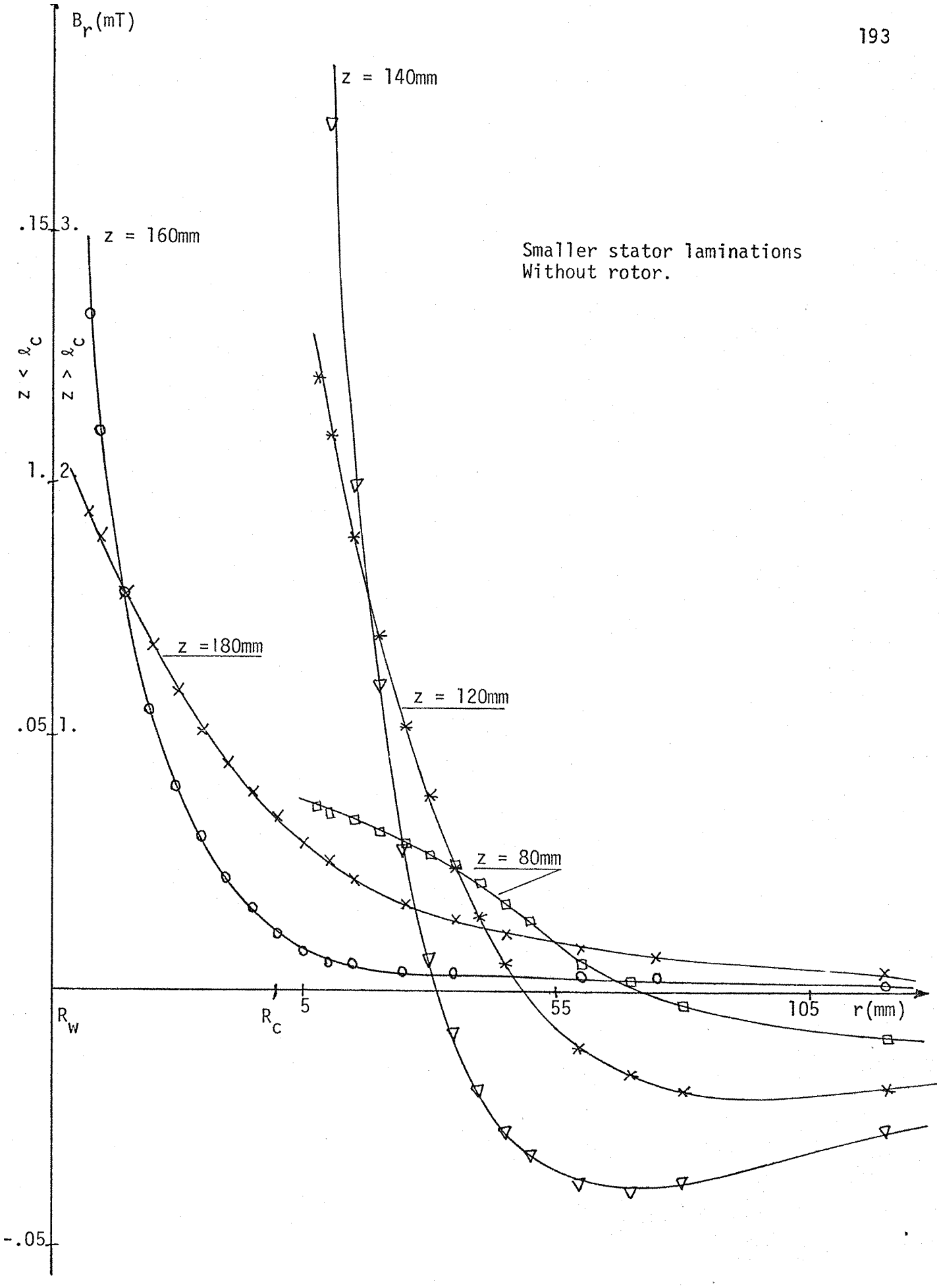

Fig. 8.2.d: Variation of the radial leakage flux against the distance from the stator core back surface.

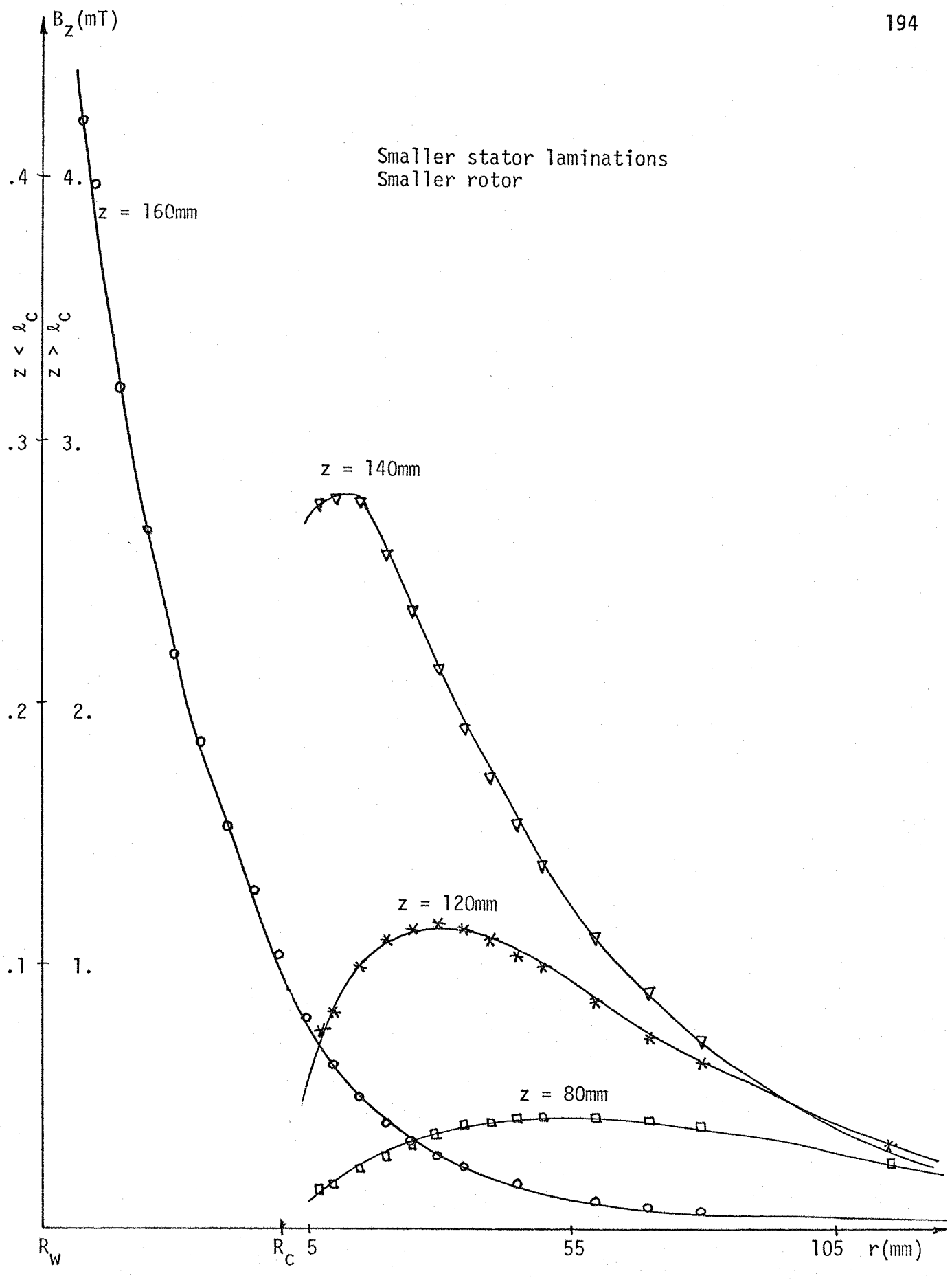

Fig. 8.3.a: Variation of the axial leakage flux density against the distance from the stator core back surface.

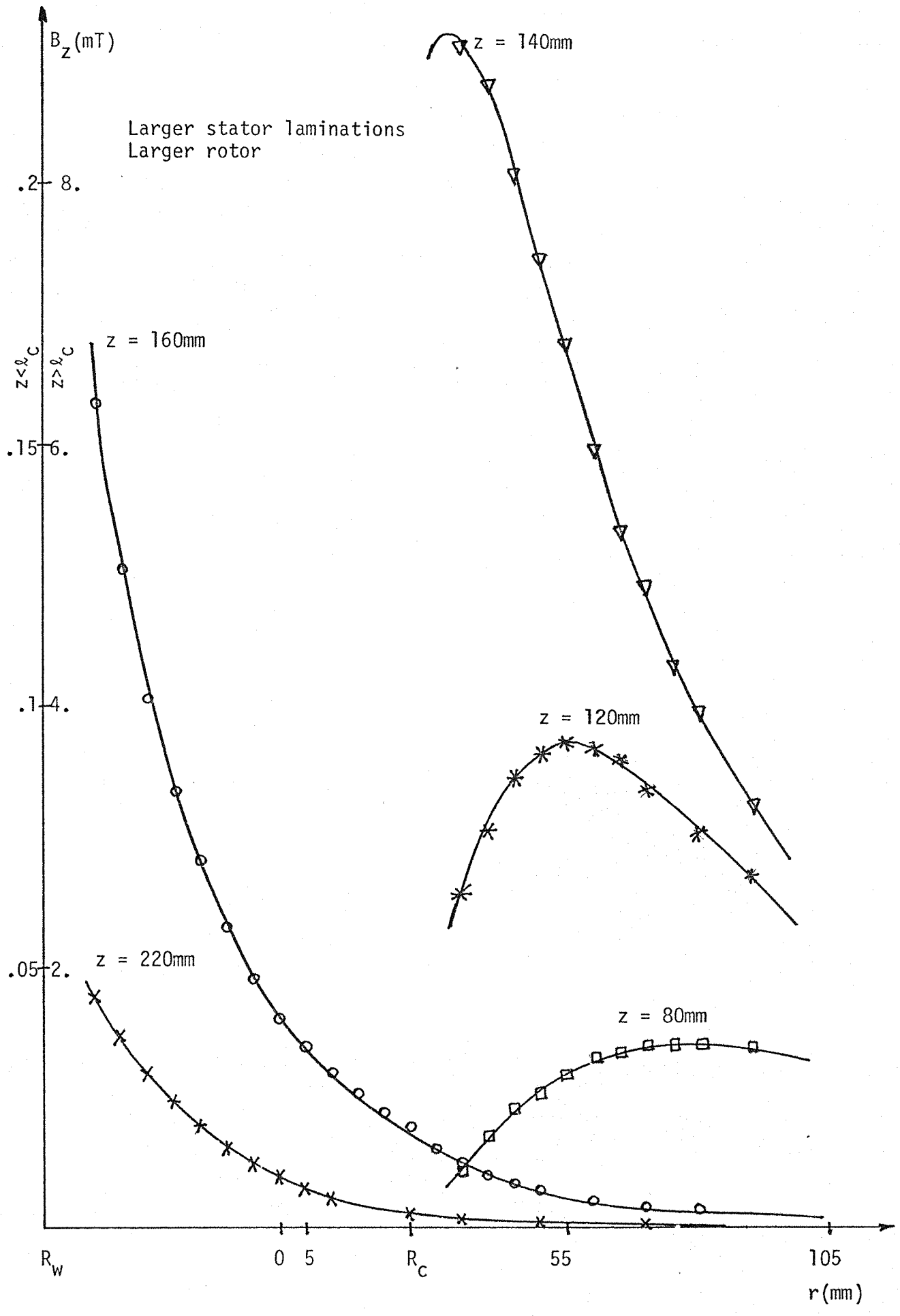

Fig. 8.3.b: Variation of the axial leakage flux density against the distance from the stator core back surface.

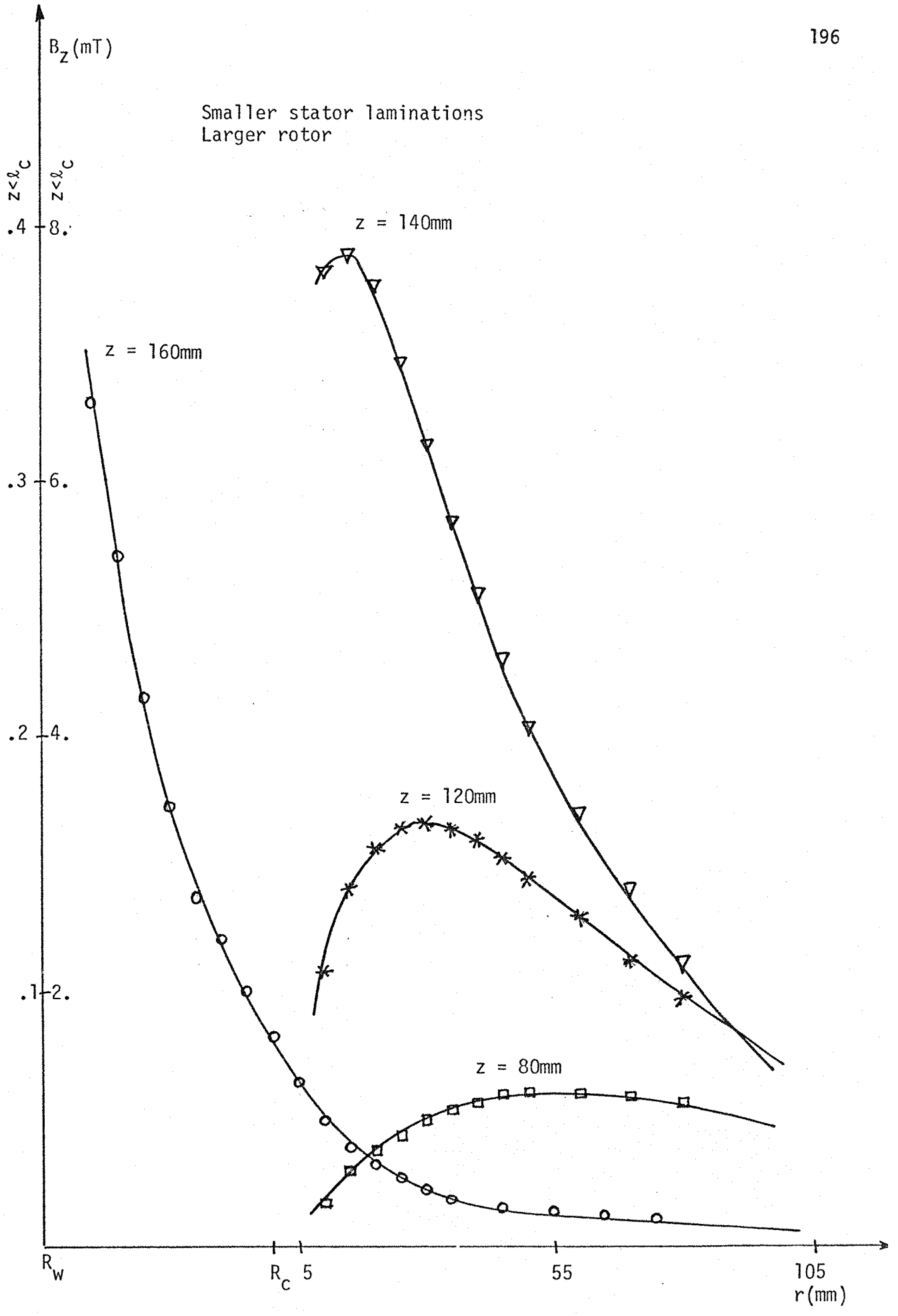

Fig. 8.3.c: Variation of the axial leakage flux density against the distance from the stator core back surface.

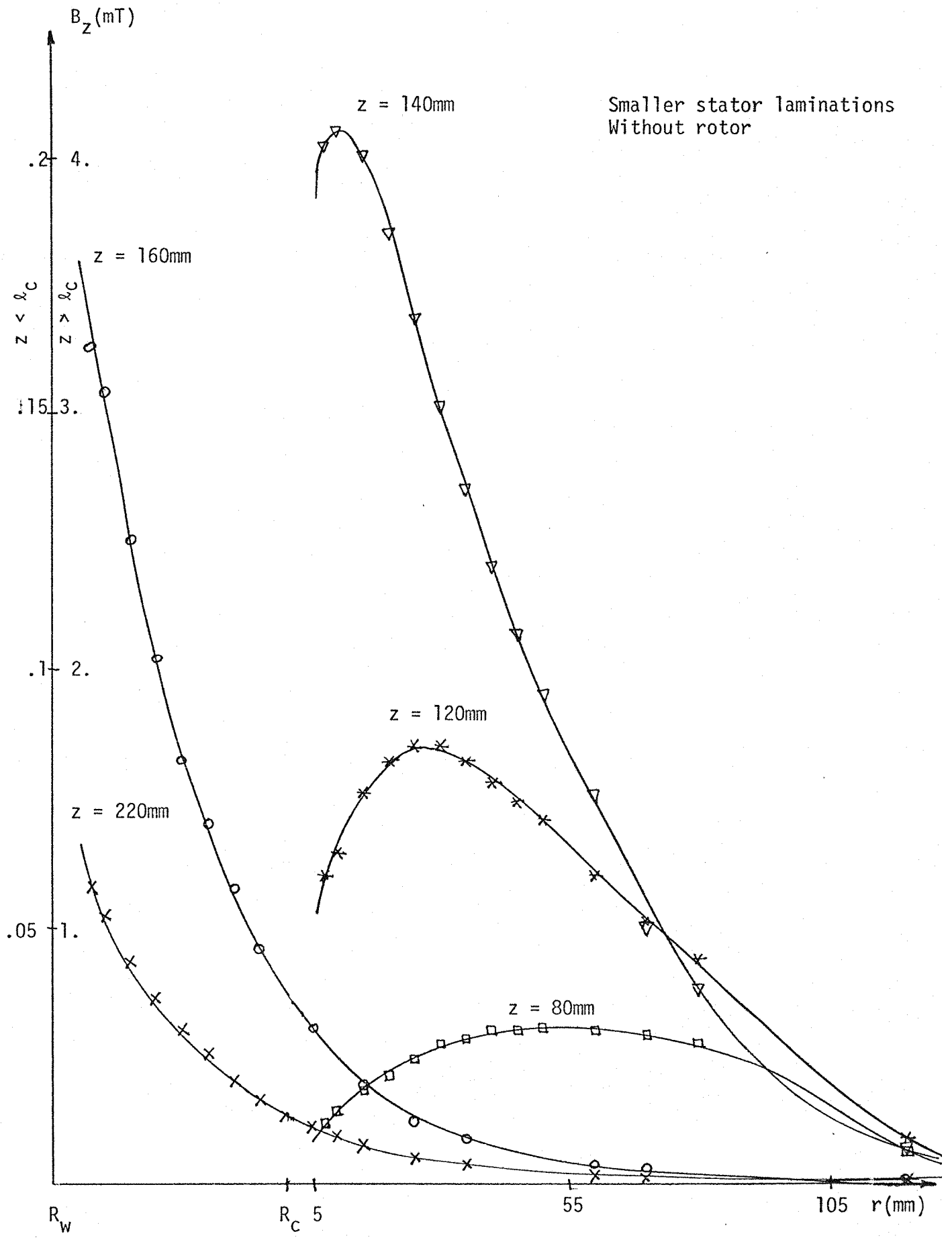

Fig. 8.3.d. Variation of the axial leakage flux against the distance from the stator core back surface.

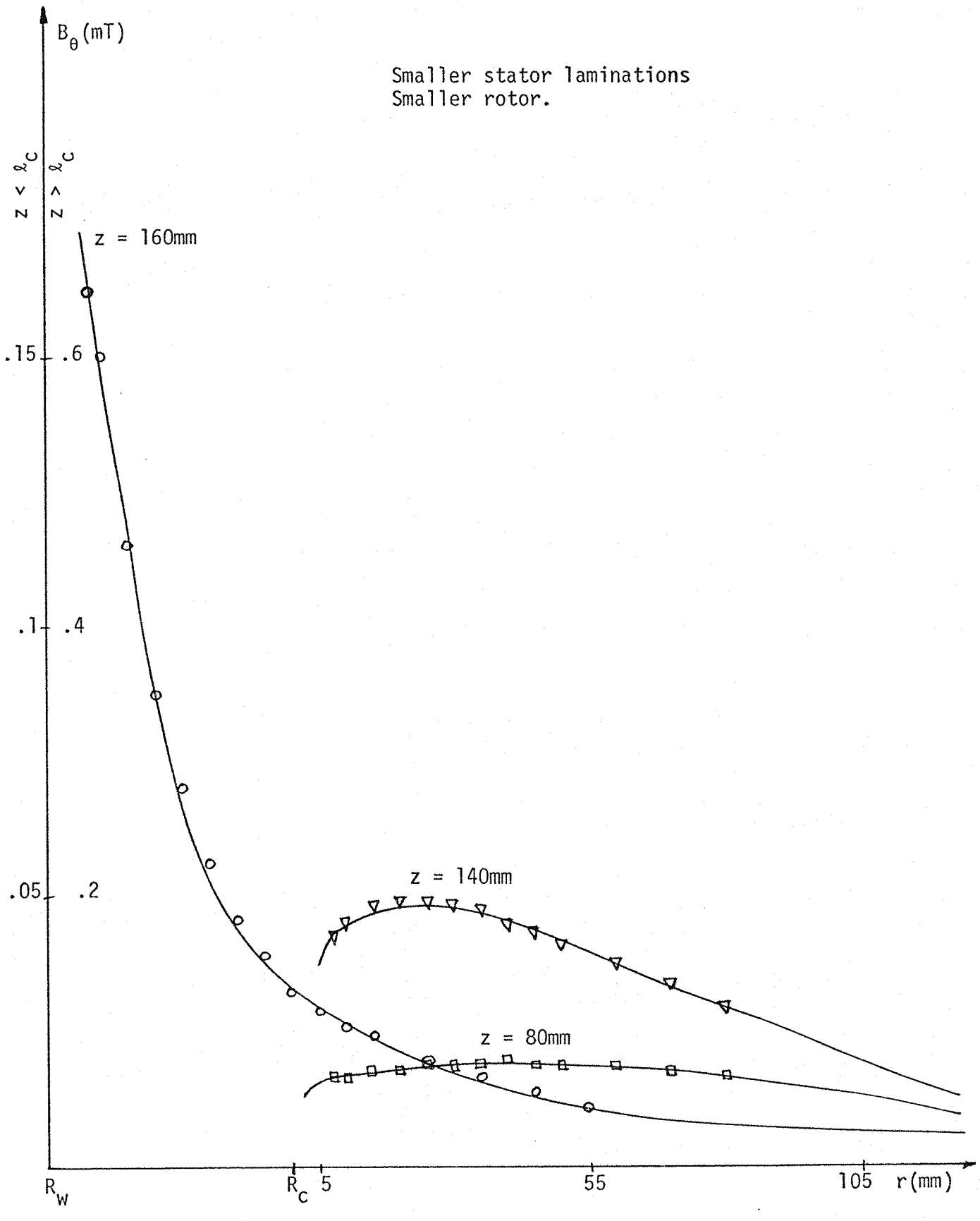

Fig. 8.4.a: Variation of the circumferential leakage fulx density against the distance from the stator core back surface.

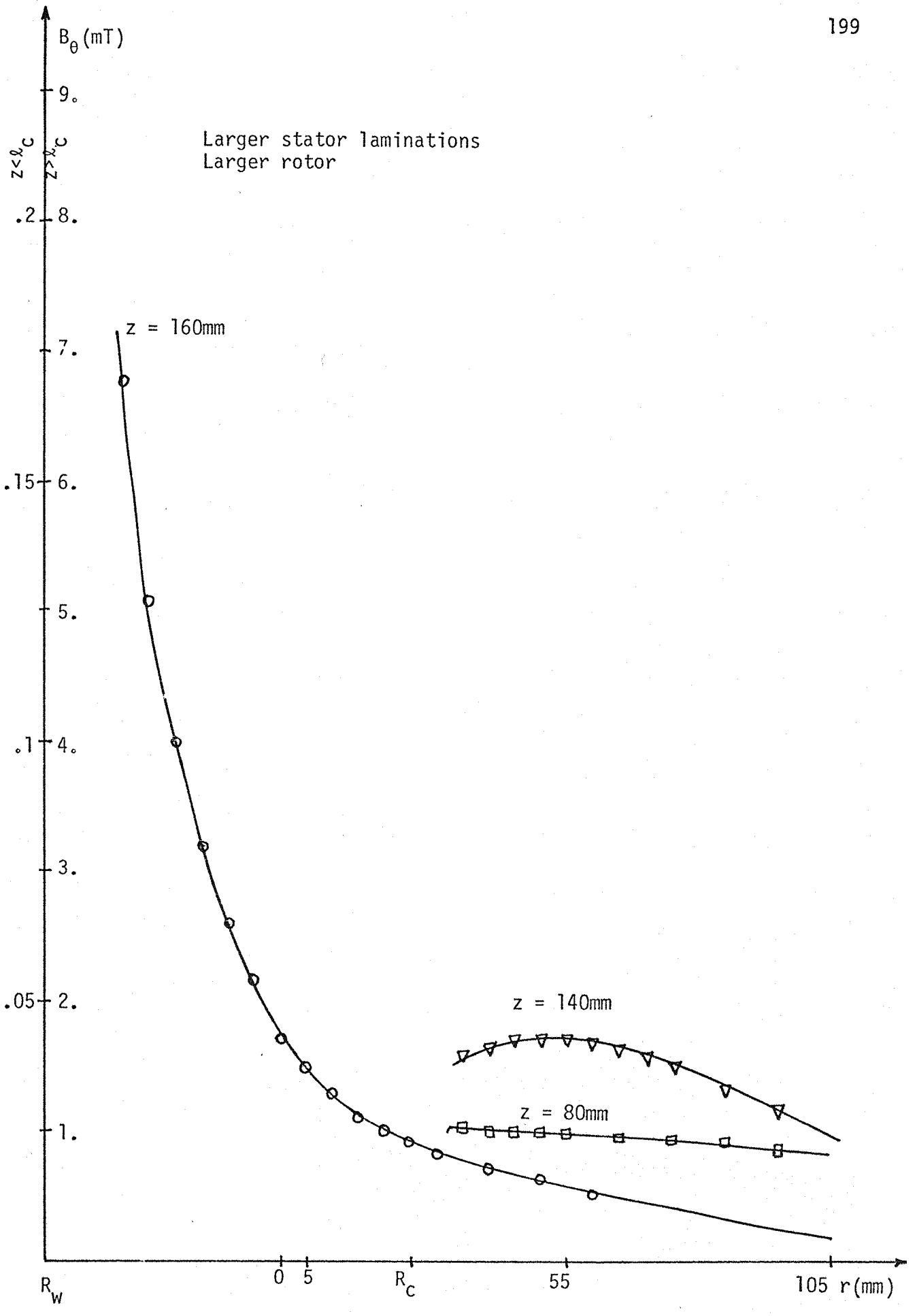

Fig. 8.4.b: Variation of the circumferential leakage flux density against the distance from the stator core back surface.

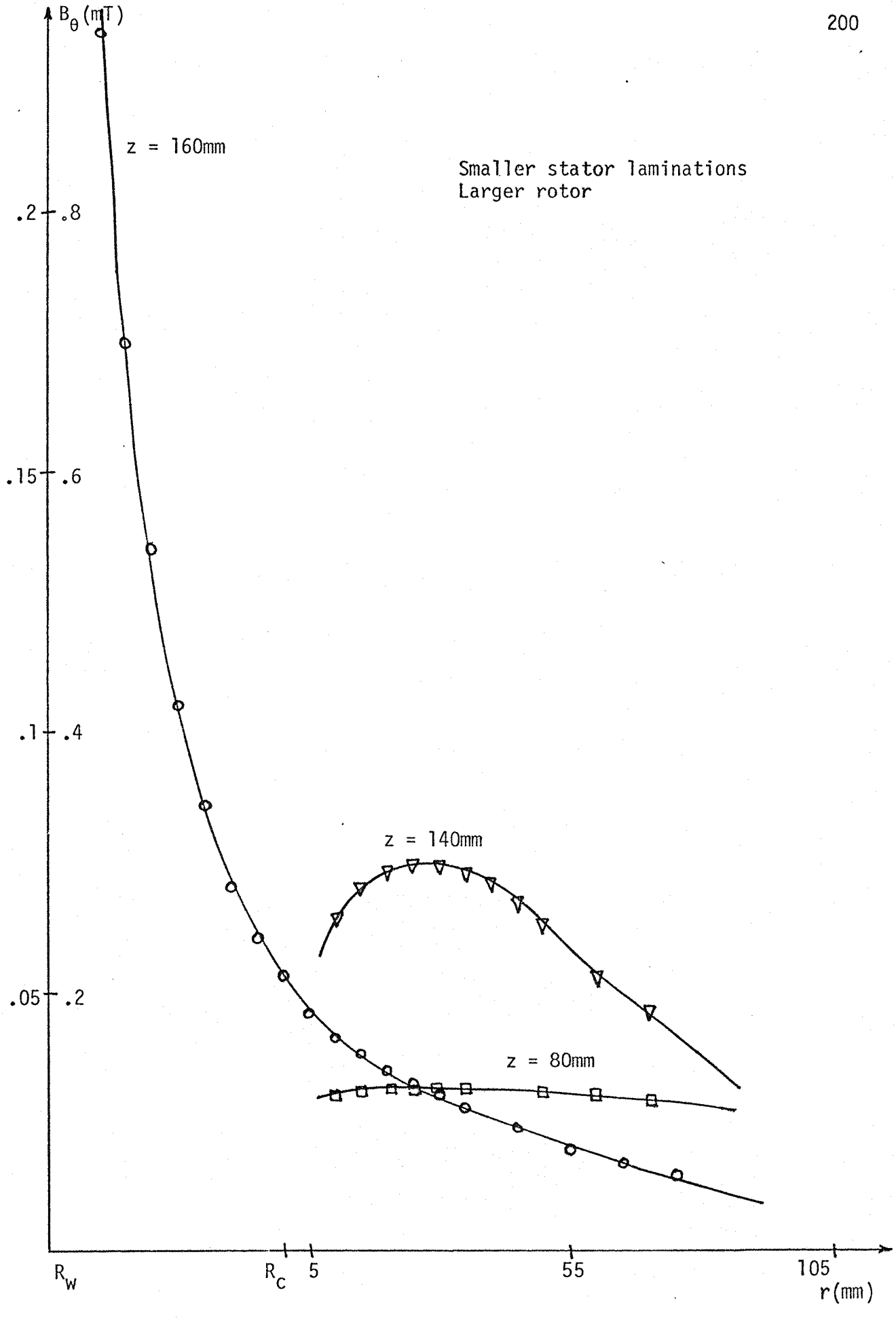

Fig. 8.4.c: Variation of the circumferential leakage flux density against the distance from the stator core back surface.

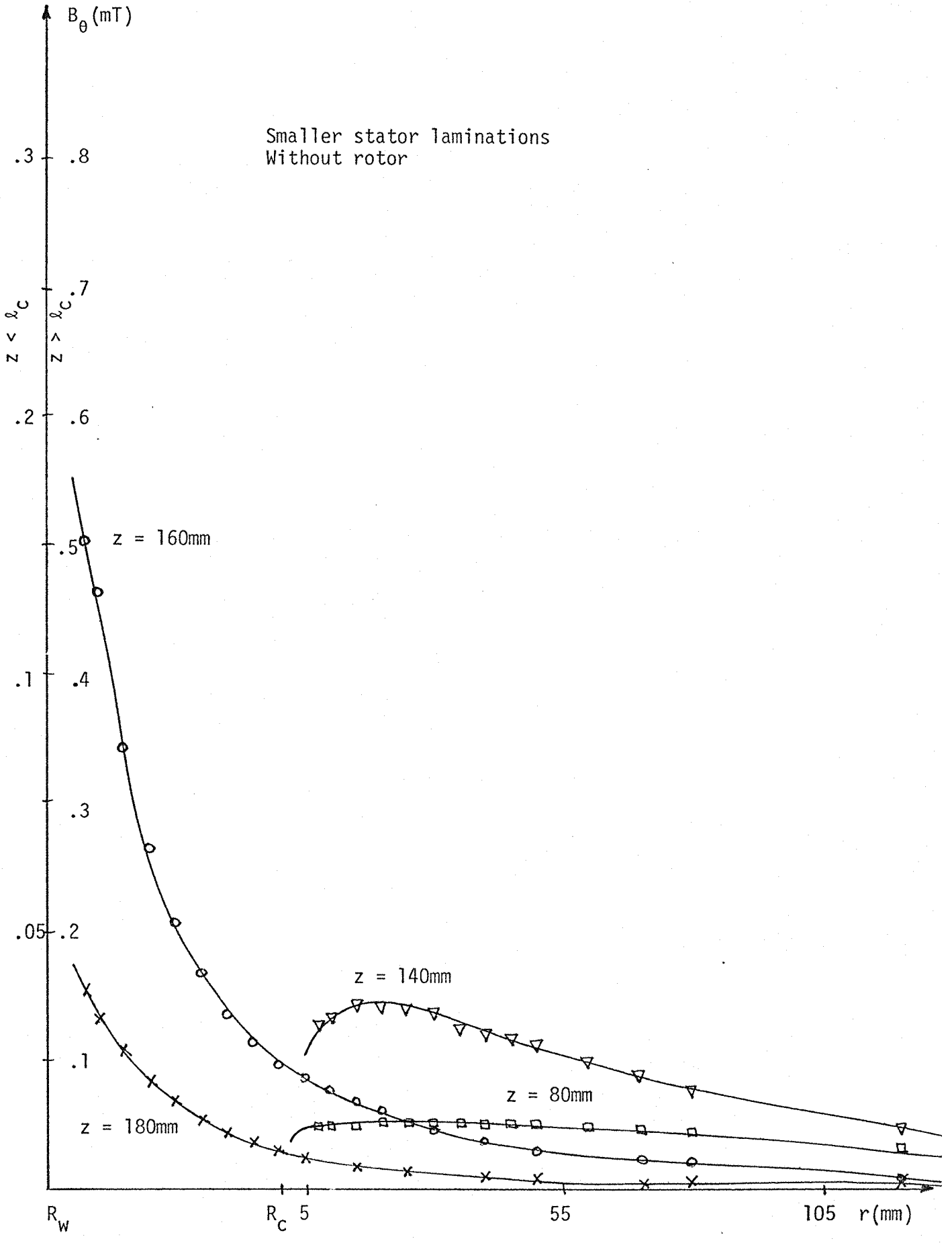

Fig. 8.4.d: Variation of the circumfernetial leakage flux density against the distance from the stator core back surface.

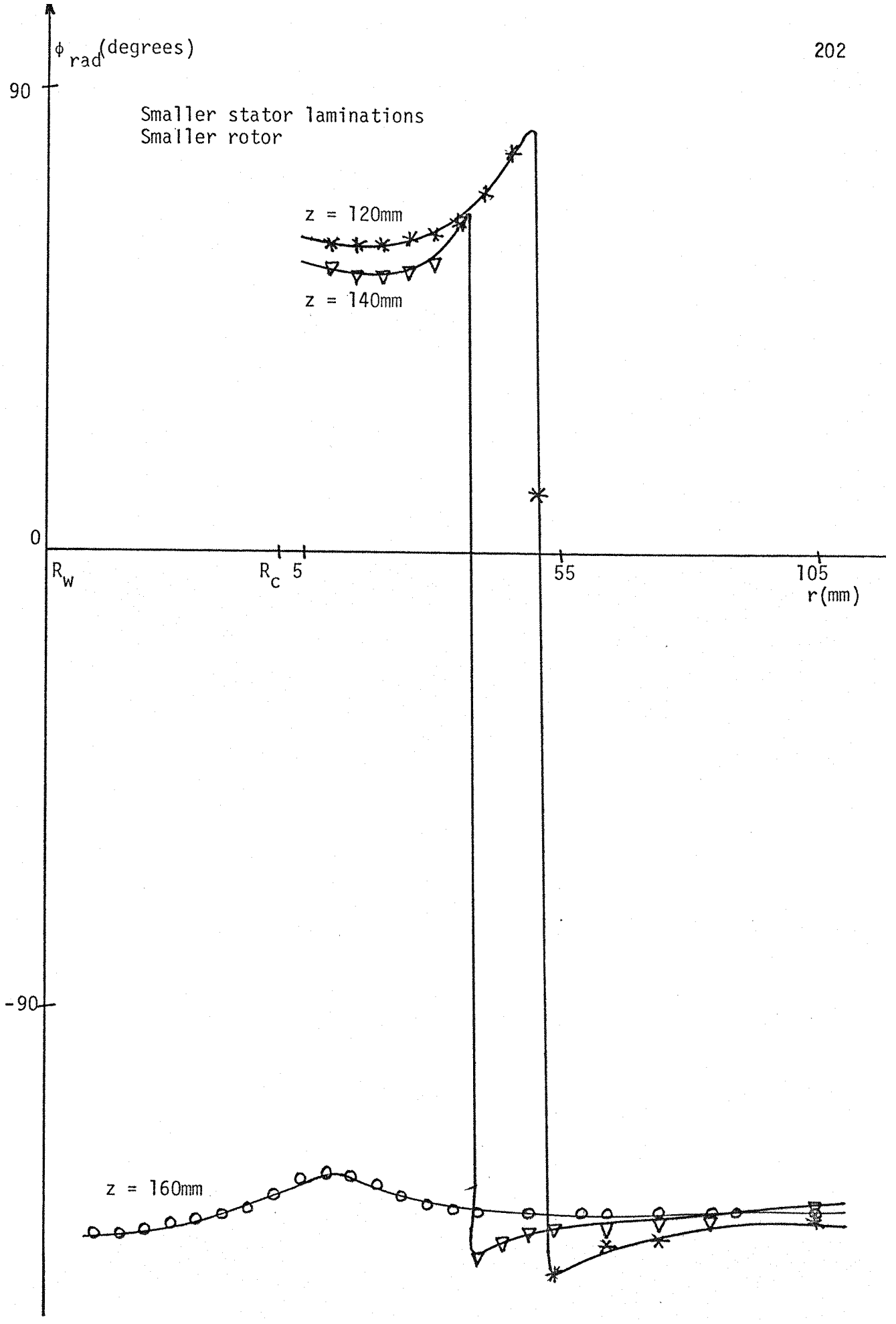

Fig. 8.5.a: Variation of the radial component phase angle against the distance from the stator core back surface.

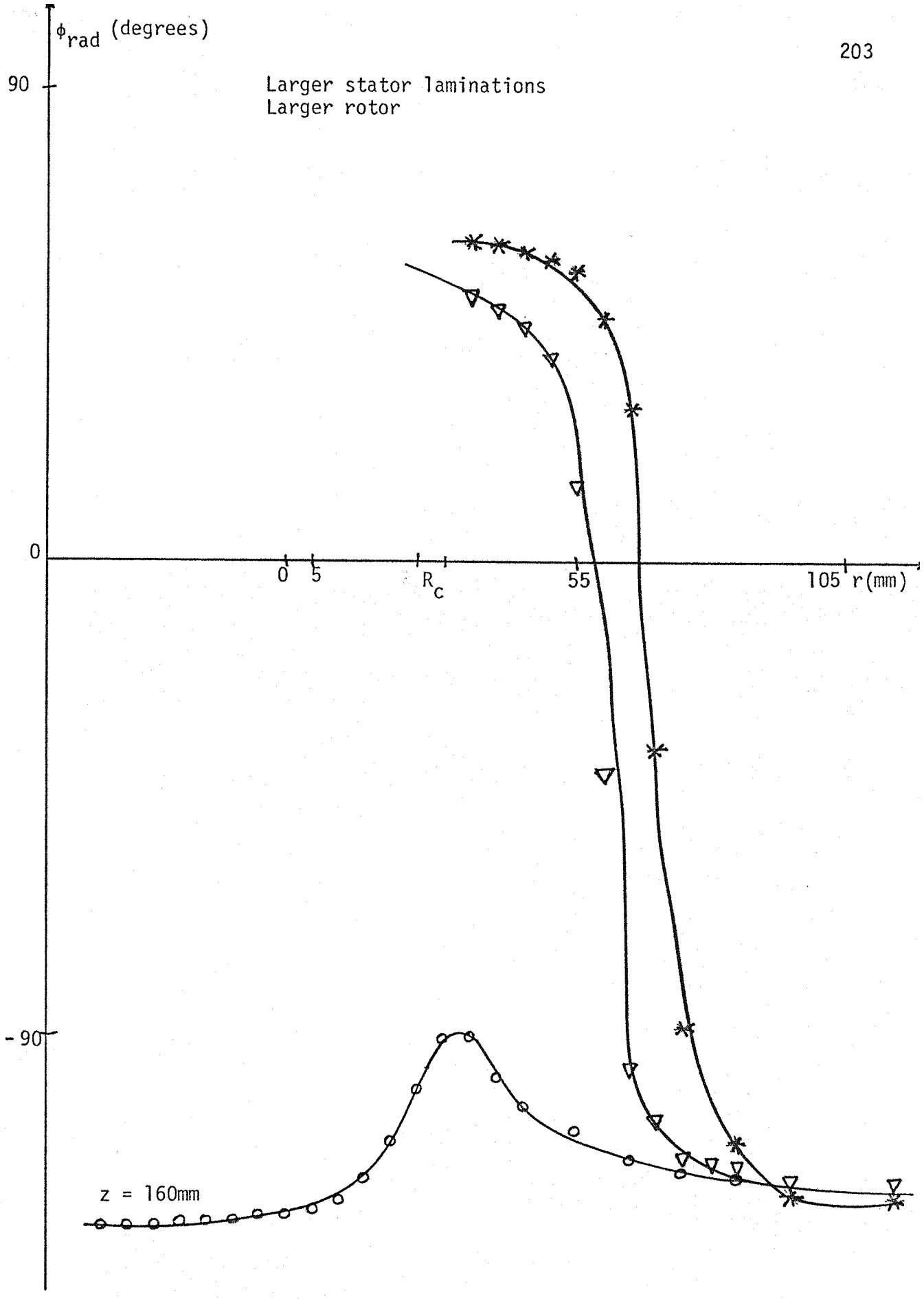

Fig. 8.5.b: Variation of the radial component phase angle against the distance from the stator core back surface.

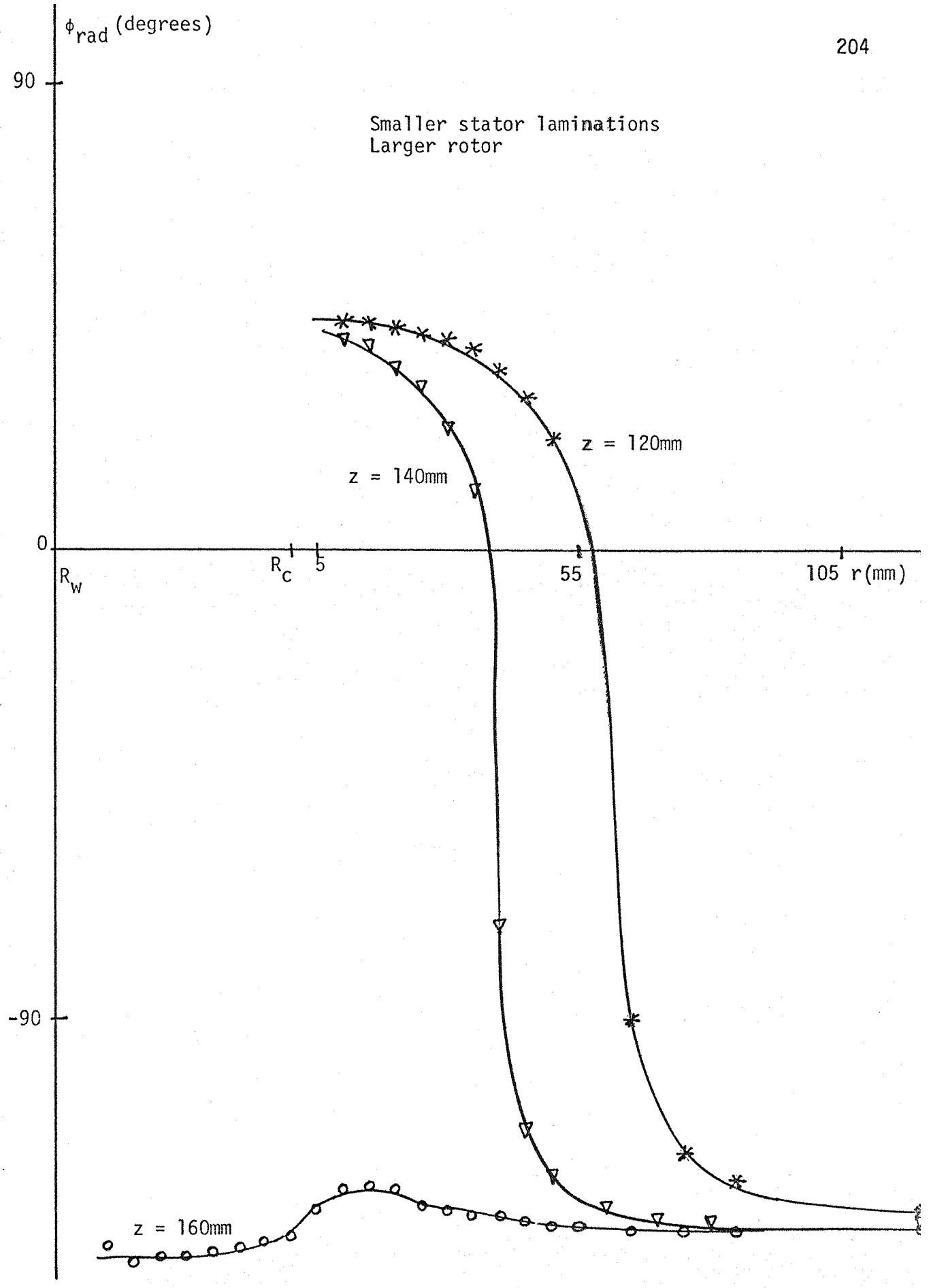

Fig. 8.5.c: Variation of the radial component phase angle against the distance from the stator core back surface.

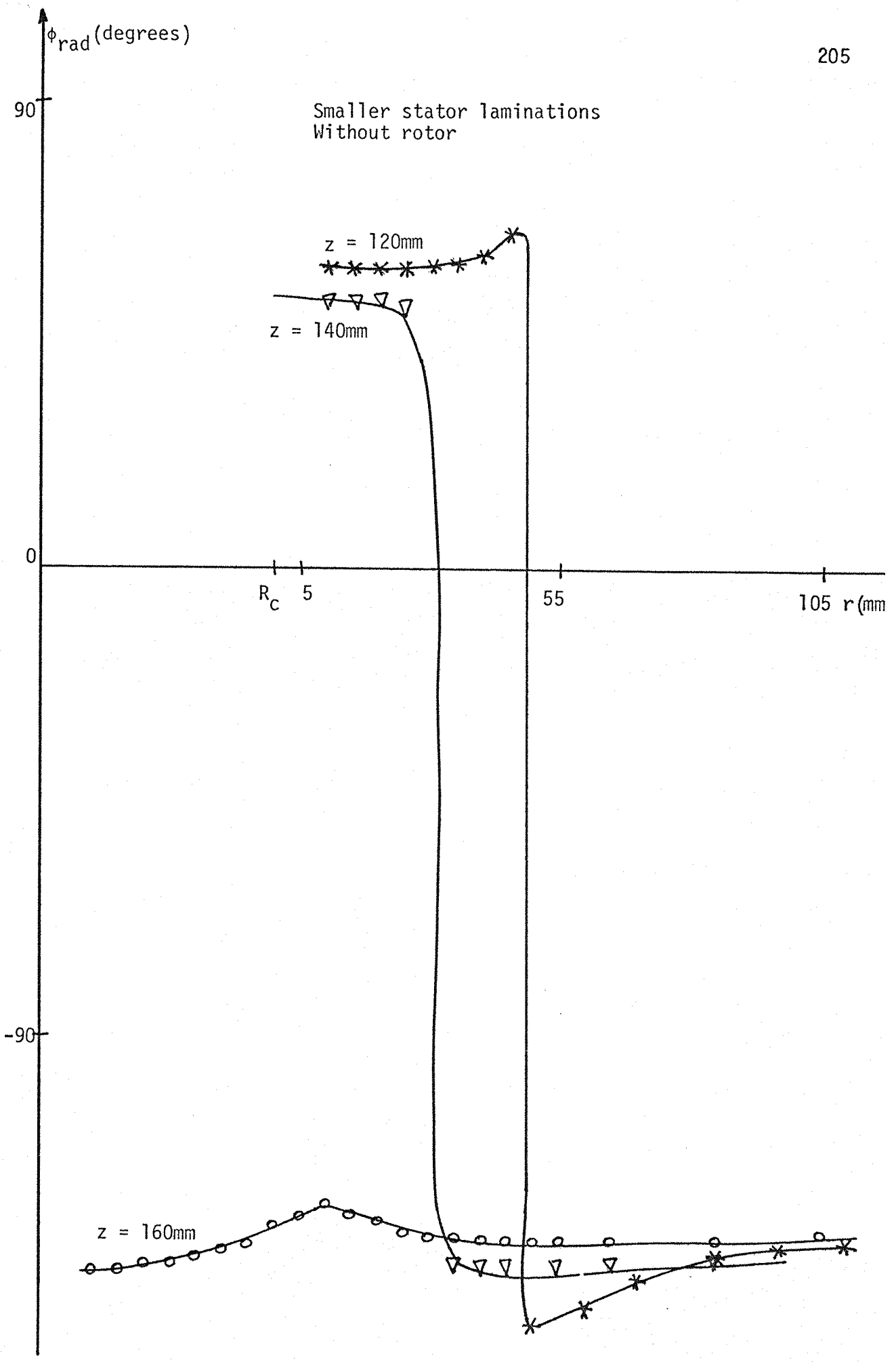

Fig. 8.5.d: Variation of the radial component phase angle against the distance from the stator core back surface.

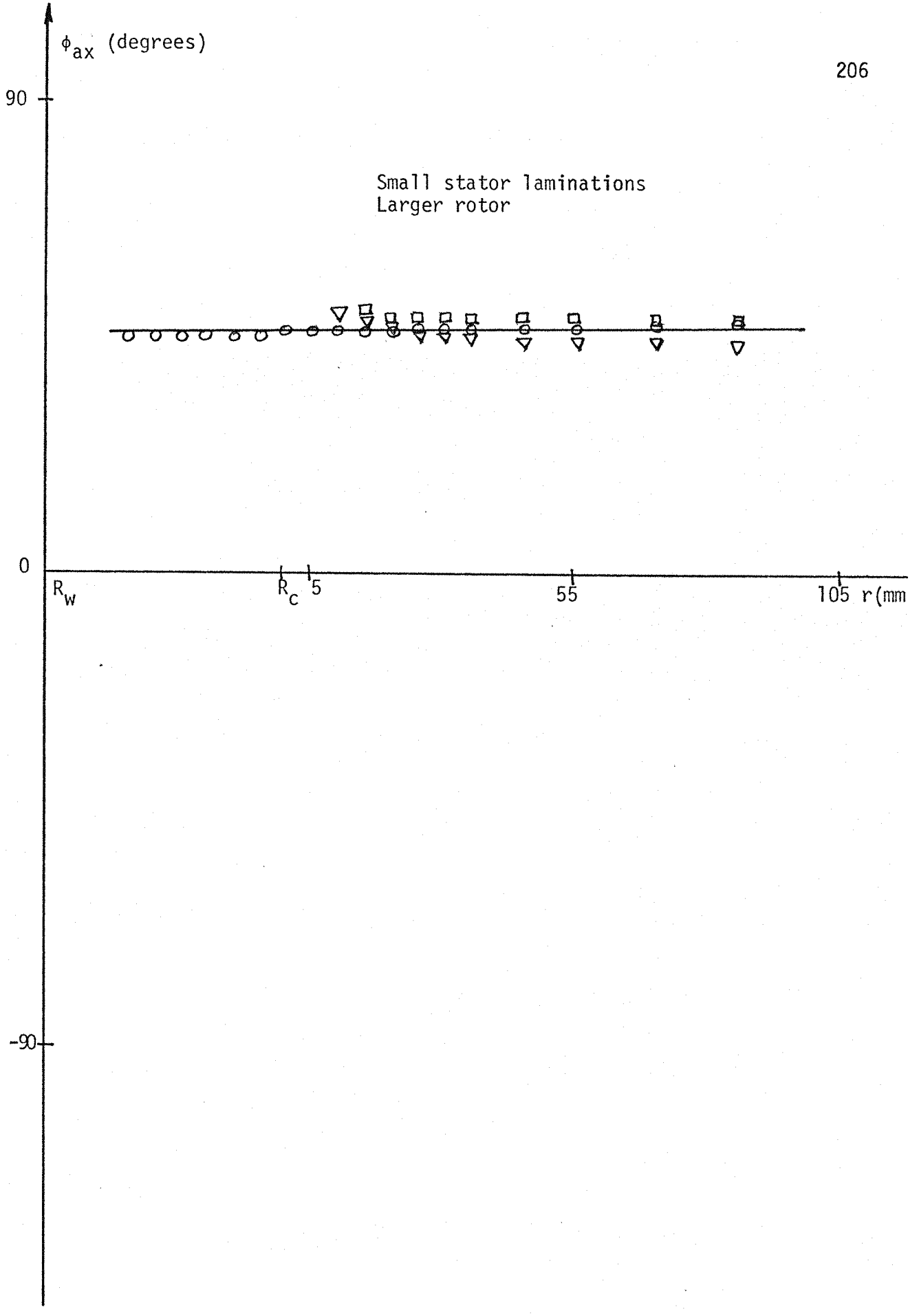

Fig. 8.6: Variation of the axial component phase angle against the distance from the stator core back surface.

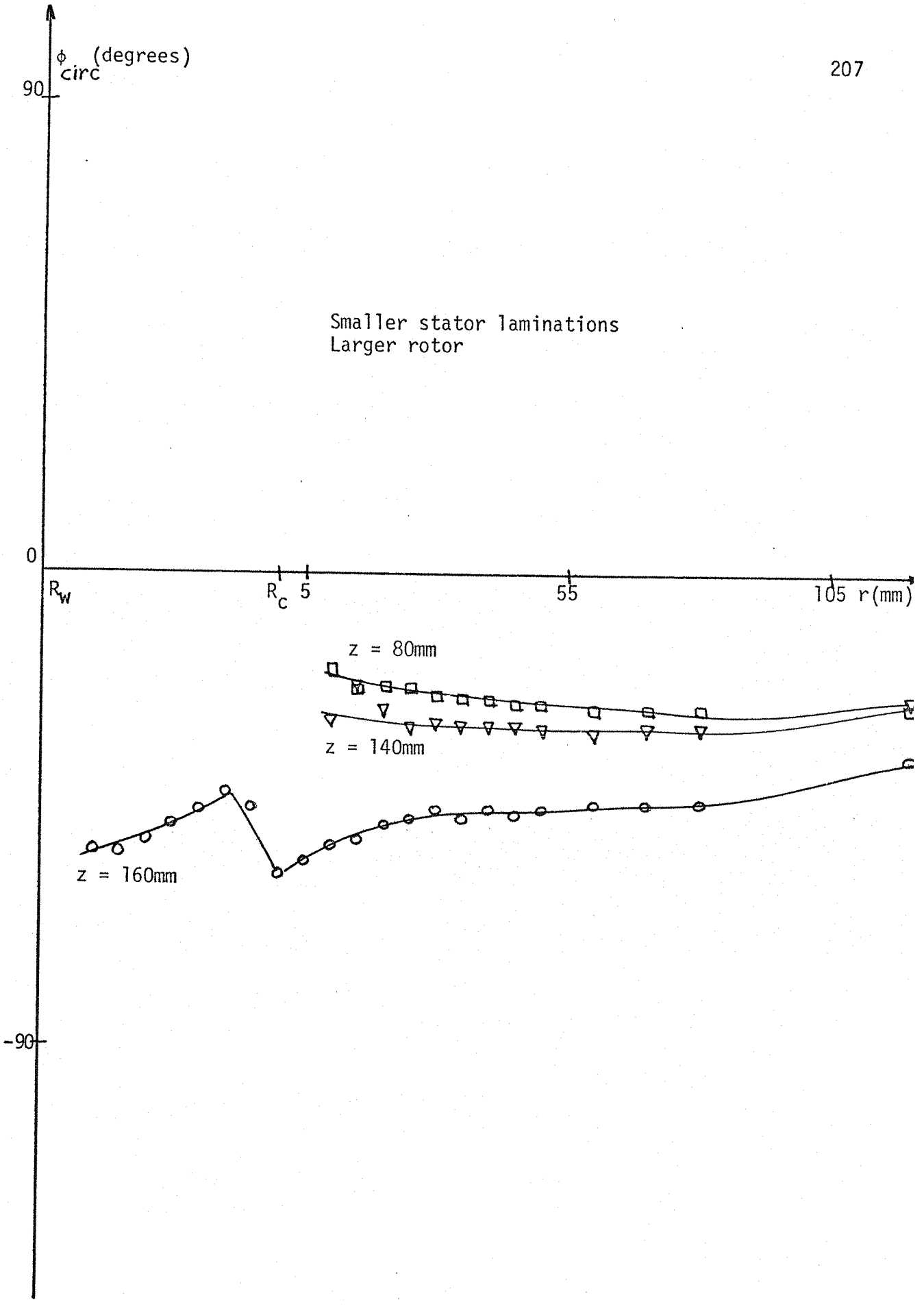

Fig. 8.7: Variation of the circumferential component phase angle with the distance from the stator core back surface.

8.2.3 Variation of the Leakage Flux Around the Circumferential Direction of the Stator Core Back

The model with the stationary rotor was constructed in such a way that the stator core had a good circumferential uniformity. However, the uniformity was not absolute; it was much better than that presented by the laboratory synchronous machine.

The supporting structure, such as clamping plates and building bars, was not constructed of magnetic material. This was not possible to have in the synchronous machine because of the higher vibrations and mechanical forces involved. The laminations were stacked in a randomised way with respect to the rolling direction. There were no butt-joints present.

Figure 8.8 shows the relative variations of the radial, axial and circumferential components of core back leakage flux around the circumferential direction at different positions along the core length. There is a smooth variation of the three components around the core back. There is no pronounced difference between the intensities of the leakage flux. This has not been obtained in the synchronous machine because of lack of circumferential uniformity, as shown in figure 6.9.

Figure 8.9 shows the variation of the phase angle of the radial, axial and circumferential components of core back leakage flux around the circumferential direction. As expected, opposite positions in the core back have a difference of the phase angle equal to 180^{o}. The curve is similar to that when just the stator winding is present (without any iron at all).

Figure 8.10 shows the relative variations of the magnetic flux density components against the circumferential position around the stator winding when no iron is present. There is also no pronounced

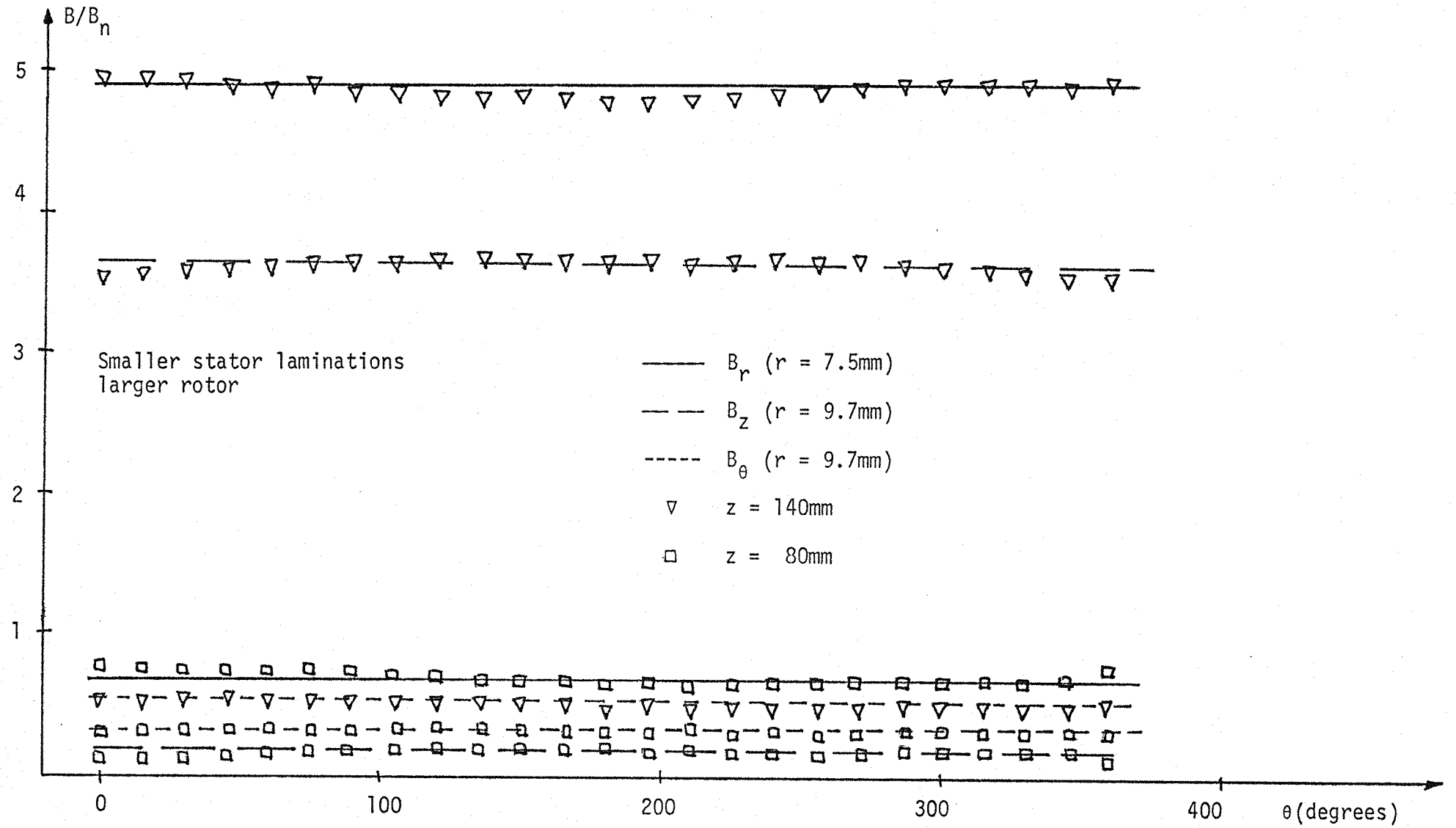

Fig. 8.8: Variation of the relative amplitude of the leakage flux density components around the circumferential direction.

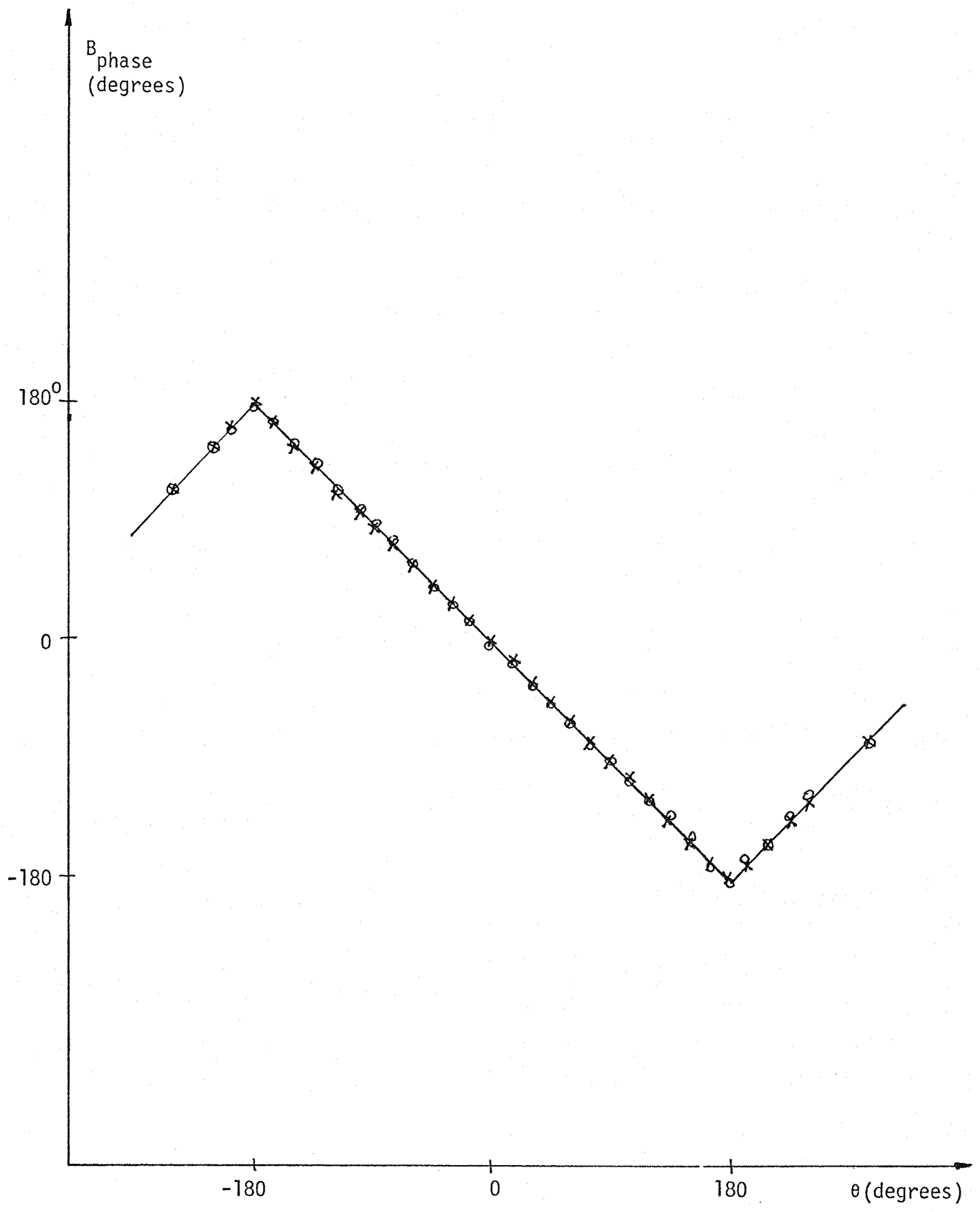

Fig. 8.9: Variation of the relative phase angle of the flux density components around the circumferential direction.

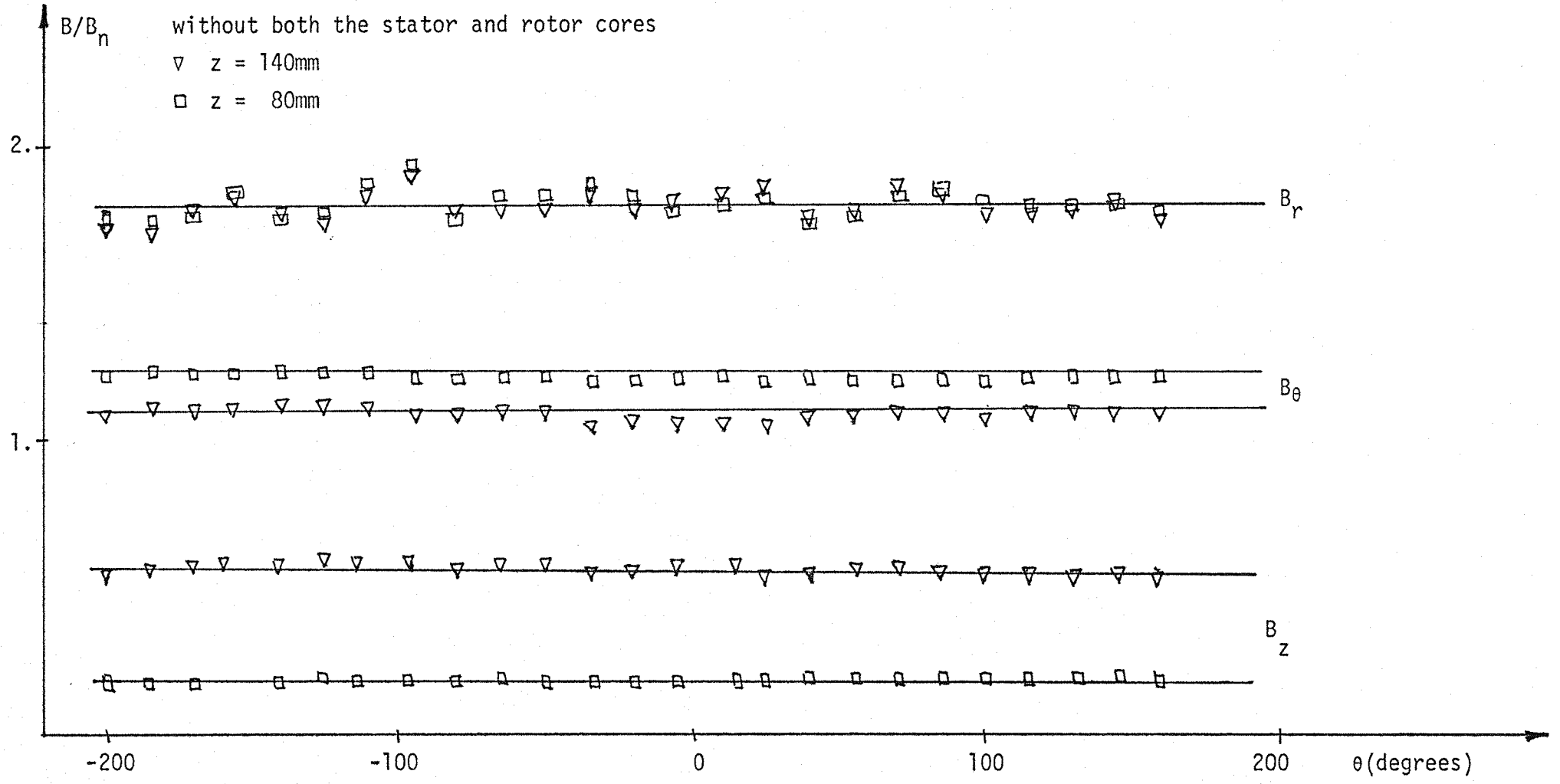

Fig. 8.10: Variation of the relative amplitude of the flux density components around the circumferential direction.

difference between the leakage flux intensities, as expected.

8.2.4 Effects of the Laminations Rolling Direction

The stator cores of synchronous machines are built up from non-oriented silicon steel laminations insulated from one another and rigidly stacked together. The big cores have laminations composed of segments. The core laminations are normally obtained from cold-rolled silicon steel sheet because it has a good magnetic quality and uniformity,[67] producing small core losses. Although the silicon steel sheet is non-oriented, it also does not have a uniform circumferential permeability because it also has anisotropic magnetic properties. Therefore, the non-oriented sheet also has a permeability in the rolling direction greater than in the direction perpendicular to the rolling direction. This means that the magnetisation is easier in the rolling direction than in the direction perpendicular to it.

The construction of the stator core with the laminations aligned according to their rolling direction can cause zones of higher concentration of leakage flux around the stator core back. The radial leakage flux impinging on the core back seeks zones of higher permeabilities. Therefore more radial leakage flux impinges on the core back in the direction parallel to the rolling direction because that direction has the highest permeability. Less radial leakage flux impinges on the core back in the direction perpendicular to the rolling direction. This phenomenon produces an increase in the magnetic surface polarity of the back of the core along the rolling direction. Once again, a position closer to the edge of the core back is more affected by the aligned rolling direction than a position closer to the centre which means that the relative increase in the leakage flux is greater at the back edge. The axial leakage flux penetrating the stator

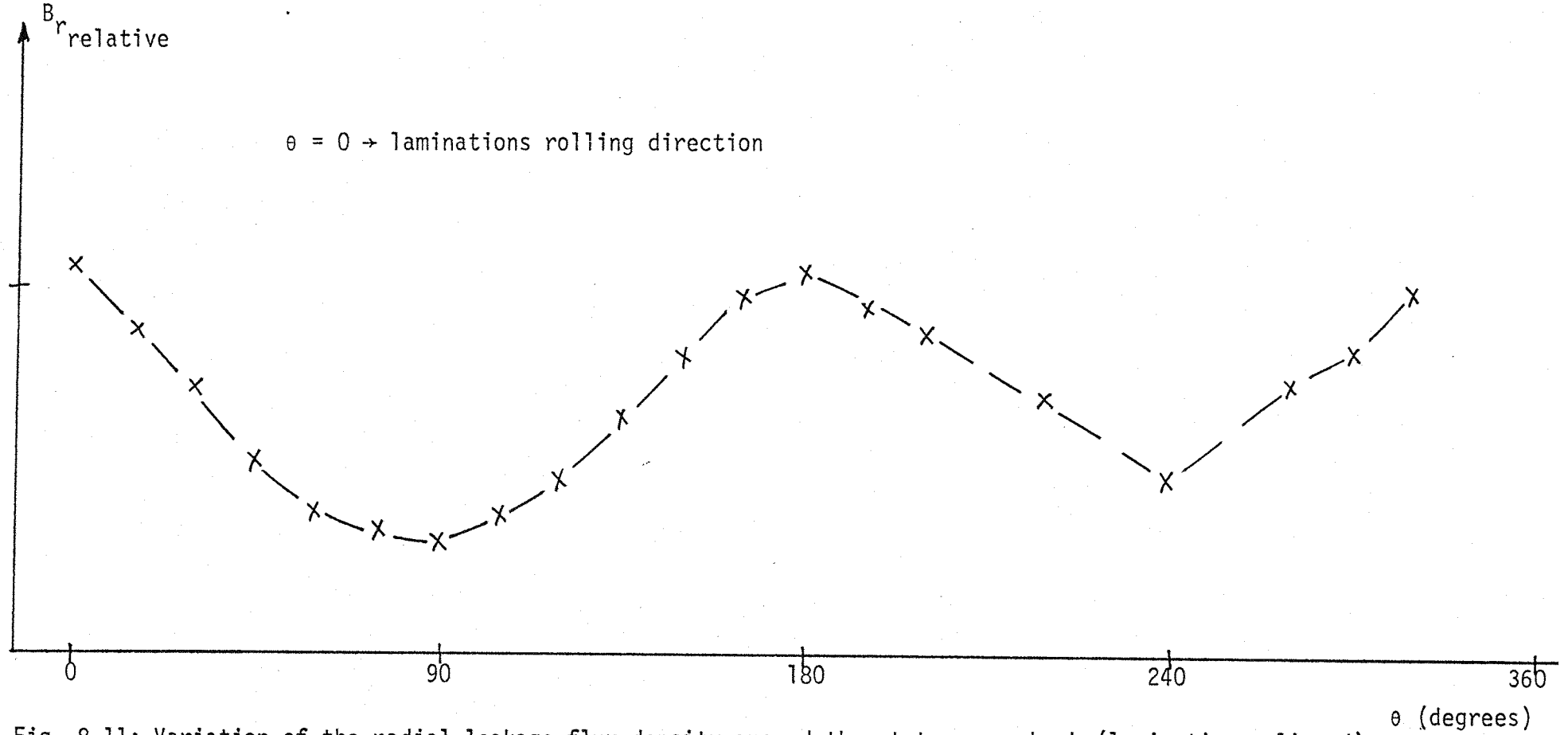

Fig. 8.11: Variation of the radial leakage flux density around the stator core back (laminations aligned)

core is also increased if the laminations are aligned.[49] The randomised arrangement of the laminations avoids the higher concentration of leakage flux caused by the alignment. The reluctanee of the stator core back surface does not vary greatly along the circumferential direction when the laminations are randomised.

Figure 8.11 shows the relative variation of the radial leakage flux density along the circumferential direction of the stator core back with the rolling direction aligned. The variation is not smooth and there is a peak of radial flux in the direction parallel to the rolling direction. The radial leakage flux impinging the core back in the direction perpendicular to the rolling direction is smaller. Figure 8.8 also shows that variation with the randomised arrangement of the laminations. The variation is smoother and there is no pronounced peak of radial flux along the circumferential direction. The discussion presented by Heck[67] confirms that the flux adopts a preferential way towards the rolling direction.

8.2.5 Effects of the Air Gap Length

A variation of the air gap length produces a variation in the magnetic surface polarity at the bore if the excitation current is kept constant. The bore magnetic surface polarity is decreased with the reduction in the length of the air gap for a fixed excitation.

Comparing the results in figure 8.1 for the cases (a) (both smaller stator and rotor cores) and (c) (smaller stator and larger rotor cores), it can be noticed that the radial, axial and circumferential components of core back leakage flux are reduced when the air gap length is increased with the utilisation of the rotor with smaller diameter. Those components of leakage flux are further reduced when the rotor is not used. However, it must be borne in mind that the

utilisation of different rotor diameters is made in order to vary the magnetic surface polarity at the bore. If the length of the air gap is shortened with a constant flux density in the air gap the magnetic surface polarity at the bore is increased. The shortening of the air gap length produces a decrease in the fringing flux, as discussed by Howe.[66] A constant flux density in the air gap is obtained with an increase in the excitation current when the air gap length is shortened.

Therefore if the air gap flux density is constant and the length of the air gap is increased the leakage flux at the stator core back is increased because of the increase in the fringing flux. The increased fringing flux produces a larger distribution of magnetic poles in both the core front and core back. Then the magnetic surface polarities at both the core front and core back are increased. Although the strongest fringing field occurs close to the bore region the core back can also be affected by the fringing flux when flux diverters such as screening plates and stepping of the corners of the core bore are utilised.

8.2.6 Effects of the Stator Core Depth

The stator core depth is determined by the diameter of the laminations. The distribution of leakage flux at the stator core back of the synchronous machine varies with the depth of the stator core. The intensity of the core back leakage flux is diminished when a deeper stator core is used. The magnetic surface polarity at the back of the core decreases because it is less affected by the magnetising leakage flux due to the other main electromagnetic sources when the core depth is increased. The relative distance from both the core bore and the overhang current sources is increased with respect to the core back surface when deeper cores are used. The distribution of magnetic poles

at the region of the core front close to the core back is also diminished with the increase in the depth of the stator core. The intensity of main flux that reaches the core back surface is also decreased at deeper stator cores.

Figures 8.1 (a, b, c, d) show that both the radial, axial and circumferential components of leakage flux at the stator core back have smaller intensities when the stator core depth is greater. The presence of a larger quantity of electromagnetic material in the radial direction produces a decrease in the length of the leakage flux path, and less leakage flux reaches the back region of the stator core.

A limiting case of diminishing the depth of the stator core was obtained with the removal of the stator laminations. The variations of the radial, axial and circumferential components of the flux produced by the excited stator winding with the smaller rotor core and in the complete absence of iron are shown from figures 8.13 to 8.18. Comparing this limiting case when the stator core is absent with those when the stator core is present it can be observed that the flux components are more spread in the first case. Therefore, a region in the core back of the machine with the stator laminations fitted in has a smaller flux intensity than in the case where the laminations are removed. This is explained by the fact that the stator iron furnishes a path of smaller reluctance to the magnetic flux concentrating a much greater quantity of magnetic flux inside the stator core. Hammond,[93] Hague,[94] and Carter[95] describe the effects of the iron in the rearrangement of the magnetic flux distribution.

Figure 8.26 (I, II and III) shows the intensity of the total leakage flux density for the cases with both the larger stator core and the small stator core and with no iron at all. The results show that the intensities of the total core back leakage flux are smallest when

the larger stator core is used. If a region at the core back is fixed, the total leakage flux when the stator core is removed is shown as case V (no iron at all).

The fact that the core back leakage flux is smaller when the stator core is deeper suggests that a stepped core back edge could diminish the concentration of leakage flux at the edge of the core back. The first lamination at the core end would have a larger diameter. The extension of the stepped region would be small compared with the stator length. However, the stator core with stepped back edge would have a more difficult construction.

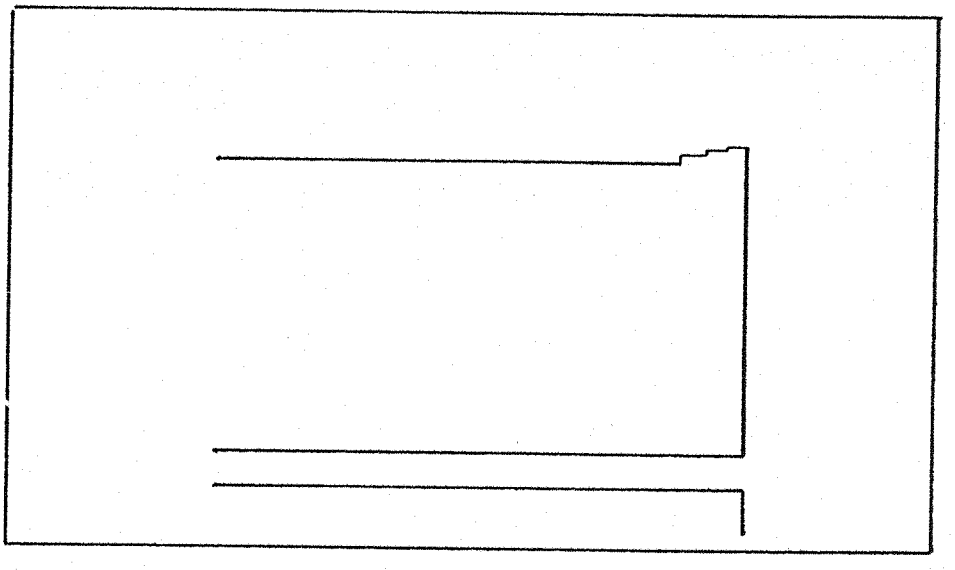

Fig. 8.12: Stator core back with stepped edge

8.2.7 Effects of the Stator Core Length

The increase in the length of the stator core increases the relative concentration of leakage flux at the edge of the stator core back with respect to the centre region, i.e. the ratio between the leakage flux at the core back edge and the core back centre rises with the utilisation of longer stator core. That is explained by the fact that the distance between the core centre region and the main electromagnetic sources increases with the increase in the stator core length.

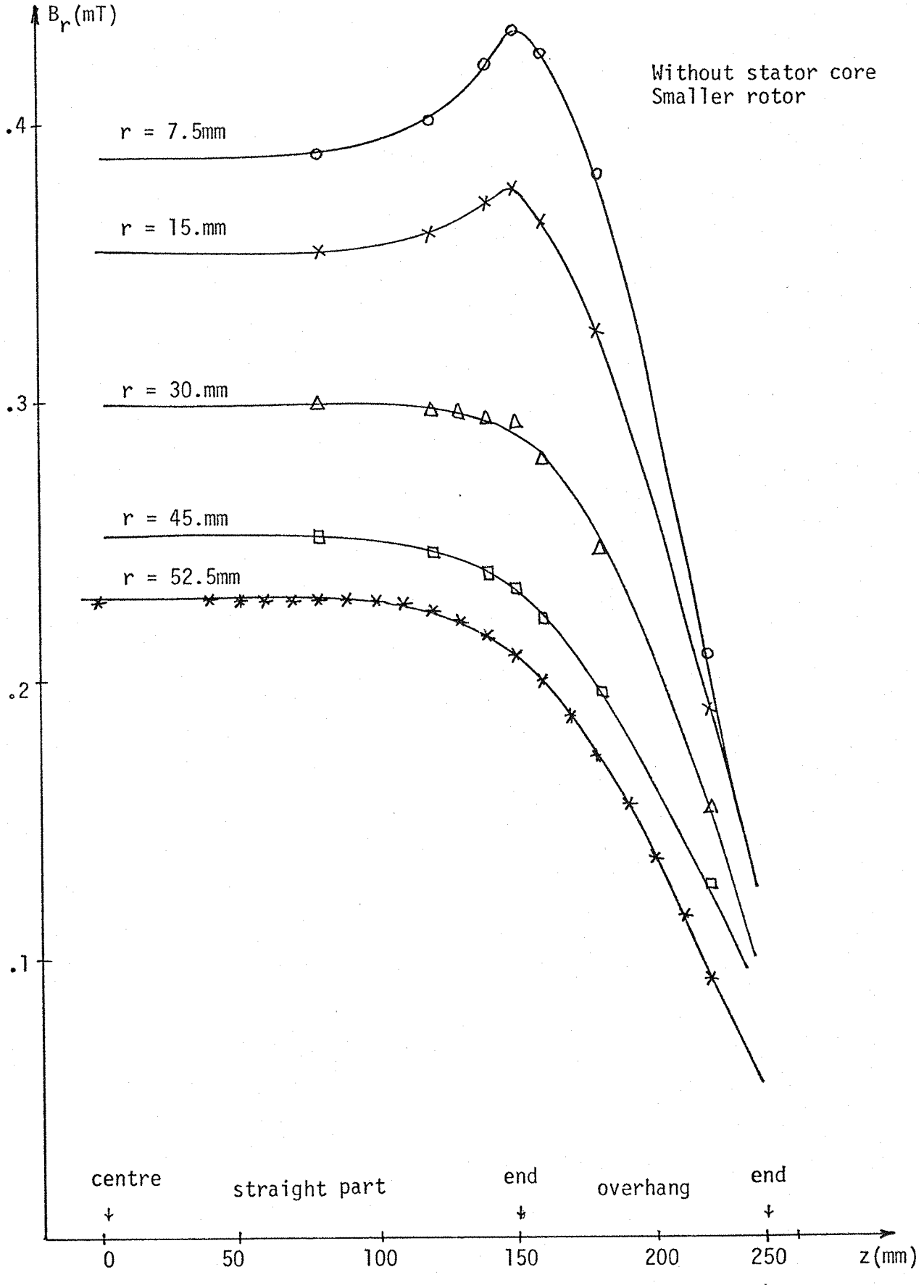

Fig. 8.13.a: Variation of the radial flux density along the stator winding length (for different distance from the surface).

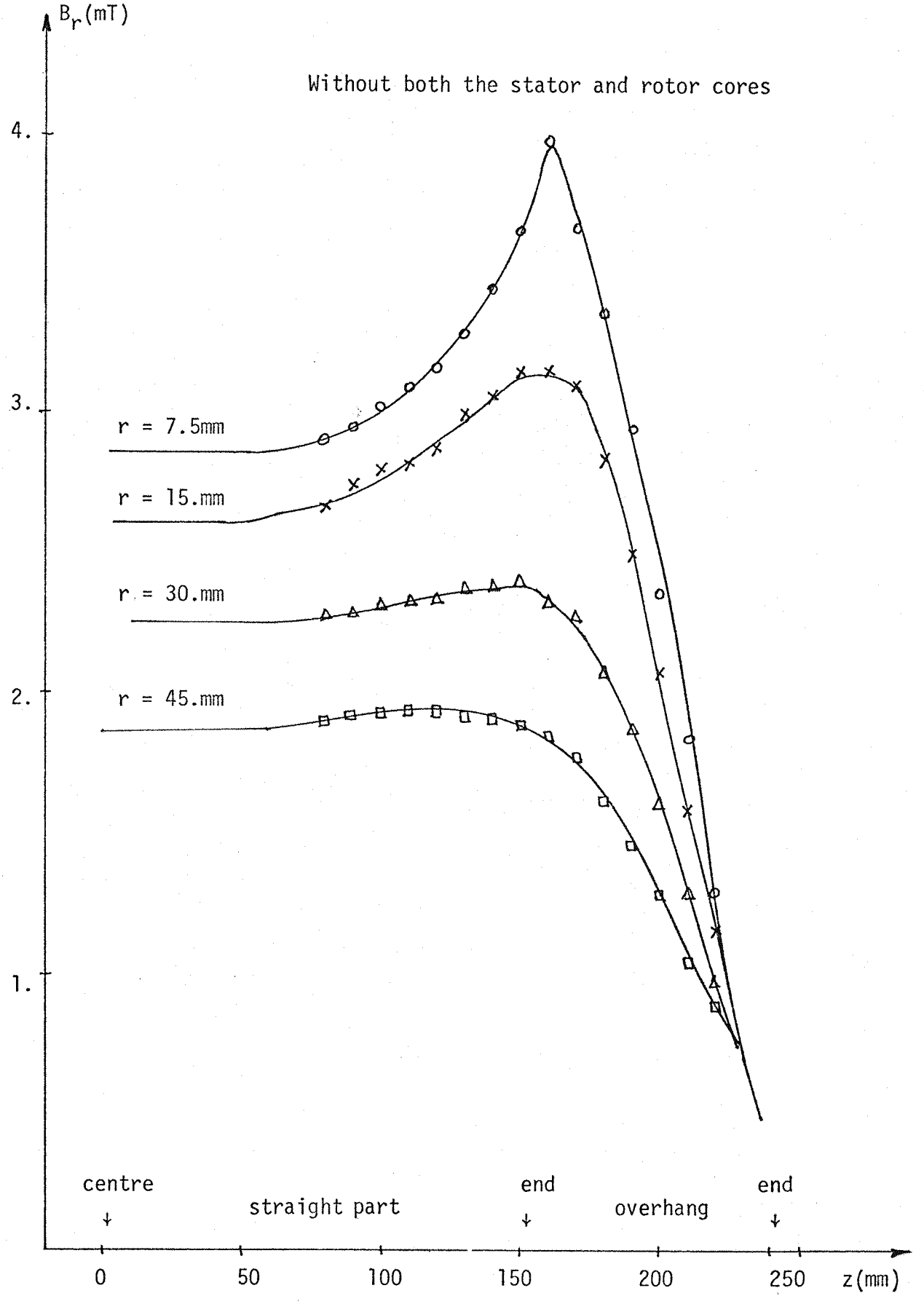

Fig. 8.13.b: Variation of the radial flux density along the stator winding lingth (for different distance from the surface).

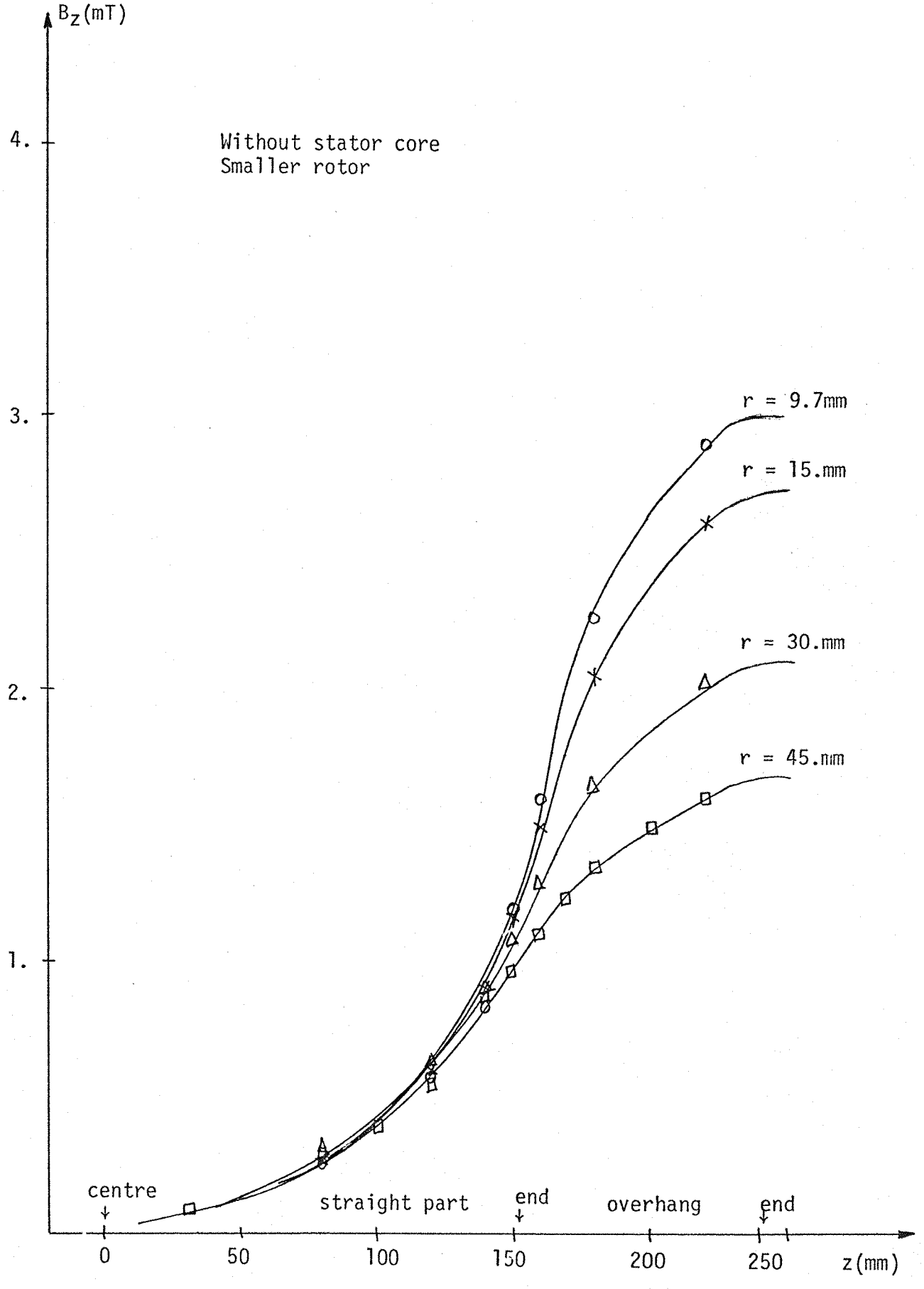

Fig. 8.14.a: Variation of the axial flux density along the stator winding length (for different distance from the surface).

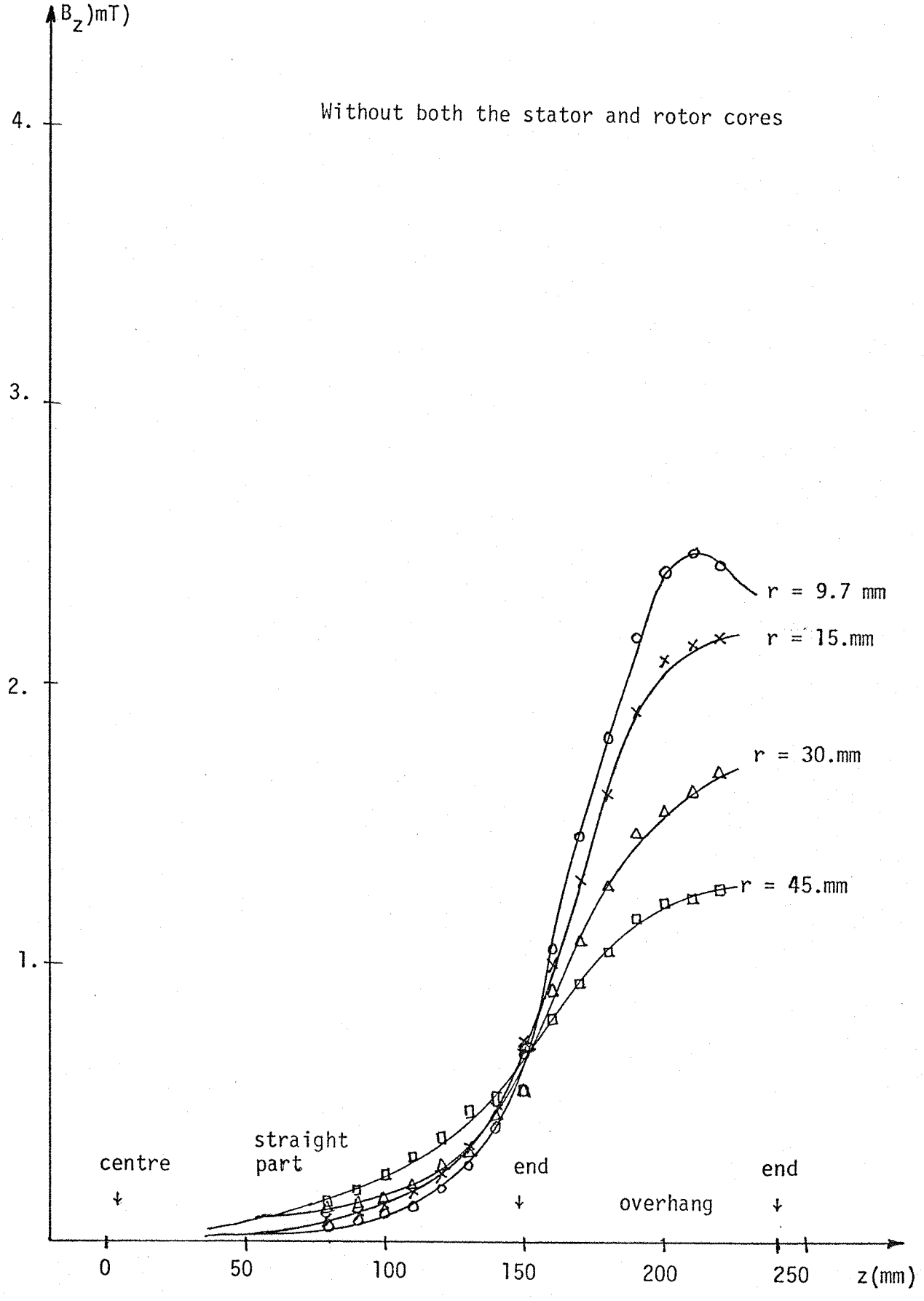

Fig. 8.14.b: Variation of the axial flux density along the stator winding length (for different distances from the surface.)

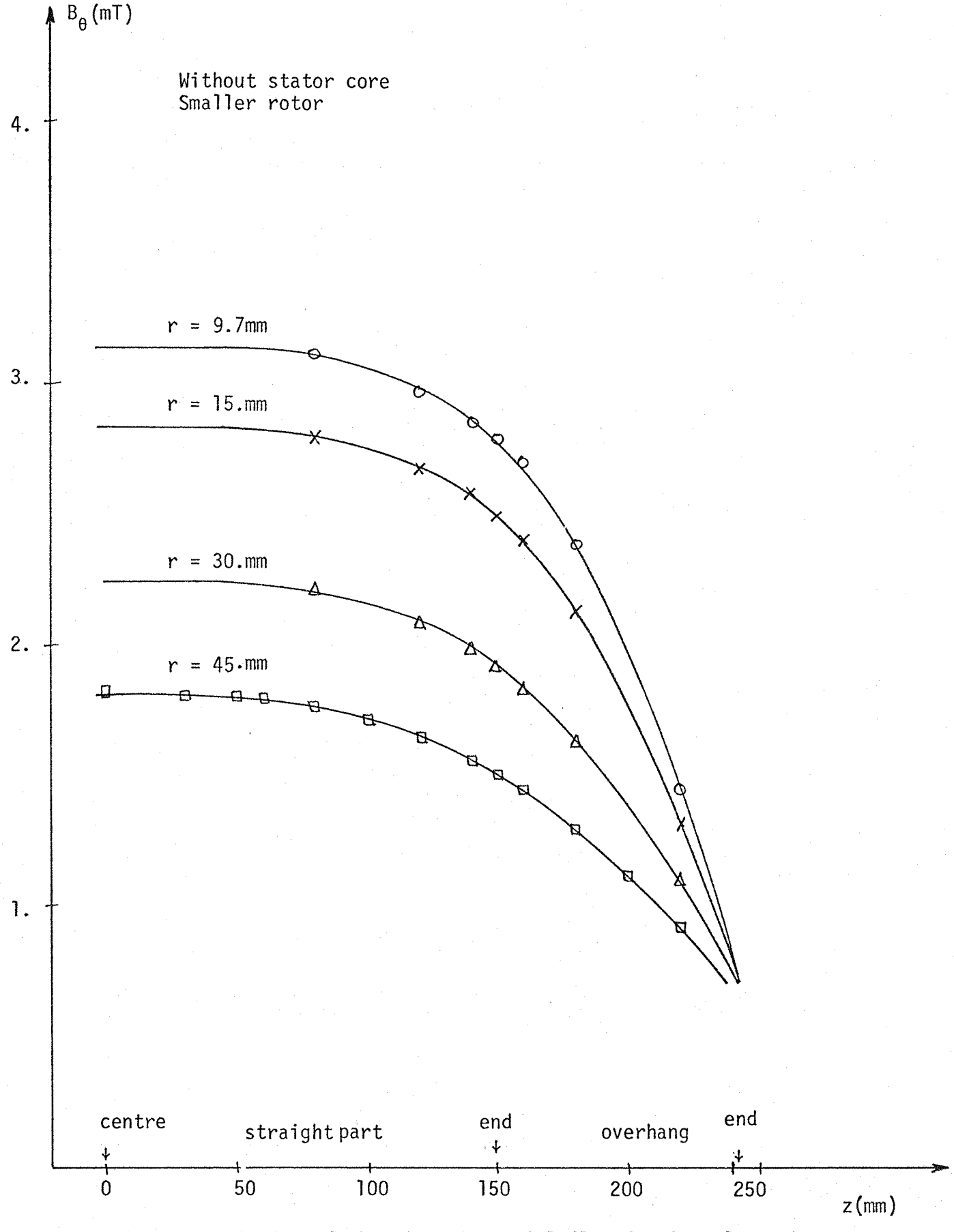

Fig. 8.15.a: Variation of the circumferential flux density along the stator widning length (for different distances from the surface).

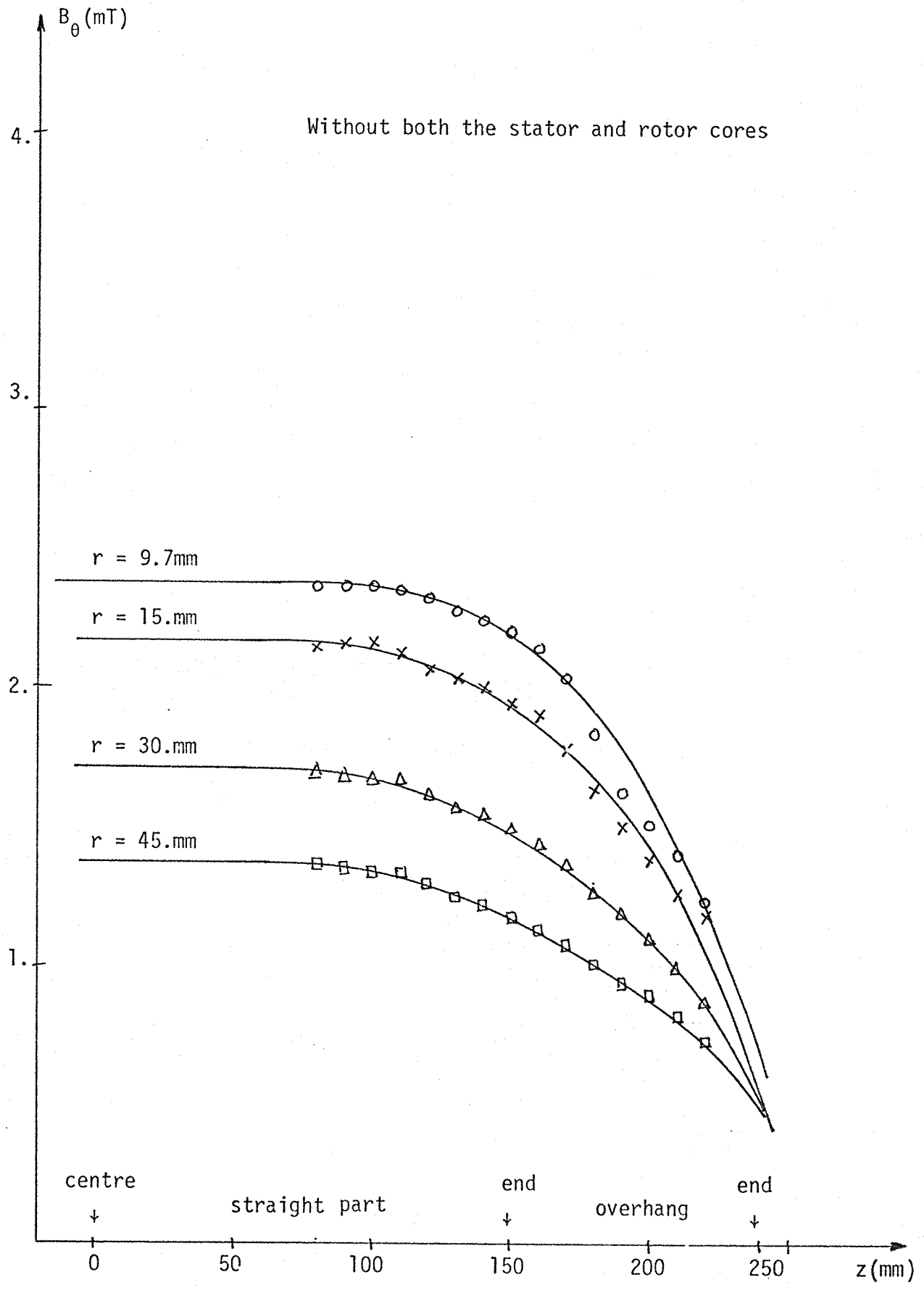

Fig. 8.15.b: Variation of the curcumferential flux density along the stator winding length (for different distance from the surface).

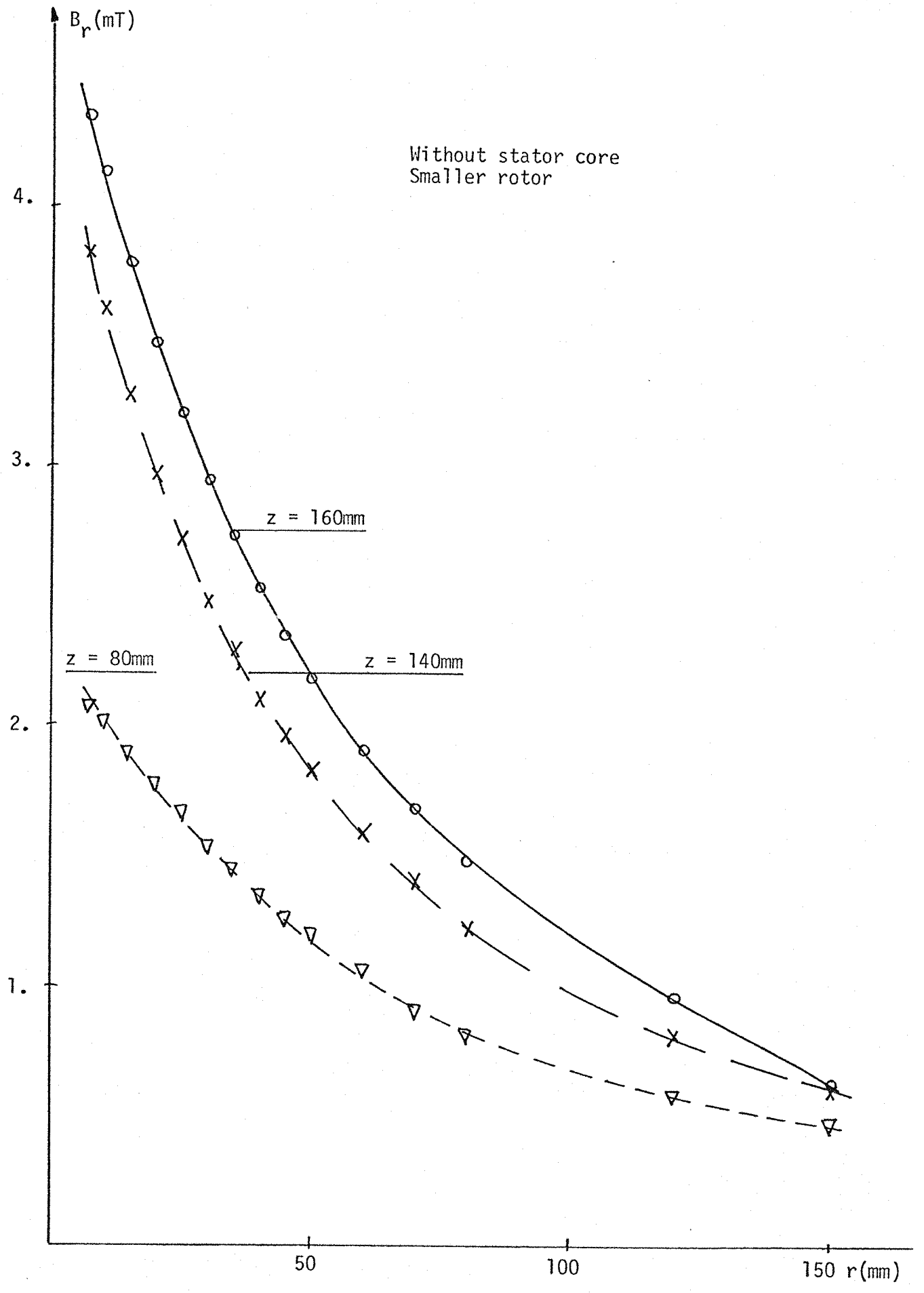

Fig. 8.16.a: Variation of the radial component of the flux density against the distance from the stator winding surface.

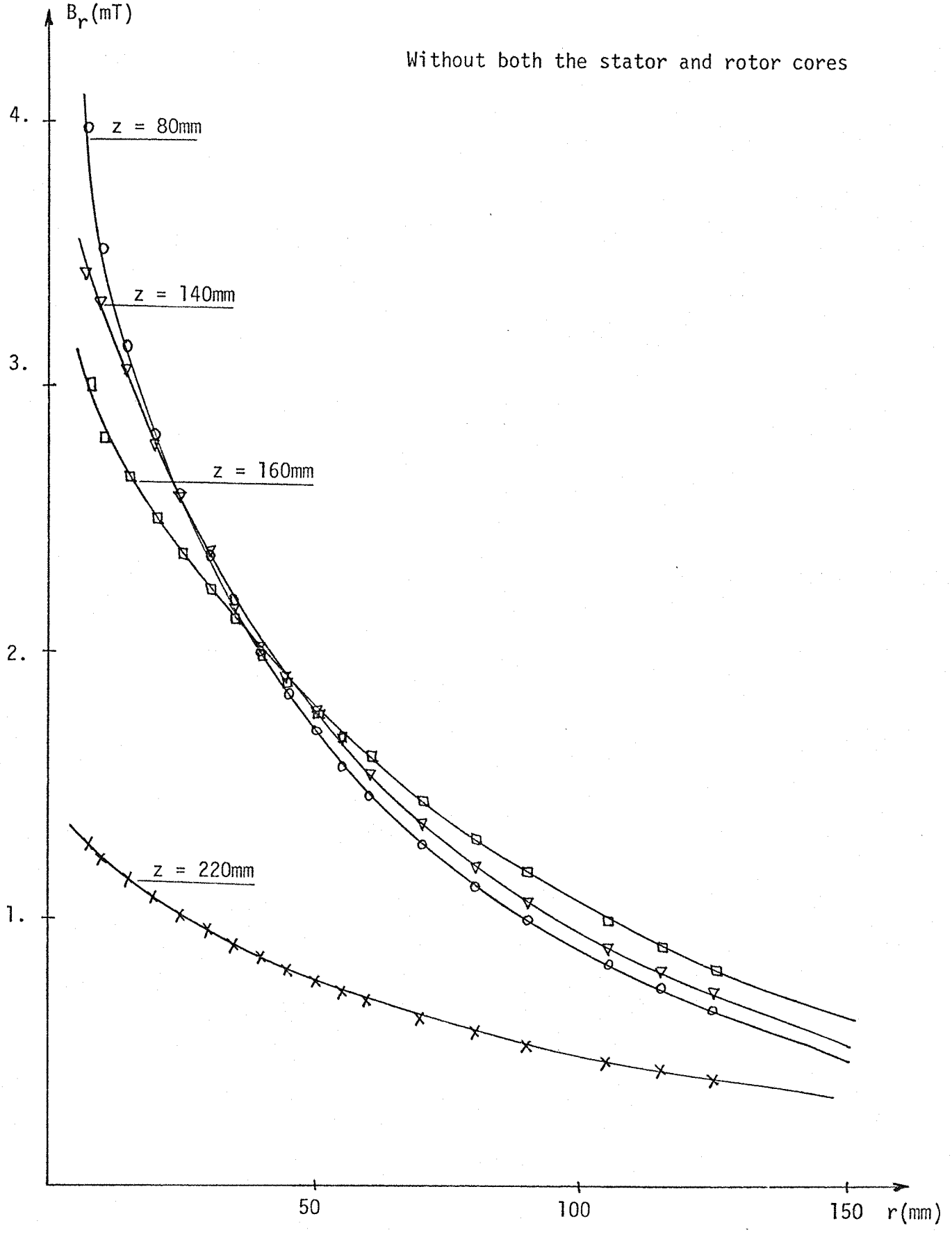

Fig. 8.16.b: Variation of the radial flux density against the distance from the stator winding surface.

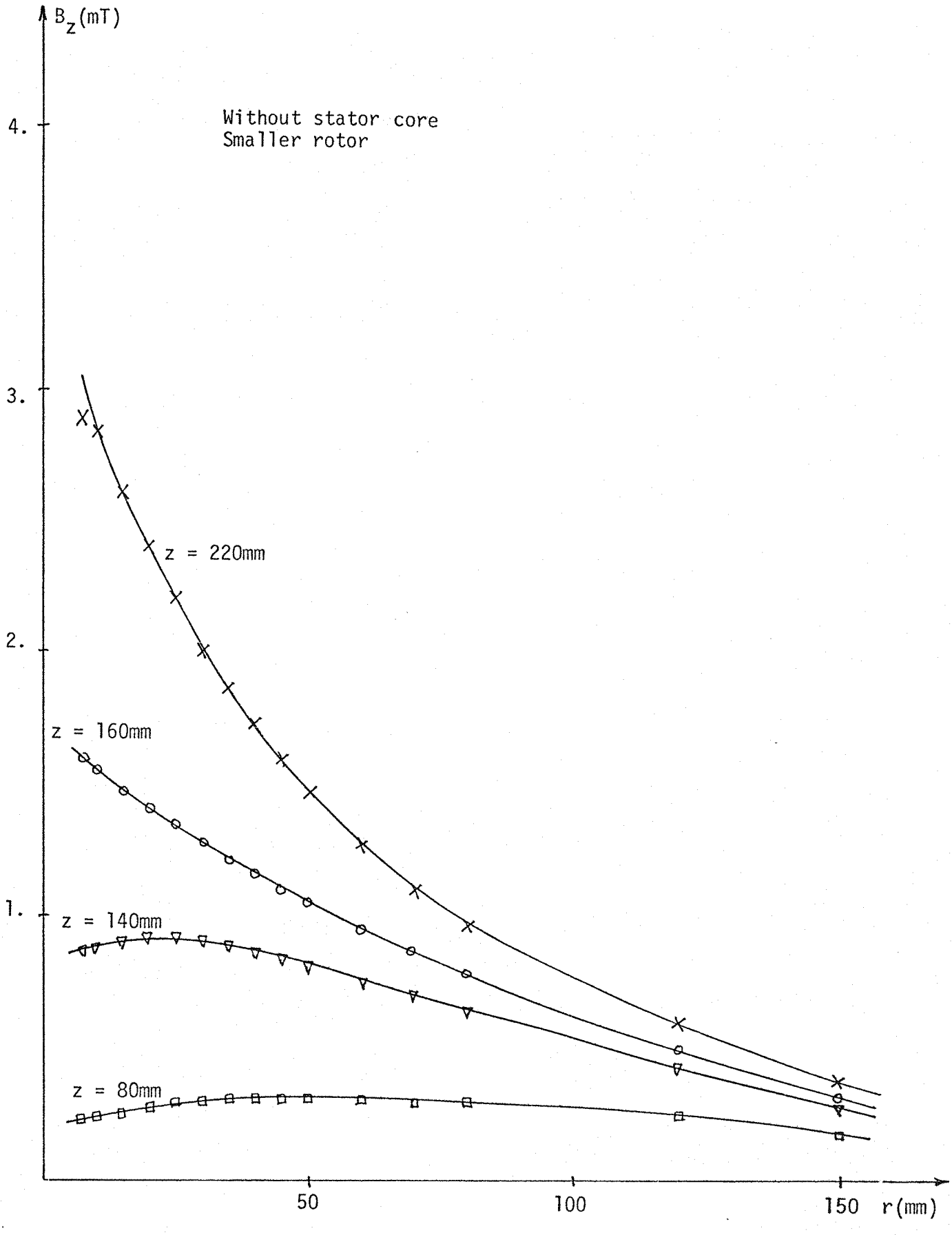

Fig. 8.17.a: Variation of the axial flux density against the distance from the stator winding surface.

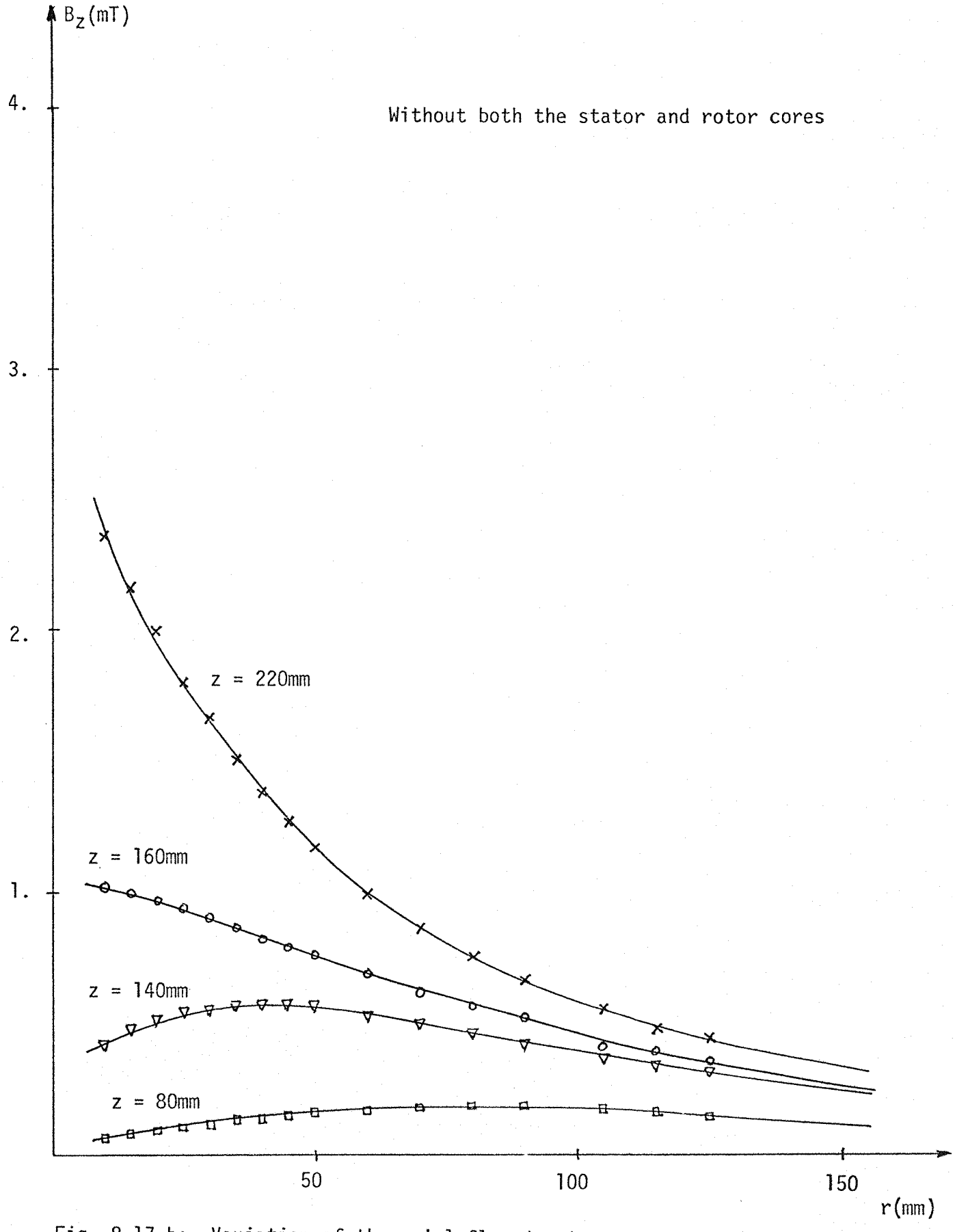

Fig. 8.17.b: Variation of the axial flux density against the distance from the stator winding surface.

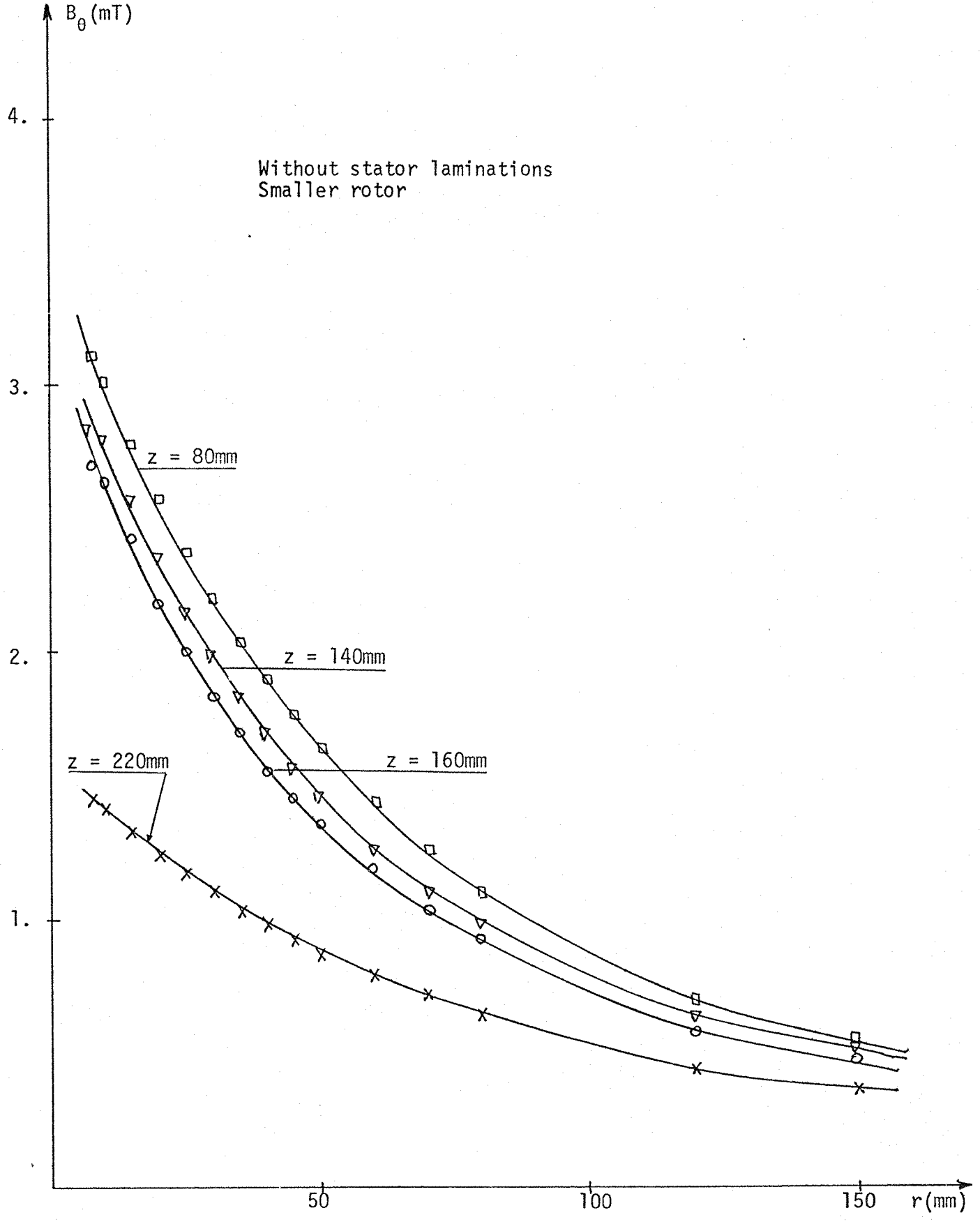

Fig. 8.18.a: Variation of the circumferential flux density against the distance from the stator winding surface.

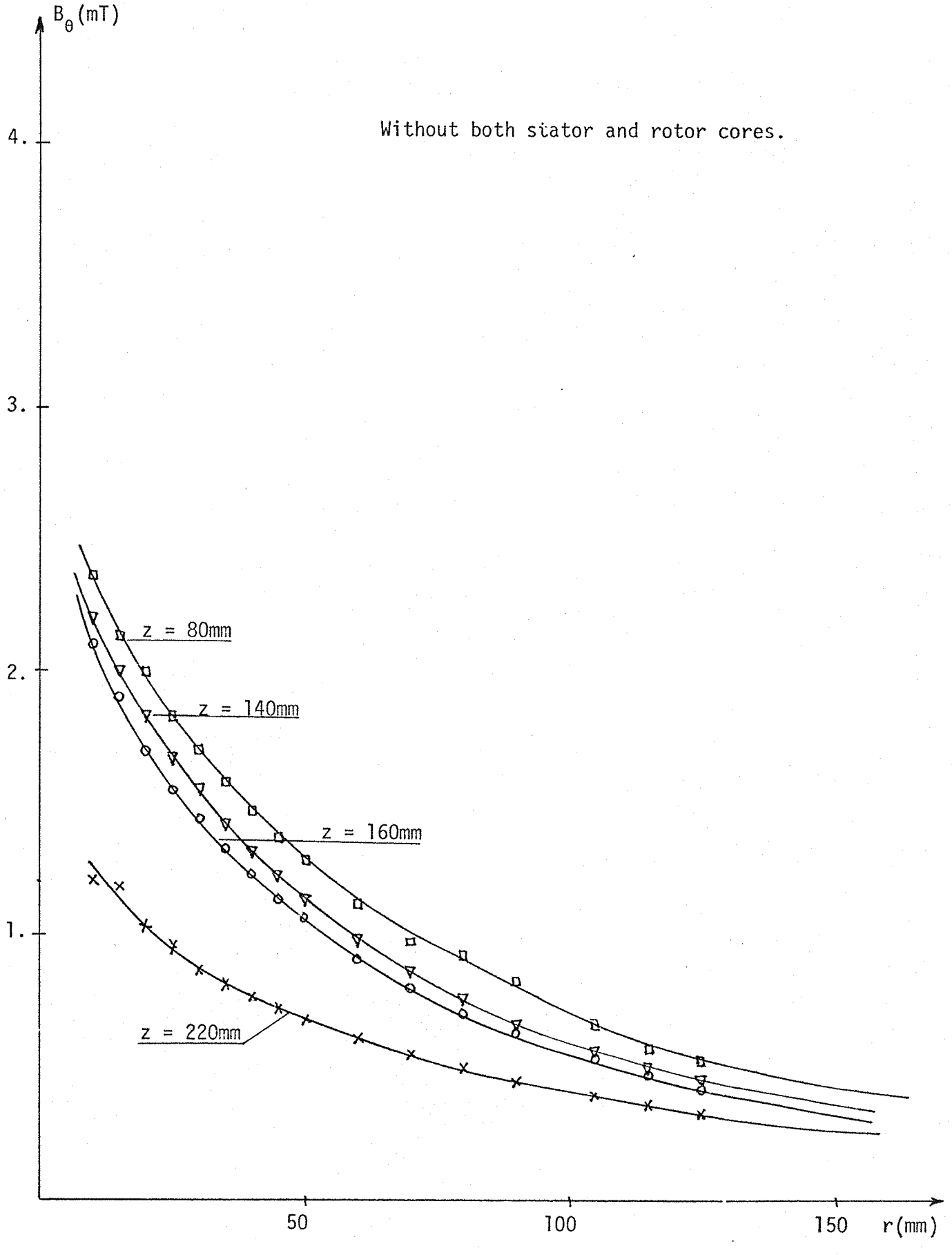

Fig. 8.18.b: Variation of the circumferential flux density against the distance from the stator winding surface.

The main electromagnetic sources are located at the end region of the synchronous machine, as described in figure 3.1. The presence of radial ventilating ducts in the core back can cause a redistribution in the core back leakage flux along the stator length.

8.2.8 Effects of the Relative Positions Between the Stator and Rotor Cores

The change in the relative position between both the stator and rotor cores affects the distribution of leakage flux at the stator core back. When the stator core extends beyond the rotor core the core back leakage flux is decreased. Actually the surface polarities at both the core front and core back decrease when the rotor is shortened with respect to the stator core. Howe[66] examines the effect of shortening the rotor on the leakage flux impinging the stator core front. He emphasises the fact that the core front leakage flux is diminished when the rotor is shorter than the stator core.

Figures 8.19 and 8.20 show the variation of the core back leakage flux with the relative position between both the stator and rotor cores. The three components of core back leakage flux are decreased when the stator core is extended further beyond the rotor core. The positive distances plotted in the horizontal axis mean that the rotor extends beyond the stator core and the negative distances the opposite.

The results obtained in both figure 8.19 and figure 8.20 suggest that a shortening of the rotor with respect to the stator core is beneficial in reducing the effects of the leakage flux at the stator core back of the synchronous machine.

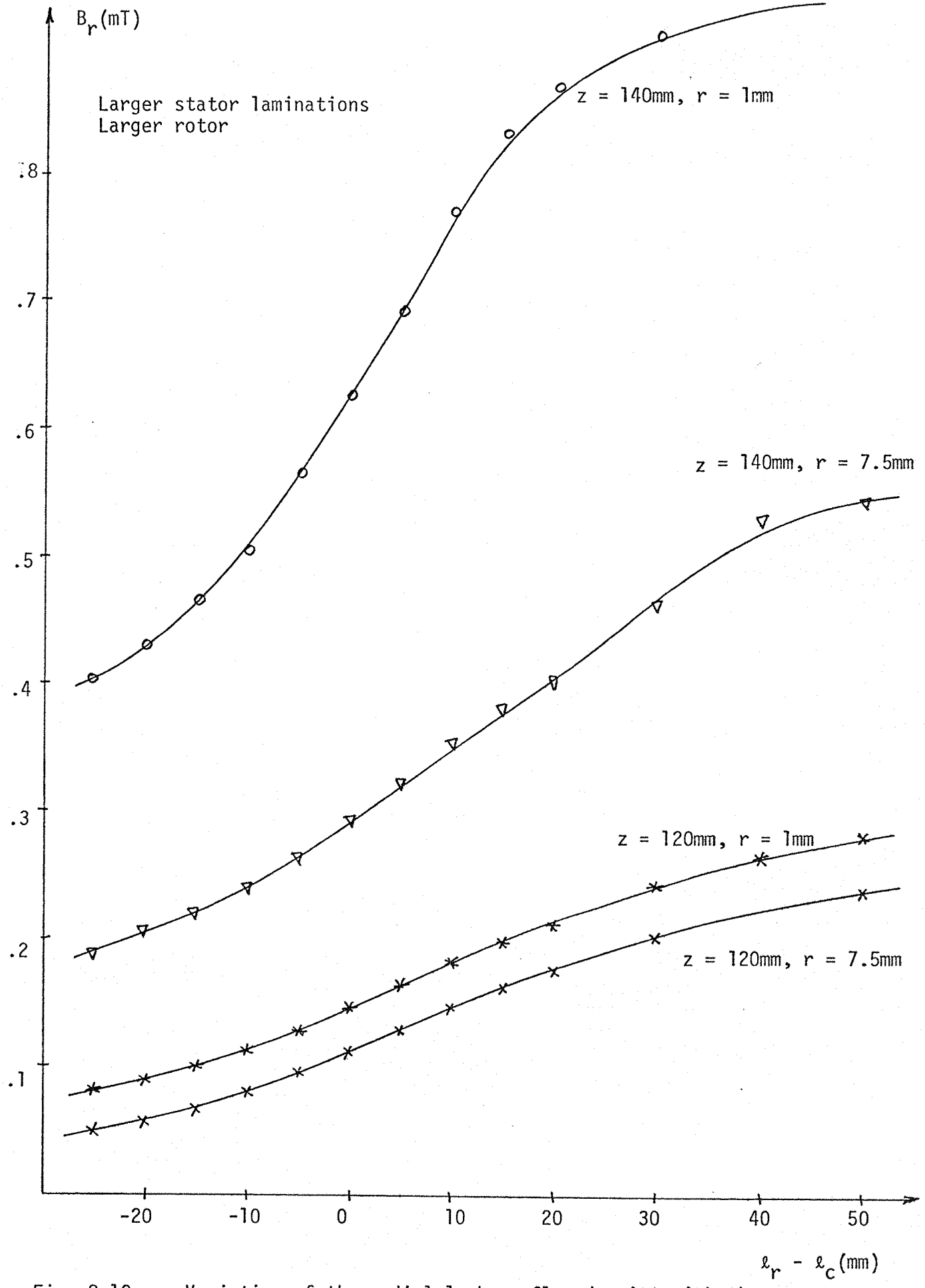

Fig. 8.19.a: Variation of the radial leakage flux density with the relative position between both the stator and rotor cores.

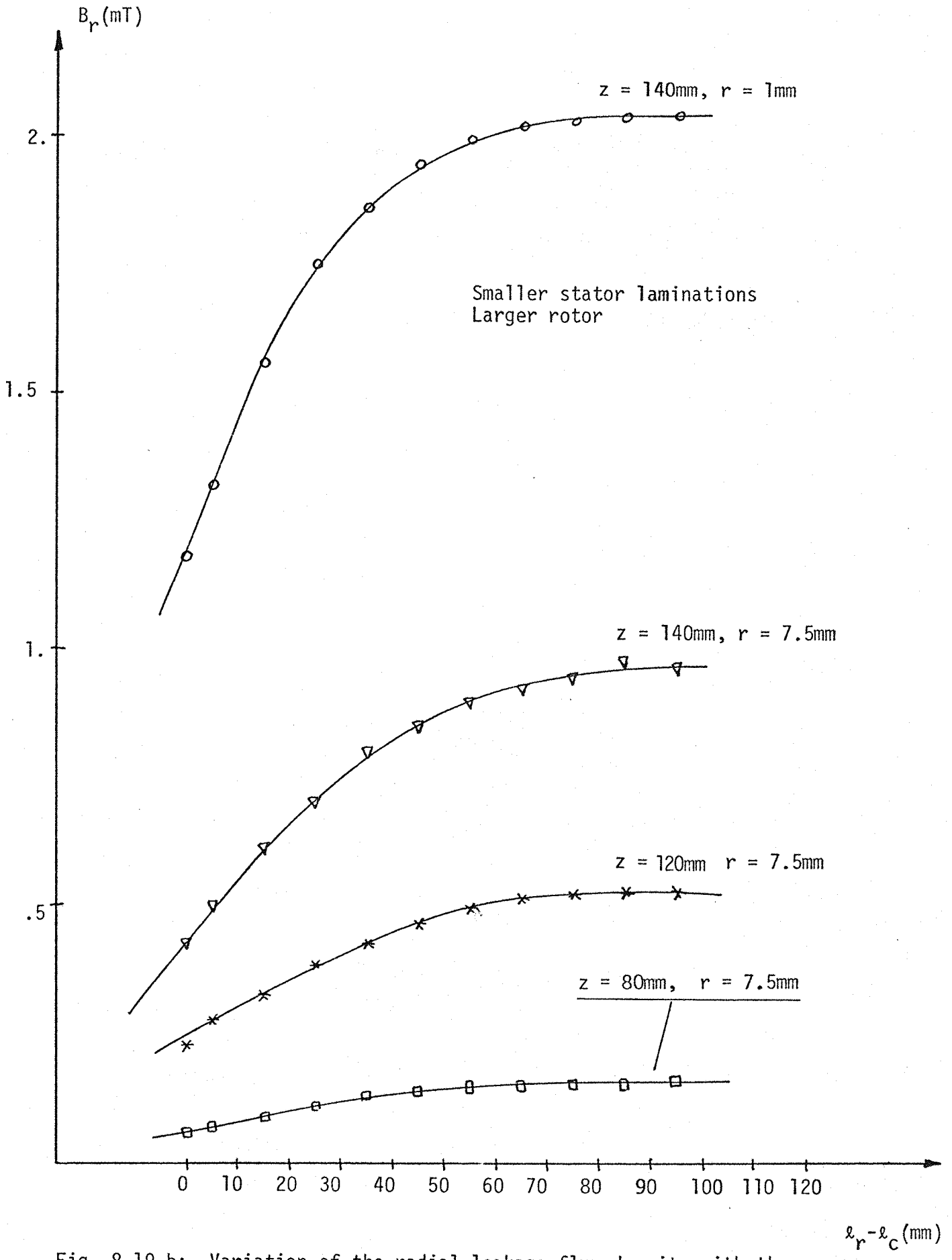

Fig. 8.19.b: Variation of the radial leakage flux density with the relative position between both the stator and rotor cores.

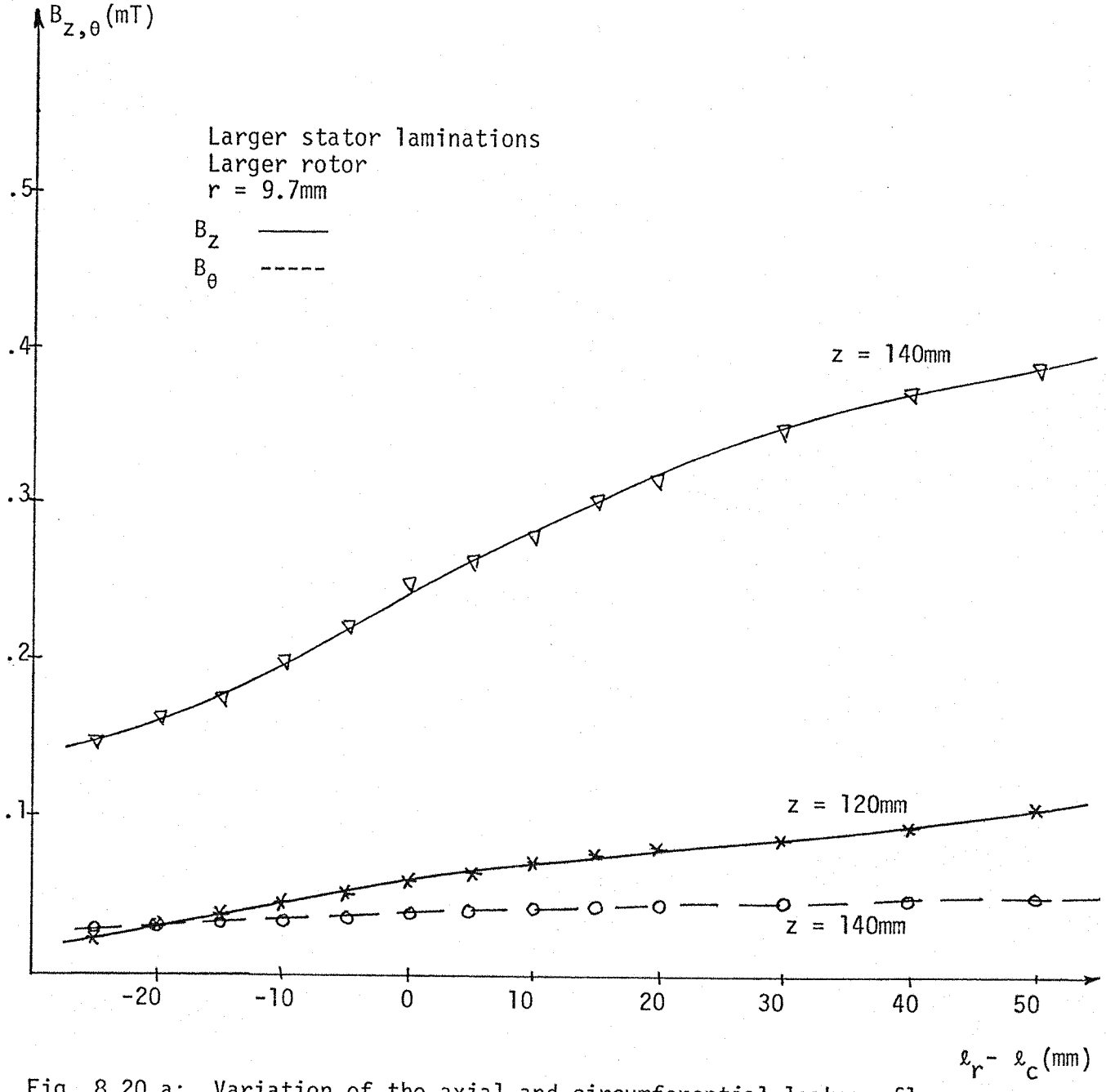

Fig. 8.20.a: Variation of the axial and circumferential leakage flux densities with the relatige position between both the stator and rotor cores.

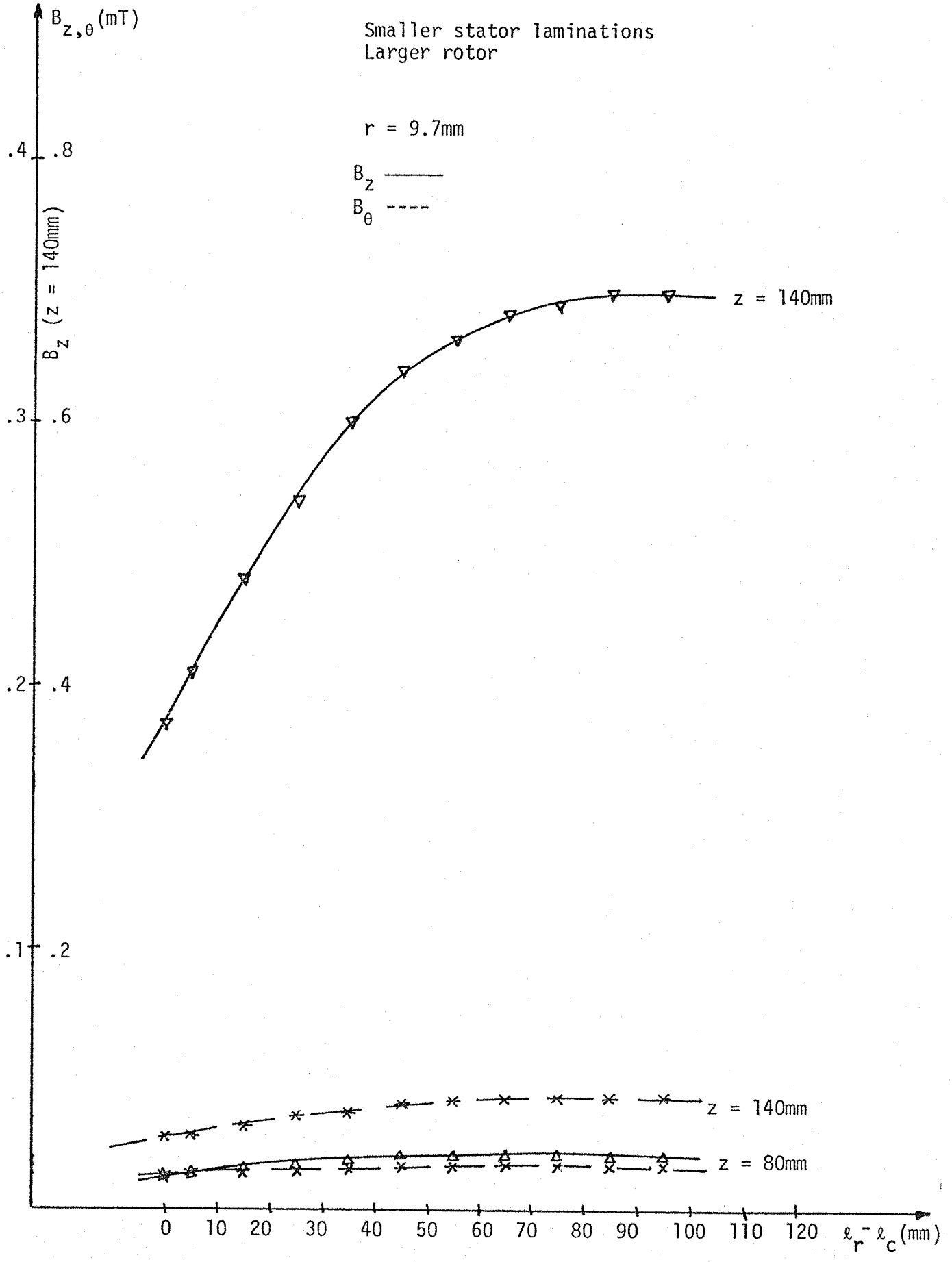

Fig. 8.20.b: Variation of the axial and circumferential leakage flux densities with the relative position between both the stator and rotor cores.

8.2.9 Effects of the Overhang Length

The overhang effects in the distribution of the leakage flux at the stator core back are discussed in further detail in section 3.2. The equations of the leakage flux components due to the different shapes of overhang are shown in section 4.3.1. Results obtained in the model with stationary rotor are shown in figure 8.21 and figure 8.22. Those results show that the core back leakage flux increases with the length of the overhang. When the overhang length is increased the leakage flux path length is also increased and a larger quantity of leakage flux reaches the core back region. Therefore the magnetic surface polarity at the stator core back is increased. Also the distribution of magnetic poles at the edge of the core front surface is affected by the change in the overhang length. The edge zone of the core back suffers a more accentuated effect from the leakage flux than the centre when the overhang length is prolonged.

8.2.10 Effects of the Overhang Current

The variation of the core back leakage flux components with the variation in the overhang current is shown in figure 8.23. The results were obtained on the model with stationary rotor and are in agreement with those results obtained in the laboratory synchronous machine operating on short circuit conditions shown in Chapter Five. Neither model was operating under saturation conditions. Therefore the leakage flux components increase linearly with the current in the overhang, as shown in figure 8.23. The sharpest increase in the core back leakage flux is obtained at the edge of the stator core back. The increase in the overhang current causes an increase in the magnetic polarities at both the bore, core front and core back surfaces. Unfortunately it was not possible to isolate the overhang current from

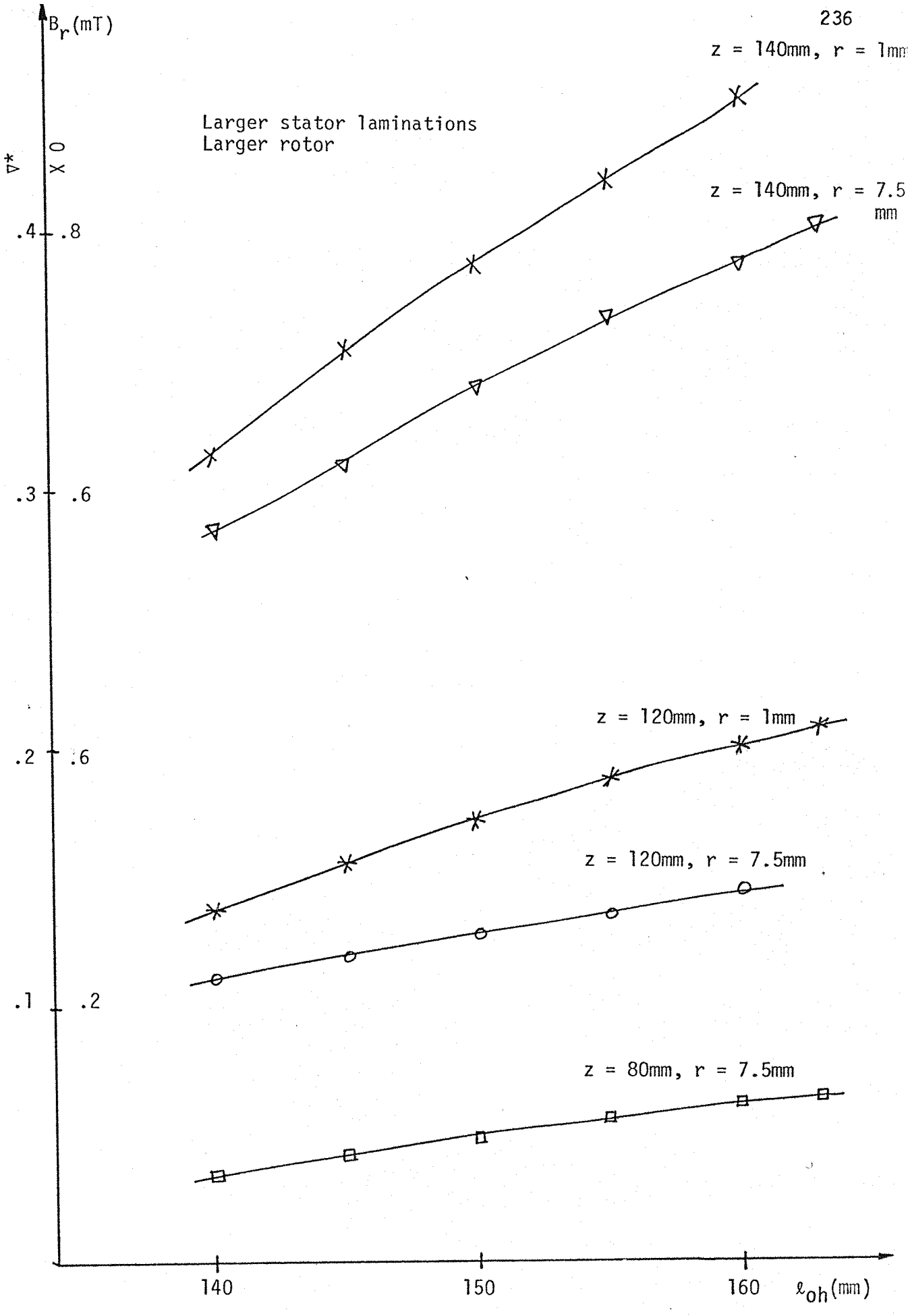

Fig. 8.21.a: Variation of the radial leakage flux density against the overhang length.

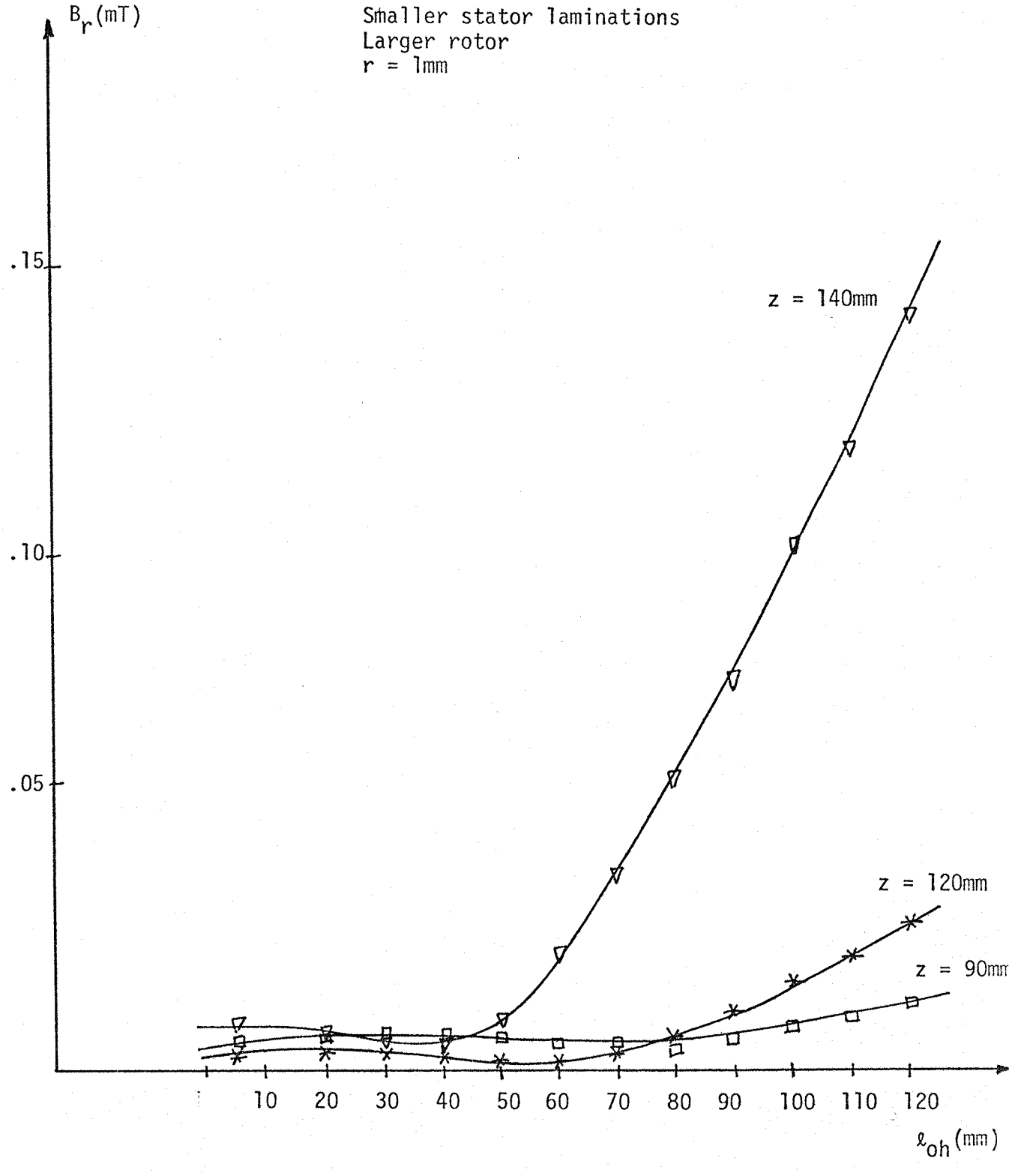

Fig. 8.21.b: Variation of the radial leakage flux density against the overhang length.

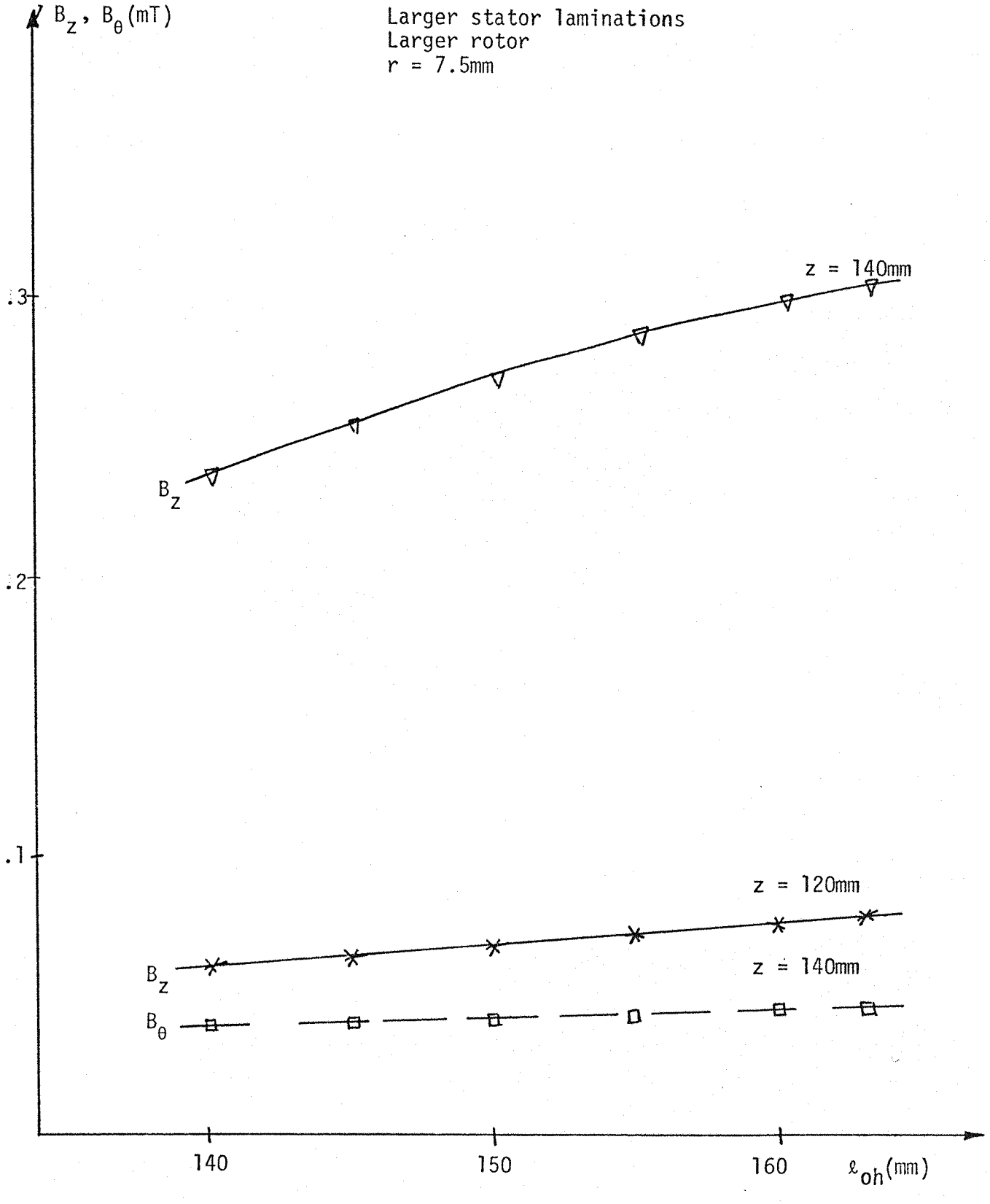

Fig. 8.22: Variation of the axial and circumferential components of leakage flux density against the overhang length.

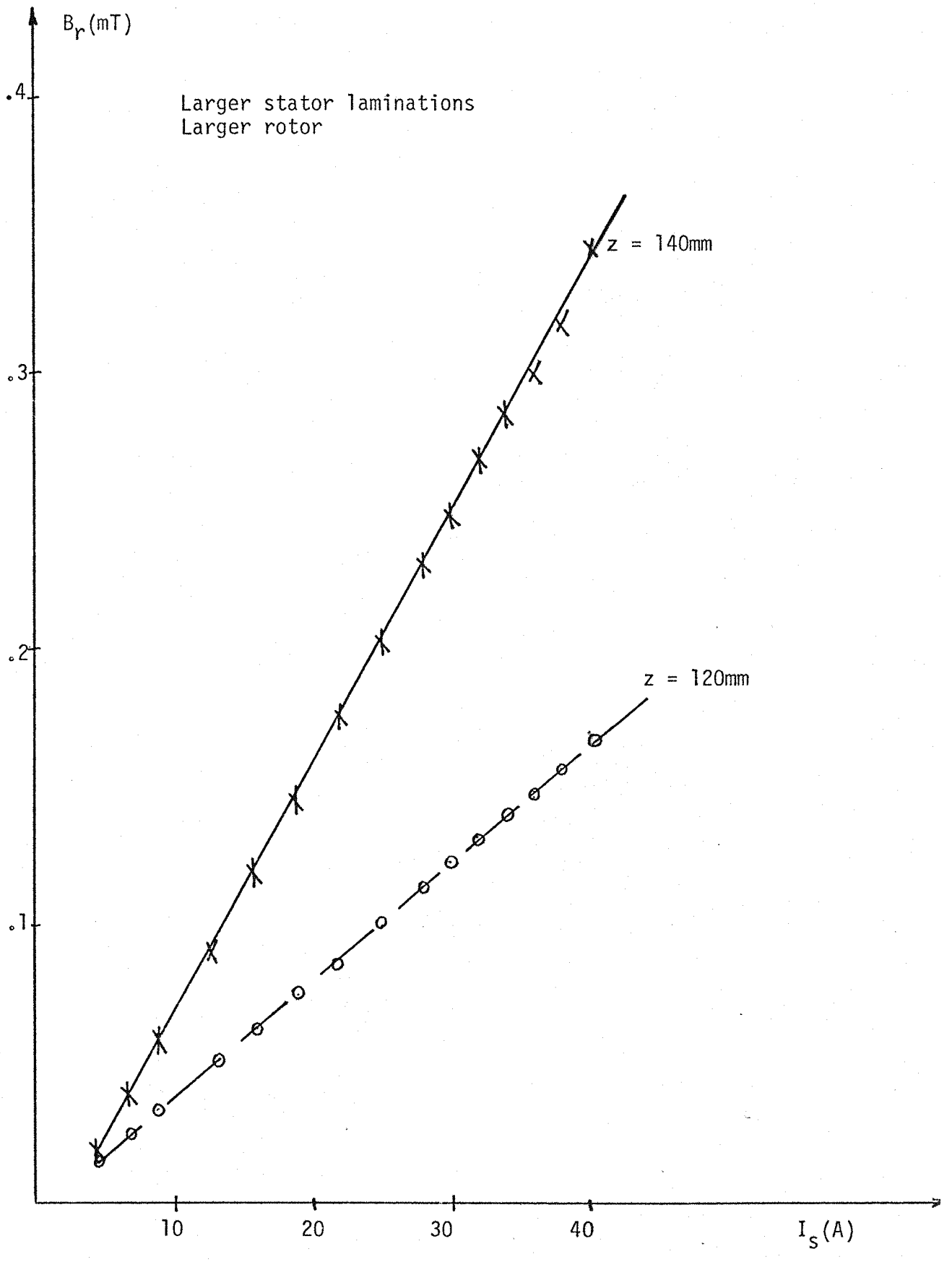

Fig. 8.23.a: Variation of the radial leakage flux density against the stator current.

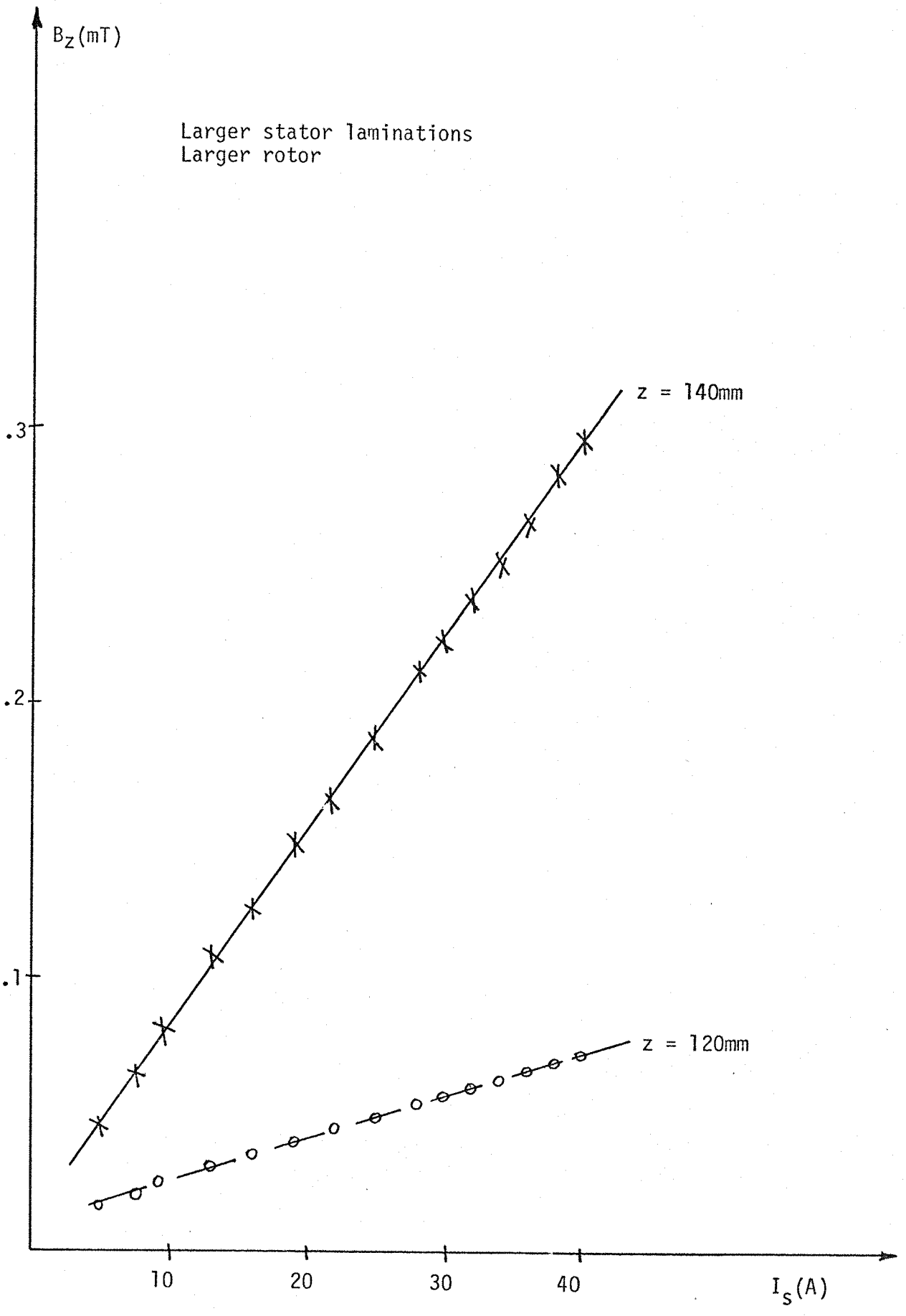

Fig. 8.23.b: Variation of the axial leakage flux density against the stator current.

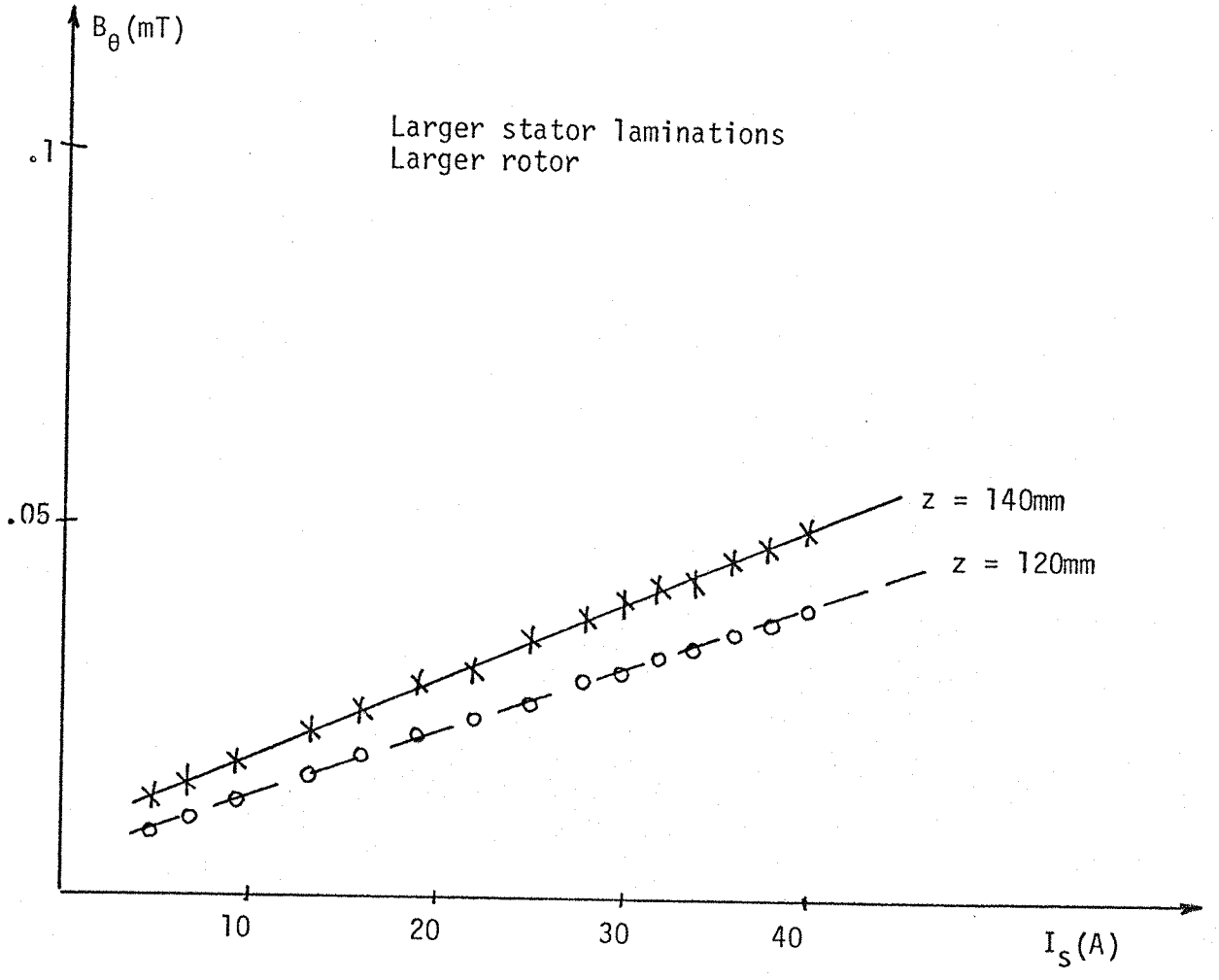

Fig. 8.23.c: Variation of the circumferential leakage flux density against the stator current.

the other sources. Both sections 3.2 and 4.3.A give theoretical support to the conclusions drawn from the experimental results.

8.2.11 Effects of Eddy Current and Screening Plate

The leakage flux impinging on the surfaces of the stator core of the synchronous machine induces eddy currents. The eddy current can be induced in the plane of laminations, back of the core, building bars, end plates and screening plates. The eddy current can produce local effects increasing the temperature. Further discussions about the eddy currents are presented in section 3.6.2. In this section attention is directed to eddy currents induced in the screening plate at the stator core front.

With the increase in the rated power output of synchronous machines the effects of the leakage flux penetrating the stator core front have been increased. Higher temperatures have been observed in the core front region due to the circulation of larger eddy currents induced by larger axial leakage flux impinging on the core front surface. In order to reduce the troublesome effects of the leakage flux, screening plates of low resistivity material have been mounted at the core front of the synchronous machine. These screening plates are generally made of either copper or aluminium.

The axial leakage flux induces eddy currents in the screening plate. The eddy current circulating in the screening plates produces a reaction field that opposes the penetration of the inducing field. The strength of the reaction field is dependent on the screening plate thickness since both the frequency and the resistivity are already fixed. If the thickness is greater than the skin depth the screening plate is seen by the axial leakage flux as a region of zero permeability and infinite conductivity. Therefore, the axial leakage flux is forced

to avoid the core front and is diverted to another direction. Close to the screening plate the leakage flux changes from the axial to the radial direction, i.e. the leakage flux adopts a direction parallel to the screening plate.

It is suggested that the existence of a screening plate at the core front of a synchronous machine can increase the leakage flux at the back of the stator core. The leakage flux diverted from the axial to the radial direction can cause a higher concentration of core back leakage flux mainly at the edge of the stator core back. The increase of core back leakage flux can induce higher eddy currents at the core back region leading to the establishment of high concentration of temperature.

The effect of the screening plate eddy current on the distribution of core back leakage flux was investigated in the model with a stationary rotor. The frequency of the stator winding current was varied. The winding current amplitude was kept constant by an appropriate adjustment in the applied stator voltage. The stator voltage needed to be increased when the frequency was increased because of the increase in the reactance of the stator winding in order to keep the current amplitude constant. Two different diameters of screening plate were used.

Figure 8.24 and figure 8.25 show the variation of the radial component of core back leakage flux against the frequency for the cases of smaller and larger screening plates at the core front, respectively. The larger laminations were used in both cases. The core back leakage flux density increases with the frequency for both cases. However, when the larger screening plate was used the leakage flux at the core back was greater than when the smaller one was used. Both screening plates produce a larger

concentration of leakage flux at the edges of the stator core back. However, when the smaller screening plate was used a greater concentration was also caused at the edge of the core front because not the complete face of the core was covered by the smaller screening plate.

The eddy current circulating in the screening plate causes a concentration of leakage flux in the region close to the screening plate edge. This conclusion suggests that the screening plate should not terminate at the core front but should be extended along the stator core back in order to avoid an increase in the leakage flux at the edge of the core back.

The amplitudes of the total leakage flux density at the air region around the stator core were obtained for the different arrangements of the model with the stationary rotor:

I	larger stator core with larger screening plate
II	larger stator core with smaller screening plate
III	larger stator core without screening plate
IV	smaller stator core without screening plate
V	stator winding only (no iron and no screening plate).

In arrangements I, II, III and IV, the larger rotor was used. Arrangement V did not have any iron at all, or screening plate.

Figure 8.26 shows the amplitudes of the total leakage flux density around the stator core for the different cases (I, II, III, IV and V). The results show that the screening plate at the core front causes an increase in the total leakage flux at the stator core back.

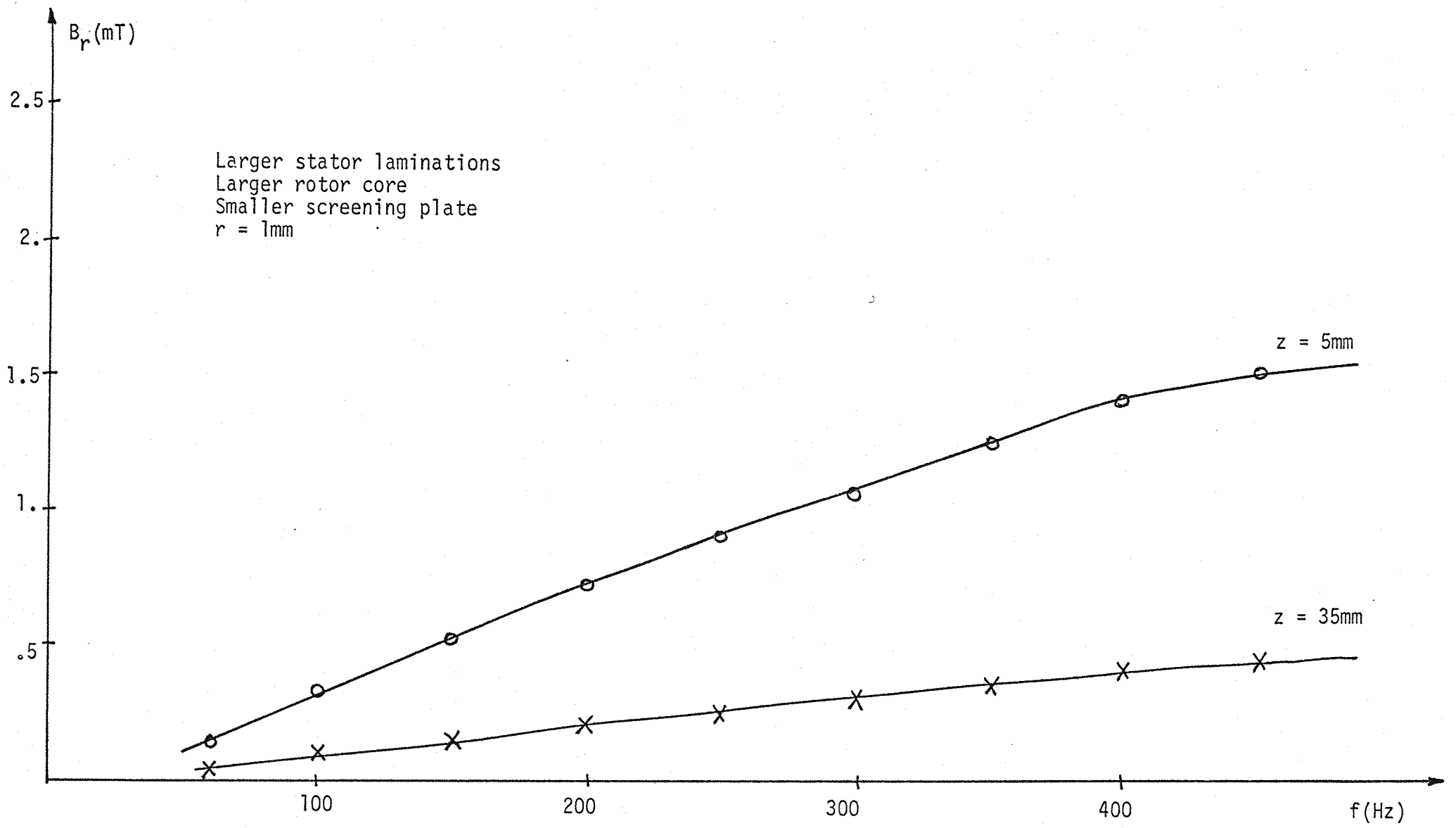

Fig. 8.24: Variation of the radial leakage flux density against the frequency.

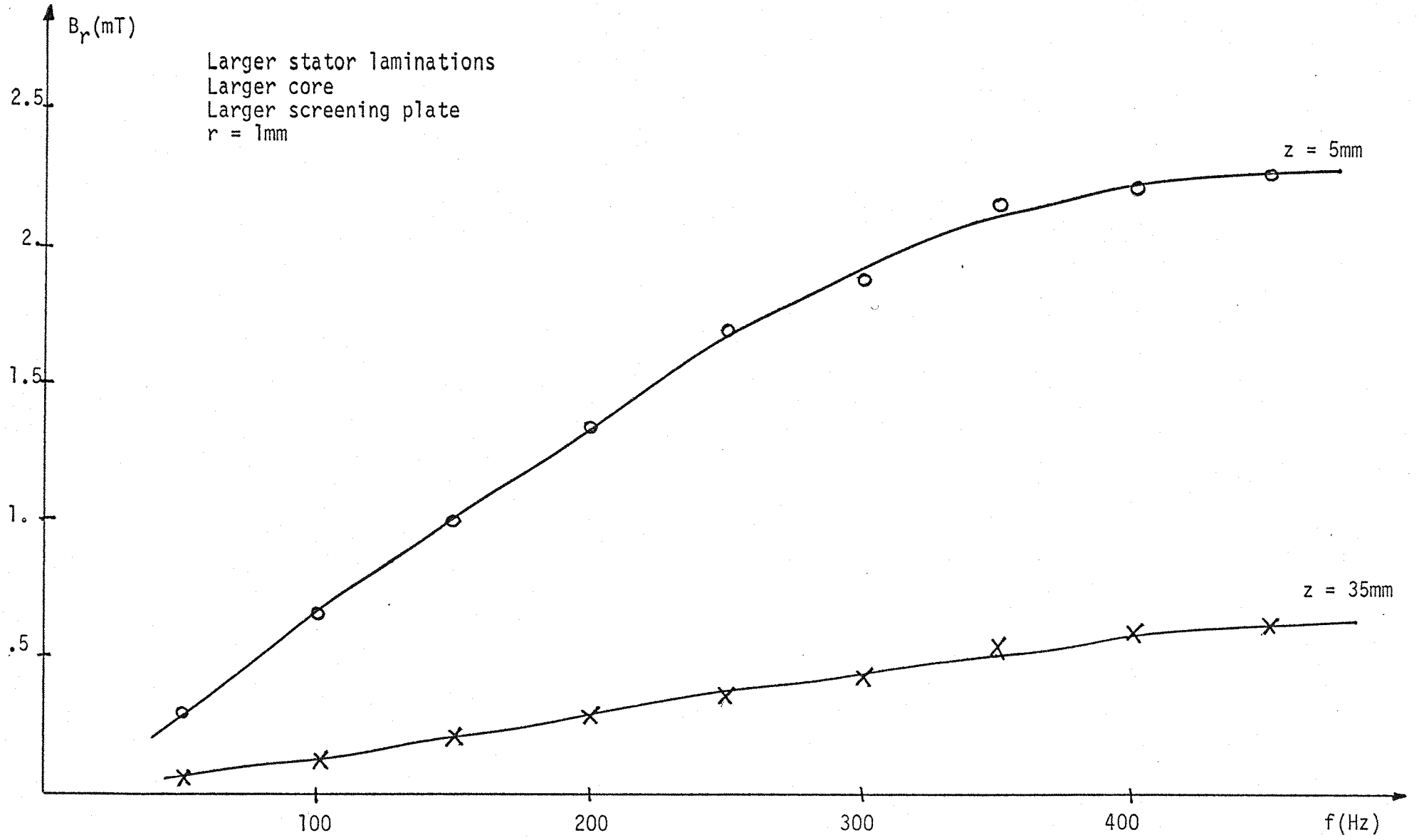

Fig. 8.25: Variation of the radial leakage flux density against the frequency.

8.2.12 Display of the 3-D Leakage Flux Density at the Core Back

The amplitudes and the phase angles of the radial, axial and circumferential components of the leakage flux density were measured in the air region for the different arrangements of the model with the stationary rotor, as described in section 8.2.10.

Baden Fuller and dos Santos[93] have designed the program which plots a vector field in space. Both the leakage flux components intensities and positions are computed. Tavner[97] has modified this program in order to add the phase angles to both the intensities and positions in the input data. The modified program is more suitable to the necessities of our specific problem. The program plots the total leakage flux density at various points in a chosen plane. The total leakage flux density is represented by arrows which give the direction and the relative amplitude of the flux density. The relative amplitude is given by the length of the arrow base. The greatest amplitude is made equal to unity. However, because of the tremendous difference between the amplitudes at certain positions over the air region, it was necessary to adopt logarithmic scale for the amplitudes at different radial positions. That scaling factor makes the reading of the magnitudes of the leakage flux density at different positions difficult. However, the greatest interest in using this powerful method of plotting the leakage flux density is directed towards the analysis in the change of direction of the leakage flux density over the air region. Figure 8.27 shows the effect of different diameters of screening plates and core depth in the distribution of core back leakage flux. The influence of the iron in the field produced by the stator winding can also be seen. Figure 8.26 helps to overcome the difficulties presented in reading the logarithmic scale used in figure 8.27.

Fig. 8.26.a: Magnitudes of the total leakage flux density

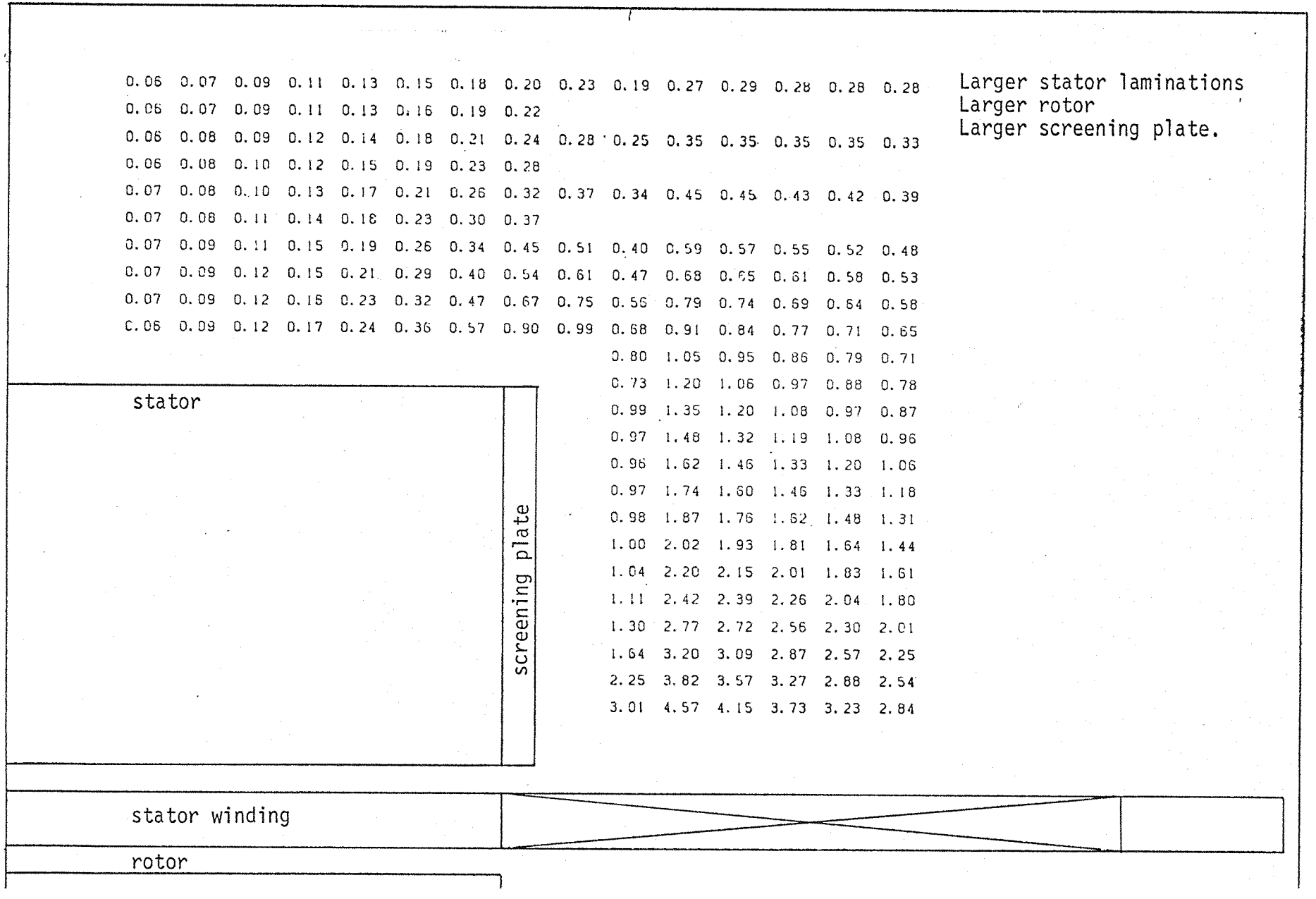

Fig. 8.26.b: Magnitudes of the total leakage flux density

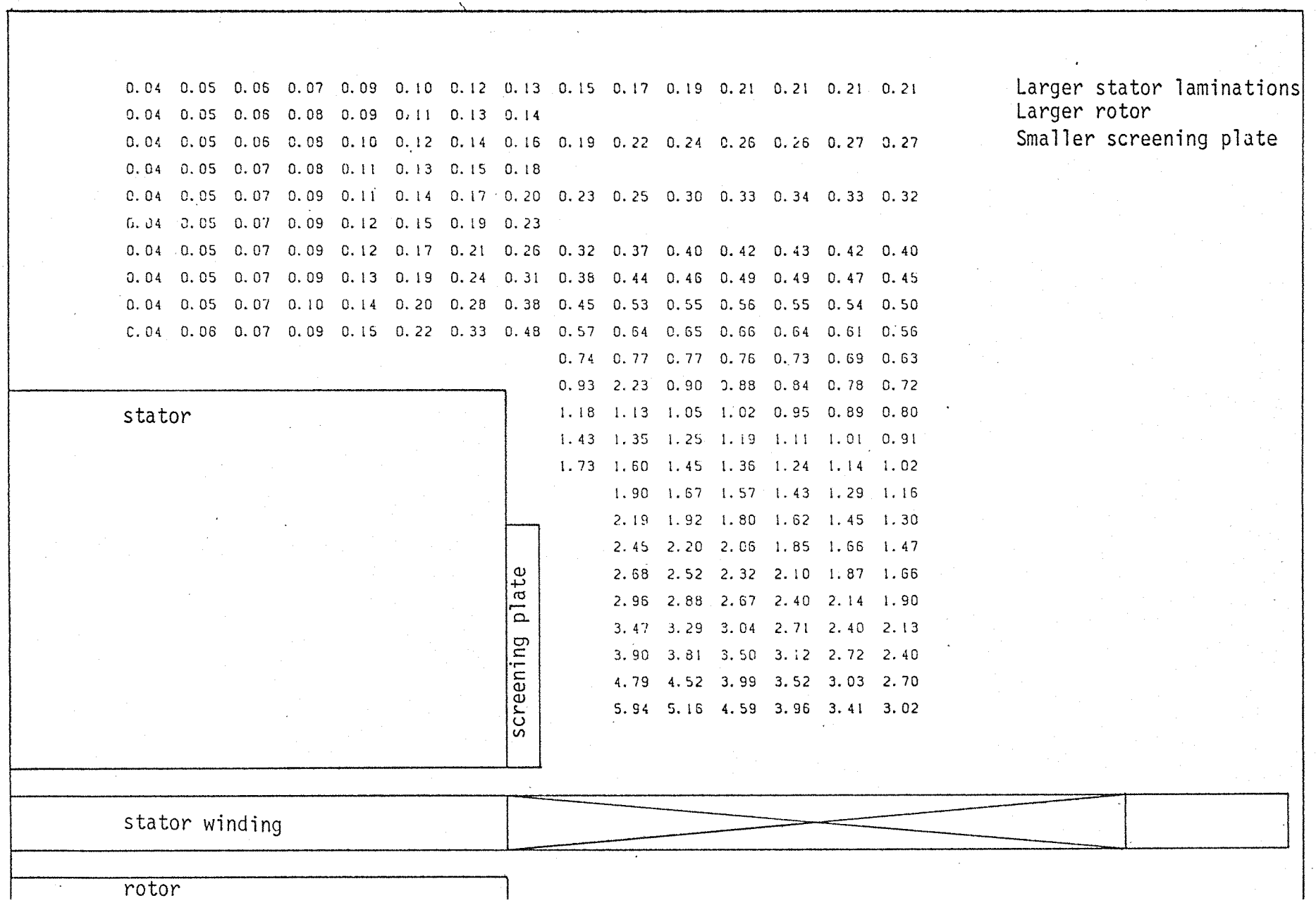

Fig. 8.26.c: Mangitudes of the total leakage flux density

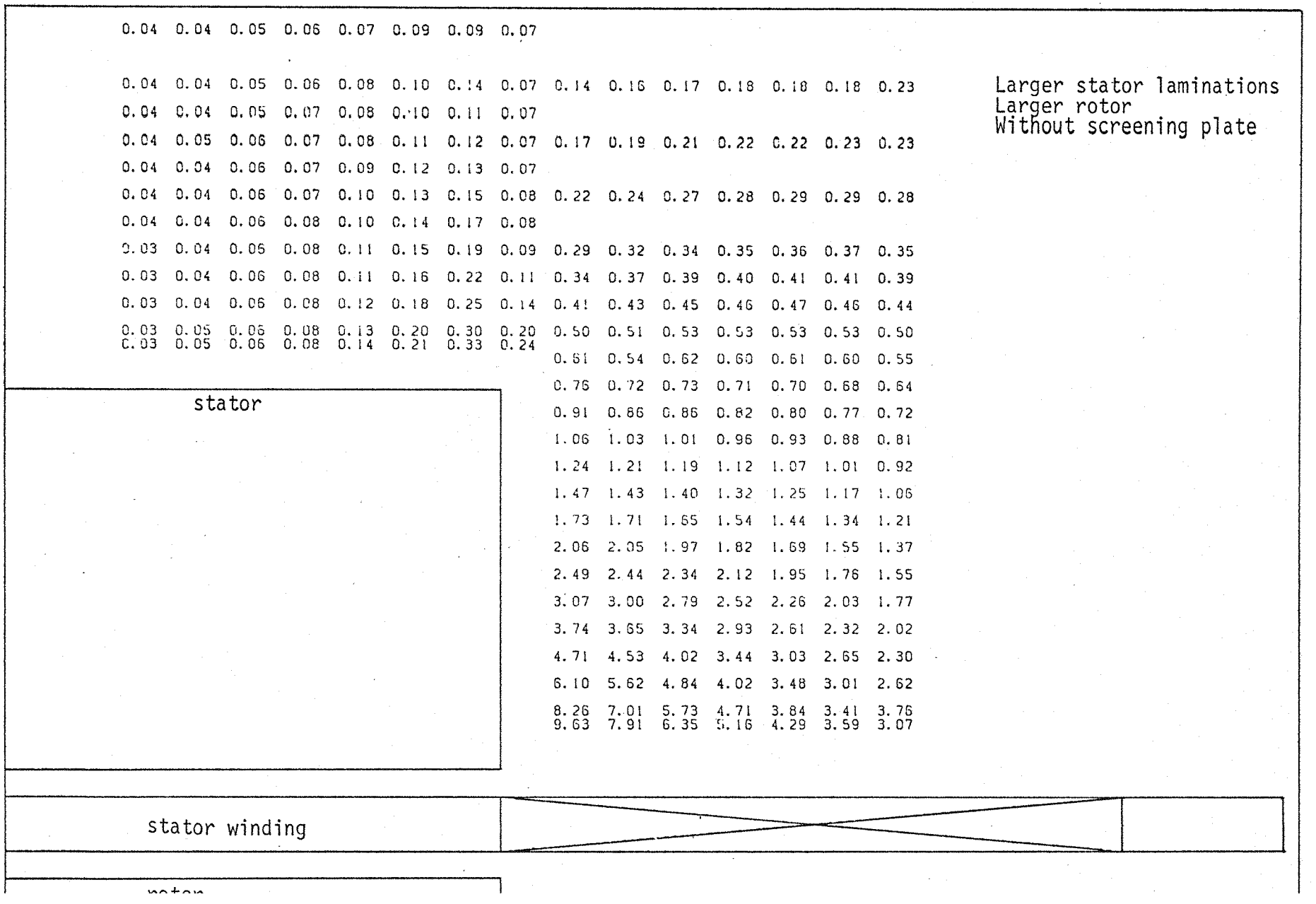

Fig. 8.26.d: Magnitudes of the total leakage flux density

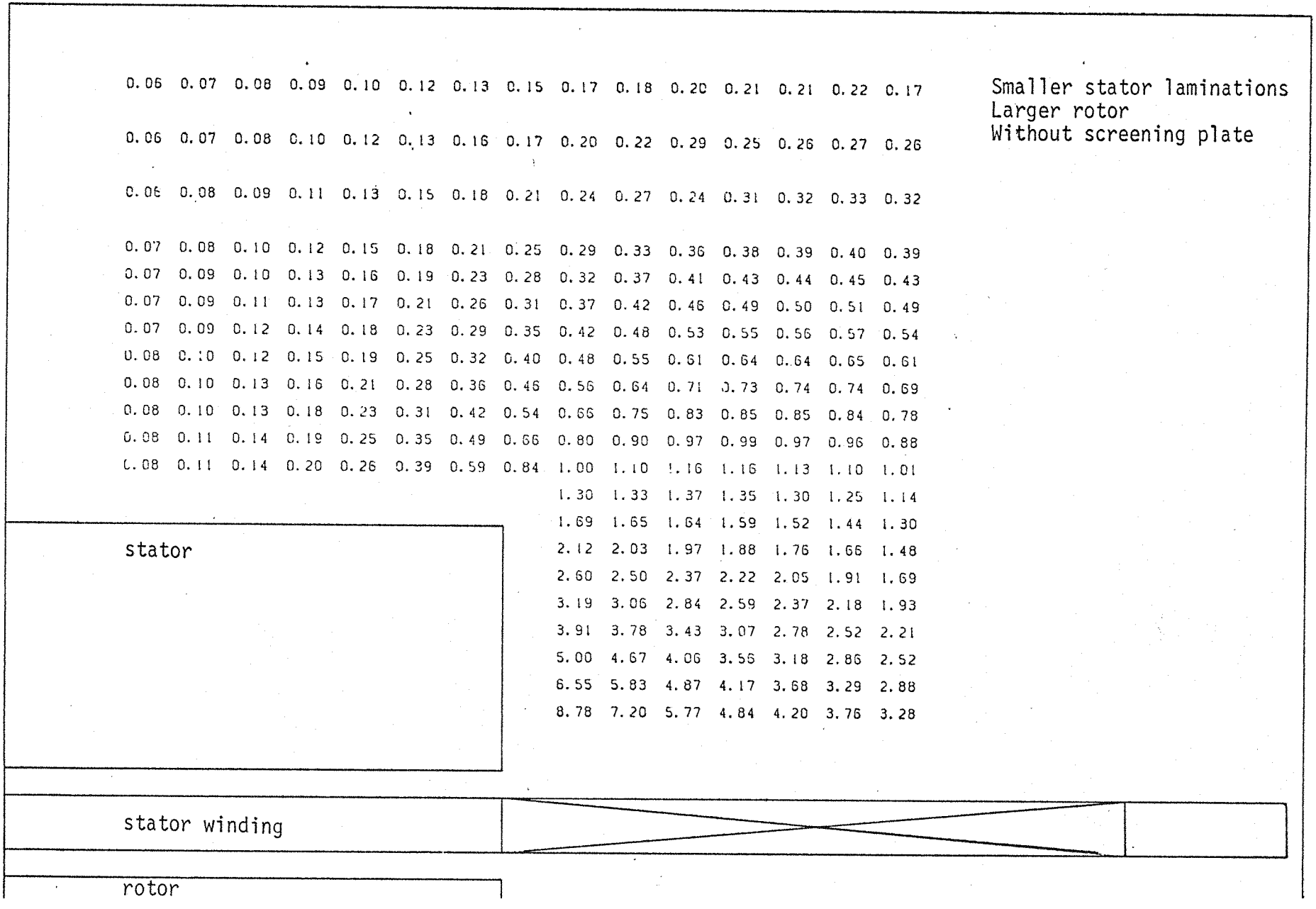

Fig. 8.26e: Magnitudes of the total flux density

0.84	0.85	0.85	0.84	0.82	0.80	0.82	0.78	0.76	0.75	0.72	0.69	0.67	0.63	0.60
0.92	0.95	0.93	0.94	0.91	0.09	0.88	0.87	0.85	0.83	0.80	0.77	0.74	0.70	0.66
1.02	1.04	1.03	1.02	1.00	0.99	0.98	0.96	0.94	0.92	0.89	0.85	0.82	0.77	0.72
1.13	1.14	1.14	1.13	1.11	1.10	1.09	1.07	1.05	1.03	0.99	0.96	0.91	0.85	0.80
1.18	1.20	1.19	1.19	1.17	1.16	1.15	1.13	1.11	1.09	1.05	1.02	0.96	0.90	0.85
1.24	1.26	1.26	1.26	1.24	1.22	1.22	1.20	1.18	1.16	1.12	1.08	1.02	0.96	0.90
1.30	1.33	1.32	1.32	1.30	1.29	1.28	1.27	1.25	1.23	1.18	1.14	1.08	1.02	0.95
1.37	1.39	1.39	1.39	1.39	1.37	1.37	1.35	1.33	1.31	1.26	1.22	1.15	1.08	1.00
1.44	1.47	1.47	1.48	1.46	1.46	1.45	1.44	1.42	1.39	1.34	1.30	1.23	1.15	1.07
1.53	1.56	1.55	1.56	1.55	1.55	1.54	1.53	1.51	1.49	1.44	1.39	1.31	1.23	1.14
1.60	1.63	1.63	1.65	1.64	1.64	1.63	1.62	1.61	1.60	1.53	1.48	1.40	1.31	1.22
1.69	1.73	1.73	1.74	1.74	1.74	1.74	1.74	1.72	1.71	1.65	1.59	1.50	1.41	1.30
1.78	1.82	1.82	1.84	1.83	1.85	1.86	1.86	1.84	1.84	1.77	1.71	1.61	1.51	1.39
1.87	1.93	1.93	1.96	1.96	1.97	1.98	1.99	1.98	1.98	1.90	1.85	1.75	1.62	1.50
1.97	2.03	2.05	2.06	2.08	2.11	2.11	2.14	2.14	2.13	2.05	1.98	1.89	1.75	1.63
2.09	2.14	2.17	2.19	2.22	2.25	2.23	2.31	2.31	2.31	2.22	2.14	2.05	1.88	1.75
2.19	2.26	2.29	2.32	2.35	2.40	2.44	2.48	2.77	2.49	2.41	2.33	2.22	2.04	1.92
2.32	2.40	2.43	2.47	2.51	2.58	2.64	2.71	2.73	2.73	2.63	2.54	2.42	2.22	2.07
2.45	2.52	2.14	2.61	2.67	2.75	2.83	2.92	2.97	2.98	2.88	2.78	2.65	2.41	2.24
2.59	2.66	2.74	2.78	2.83	2.96	3.06	3.20	3.27	3.28	3.17	3.05	2.88	2.62	2.43
2.72	2.81	2.88	2.94	3.01	3.15	3.32	3.50	3.60	3.65	3.51	3.37	3.18	2.86	2.63

Stator winding only, no iron and no screening plate.

straight part | overhang

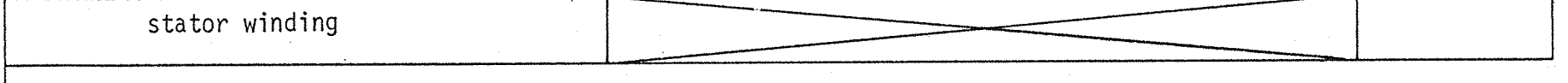

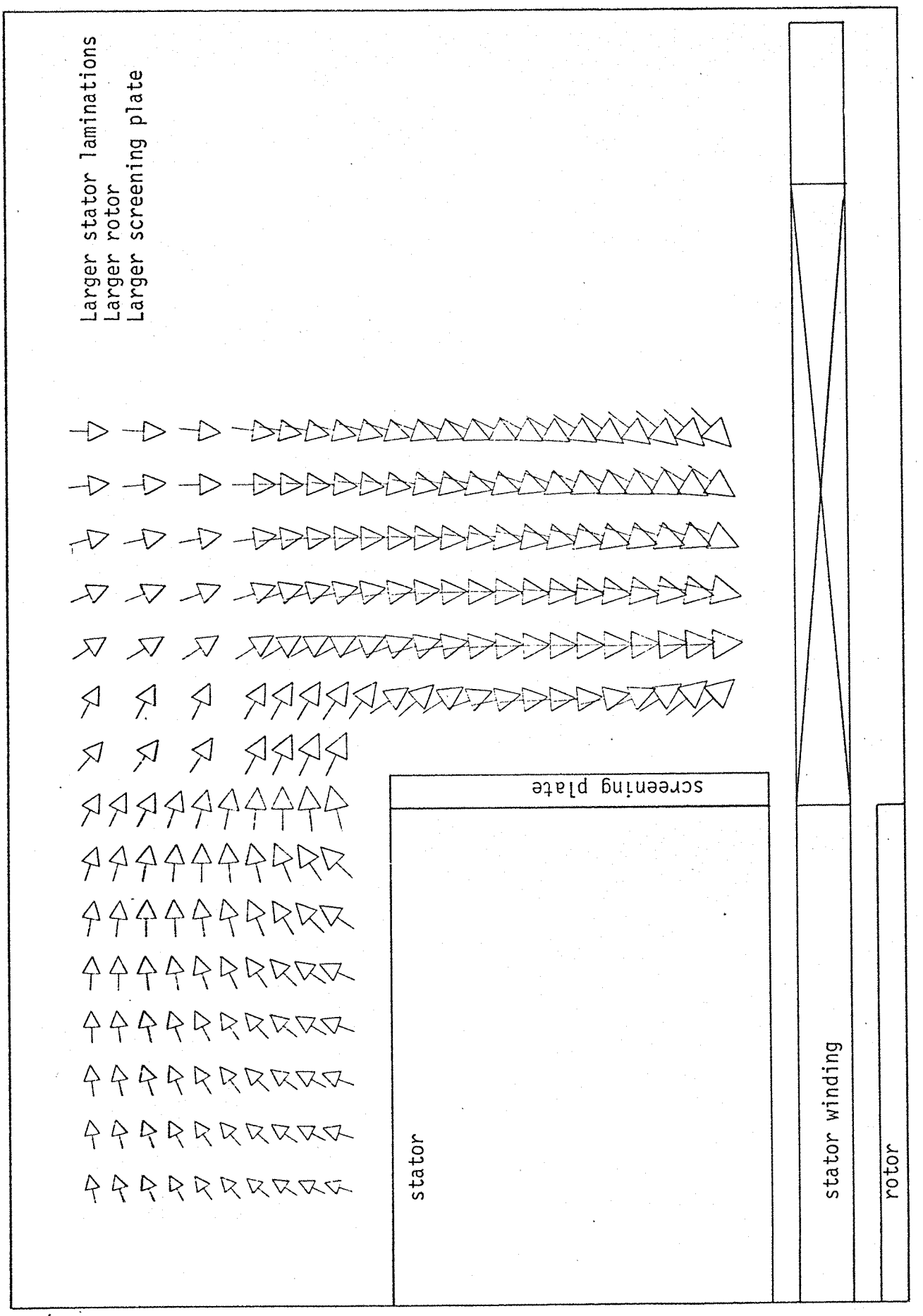

Fig. 8.27.I: 3-D leakage flux density vectors

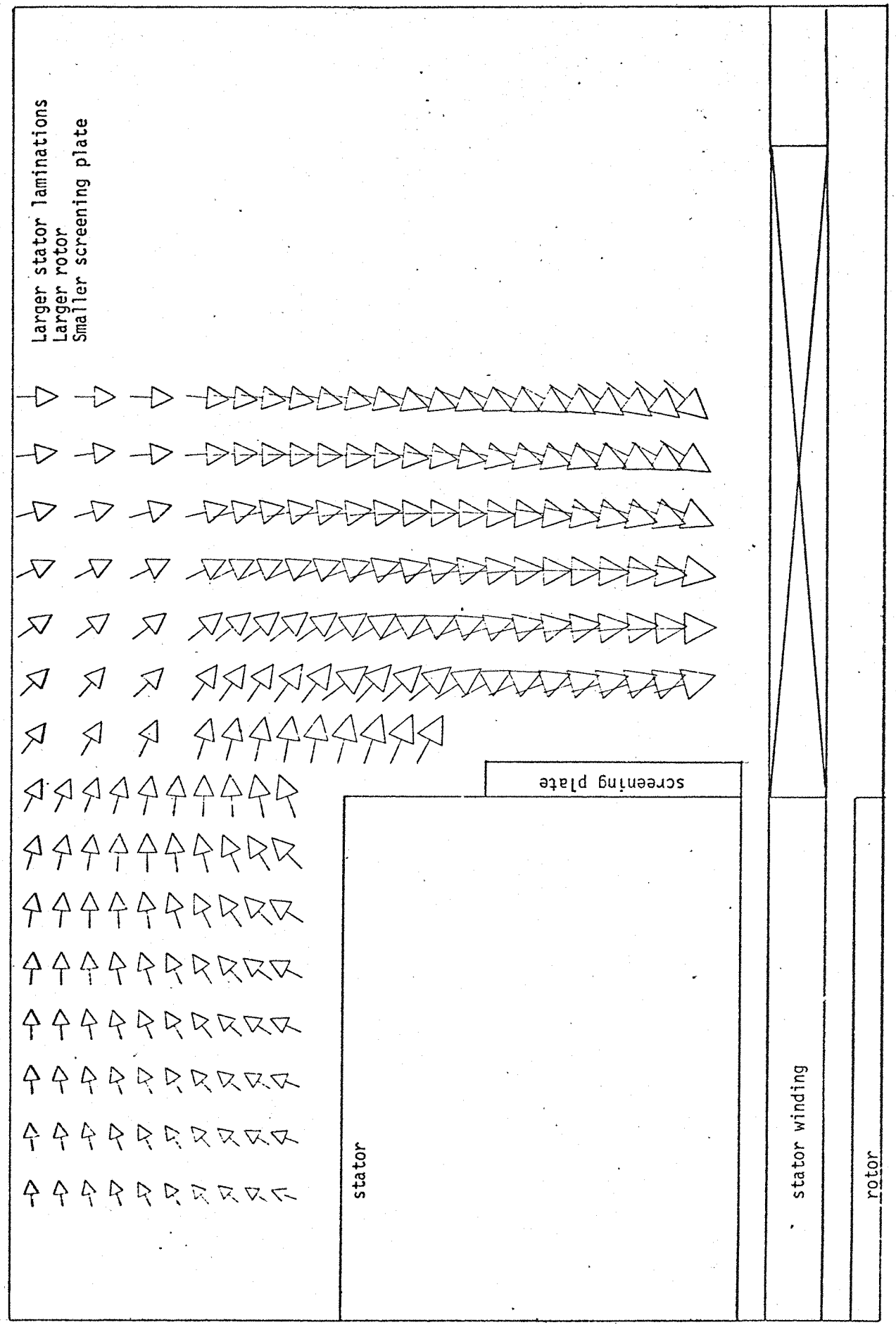

Fig. 8.27.II: 3-D leakage flux density vector

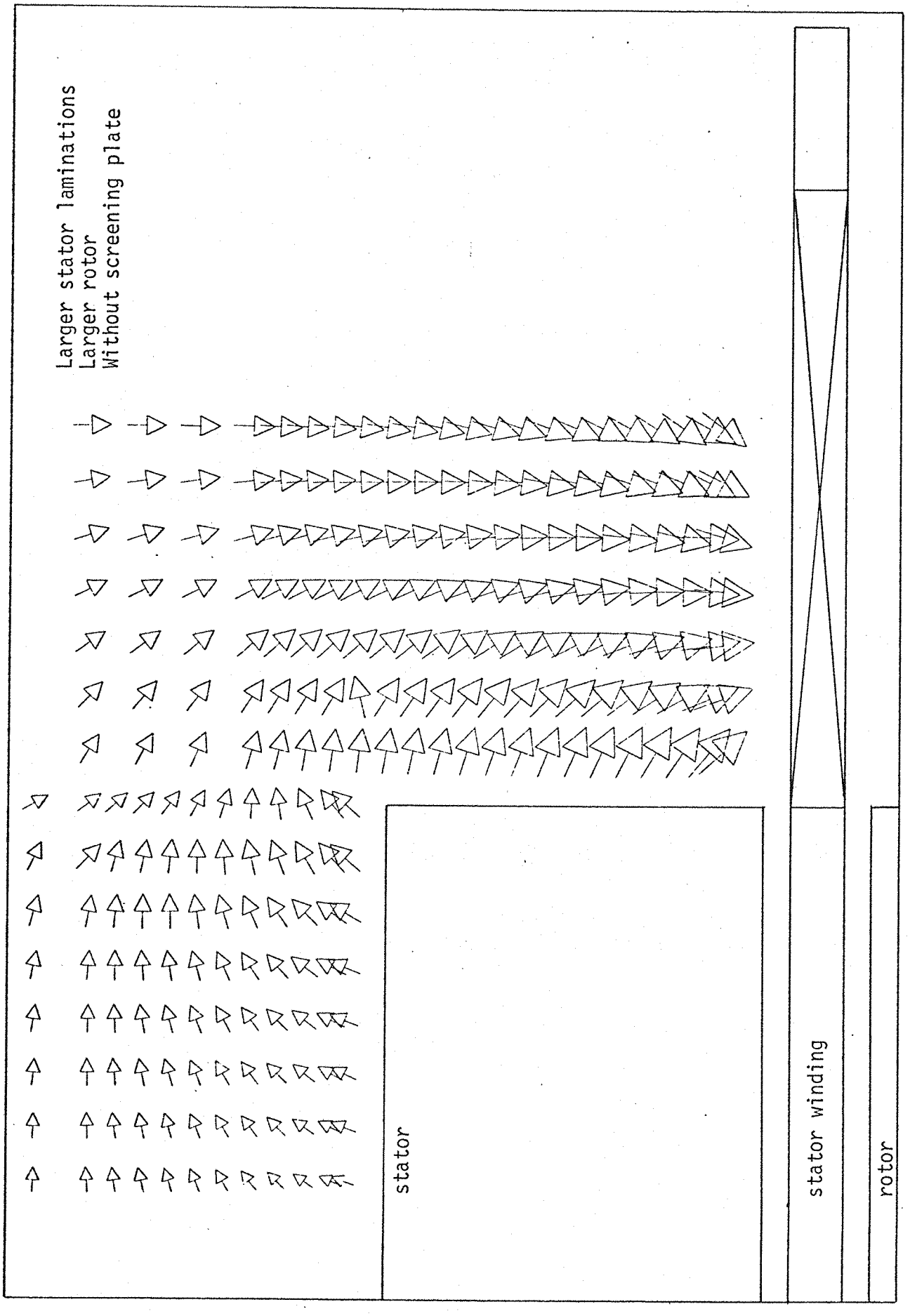

Fig. 8.27. III : 3-D leakage flux density vectors

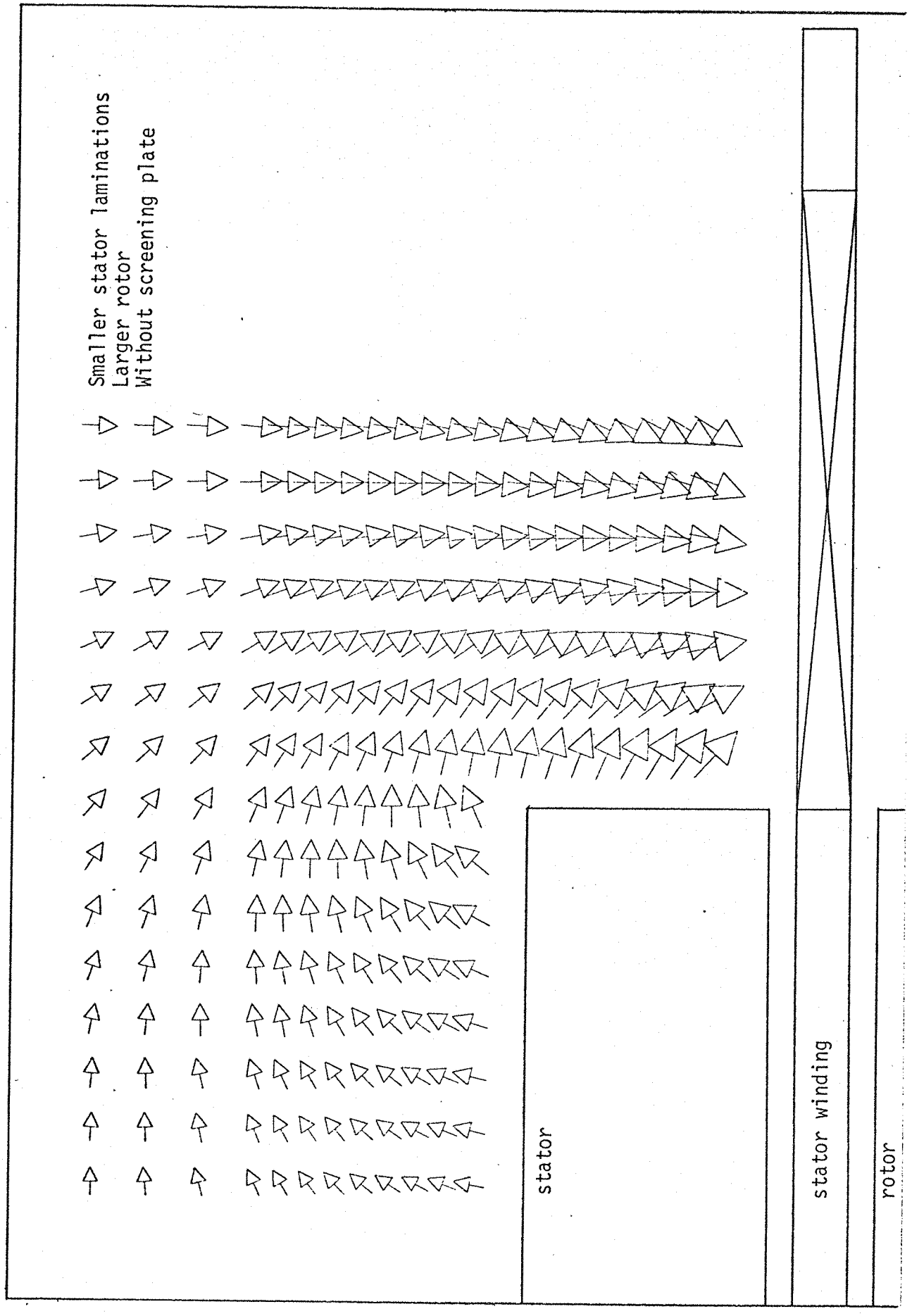

Fig. 8.27.IV: 3-D leakage flux density vector

Fig. 8.27.V: 3-D magnetic flux density vectors

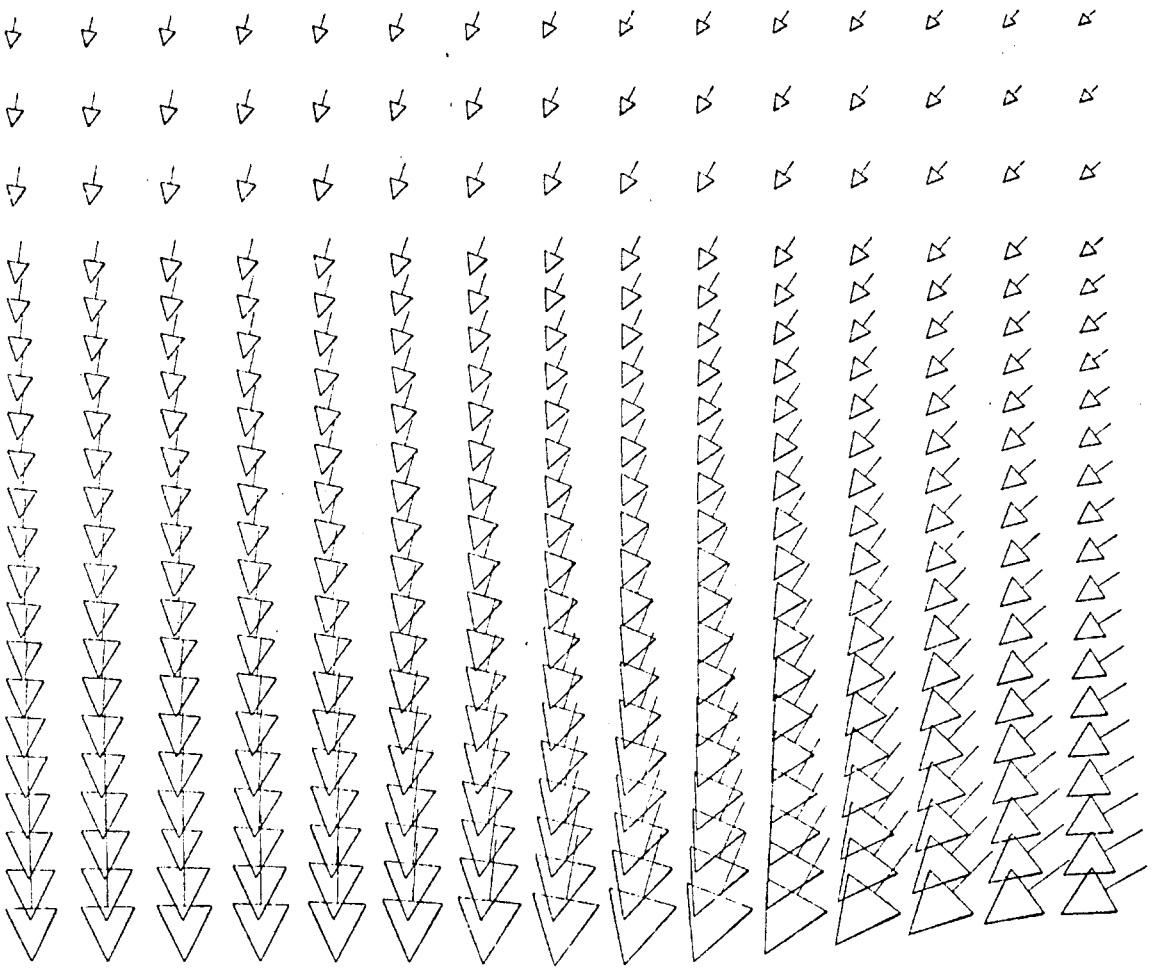

Just the stator winding without both the stator and rotor cores and without any screening.

stator winding.

8.3 ELECTROMAGNETIC STRESS OF THE STATOR CORE BACK FIELD

The concept of electromagnetic stress has been invented to account for the manner in which forces are transmitted in magnetic materials.[51,60] The electromagnetic stress is actually defined as the ratio force per unit area. The electromagnetic stress is manifested at the iron/air boundary of the stator core back because of the large variation in the permeability at that boundary. The iron permeability is much larger than the permeability in the air. The magnetic flux density between air and the stator core back surface is everywhere normal to the iron/air boundary in the air region ($\mu_{iron} \to \infty$).

The electromagnetic stress of the core back magnetic field is given by:

$$\sigma = \frac{1}{2} H.B$$

but at the air region the relationship between B and H is linear:

$$B = \mu_o H$$

Therefore

$$\sigma = \frac{1}{2} \mu_o H^2$$

or

$$\sigma = \frac{1}{2\mu_o} B^2$$

The relationship between the force and the stress is given by:

$$dF = \sigma ds$$

The force on the stator core back can, therefore, be determined by integrating the electromagnetic stress over the core back surface, using the magnetic flux density in the air region of the stator core back. The electromagnetic stress of the core back

magnetic field is in such a direction that it attempts to pull the stator core back into the air region. The figures given in section 6.3.5.A show the power spectrum density (PSD) of the core back leakage flux components. The amplitudes of the harmonics content are porportional to the square of the magnetic flux density. Therefore the power spectrum density figures can also be used to identify the harmonics contribution to the electromagnetic stress. When the saturation in the stator core is increased the magnitudes of the odd harmonics in the electromagnetic stress are also increased. The higher the level of saturation, the higher is the magnitude of the third harmonic content in the electromagnetic stress of the magnetic field at the stator core back.

CHAPTER NINE

CONCLUSIONS AND SUGGESTIONS FOR FURTHER WORK

In view of the constant increase in the size of the synchronous machine and due to recent observations at power stations of the damage of stator cores, a need has arisen to analyse the distribution of leakage flux density at the stator core back. The core back leakage flux may cause large circulating currents in the building bars of the synchronous machine which can lead to damage of the stator laminations in contact with the building bars. In order to minimise the effects of these circulating currents, the stator core is built up with just one building bar in contact with the laminations to provide the stator core earthing and all the others are insulated from the laminations.

The distribution of leakage flux at the stator core back varies lengthwise along the core back. The radial, axial and circumferential components of leakage flux have higher intensities at the edge of the core back. That is explained by the fact that the main electromagnetic sources are placed closer to the core back edge. The main electromagnetic sources of core back leakage flux are: polarity on disc surfaces at the core front, polarity on the back of the core, bore polarity and overhang current. The magnetic polarity on the core back surface has the largest contribution to the leakage flux at the core back surface. The intensity of the core back leakage flux decreases with the distance from the surface of the stator core.

The shape of the core back leakage flux distribution does not depend on the operational conditions of the synchronous machine, i.e. either during short and open circuit or on-load conditions the largest concentration of leakage flux is at the edge of the core back surface. However, the intensities of the leakage flux at the stator core back

depends on a large number of variables, including the geometry of the stator core and its supporting structure, the geometry of the overhang, the distribution of eddy currents, levels of saturation in the stator core, the overhang current and the power factor. These variables produce a larger effect in the leakage flux at the edge of the stator core back. Both the building bars and the radial ventilating ducts can affect the distribution of core back leakage flux introducing areas of higher concentration of leakage flux. However, the effects of both the building bars and the radial ventilating ducts are localised and they affect just the distribution of core back leakage flux in the surrounding areas.

The increase in the overhang current increases the intensity of leakage flux at the stator core back. Therefore it is expected that the effects of core back leakage flux are amplified on large synchronous machines.

When the synchronous machine is operating under saturating conditions the core back leakage flux is increased. The waveforms of the core back leakage flux are distorted by the saturation effects and the magnitudes of odd harmonics are increased. The increase in the odd harmonic magnitude can cause increased losses in the building bars and can also damage both the insulation between adjacent laminations and the insulation between the insulated building bars and the laminations. This causes the establishment of circulating currents which can produce spots of high temperature at the stator core.

The power factor also affects the leakage flux at the stator core back. A synchronous generator operating at leading power factor has a larger leakage flux at the core back than at lagging power factor. Intuitively one might expect that the core back leakage flux should be stronger at lagging power factor when the field current is larger.

However, it must be remembered that the resultant vector field is obtained as the vector sum of the stator and rotor field components which are arithmetically subtracted one from the other producing less leakage flux at a lagging power factor.

The stator core geometry also plays an important role in the distribution of leakage flux at the core back. The depth of the stator core changes the magnitude of the core back leakage flux. A deeper stator core has a smaller core back leakage flux because the distance between the main electromagnetic sources and the core back is increased. Also less magnetising leakage flux reaches the core back. The latter effect causes the magnetic polarity at the core back surface to be diminished. This suggests that an inwards stepping of the core back edge attenuates the concentration of leakage flux at the edge. However, the stator core back with stepped edges would have difficulties in construction. An increase in the core length produces a decrease in the leakage flux at the centre of the core back because the main electromagnetic sources located at the stator end are more distant when longer cores are used. A shorter air gap with constant air gap flux decreases the leakage flux at the core back because the magnetising fringing flux is diminished.

The relative position between both the stator and the rotor cores is also important in the distribution of core back leakage flux. Results obtained in this research suggest that a shortening in the rotor with respect to the stator core diminishes the leakage flux at the core back. This is because the rotor shortening diminishes the magnetising axial leakage flux at the core front. The increase in the length of the overhang increases the core back leakage flux because of the increase in the length of the leakage flux path.

Synchronous machines having the stator core laminations

aligned with respect to the rolling direction can have increased intensity of leakage flux impinging the stator core back at a direction parallel to the rolling direction of the laminations. The aligned rolling direction can therefore establish areas of higher concentration of leakage flux around the circumferential position of the core back.

The eddy current circulating in the screening plate can produce a reaction field that is strong enough to divert the axial leakage flux at the core front to the back of the stator core. That effect increases the concentration of leakage flux at the edge of the stator core back. This suggests that a screening plate extended over the core back edge can diminish the concentration of leakage flux at the core back edge.

The determination of the leakage flux density in the air region at the stator core back is important for two main reasons: firstly, it helps to estimate the leakage flux inside the stator core back and secondly, it can be used to determine the effects of the leakage flux penetrating the building bars. The use of the boundary conditions at the core back surface enables the establishment of the leakage flux density inside the core back given the leakage flux at the air region. The core back leakage flux density also helps in obtaining the electromagnetic stress of the core back magnetic field. The concept of electromagnetic stress has been invented to account for the manner in which forces are transmitted in magnetic materials. The integration of the electromagnetic stress over the core back surface gives the force pulling the stator core back into the air region. Considering that the effects of the core back leakage flux in the reliability of the stator core back of large synchronous machines have become more accentuated, further attention should be given to the analysis of this leakage flux. It is suggested that an investigation

be made of the effects of both the radial ventilating ducts and the butt-joints in the distribution of leakage flux at the stator core back. The construction of a copper cage to act as part of the stator core structure is also suggested in order to investigate the effects of the induced current flowing in the structure due to the leakage flux at the core back. The investigation of the leakage flux at the stator core back when the synchronous machine is operating under transient conditions is also important to the stator core reliability since the effects of the core back leakage flux are expected to be much greater during the transients.

REFERENCES

1. NEIDHOEFFER, G. and SCHWENGELER, A.: "The application and significance of magnetic materials in large generator construction", Journal of Magnetism and Magnetic Materials, North-Holland Publishing Co., 1978, 9, pp112-22.

2. ABEGG, K.: "The growth of turbogenerators", Phil. Trans. R. Soc. Lond., 1973, 275, pp51-67.

3. VICKERS, V.J.: "Recent trends in turbogenerators", Proc. IEE, 1974, 121(11), pp1273-306.

4. SAY, M.G.: "Alternating current machines", (Pitman, 1978).

5. NOSER, R.R. and POHL, H.: "Cooling large turbogenerators without hydrogen", IEEE Winter Power Meeting, New York, 1971, pp2101-07.

6. HOLLEY, C.H. and TAYLOR, H.D.: "Direct cooling of turbine-generator fields windings", Trans. AIEE, 1954, 73(3), pp542-50.

7. BAUDRY, R.A. and HELLER, P.R.: "Ventilation of inner-cooled generators", ibid, 1954, 73(3), pp500-08.

8. DEMERDASH, N.A., GARG, V.K. and HAMILTON, H.B.: "Effect of ventilating holes on radial flux and losses in stator slots of turbogenerators", IEEE Trans. PAS, 1975, PAS-94(4), pp1177-80.

9. WINCHESTER, R.L.: "Stray losses in the armature end iron of large turbine generators", Proc. IEE, 1955, 74(3), pp381-91.

10. JACOBS, D.A.H., MINOSS, R.H., MYERSCOUGH, C.J., ROLLASON, M.L.J. and STEEL, J.G.: "Calculation of losses in the end region of turbogenerators", ibid, 1977, 124(4), pp356-62.

11. HENSMAN, G.O., MUHLHAUS, J., MYERSCOUGH, C.J.: "Calculation and measurement of magnetic fields in turbogenerator end-regions", ibid, 1976, 123(9), pp887-92.

12. HAMMOND, P.: "The calculation of the magnetic field of rotating machines. Pt. 1 - The field of tubular current", ibid, 1959, 106(C), pp158-64.

13. ASHWORTH, D.S. and HAMMOND, P.: "The calculation of the magnetic field of rotating machines. Pt. 2 - The field of turbogenerator end windings", ibid, 1961, 108(A), pp527-38.

14. HAMMOND, P.: "The calculation of the magnetic field of rotating machines. Pt. 3 - Eddy currents induced in a solid slab by a circular current loop", ibid, 1962, 109(C), pp508-

15. STOLL, R.L. and HAMMOND, P.: "The calculation of the magnetic field of rotating machines. Pt. 4 - Approximate determination of the field and the losses associated with eddy currents in conducting surfaces", ibid, 1965, 112(11), pp2082-94.

16. STOLL, R.L. and HAMMOND, P.: "The calculation of the magnetic field of rotating machines. Pt. 5 - Field in the end region of turbogenerators and the eddy current loss in the end plates of stator cores", ibid, 1966, 113(11), pp1793-804.

17. HOWE, D. and HAMMOND, P.: "Examination of the axial flux in stator cores with particular reference to turbogenerators", ibid, 1974, 121(12)- pp1536-42.

18. HOWE, D. and HAMMOND, P.: "Distribution of axial flux on the stator surfaces at the ends of turbogenerators", ibid, 1974, 121(9), pp980-90.

19. TAVNER, P.J., HAMMOND, P. and PENMAN, J.: "Contribution to the study of leakage fields at the ends of rotating electrical machines", ibid, 1978, 125(12), pp1339-49.

20. TAVNER, P.J., PENMAN, J., STOLL, R.L. and LORCH, H.O.: "Influence of winding design on the axial flux in laminated stator cores", ibid, 1978, 125(10), pp948-56.

21. LAWRENSON, P.J.: "The magnetic field of the end-windings of turbo-generators", ibid, 1961, 108(A), pp538-53.

22. HAWLEY, R., EDWARDS, I.M., HEATON, J.M. and STOLL, R.L.: "Turbogenerator end-region magnetic fields: Qualitative prediction by field plotting", ibid, 1967, 114(8), pp1107-14.

23. OKUDA, H.: "Calculation of magnetic field distribution in the end zone of generator winding", Electrical Eng. in Japan, 1969, 89(11), pp27-33.

24. SMITH, R.T.: "End component of armature leakage reactance of round-rotor generators", Trans. AIEE, 1963, 82, pp562-72.

25. REECE, A.B.J. and PRAMANIK, A.: "Calculation of the end-region field of a.c. machines", Proc. IEE, 1965, 112(7), pp1355-68.

26. MYERSCOUGH, C.J.: "Calculation of the magnetic fields in the end regions of turbogenerators", ibid, 1974, 121(7), pp653-56.

27. CARPENTER, C.J.: "The application of the method of images to machine end-winding fields", ibid, 1960, 107(A), pp487-500.

28. TEGOPOULOS, J.A.: "Current sheets equivalent to end-winding currents of turbine-generator stator and rotor", Trans. AIEE, 1963, 81(3), pp695-700.

29. TEGOPOULOS, J.A.: "Flux impinging on the end plate of turbine generators", ibid, 81(3), pp700-07.

30. TEGOPOULOS, J.A.: "Determination of the magnetic field in the end zone of turbine generators", ibid, 81(3), pp562-72.

31. OBERRETL, K.: "Leakage fields, eddy current losses, temperature rise, forces and parasitic sheet-fusion in the end zone of turbo-generators" (translated from German), Elektrotechnik und Maschinenbau, 1963, 80, pp539-50.

32. PHEAR, H.W. and MALLOCK, R.R.M.: "The effect of the joints in the plates of a laminated iron core on the d.c. ampere-turns required for its magnetisation", Journal IEE, 1936, 79, pp560-64.

33. BUTLER, O.I.: "Determination of the d.c. magnetisation characteristics of laminated cores using overlapping joints", ibid, 1947, 94, pp27-32.

34. JONES, M.A., MOSES, A.J. and THOMPSON, J.E.: "Flux distribution and power loss in the mitered overlap joint in power transformer cores", IEEE Trans. on MAG, 1973, MAG-9, pp114-22.

35. STOLL, R.L.: "The effect of butt joints in large a.c. machines", Proceedings of the International Conference on Electrical Machines, Vienna, 1976, pp165-70.

36. STOLL, R.L.: "Eddy-current losses at the joints of laminated cores", Proceedings of the International Conference on Electrical Machines, Brussels, 1978, paper G2/3, pp1-12.

37. HOWE, D, JACK, A.G., and BENNETT, J.: "Examination of the flux distribution in segmented stator cores", ibid, (to be published).

38. CHALMERS, B.J.: "Electromagnetic problems of a.c. machines", (Chapman and Hall, Ltd., 1965).

39. NITSCHE, E.: "Fields and forces in end-windings of synchronous machines at sudden short-circuits", Proceedings of the International Conference on Electrical Machines, Vienna, 1976, paper G3/5, pp1-10.

40. BRANDL, P.: "Forces on the end winding of a.c. machines", Brown Boveri Rev., 1980, 2, pp128-34.

41. JACKSON, R.J.: "Interlamination voltages in large turbo-generators", Proc. IEE, 1978, 125(11), pp1232-38.

42. SINGLETON, R.C.C., MARSHALL, P. and STEEL, J.G.: "Axial magnetic flux in synchronous machine: The effect of operating conditions", IEEE - PES - Winter Power Meeting, New York, February 1980.

43. JAYAWANT, B.V.: "Flux distribution in a permeable sheet with a hole near an edge", Proc. IEE, March 1960, Monograph No. 368, pp238-41.

44. JACKSON, R.L.: "Factors affecting the eddy-current loss in steel clamping bolts", ibid, 1965, 112(12), pp2353-58.

45. WALKER, J.H., ROGERS, G.J. and JACKSON? R.L.: "Pressing and clamping laminated cores", ibid, 1964, 111(3), pp565-77.

46. HAMMOND, P. and MARIOTONI, C.A.: "External flux leakage of synchronous machines", Proceedings of the International Conference on Electrical Machines, Athens, 1980, pp1573-80.

47. ZIJESTRA, H.: "Experimental methods in electromagnetism: Measurement of magnetic quantities", (North Holland Publishing Co., 1967).

48. HAMMOND, P.: "Sources and fields - some thoughts on teaching the principles of electromagnetism", Inst. J. Elect. Eng. Educ., 1969, 7, pp65-76.

49. TAVNER, P.J.: "Axial flux distribution in laminated steel cores, with particular reference to the end region magnetic field of large turbogenerators", Ph.D. Thesis, University of Southampton, 1978.

50. MOULIN, E.G.: "The principles of electromagnetism", (Clarendon Press, 1955).

51. HAMMOND, P.: "Applied electromagnetism", (Pergamon Press, 1971).

52. HAMMOND, P.: "Leakage flux and surface polarity in iron ring stampings", Proc. IEE, 1955, 102C, pp138-47.

53. STEEL, J.G.: "Soft-magnetic materials in large turbo-generators", IEEE Trans. on MAG, 1974, MAG-10(2), pp151-54.

54. STOLL, R.L.: "The analysis of eddy currents", (Clarendon Press, 1974).

55. LAMMERANER, J. and STAFL, M.: "Eddy currents", (Iliffe Books Ltd., 1966).

56. STAFL, M.: "Electrodynamics of electrical machines", (Iliffe Books Ltd., 1967).

57. ZAHN, M.: "Electromagnetic field theory: a problem solving approach", (John Wiley and Sons, 1979).

58. PANOFSKY, W.K.H. and PHILIPS, D.M.: "Classical electricity and magnetism", (Addison-Wesley, 1955).

59. KIP, A.F.: "Fundamentals of electricity and magnetism", (McGraw-Hill Kogakusha Ltd., 1969).

60. BOAST, W.B.: "Vector fields - A vector foundation of electric and magnetic fields", (Harper and Row, and John Weatherall Inc., 1964).

61. DAVIES, E.J.: "Airgap windings for large turbogenerators", Proc. IEE, 1971, 118(3/4), pp529-35.

62. SPOONER, E.: "Fully slotless turbogenerators", ibid, 1973, 120(12), pp1507-18.

63. ANDERSON, A.F., BUMBY, J.R. and HASSALL, B.I.: "Analysis of helical armature windings with particular reference to superconducting a.c. generators", ibid, 1980, 127C(3), pp129-44.

64. FITZGERALD, A.E., KINGSLEY, and KUSKO, A.: "Electric machinery", (McGraw-Hill Inc., 1975).

65. LIWSCHITZ-GARIK, M. and WHIPPLE, C.C.: "Electric machinery", (D. Van Nostrand Co. Inc., 1950).

66. HOWE, D.: "End effects in the magnetic field of large electrical machines", Ph.D. Thesis, University of Southampton, 1976.

67. HECK, C.: "Magnetic materials and their applications", (Butterworth and Co. (Publishers) Ltd., 1974).

68. WALKER, J.H.: "Large a.c. machines - design, manufacture and operation", (Bharat Heavy Electricals Limited, 1979).

69. CARPENTER, C.J.: "Theory of flux penetration into laminated iron and associated losses", Proc. IEE, 1977, 124(7), pp659-64.

70. OBERRETL, K.: "Magnetic fields, eddy currents, and losses, taking the variable permeability into account", IEEE Trans. PAS, 1969, PAS-88(11), pp1646-57.

71. LANGLOIS-BERTHELOT, R.: "Electro-magnetic machines", (Macdonald and Co. (Publishers) Ltd., 1953).

72. LEE, E.W.: "Eddy-current losses in thin ferromagnetic sheets", Proc. IEE, February 1958, Monograph No. 284, pp337-42.

73. AGARWALL, P.D.: "Eddy-current losses in solid and laminated iron", AIEE Trans. PAS, 1959, PAS-78(1), pp169-81.

74. BARTH, J.B.: "Alternating electromagnetic fields, eddy currents and power loss in solid iron", Proc. IEE, 1973, 120(11), pp1454-61.

75. O'KELLY, D.: "Flux penetration and core loss in solid iron", IEEE Trans. on MAG, 1975, MAG-11(1), pp55-60.

76. CHURCHILL, R.V.: "Fourier series and boundary value problems", (McGraw-Hill Book Company Inc., 1941).

77. KREYSIG, E.: "Advanced engineering mathematics", (John Wiley and Sons Inc., 1972).

78. MIGLEY, D. and SMETHURST, S.W.: "Magnetic field problem with axial symmetry and its solution in terms of Fourier-Bessel expansions", Proc. IEE, 1963, 110(8), pp1465-72.

79. MCLACHLAN, N.W.: "Bessel functions for engineers", (Clarendon Press, 1961).

80. MOON, P. and SPENCER, D.E.: "Field theory for engineers", (D. Van Nostrand Co. Inc., 1961).

81. MATSCH, L.W.: "Electromagnetic and electromechanical machines", (International Textbook Company, 1972).

82. SEELY, S.: "Electromechanical energy conversion", (McGraw-Hill Book Company Inc., 1962).

83. ADKINS, B. and HARLEY, R.G.: "The general theory of alternating current machines: application to practical problems", (Chapman and Hall Ltd., 1975).

84. Department of Electrical Engineering - M.I.T.: "Magnetic circuits and transformers", (The M.I.T. Press, 1974).

85. BRAILSFORD, F. and BURGESS, J.M.: "Internal waveform distortion in silicon-iron laminations for magnetisation at 50c/s", Proc. IEE, May 1961, Monograph No. 446, pp458-62.

86. DUNFIELD, J.C. and BARTON, T.H.: "Effects of m.m.f. and permeance harmonics in electrical machines - with special reference to a synchronous machine", ibid, 1967, 114(10), pp1443-50.

87. SAMAHA-FAHMY, M. and BARTON, T.H.: "Harmonic effects in rotating electric machines", paper T74 011-3, IEEE - PES - Winter Meeting, New York, 1974.

88. BEAUCHAMP, K.G.: "Signal processing: using analog and digital techniques", (George Allen and Unwin Ltd., 1973).

89. Central Electricity Generating Board (C.E.G.B.): "Modern power station practice: Operation and efficiency - Vol. 7", (Pergamon Press, 1971).

90. RICHARDSON, P.: "Design and application of large solid-rotor asynchronous generators", Proc. IEE, 1958, 105A, pp332-46.

91. MASON, T.H., AYLETT, P.D. and BIRCH, F.H.: "Turbo-generator performance under exceptional operating conditions", ibid, 1959, 106A, pp357-80.

92. ESTCOURT, V.F., HOLLEY, C.H., JOHNSON, W.R. and LIGHT, P.H.: "Underexcited operation of large turbine generators on pacific gas and electric company's system", AIEE Trans., 1953, 72(3), pp16-22.

93. HAMMOND, P.: "The magnetic screening effect of iron tubes", Proc. IEE, 1956, 103C, pp112-20.

94. HAGUE, B.: "The principles of electromagnetism applied to electrical machines", (Dover, 1962).

95. CARTER, G.W.: "The electromagnetic field in its engineering aspects", (Longman, 1967).

96. BADEN FULLER, A.J. and DOS SANTOS, M.L.X.: "New method for the display of three-dimensional vector fields", ibid, 1980, 127A(7), pp435-42.

97. TAVNER, P.J.: "Private correspondence".